ANALYSIS OF THE INTERACTION BETWEEN PENTRAXINS AND *LEISHMANIA* PHOSPHOGLYCANS

Eu Shen Seow

Thesis submitted in accordance with the requirements for the degree of

Doctor of Philosophy

of the
University of London

March 2021

Department of Infection Biology

Faculty of Infectious and Tropical Diseases

LONDON SCHOOL OF HYGIENE & TROPICAL MEDICINE

No funding received

Research group affiliation: Raynes Group

Declaration of work

I, Eu Shen Seow, confirm that the work presented in this thesis is my own. Where information has been derived from other sources, I confirm that this has been indicated in the thesis.

Abstract

CRP, a major acute phase protein, has also been shown to bind to *Leishmania* lipophosphoglycan (LPG) phosphorylated disaccharide repeats in a calcium-dependent manner. Similar structures have been observed in the promastigote secretory gel (PSG) components filamentous proteophosphoglycan (fPPG) and secreted acid phosphatase (ScAP). We investigate the ability of CRP, as well as related innate immune proteins, to bind to these *Leishmania* phosphoglycans, to determine their potential mechanisms as virulence factors of mammalian infection.

CRP binding of PSG was shown to be calcium-dependent and on the same binding cleft involved in PC-binding. PSG from a range of *Leishmania* species (*L.aethiopica, L.panamensis, L.donovani, L.infantum, L.mexicana, L.tropica, L.amazonensis,* and *L.major*), as well as LPG derived from different *L.mexicana* promastigote stages, had the ability to bind to CRP and SAP with widely varying binding capacities. ScAP was determined to be the major CRP binding component in PSG. CRP-PSG binding was shown to be a high avidity and multimeric interaction.*L.mexicana* LPG stage-specific variations in size and pentraxin binding characteristics, as well as calcium-dependent binding of CRP and SAP, was demonstrated.

CRP, but not SAP, binding to LPG was directed at the phosphorylated disaccharide repeats. A novel, orientation-dependent interaction of SAP binding to *L.mexicana* LPG was observed. LPG appeared to undergo a conformational change at a threshold of CRP binding (~2.5 µg/ml), affecting subsequent CRP binding affinity. Stage-variable LPG-PSG interaction dependent on CRP and calcium was demonstrated, with interaction being significantly greater in LPG derived from infectious stage promastigotes.

PSG-CRP and LPG-CRP complex, but not LPG-SAP, was shown to be capable of binding C1q. PSG-CRP complex-mediated complement generation was shown to be primarily via the classical pathway (CP), with minor alternative pathway (AP) contribution.

Dedication

To my family

Acknowledgements

Utmost gratitude and credit must be given to my primary supervisor, Professor John Raynes, who fuelled this project with a steady supply of practical advice, assistance, patience and beer.

Many thanks also to Matthew Rogers, who grew the *Leishmania* cultures from which the necessary materials for this study were derived, and his invaluable insight from the perspective of entomology and parasitology, which contributed greatly to the development and direction of this study.

A special mention to my co-supervisor Dr Jackie Cliff, who provided practical guidance and advice when needed.

Credit also to Dr Jan-Hendrick Schroeder, whose early work in the *Leishmania* secretome helped provide the early foundation on which the rest of this study was built.

I am grateful to the contribution of Dr Thomas Ilg, whose kind donation of *Leishmania*-specific antibodies to the Raynes Group enabled much of the presented work to be performed.

And last but not least, thank you to the crew of lab 420 and the Department of Infection Biology corner in the 4th floor for the much-needed banter, cakes and coffee!

Table of contents

Cover page 1

Declaration of work 2

Abstract 3

Dedication 4

Acknowledgements 5

Table of contents 6

Figures 15

Tables 21

Abbreviations 22

CHAPTER 1: Introduction 30

1.1: The Innate Immune Response 30

1.1.1: Innate Immunity 30

1.1.2: The Acute Phase Proteins 32

1.1.3: Regulation of the Acute Phase Response 34

1.1.4: Pathogen modulation of host immunity 34

1.1.5: Innate Recognition of Carbohydrate epitopes 36

1.2: Pentraxins 37

1.2.1: C-Reactive Protein (CRP) 40

1.2.1.1: Expression 40

1.2.1.2: Structure 42

1.2.1.3: Ca^{2+} dependent binding 45

1.2.1.4.: Ca^{2+} independent binding 46

1.2.1.5: Interactions with Complement 49

1.2.1.6: Cell surface CRP receptors 50

1.2.2: Serum Amyloid P component (SAP) 52

1.2.2.1: Expression 52

1.2.2.2: Structure 52

1.2.2.3: Ligand Binding and Specificity 53
1.2.2.4: Antimicrobial action 55
1.2.2.5: Wound resolution and anti-fibrosis 55
1.2.2.6: Amyloid Fibril Formation 57
1.2.2.7: Interactions with Complement 57
1.3: Complement 59
1.3.1: The Complement System 59
1.3.2: The Classical Pathway 61
1.3.3: The Alternative Pathway 62
1.3.4: The Lectin Pathway 63
1.4: *Leishmania* 68
1.4.1: Leishmaniasis 68
1.4.2: Life cycle 68
1.4.3: Clinical Symptoms 72
1.4.4: Treatment and therapeutic strategies 73
1.4.5: Vaccination 74
1.4.6: Vector Control 76
1.4.7: Immune response against *Leishmania* infection 77
1.4.8: Immune evasion and modulation by *Leishmania* parasites 82
1.5: *Leishmania* phosphoglycan products 86
1.5.1: Lipophosphoglycan (LPG) 86
1.5.1.1: Expression 86
1.5.1.2: Structure 87
1.5.1.3: Stage-specific variations 88
1.5.1.4: Species specific variations 91
1.5.2: Filamentous Proteophosphoglycan (fPPG) 93
1.5.2.1: Expression 93
1.5.2.2: Structure 93
1.5.2.3: Function: Promoting survival in sandfly gut lumen 96
1.5.2.4: Function: Promoting mammalian infection via sandfly gut obstruction 96

1.5.2.5: Function: Modulation of macrophages 100
1.5.3: Secreted Acid Phosphatase (ScAP) 101
1.5.3.1: Expression 101
1.5.3.2: Structure 103
1.5.3.3: *L.mexicana* ScAP 105
1.5.3.4: *L.donovani* ScAP 107
1.5.3.5: ScAP: Function 107
1.6: Innate Immune recognition of *Leishmania* 109
1.7: Hypothesis and aims 111
CHAPTER 2: Materials and methods 113
2.1: Buffers 113
2.2: ELISA 113
2.3: SDS-PAGE 114
2.4: Western and ligand blotting 116
2.5: Protein gel staining 118
2.6: Carbohydrate quantification assay 119
2.7: Serum 120
2.7.1: Extraction 120
2.7.2: Serum depletion of pentraxins 120
2.7.2.1: Affinity chromatography 120
2.7.2.2: Magnetic bead depletion of CRP 121
2.7.3: Determination of pentraxin concentration 121
2.7.3.1: CRP-detection ELISA 121
2.7.3.2: SAP-detection ELISA 122
2.8: Pentraxins 123
2.8.1: Purification 123
2.8.1.1: Ca^{2+} dependent affinity chromatography 123
2.8.1.2: Anion Exchange Chromatography 123
2.8.2: Biotinylation 124
2.8.2.1: CRP-biotin 124

2.8.2.2: SAP-biotin 125
2.9: Pentraxin ligands 126
2.9.1: Phosphorylcholine-conjugated bovine serum albumin (PCBSA) 126
2.9.2: Phosphoethanolamine cellulose (PEC) 126
2.9.2.1: Generation 127
2.9.2.2: Purification 127
2.10: Promastigote Secretory Gel (PSG) 128
2.10.1: Generation 128
2.10.2: Purification 128
2.10.2.1: Anion Exchange Chromatography 128
2.10.2.2: Hydrophobic Interaction chromatography 129
2.10.2.3: Ultracentrifugation 129
2.10.3: Quantification and Verification 130
2.10.4: Biotinylation 130
2.11: Lipophosphoglycan 132
2.11.1: Generation 132
2.11.2: Purification 132
2.11.3: Quantification and verification 133
2.11.4: Biotinylation 133
2.12: Pentraxin binding to *Leishmania* PSG 134
2.12.1: Western/ligand blot and protein gel staining 134
2.12.2: PSG-pentraxin ELISA 134
2.13: Complement assays 136
2.13.1: C1q capture assay 136
2.13.2: C1q binding assay 136
2.13.3: C3d Deposition assay 137
2.13.4: C3bi Deposition assay 137
2.14: PSG-MBL binding ELISA 139
2.15: Characterisation of LPG interactions with pentraxins 140
2.15.1: SDS-PAGE, western and ligand blotting 140

2.15.2: LPG-pentraxin ELISA 140
2.16: LPG-PSG ELISA 142
2.17: Surface plasmon resonance analysis of pentraxin interaction with PSG 143
2.17.1: PSG immobilisation 143
2.17.1.1: Amine coupling of PSG 143
2.17.1.2: Analysis of pentraxin binding 143
2.17.2: Desthiobiotin attachment for regenerable surface 144
2.17.2.1: Amine coupling of desthiobiotin 144
2.17.2.2: Analysis of PSG binding to captured CRP-biotin 145
2.17.2.3: Analysis of CRP binding to captured PSG 145
2.17.2.4: Indirect assay of CRP binding 146
2.18: Surface plasmon resonance analysis of pentraxin interaction with LPG 147
2.18.1: Aldehyde coupling of PSG 147
2.18.2: Hydrophobic attachment to alkyl surface 148
2.18.3: Analysis of pentraxin binding 148
2.19: Statistical analysis 149
CHAPTER 3: Results 150
3.1: Material generation, purification and quantification 150
3.1.1: Generation of Generation of the CRP ligand PCBSA 150
3.1.2: Purification of SAP ligand PEC 153
3.1.3: Purification of PSG 155
3.1.4: Purification of CRP and SAP from serum 158
3.1.5: Purification of Biotinylated of CRP and SAP 161
3.1.6: Serum depletion of SAP and CRP by affinity chromatography 163
3.1.7: Depletion of CRP from serum using Magnetic beads 166
3.1.8: Quantification of LPG using carbohydrate assay was more accurate than weight estimation of lyophilised LPG 168

3.1.9: PSG is a heterogeneous material (fPPG and ScAP) 170
3.2: Characterisation of CRP binding to *Leishmania* PSG 173
3.2.1: Binding of CRP to PSG is affected by the PC binding site 173
3.2.2: CRP binding to PSG is calcium-dependent and magnesium-independent 175
3.2.3: PSG from different *Leishmania* species have widely varying CRP binding capacities 179
3.2.4: CRP binding to PSG is not dependent on LPG 184
3.2.5: Secreted acid phosphatase is responsible for the majority of CRP binding capacity in *L.mexicana* PSG 189
3.3: Investigation of complement activation potential by CRP-PSG complex 192
3.3.1 PSG-CRP complex is capable of binding C1q 192
3.3.2: PSG-CRP complex activates to classical complement pathway to generate C3 convertase 197
3.3.3: PSG-CRP complex classical pathway activation is not due to LPG contamination 203
3.4: Investigation of potential PSG interaction with the Lectin Pathway of complement activation 205
3.4.1: PSG is capable of binding to Mannose Binding Lectin 205
3.4.2: MBL binding of PSG appears to be independent to the presence of Ca^{2+} 208
3.5: Investigating interaction of SAP with *Leishmania* PSG 210
3.5.1: PSG from different *Leishmania* species have varying SAP binding capacities 210
3.5.2: fPPG has a higher SAP binding capacity than ScAP for a given quantity of material 214
3.6: Characterisation of LPG interactions with CRP 217
3.6.1: *Leishmania* promastigotes produce LPG of different sizes at different life cycle stages 217

3.6.2: Metacyclic LPG has greater CRP binding capacity than nectomonad stage LPG 219
3.6.3: CRP binds Metacyclic and Nectomonad stage LPG in a Ca^{2+} dependent manner 223
3.6.4: CRP binds to LPG via the PC binding site 225
3.7: Characterising SAP binding to different stages of LPG expressed by different *Leishmania* promastigote stages 227
3.7.1: Nectomonad LPG possesses greater SAP binding capacity than metacyclic LPG 227
3.7.2: CRP binds Metacyclic and Nectomonad stage LPG in a Ca^{2+} dependent manner 230
3.8: CRP inhibits SAP binding to PSG at high concentrations 232
3.9: Investigation of the ability of LPG to activate the classical complement pathway in complex with different pentraxins 235
3.9.1: CRP-LPG complex is capable of binding the classical complement pathway initiator molecule C1q 235
3.9.2: SAP-LPG complex is unable to activate the classical complement pathway 237
3.10: The influence of CRP in the adherence of different *Leishmania* promastigote stages to PSG 239
3.10.1: Biotinylated *L.mexicana* WT PSG maintains CRP binding capacity 239
3.10.2: CRP increases LPG-PSG complex formation to a greater extent in metacyclic-stage LPG 242
3.11: Investigating CRP-PSG binding kinetics using Surface plasmon resonance techniques 244
3.11.1: Initial attempts at immobilisation of PSG ligand 244
3.11.2: Immobilised CRP binds avidly to *L.mexicana* PSG 246

3.11.3: PSG-biotin immobilised exhibits high avidity to CRP analyte 249
3.11.4: Surface plasmon resonance: Comparison of CRP binding kinetics between different *Leishmania* species 251
3.11.5: PSG binding to CRP is based on multiple low-affinity binding events 259
3.11.6: CRP binding to immobilised PSG is affected by ligand capture method and heterogenous composition 261
3.12: Investigating pentraxin binding to LPG using surface plasmon resonance techniques 268
3.12.1: Early LPG ligand Immobilisation strategies 268
3.12.2: Metacyclic-stage LPG exhibits higher CRP binding avidity than Nectomonad LPG at higher ligand densities 269
3.12.3: CRP analyte association with *L.mexicana* metacyclic LPG ligand is not influenced by mass transport effect 282
CHAPTER 4: Discussion 285
4.1: Preface 285
4.2: Pentraxin purification and modification 285
4.2.1: Pentraxin purification 285
4.2.2: Biotinylation of SAP 286
4.2.3: Conclusions 289
4.3: Composition of PSG 290
4.3.1: PSG derived from promastigote culture supernatant 290
4.3.2: Corroboration of PSG purified in-house with previous work 290
4.3.3: Individual characterisation of PSG components 291
4.3.4: Conclusions 292
4.4: PSG Binding to pentraxins 293
4.4.1: Binding affinity and capacity of PSG to pentraxins 293
4.4.2: LPG is not a major CRP binding component in PSG 294

4.4.3: Individual pentraxin binding characteristics of the PSG components fPPG and ScAP 294
4.5: PSG-driven complement activation 296
4.5.1: Classical Pathway activation by CRP-PSG complex 296
4.5.2: Lectin pathway activation via MBL-binding 296
4.5.3: *Leishmania* survival and complement 297
4.5.4: ScAP and intracellular nutrition 299
4.5.5: Conclusions 300
4.6: Characterisation of pentraxin binding to *L.mexicana* LPG 302
4.6.1: CRP binding to LPG 302
4.6.2: LPG binding to SAP 303
4.6.3: CRP and SAP binding sites on LPG 304
4.6.4: Conclusions 305
4.7: Surface Binding Resonance 307
4.7.1: Binding kinetics 307
4.7.2: PSG orientation and ligand availability 307
4.8: LPG-PSG interaction 309
4.8.1: LPG and PSG in the arthropod digestive tract 309
4.8.2: LPG and PSG in the mammalian host 310
4.9: Role of Serum Amyloid P (SAP) in innate immunity 311
4.10: The lectin pathway in *Leishmania*-mediated complement activation 312
4.11: Phosphorylcholine containing molecules: The search for an immunomodulatory small molecule derivative 313
4.12: Summary 316
References 323

Figures

Figure 1 Diagram of the acute phase response, including activation stimuli and downstream effects 33

Figure 2 Comparison of properties of the classical pentraxins CRP and SAP 39

Figure 3 The physiological structure of human C-reactive protein and its complex with phosphocholine 44

Figure 4 GRASP representation of the 'A' face of the CRP protomer and charge profile surrounding the PC-binding cleft 48

Figure 5 Flow diagram of the complement cascade in in relation to the three activation pathways 60

Figure 6 Structural comparison of C1q with MBL and ficolin oligomers, and the location of associated serine proteases 65

Figure 7 Illustration of the life cycle of *Leishmania* species parasites within human and sandfly hosts 70

Figure 8 Differential expression of cell membrane surface markers between promastigote and amastigote stage *Leishmania* 89

Figure 9 Stage and species dependent side-chain modifications in *Leishmania* LPG 92

Figure 10 Image of *L.mexicana* PSG three-dimensional structure using Scanning Electron Microscopy (SEM) 95

Figure 11 Location of PSG obstruction in *Leishmania* infected sandflies digestive tract 97

Figure 12 Regurgitation Model of *Leishmania* Infection 99

Figure 13 Microscopy of *L.mexicana* promastigotes from infected *Lutzomiya longipalpis* midguts, with additional phase contrast illumination 102

Figure 14 Comparison of O and N-linked glycosylation in *L.mexicana* ... 104

Figure 15 Imaging of *L.mexicana* ScAP ... 106

Figure 16 PC-BSA conjugation produces two ligands of different molecular weights ... 151

Figure 17 Protein gel staining and ligand blot analysis of PCBSA ... 152

Figure 18 Quantification of PEC using Phenol-H_2SO_4 assay ... 154

Figure 19 Anion Exchange chromatography of PSG ... 156

Figure 20 Hydrophobic Interaction chromatography of PSG ... 157

Figure 21 Purification of CRP by sequential calcium-dependent PC-sepharose affinity chromatography and anion exchange chromatography ... 159

Figure 22 Purification of SAP by sequential calcium-dependent PE-sepharose chromatography and anion exchange chromatography ... 160

Figure 23 Western blot analysis of biotinylated CRP and SAP ... 162

Figure 24 Standard curve generated using CRP-standardised serum and table of serum CRP concentrations before and after affinity chromatography depletion ... 164

Figure 25 Standard curve generated using SAP-standardised serum and table of serum SAP concentrations before and after affinity chromatography depletion ... 165

Figure 26 M-bead depletion of CRP in serum shows significant reduced complement activation ... 167

Figure 27 Quantification of LPG via carbohydrate assay against a mannose standard ... 169

Figure 28 LT6 binding *L.mexicana* PSG from culture supernatants ... 171

Figure 29 LT6 binding to native *L.mexicana* PSG ... 172

Figure 30 PC inhibits CRP binding of PSG ... 174

Figure 31 PSG binding to CRP is dependent on calcium and independent of magnesium 176

Figure 32 CRP binding to WT PSG is dose and Ca^{2+} dependent 177

Figure 33 CRP binding of PSG from different species is also a calcium-dependent interaction 178

Figure 34 PSG from different *Leishmania* species exhibit widely varying CRP binding capacities 180

Figure 35 Different *Leishmania* species produce varying levels of CRP binding components 181

Figure 36 Different *Leishmania* species produce high-molecular weight PSG components that bind to CRP 182

Figure 37 PC inhibits CRP binding of PSG in multiple species 183

Figure 38 CRP binding of PSG is independent of LPG 186

Figure 39 CRP binding to PSG is not dependent on LPG 187

Figure 40 CRP binding to PSG is not dependent on LPG and corresponds to PG synthesis in *Leishmania* PSG 188

Figure 41 ScAP provides the majority of CRP binding capacity in PSG 190

Figure 42 ScAP provides the majority of CRP binding capacity in PSG 191

Figure 43 PSG-CRP complexes are capable of binding to C1q 193

Figure 44 C1q binding of PSG-CRP complex is Ca^{2+} dependent 195

Figure 45 PC inhibits C1q binding of *L.aethiopica* PSG-CRP complex 196

Figure 46 Complement activation by *L.mexicana* PSG is time sensitive 198

Figure 47 *L.mexicana* PSG activates the classical complement pathway and is increased by CRP binding 199

Figure 48 PSG activates complement primarily via the classical pathway 200

Figure 49 PSG and PCBSA activates classical complement pathway activation via CRP 202

Figure 50 PSG causes a statistically significant increase in classical complement activation as measured by C3d deposition 204

Figure 51 PSG from different *Leishmania* species exhibit widely varying MBL binding capacities 206

Figure 52 MBL binding of PSG is not entirely calcium-dependent 209

Figure 53 PSG from different *Leishmania* species exhibit widely varying SAP binding capacity and is dependent on serum components; SAP binds to different PSG component than CRP 211

Figure 54 SAP binds to different components in PSG compared to CRP 213

Figure 55 SAP binding of PSG is not LPG dependent 215

Figure 56 fPPG provides the majority of SAP binding capacity in PSG 216

Figure 57 Promastigote stages produce LPG of different molecular weight 218

Figure 58 Metacyclic LPG has a higher CRP binding capacity than nectomonad LPG 220

Figure 59 Metacyclic LPG has a higher CRP binding capacity than nectomonad LPG 221

Figure 60 CRP binding to purified *L.mexicana* LPG 222

Figure 61 CRP binding to LPG is dependent on calcium and independent of magnesium 224

Figure 62 CRP binds to the phosphorylated disaccharide repeats on LPG 226

Figure 63 Nectomonad LPG has a higher SAP binding capacity than Metacyclic LPG 228

Figure 64 SAP-biotin binding to purified *L.mexicana* LPG 229

Figure 65 SAP binding to LPG is dependent on Ca^{2+} and independent of Mg^{2+} 231

Figure 66 SAP does not inhibit CRP binding to LPG 233

Figure 67 CRP inhibits SAP binding to LPG 234

Figure 68 CRP-LPG complexes are capable of binding to the classical complement pathway initiator C1q 236

Figure 69 SAP-LPG complexes are not capable of binding to the classical complement pathway initiator C1q 238

Figure 70 Biotinylation of PSG does not affect CRP binding capacity 241

Figure 71 CRP can act as bridge between LPG and PSG 243

Figure 72 *L.mexicana* WT PSG exhibits strong interaction with CRP 247

Figure 73 ScAP is a major component of PSG binding to CRP 248

Figure 74 CRP binding to *L.mexicana* PSG biotin immobilised onto neutravidin surface, with residual analysis of dissociation 250

Figure 75 *L.mexicana* WT PSG exhibits binding avidity to immobilised CRP-biotin 253

Figure 76 *L.donovani* PSG exhibits binding avidity to immobilised CRP-biotin 253

Figure 77 *L.panamensis* PSG exhibits binding avidity to immobilised CRP-biotin 254

Figure 78 *L.aethiopica* PSG exhibits binding avidity to immobilised CRP-biotin 255

Figure 79 *L.major* PSG binding to CRP-biotin insufficient to calculate binding kinetics 257

Figure 80 *L.tropica* and *L.amazonensis* PSG exhibit poor CRP binding avidity 258

Figure 81 *L.mexicana* WT PSG association rate to CRP-biotin is reduced at high flow rates 260

Figure 82 *L.mexicana* WT PSG captured on CRP-biotin exhibits greater CRP binding capacity compared to directly immobilised PSG 263

Figure 83 CRP-biotin captured *L.mexicana* PSG exhibits increased binding sites for CRP 263

Figure 84 CRP-biotin captured *L.panamensis* PSG exhibits increased binding sites for CRP 265

Figure 85 CRP-biotin captured *L.donovani* PSG exhibits increased binding sites for CRP 266

Figure 86 CRP exhibits similar binding avidity to metacyclic LPG at low ligand densities 270

Figure 87 CRP exhibits similar binding avidity to nectomonad LPG at low ligand densities 271

Figure 88 CRP binding to *L.mexicana* metacyclic LPG immobilised at high density exhibits changes in kinetics at higher CRP concentrations, with residual analysis of dissociation 272

Figure 89 CRP at higher concentrations shows changes in kinetics of binding to nectomonad LPG from *L.mexicana* immobilised at high ligand density, with residual analysis of association 274

Figure 90 CRP exhibits no change in kinetics of binding to PCBSA, with residual analysis of association 277

Figure 91 CRP exhibits no change in kinetics of binding to ES-62, with residual analysis of association 280

Figure 92 CRP analyte association rate to *L.mexicana* metacyclic LPG ligand is not mass transfer dependent 283

Figure 93 CRP analyte association rate to *L.mexicana* nectomonad LPG ligand is not mass transfer dependent 284

Figure 94 Ligand binding site structure for CRP and SAP 288

Figure 95 Model of proposed PSG innate immune manipulation and how it may promote *Leishmania* survival and persistence 299

Figure 96 Proposed mechanism of CP inactivation by the *Acanthocheilonema viteae* CRP-ligand ES-62, compared to complement activation by conventional CRP ligands 314

Figure 1 Summary of the initial research topics, the conclusions drawn and their potential, wider impact/relevance to the field 322

Tables

Table 1 Table of C-Reactive Protein Receptors according with their associated function and location 51

Table 2 Table of human and rodent ficolins according to site of expression, ligand specificity and target pathogens 66

Table 3 Table of kinetic values for SPR of CRP analyte binding to ligand WT *L.mexicana* PSG captured on CRP-biotin 264

Table 4 Table of kinetic values for SPR of CRP analyte binding to ligand *L.mexicana* metacyclic LPG immobilised by hydrophobic attachment 273

Table 5 Table of kinetic values for SPR of CRP analyte binding to ligand *L.mexicana* Nectomonad LPG immobilised by hydrophobic attachment 275

Table 1 Table of kinetic values for SPR of CRP analyte binding to ligand PCBSA immobilised by amine coupling 278

Table 7 Table of kinetic values for SPR of CRP analyte binding to ligand ES-62 281

Table 8 Table of CRP binding interaction to PSG in different *Leishmania* species observed with various experimental techniques in the course of this study 317

Abbreviations

AAM	Alternatively activated macrophage
AMG	Anterior midgut
AP	Alternative pathway of complement
APP	Acute phase protein
Asn	Asparagine
Asp	Aspartate
BCIP	5-bromo-4-chloro-3-idonyl phosphate
BSA	Bovine Serum Albumin
C1q, C3d etc.	Complement components
C/EFB	CCAAT-enhancer-binding protein
CAM	Classically activated macrophage
CBS	Calcium-binding site
CCAAT motif	Cytosine-cytosine-adenosine-adenosine-thymidine box
CCL	C-C motif chemokine ligand
CD80, CD86 etc.	Clusters of differentiation
CP	Classical pathway of complement
CRD	Carbohydrate recognition domain
CRP	C-reactive protein
CL	Collectin
CPHPC	(2R)-1-[6-[(2R)-2-Carboxypyrrolidin-1-yl]-6 oxohexanoyl]pyrrolidine-2-carboxylic acid
CR1, CR3 etc.	Complement receptors

CRD	C-type carbohydrate recognition domain
CtL	Cutaneous leishmaniasis
CTLA-4	Cytotoxic T-lymphocyte associated protein 4
CV	Cibarial valve
CWPS	Cell wall polysaccharide
DAG	Diacylglycerol
DC	Dendritic cell
DCtL	Diffuse cutaneous leishmaniasis
DC-SIGN	Dendritic Cell-Specific Intercellular adhesion molecule-3-Grabbing Non-integrin
DNA	Deoxyribonucleic acid
DESPIAD	Depletion of Serum amyloid P component In Alzheimer's Disease
dH_2O	Distilled water
DMSO	Dimethyl Sulfoxide (DMSO
DTH	Delayed-type hypersensitivity
EDC	N-(3-Dimethylaminopropyl)-N′-ethylcarbodiimide
EDTA	Ethydiaminetetra-acetic acid
EGTA	Ethylene glycol tetra-acetic acid
ELISA	Enzyme-linked immunosorbent assay
$Fc_\gamma RI$, $Fc_\gamma RII$ etc.	IgG FC receptors
Fc	Fragment crystallisable region
FC	Flow cell
FDA	Food and Drug Administration (United States of America)
FG	Foregut
fMLP	*N*-formyl-methionine-leucine-phenylalanine

fPPG	Filamentous proteophosphoglycan
Gal	Galactose
GalNAc	N-acetylgalactosamine
Glc	Glucose
Glu	Glutamate
GP63	Glycoprotein 63
GPI	Glycosylphosphatidylinositol
GSL	glycosphingolipid
HBS	HEPES-buffered Saline
HEPES	4-(2-hydroxyethyl)-1-piperazineethanesulfonic acid
HG	Hindgut
His	Histidine
HIV	Human Immunodeficiency Virus
HRP	Horseradish peroxidase
Hs-CRP	Highly sensitive C reactive protein assay
IFN-γ	Interferon-γ
IgG, IgM etc.	Immunoglobulin classes
IL-8, IL-13 etc.	Interleukins
iNOS	Inducible nitric oxide synthase
IR	Infrared
ITAM	Immunoreceptor tyrosine-based activation motif
ITIM	Immunoreceptor tyrosine-based inhibitory motifs
k_a	Association Rate Constant
K_A	Association Constant
k_d	Dissociation Rate Constant

K_D	Dissociation Constant
kDa	Kilodalton
KLR	Killer cell C-type lectin receptor
LAIR-1	Leukocyte-associated immunoglobulin-like receptor 1
LDL	Low density lipoprotein
LOX-1	Lectin-like oxidized low density lipoprotein receptor-1
LP	Lectin pathway of complement
LPG	Lipophosphoglycan
LPS	Lipopolysaccharide
Lys	Lysine
m	Minutes
M1, M2 etc.	Macrophages
Man	Mannose
MAPK	Mitogen activating protein kinase
MASP	Mannose-Associated Serine Protease
MBL	Mannose binding lectin
mCRP	Monomeric C reactive protein
ML	Mucocutaneous leishmaniasis
MOβDG	Methyl 4,6-0-(1-carboxyethylidene)-β-D galactopyranoside
mRNA	Messenger RNA
NBT	Nitro blue tetrazolium
NIR	Near-infrared
NHS	N-hydroxysuccinimide
NK	Natural killer cells
nor-NOHA	N^{ω}-hydroxy-nor-Arginine

OD	Optical density
PAGE	Polyacrylamide gel electrophoresis
PAMP	Pathogen associated molecular pattern
PBMC	Peripheral blood mononuclear cell
PBS	Phosphate-buffered saline
PC	Phosphorylcholine
PCBSA	Phosphorylcholine-conjugated bovine serum albumin
pCRP	Polymeric C reactive protein
PE	Phosphoethanolamine
PEC	Phosphorylethanolamine cellulose
PG	Phosphoglycan
PKC	Protein kinase C
PKDL	Post Kala-Azar dermal leishmaniasis
PKT	Tyrosine protein kinase
PMN	Polymorphonuclear leukocytes
PO_4	Phosphate
PPG	Proteophosphoglycan
PRR	Pattern recognition receptors
PS	Phosphatidylserine
PSG	Promastigote secretory gel
PTX3	Pentraxin 3
PVDF	Polyvinylidene fluoride
RNA	Ribonucleic acid
R_{eq}	Response Units at equilibrium
RI	Response units detected at beginning of analysis

R_{max}	Maximum observed response units
R_{obs}	Observed rate constant
RU	Response units
s	Seconds
SAA	Serum amyloid A
SAP	Serum Amyloid P
ScAP	Secreted acid phosphatase
SD	Standard deviation
SDS	Sodium dodecyl sulphate
SEM	Scanning electron microscopy
Ser	Serine
SG	Salivary Glands
SLE	Systemic lupus erythematosus
SpA	Surface Protein A
sPLA2	Secreted phospholipase A2
SPR	Surface plasmon resonance
SPS	Sodium polyanethole sulphonate
SV	Stomodeal valve
Spp.	Species
TEMED	N,N,N′,N′-Tetramethylethylenediamine
Th1, 2 etc.	Helper T-cells
TLR	Toll-like receptor
T_{reg}	Regulatory T-cells
TBS	Tris-buffered saline
TCM	Central memory T-cell

TEM	Effector memory T-cell
TCR	T-cell receptor
TGFβ	Tumour growth factor β
TMB	3,3',5,5'-Tetramethylbenzidine
TMG:	Tegmental midgut
Tris	2-Amino-2-(hydroxymethyl) propane-1,3-diol
TNF-α	Tumour necrosis factor α
Tyr	Tyrosine
VBS	Veronal-buffered saline
VL	Visceral leishmaniasis
VLDL	Very low-density lipoprotein
WT	Wild type

Chapter 1
Introduction

1.1: The Innate Immune Response

1.1.1: Innate Immunity

Innate immunity is the first-line defence against antigenic and pathogenic challenges. It is characterised by rapid deployment/response and a lack of memory formation, with subsequent insult from the same pathogen not eliciting a stronger response or resulting in quicker clearance and/or resolution (Dunkelberger and Song, 2010). Innate immunity is associated with a number of protein mediators and mechanisms, with outcomes including opsonisation of pathogens, direct killing and triggering local inflammatory responses in the wound site.

Innate immunity is mediated by a number of cell populations, including polymorphonuclear cells (PMNs: neutrophils, basophils and eosinophils), mast cells, monocytes, macrophages, dendritic cells and lymphocytes species with limited receptor variation (e.g. Natural Killer Cells, B1 lymphocytes, γδ T-cells). Epithelial and endothelial cells, in addition to providing a physical barrier to potential infection or injurious challenge and secreting antimicrobial factors (e.g. defensins, mucins, surface protein A), play a crucial role in early chemokine signalling and determination of the local immune environment. Mast cell and tissue resident macrophages play a key role in the initial stages of innate immunity through antimicrobial action and chemokine release; it is the rapid generation of the chemokine gradient (e.g. IL-8, CCL2) that signals innate immune cells (e.g. PMNs, monocytes) in the circulation to migrate (i.e. chemotaxis) to the relevant site. Recognition of pathogen associated molecular patterns (PAMPs) by cell surface pattern recognition receptors (PRRs) on both

resident and recently migrated immune cells determines the cellular responses triggered, ranging from further cytokine release to modulate the local immune environment (e.g. Th1 vs Th2 typing), the secretion of antimicrobial factors (e.g. Neutrophil Extracellular Traps) and phagocytosis.

There are non-cellular immune components involved in innate immunity as well. The complement system consists of a series of zymogens which, when activated, mediate a number of immune-relevant actions, including inflammation, opsonisation and the formation of antimicrobial complexes. Acute phase proteins (APPs) such as C-reactive protein (CRP) and serum amyloid A (SAA) contribute to innate immunity through a variety of actions (Section 1.1.2). The pentraxin serum amyloid P component (SAP) is a constitutively expressed protein, which has been reported to have a number of immune relevant functions.

Modulation of the inflammatory response is required in order to prevent pathology and disease manifestation. A number of immuno-modulatory mechanisms exist in order to prevent pathology from the excess inflammation and/or immune dysregulation observed in rheumatoid arthritis, systemic lupus erythematosus (SLE) and asthma, as well as the 'cytokine storm' scenario responsible for sepsis (Schulte et al., 2013).

Immune modulation is also a survival strategy used by various parasitic organisms to reduce clearance by the host immune response and increase the likelihood of survival. This ranges from true downregulation of the overall immune response (e.g. triggering a T_{reg}-like response); to altering the immune response to one which is not associated with parasite clearance (e.g. Th1 responses are associated with *Leishmania* clearance in the mammalian host, whereas Th2 response are associated with *Leishmania* survival) (McSorley and Maizels, 2012). The Hygiene Hypothesis postulates that the increase in autoimmune disorders in developed western countries is linked to the reduction in immune system priming by assorted pathogenic organisms during childhood (Okada et al., 2010).

1.1.2: The Acute Phase Proteins

APPs are defined as a group of proteins which are highly upregulated as part of the initial immune response to insult or infection. This increase in serum concentration varies greatly, from 2 to 3-fold increase in some cases to potentially over a thousand-fold in others, such as CRP. As this increase is triggered as part of the inflammatory response, there is a reasonable assumption that certain APPs have a role in the innate immunity against pathogens, or alternatively regulate the immune response in both the local and systemic environments, the remodelling of damaged tissue and/or otherwise bringing the host organism back to a state of pre-challenge homeostasis (Figure 1). The importance of major APPs, such as CRP and SAA can be inferred by the lack of reported deficiencies, suggesting that they essential to the viability of host organism survival.

The acute phase response is associated with and triggered by the cytokines IL-1, IL-6 and TNF-α, and is associated with a number of physiological effects, including pyrexia, somnolence, oedema and changes in hormonal and micronutrient levels (Raynes, 1994). There is evidence that different combinations of acute phase trigger cytokines influence the type and level of APPs in circulation, with most regulation of APP occurring at the level of post-transcriptional modulation of protein synthesis. While APPs have a diverse range of functions, they may be broadly classified as complement components (e.g. C1q, C3, C5 etc.), coagulation proteins (e.g. Fibrinogen, Von Willebrand Factor etc.), protease inhibitors (e.g., α1-antitrypsin), transport or metal binding proteins (e.g. Ferritin), Inflammation Regulating Proteins (e.g. Albumin) and innate immune proteins (e.g. sPLA2, CRP and SAA). The major acute phase proteins undergo the most dramatic increase in serum concentration during inflammatory events. CRP, which is of particular interest to this study, is used as a clinical marker for a patients' inflammatory state, due to the rapidity (exponential decrease in serum concentration 18-20 hours post infection) and fold increase (1000 fold in some bacterial infections) of CRP concentrations in response to inflammation.

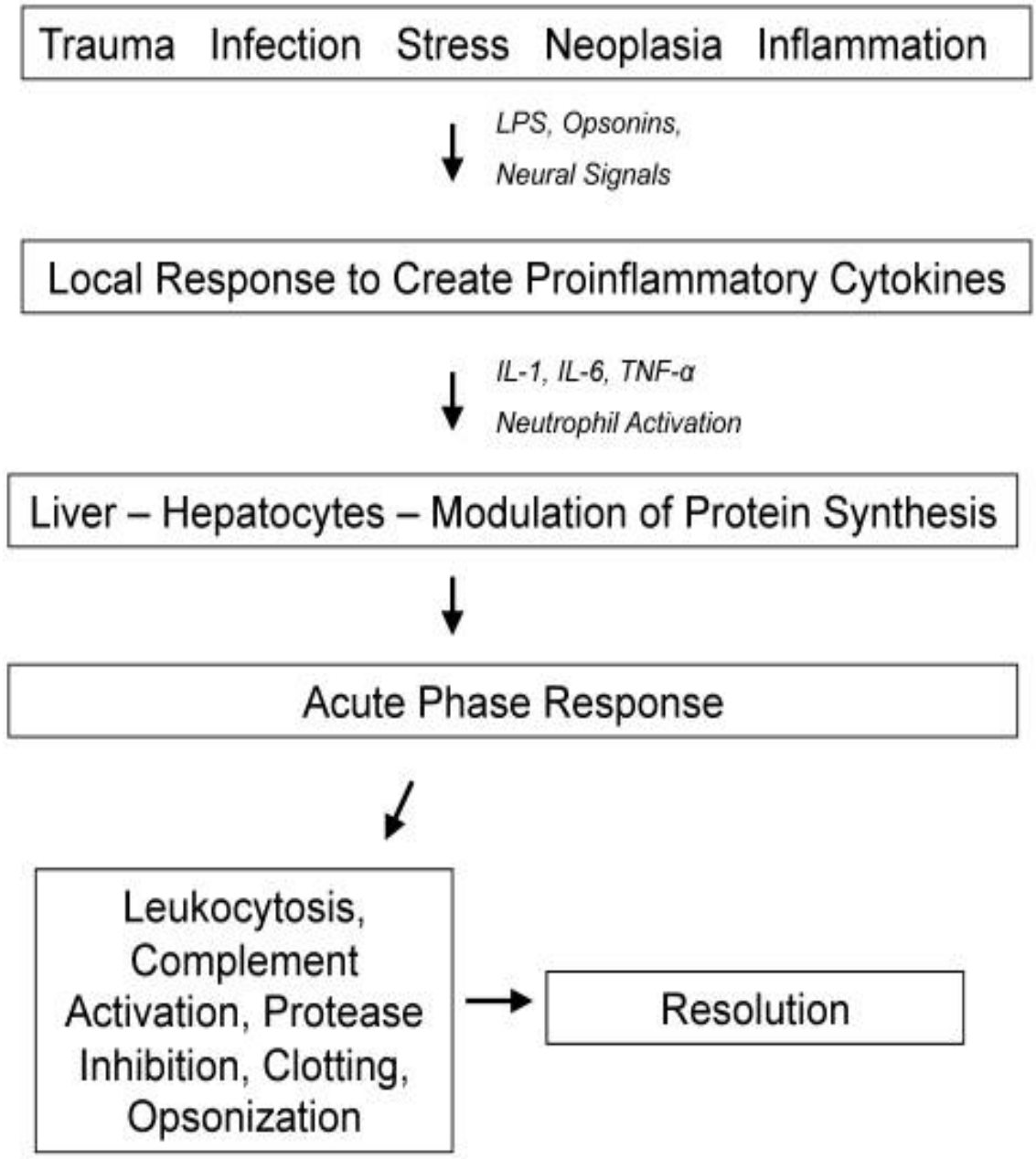

Figure 2: Diagram of the acute phase response, including activation stimuli and downstream effects (Cray et al., 2009).

LPS: Lipopolysaccharide
IL: Interleukin
TNF-α: Tumour Necrosis Factor Alpha

1.1.3: Regulation of the Acute Phase Response

The acute phase response must be, by necessity, tightly regulated in order to prevent it from harming the host organism instead of resolving infection and insult. This is particularly true for cytokines such as TNF-α and IL-1, which have the ability to substantially upregulate to synthesis of other downstream cytokines. Regulatory mechanisms to prevent this exist on multiple levels, including adrenal gland-derived glucocorticoid hormones and IL-10 release by Regulatory T lymphocytes (T_{reg}).

The most dramatic example of a potentially dangerous dysregulation of the acute phase response can be seen in sepsis, during which systemic inflammation triggers a cascade of cytokine releases, resulting in a 'cytokine storm', a potentially fatal condition particularly in the absence of effective clinical intervention. As such, it is unsurprising that many APPs do not contribute to an increase in inflammatory symptoms (e.g. fever, swelling, swelling) and instead act as negative feedback mechanism to prevent a runaway inflammatory response to challenge which may damage the host instead.

1.1.4: Pathogen modulation of host immunity

Many helminths promote an immune-regulatory state in the host in order to avoid elimination by an appropriate inflammatory response. This often results in cases of asymptomatic, chronic infection, associated with high parasite load and arguably the most advantageous state for the parasite organism. Immunopathology is associated with a failure to maintain the regulatory state, and is generally associated with low parasite loads in the host(McSorley and Maizels, 2012).

An example of this spectrum of helminth infection states can be seen in lymphatic filarial nematode infection (e.g. *Brugia malayi* and *Wuchereria Bancrofti*) in long-term exposure populations. The 'endemic normal' proportion of the population are uninfected and are apparently immune to filarial infection. Asymptomatic filarial infection is associated with the suppression of Th1 (e.g. IFN-γ) and some Th2 (e.g. IL-5) cytokines, while the levels of IL-10 (an immune-regulatory cytokine) and CTLA-4 positive (an inhibitory marker) T-cells

increases. Immunopathology in filarial infection takes the form of chronic lymphatic inflammation and elephantiasis, and is associated with low number of T-regulatory (Foxp3+) cells and higher levels of Th1 and Th17 cells, with Th17 type responses being associated with parasite load reduction (Harnett†, 2006).

The immunomodulatory capabilities of helminths have been linked to the hygiene hypothesis, which links the increased incidence of autoimmune disorders, such as rheumatoid arthritis and SLE, in highly developed countries to a decrease in parasitic infection and incidence, leading to a lack in appropriate priming and modification of the immune response. This has led to research of helminth-derived products for their therapeutic potential(Eason et al., 2016, Lumb et al., 2017, Pineda et al., 2014).

ES-62 is a 62kDa, tetrameric, PC-containing molecule with immunomodulatory properties, produced by *Acanthochelionema viteae*, a rodent filarial nematode. ES-62 is a secreted factor, containing phosphorylcholine (PC) moieties attached via a flexible tail to the main component protein structure. The positioning of the PC moiety at the end of a flexible structure is important to its function, as other PC containing molecules without this distinction, such as *Streptococcus pneumoniae* bacterial cell wall polysaccharide (CWPS), which is linked to the cell wall and cytoplasmic membrane of gram-positive bacteria, elicits an immune response (e.g. complement activation) detrimental to the pathogen's survival and persistence. (Hewitson et al., 2009). ES-62 has immunomodulatory effects via its effect on dendritic cells and macrophages by interfering with Toll-like receptor 4 (TLR4) signalling, reducing the synthesis of pro-inflammatory cytokines, such as TNF-α and IL-6, and Th1-polarising cytokines such as IL-12. ES-62 also reduces complement activation and C3 convertase formation following binding to CRP (Ahmed et al., 2016). Lipophosphoglycan (LPG) that coats the *Leishmania* parasite may have a role in regulating the host immune response to promote *Leishmania* infection in the mammalian host. One of the most studied potential actions is LPG's potential effects on macrophages, particularly relevant as macrophages are the chief host cell for *Leishmania* replication. LPG ligation of CR1 or CR3, both of which are expressed on the macrophage surface, does not trigger oxidative burst a key antimicrobial mechanism following phagocytosis (Ueno and Wilson, 2012). In addition, LPG ligation of CR3 appears to inhibit the release of IL-12, a key promoter of cell-

mediated immunity. LPG also appears to inhibit fusion of the endosome and phagosome, which may be due to bilayer stabilisation from LPG insertion. However, recent studies suggest that LPG is not an essential virulence factor for mammalian infection, with LPG-deficient *L.major* mutant promastigotes being able to establish infection in animal models of infection in the same manner as wild type parasite. In addition, *L.mexicana* mutants expressing with LPG deficient in Gal-Man-PO_4 repeats with intact mannose end caps, or deficient in both Gal-Man-PO_4 repeats and downregulated mannose end caps, were capable of macrophage infection and replication in the phagolysosome in the same manner as WT *L.mexicana*, as well as being capable of establishing infection in mice (Ilg, 2000a, Ilg et al., 2001).

1.1.5: Innate Recognition of Carbohydrate epitopes

The adaptive immune response to pathogens is largely based on recognition of peptides and protein moieties, although CD1 presentation of carbohydrate ligands to γδ T-cell receptors (TCR) has been reported (Cobb and Kasper, 2005). Antibodies directed against pathogen glycosylated products, such as *S.pneumoniae* C-polysaccharide may be not be protective in humans, despite appearing to confer protection in animal models (Frasch and Concepcion, 2000).

The innate immune system, on the other hand, has several mechanisms by which glycosylated antigens may be recognised. B1-cells, a subset of B-lymphocytes which have no memory function in response to previous pathogenic challenge and are capable of responding without T-cell activation, produce natural antibodies which may be carbohydrate specific and capable of eliciting of protective response (Hoffman et al., 2016). In addition, Natural Killer (NK) cells also express killer cell C-type lectin receptors (KLRs) on their cell surface which may be attached to both stimulatory or inhibitory intracellular signalling motifs, implying a potential for protective immune responses against carbohydrate ligands (Bartel et al., 2013).

1.2: Pentraxins

Classical, short pentraxins are cyclic, homomeric pentamers consisting of 5 non-covalently linked identical subunits with Ca^{2+} dependent ligand binding characteristics.

Pentraxins are an ancient group of proteins, with C-reactive protein (CRP) in particular being found as far back in the evolutionary timeline as the horseshoe crab, suggesting an important physiological function for them. The classical pentraxins, CRP and Serum Amyloid P (SAP), are well-conserved proteins, with reported polymorphisms in CRP being restricted to non-expressed intron regions, suggesting their importance in viability of complex organisms (Volanakis, 2001). In addition, there has been no recorded deficiency in humans of either pentraxin. It will the classical pentraxins that will be the main focus of investigation in our study.

Aside from the classical, 'short', pentraxins (CRP and SAP), studies have revealed a series of related 'long' pentraxins, such as pentraxin 3 (PTX3), apexin (i.e. P50) and neuronal pentraxin I (NPI), which are much larger than the classical pentraxins but share C-terminus homology with the classical pentraxins. In addition, 'long' pentraxins' do not share the homo-pentameric quaternary protein structure of CRP and SAP (Goodman et al., 1996).

PTX3 is a soluble pattern recognition molecule which exhibits binding specificity to a wide variety of pathogenic ligands, including those found on viruses (e.g. H3N2 *influenza*, *cytomegalovirus*), bacteria (e.g. *Staphylococcus aureus*) and fungi (e.g. *Aspergillus fumigatus*), with binding thought to be mediated by region found on its N-terminal domain. Immune functions ascribed to PTX3 include complement activation, opsonisation and neutralisation. PTX3 synthesis occurs in a number of immune cells following Toll-like Receptor (TLR) activation, including phagocytes, neutrophils and myeloid dendritic cells (Hajishengallis and Russell, 2015, Roy et al., 2017).

The pentraxins C-reactive proteins (CRP) and Serum Amyloid Protein (SAP) share a degree high degree (approximately 51%) of homology and have a number of well-documented immune functions, including opsonisation and activation of the classical complement pathway. Broadly speaking, in regard to

mammalian species, one of these pentraxins would be a major APP, with the other being having expression levels which are relatively unaffected by the host organism's inflammatory state. For humans, CRP is the APP, whereas the opposite is true for mice (i.e. SAP is the APP).

CRP is the quintessential acute phase protein, with serum levels of CRP rapidly experiencing up to a 1000-fold increase (less than 3 µg/ml in healthy individuals, up to 300 µg/ml) in cases of infection and subsequent inflammation. 10000-fold increases have been recorded in clinical trials of IL-6 for cancer treatment, from 0.1 µg/ml to 1 mg/ml following cytokine therapy (Banks et al., 1995). SAP does not exhibit a sharp increase in concentration following infection, but an increase in circulating SAP concentration in infection of murine models is observed. A figure summarising comparison between CRP and SAP is provided (Figure 2).

	C-reactive protein (CRP)	Serum amyloid P (SAP)
Fc receptor binding	Yes	Yes
Calcium-dependent ligand binding	Yes	Yes
Complement activation through C1q	Yes	Yes
Ligands	Phosphocholine snRNP (Sm, RNP) Histones Apoptotic cells Oxidized LDL	Phosphoethanolamine DNA, chromatin Heparin Apoptotic cells Amyloid fibrils
Major synthetic site	Liver	Liver
Inducers	IL-6 (acute phase reactant)	Constitutive
Structure	Cyclic pentamer 115,135 Da Each subunit 23,027 Da 206 amino acids	Cyclic pentamer 127,310 Da Each subunit 25,462 Da 204 amino acids
Glycosylation	No	Yes
Chromosomal location	1q23.2	1q23.2

Figure 3: Comparison of properties of the classical pentraxins CRP and SAP. (Du Clos, 2013)

1.2.1: C-Reactive Protein (CRP)

1.2.1.1: Expression

C-reactive protein is predominantly synthesised in the liver, with regulation occurring at the transcriptional level in response to pro-inflammatory cytokines. In particular, IL-6 appears to have a major role in promoting CRP synthesis by upregulating the transcriptional factors C/EFBβ and C/EFBδ (Black et al., 2004). IL-6 signalling may be enhanced by TNF-α and IL-1β, with co-signalling resulting in increased CRP synthesis (Brooks et al., 2010).

Following initial cytokine signalling, CRP is rapidly upregulated, with protein secretion signalling increase being observable as little as 6-8 hours later, typically peaking between 24-48 hours from initial stimulation. CRP concentrations in circulation are maintained as long as the inflammatory stimulus is present and falling rapidly once this is removed, with CRP having a half-life of approximately 19 hours. It is this rapid response to the absence and presence of inflammatory stimuli which makes it an effective clinical biomarker for a patient's inflammatory state (Ridker, 2003).

Cytokine signalling by visceral adipose tissue has been linked to CRP levels, with hyperleptinemia and hypoadiponectinemia upregulating hepatic synthesis of CRP. These two cytokines are commonly associated with obesity and insulin resistance (Scotece et al., 2012, Puglisi and Fernandez, 2008). Given the role of adipose tissue cytokine signalling, it has been categorised as an endocrine organ, particularly influential the signalling responsible for the chronic inflammation observed in obesity cases, as well as having immunomodulatory effects exerted through the release of cytokines IL-1β, IL-6 and resistin. There are reports that adipocytes may also be an extrahepatic site of CRP production in response to inflammatory cytokines (Singh et al., 2007).

Although the consensus is that the liver is the main site for CRP synthesis, CRP mRNA has been detected in a number of extrahepatic sites, including the lungs, renal cortical tube epithelium, lymphocytes, adipose tissue and atherosclerotic lesions. Studies have suggested that it is the sustained, low levels of local CRP synthesis by coronary smooth muscle cells in response to inflammatory cytokines which may predict increased risk of cardiovascular conditions,

possibly by activating nearby endothelial cells. Of note, independent studies have found a monomeric form of CRP (mCRP) appears in relatively high concentrations in certain extrahepatic compartments, such as smooth muscle cells, adipocytes and atheromatous plaque inflammatory cells, while polymeric CRP is thought to have net anti-inflammatory effects, mCRP has been shown to promote inflammatory activity. This is supported by *in vivo* studies that demonstrates that mCRP has pro-inflammatory effects on striated muscle and atherosclerotic plaque tissue. This effect is seen in both mice (Pepys et al., 2006) and humans (Braig et al., 2017) within infarcted myocardial tissue.

There is no monomeric CRP found in the hepatocyte-derived serum form. Crucially, mCRP is insoluble, making it unlikely that if it were in circulation that it would be able to travel to the tissue sites where it is observed. While this could be due to the clinical assay for CRP in serum (hs-CRP assay) being unable to detect mCRP, either in its conventional or resolubilised form, flow cytometry and immunoassays specific to mCRP have found little evidence of mCRP in circulation.

It is also possible that tissue association of mCRP may be due to factors in the local environment causing subunit dissociation of polymeric CRP. Indeed, this phenomenon has been observed to occur on the membrane surfaces of cells undergoing apoptosis, pathogenic membranes, activated platelets found of atherosclerotic plaques. The presence of exposed phosphatidylcholine, a membrane phospholipid containing a CRP-binding, polar PC head, in both scenarios appears to be a key component of pCRP binding and subsequent dissociation/mCRP generation (Ji et al., 2007). Studies have shown that initial binding of pCRP to membrane surfaces causes an initial conformational change due to hydrophobic insertion, followed by cleavage in intra-subunit disulphide linages by reducing agents such as thioredoxin (Di Napoli et al., 2018). However, other reports have shown that human CRP does not contain any intra-subunit disulphide subunits, although they are present in the CRP of other species, such as rats (de Beer et al., 1982).

There are reports of intermediate forms of mCRP formed with distinct binding affinity and structural characteristics. Initial pCRP subunit dissociation generates $mCRP_m$ which retains similar binding profile to pCRP, as well as a

similar structure to pCRP subunits. Upon dissociation from phosphatidylcholine triggered by complement component binding, $mCRP_m$ (dissociation on membrane) becomes $mCRP_s$ (conversion in solution), as structurally distinct mCRP variant reported to have strong atherogenic properties, including the induction of pathological angiogenesis and the promotion of platelet formation and aggregation (Ji et al., 2007).

CRP (pCRP) when ligand bound binds strongly to Fc-gamma RI and to a lesser extend Fc-gamma RII(Bodman-Smith et al., 2004, Bodman-Smith et al., 2002b). Fc-gamma RII receptors are found on endothelial cells, platelets, macrophages and monocytes, triggering the release of inflammatory mediators.

1.2.1.2: Structure

CRP is formed of 5 identical subunits, each approximately 36 Angstroms in diameter and consisting of 206 amino acid residues with a single internal disulphide bond. The protomers/subunits are arranged into a toroid that is approximately 102 Angstroms in diameter, with the central pore having a diameter of approximately 30 Angstroms. The pentamer is stabilised by non-covalent interactions between amino acid residues 115-123 of one subunit and 40-42 & 197-202 the adjacent subunit. Anti-parallel β-strands, interconnected by loops and opposite the calcium and ligand-binding face, form the core of each subunit (Volanakis, 2001).

Each subunit has two Ca^{2+} binding sites, binding to which causes conformational change in several defined regions of each subunit (Amino acid residues 140-150, 67-72, 85-91, 43-49) which is thought to facilitate ligand binding, forming the ‘recognition’ face of CRP (Volanakis, 2001).

Each subunit also contains a C1q binding site on the opposite, ‘effector’ face of CRP, associated with a cleft formed of carboxyl terminal of an α-helix (residues 168-176) and a loop (residues 177–182) on one end, and the carboxyl and amino terminus of each CRP subunit on the other. It has been reported that this cleft is also responsible for FcγR binding of CRP. A minimum of 2 CRP molecules are required for C1 activation (Gaboriaud et al., 2003).

The Ca^{2+} dependent binding sites of CRP are all arranged on the same face of the ring/toroid structure, allowing for multiple binding interactions between CRP and polymeric, high density ligands, such as *Streptococcus pneumoniae* C-polysaccharide, which is highly expressed as part of the bacteria's cell wall structure (Jiang et al., 1991). CRP binding to the pathogen correlates directly to the number of subunits bound to ligand, with single subunit binding events being far more likely to lead to dissociation of CRP from the pathogen surface compared to when multiple subunits are bound (Figure 3).

CRP is a well-conserved protein, but structural differences between species do exist. For example, rat CRP exhibits glycosylation, as well as an inter-subunit disulphide bond not present in the human variant. CRP derived from *Limulus polyphemus* (horseshoe crab), has been shown to be arranged in a hexameric fashion (Tennent et al., 1993).

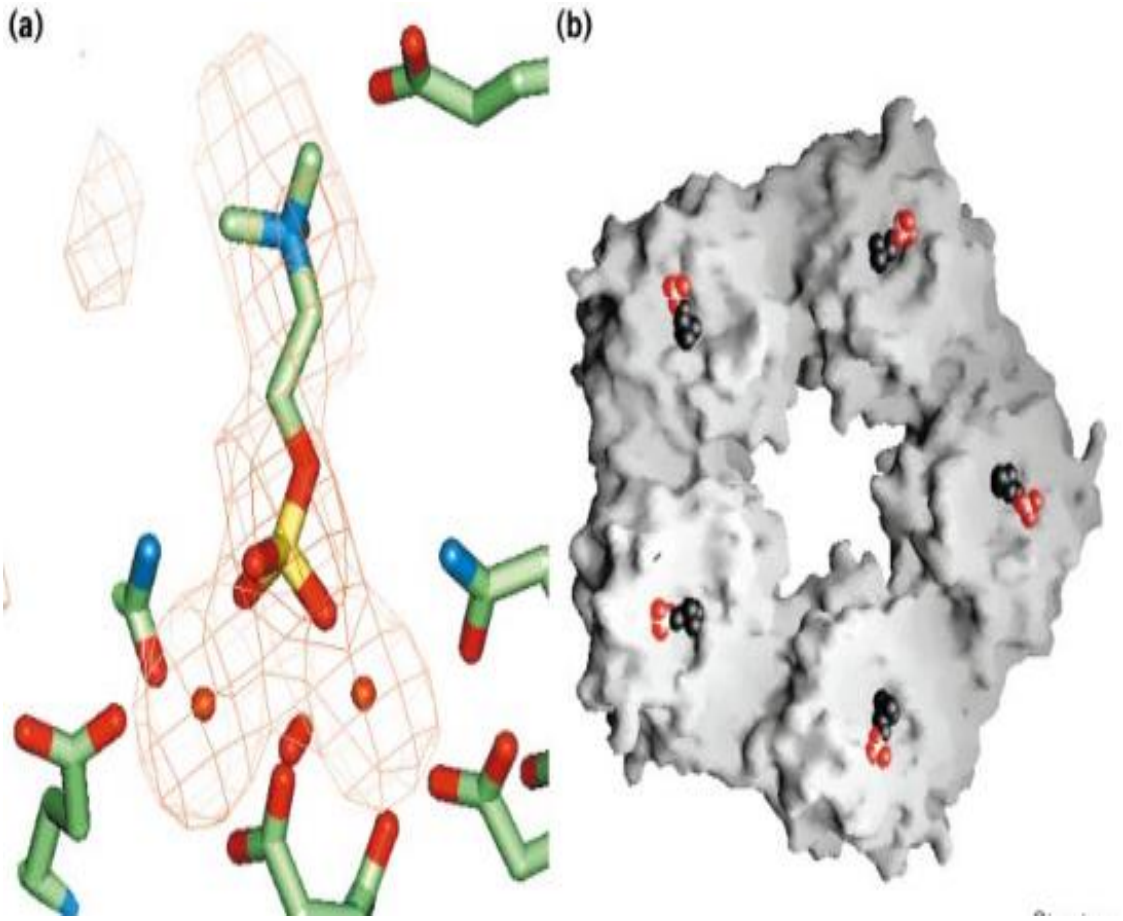

Figure 4: The physiological structure of human C-reactive protein and its complex with phosphocholine (Thompson et al., 1999).

Left (A): Fourier map (2.5 Angstrom resolution), displaying the positions of two Ca^{2+} ions (orange) relative to a phosphocholine molecule in the binding cleft. Right (B): GRASP representation of CRP, displaying the pentameric structure of CRP with PC (black) and Ca^{2+} binding (orange) sites arranged on the same face.

1.2.1.3: Ca^{2+} dependent binding

CRP binds a variety of molecules due to Ca^{2+} dependent binding of PC moieties, a common component in a variety of fungal, bacterial and parasitic products. In this manner, CRP acts as an important innate immune opsonin for complement activation via C1q and classical complement pathway activation. In addition, CRP's affinity to PC could contribute to a role in apoptotic cell clearance, due to cell membrane phosphatidylcholine, as well as the membrane lipid components sphingomyelin and lecithin, all of which contain PC, being exposed during cell membrane damage and disruption (Biro et al., 2007, Du Clos, 2013, Thompson et al., 1999, Tsujimoto M, 1983). The PC binding site on each CRP subunit is located on the lateral face, with prior calcium binding to hydrophobic pockets being necessary for ligand binding site availability, which in turn induces the conformational change required for binding to C1q and activation of the classical complement pathway.

Since the observation of CRP binding to C-polysaccharide, it has been common consensus thought that PC is the main ligand for CRP calcium-dependent binding. PC is found common occurring in many organisms, being expressed in microbial pathogen cell membranes as part of phosphatidylcholine in a similar manner previously discussed in human cell membranes. PC-containing molecules are produced and associated with a range of different microorganisms and cellular structures. In particular, many filarial nematodes (e.g. *Brugia malayi* and *Wucheria bancrofti*) have a number of secreted products with heavy PC substitution in its structure. The most widely studied of these PC ligands is ES-62, a tetrameric glycoprotein secreted by the murine filarial nematode *Acanthocheilonema viteae* that is being investigated for its immunomodulatory and anti-inflammatory properties. The potential of ES-62 for the control of clinical inflammatory conditions has led to increased interest and research in other PC containing filarial and artificial products for therapeutic value(Harnett and Harnett, 2006, Lumb et al., 2017, Pineda et al., 2014).

There have been reports that monomeric CRP (mCRP) binds to low density lipoprotein (LDL), as well as very low-density lipoprotein (VLDL) to a lesser extent. Native state pentameric CRP (pCRP) has also been show to exhibit LDL-binding properties following modifications to make LDL more immunogenic, likely linked to structural modifications that increased exposure of PC epitopes,

such as oxidation (LDL-ox), hydrolytic enzymatic modification (E-LDL) and minimal modification with phosphatidylcholine residues (mmLDL). Separate studies have demonstrated the presence of aldehyde-PC modifications in two of these modified LDL species (LDL-ox and mmLDL) (Itabe et al., 2003). The binding of pCRP to LDL-ox has been shown to lead to opsonisation, macrophage phagocytosis, and enhancing CRP binding to E-LDL, which then go on to form foam cells, a key component in atherosclerotic plaque histology. Aside from promoting the direct phagocytosis of lipoproteins, *in vivo* experiments have demonstrated that CRP stimulates cholesterol accumulation in macrophages. While pCRP binding to LDL-ox appears to have an anti-inflammatory effect, this action is not seen with mCRP, further highlighting the different mechanisms of actions of the two forms of CRP and the importance of determining the isoform present in the relevant environment (Di Napoli et al., 2018).

CRP has been previously reported to bind to and precipitate galactans in a calcium-dependent manner. However, it should be noted that it was the associated phosphate groups present on the bound carbohydrate that was responsible for CRP binding. This may be linked to binding of CRP to *Leishmania* phosphoglycosylated products, which will be discussed later. While an instance of direct carbohydrate binding by CRP has been reported, they have largely taken place at non-physiological conditions (pH 5-6) which likely caused protein denaturation and subunit dissociation. (Kottgen et al., 1992).

1.2.1.4.: Ca^{2+} independent binding

CRP has been shown to be capable of binding some polycationic molecules (e.g. poly L-lysine) in a Ca^{2+} independent manner (Potempa et al., 1981). A separate study also demonstrates that CRP binding to some cations led to depletion of complement components.

Cationic structures that bound to CRP but did not activate the complement system (e.g. human lysozymes, poly-L-ornithine) were found to inhibit CRP-mediated complement component consumption driven by both active polycations and *S.pneumoniae* C-polysaccharide, suggesting that binding sites

Ca^{2+} dependent and independent binding sites on CRP may share regions or at be proximal to each other (Siegel et al., 1975).

CRP binding to polycationic structures may be due to several anionic groups present on the CRP ligand-binding face facilitating charge-based interactions, as opposed to the high-specificity ligand-receptor interaction such as that between CRP and PC (Siegel et al., 1975). This may also account for observed CRP binding to other highly cationic, autologous molecules such as histones and ribonucleoproteins. The potential for CRP to be bound in such disparate fashion necessitates careful observation of any novel binding observation to ensure proper classification and characterisation (Figure 4) .

Non-specific adherence of CRP to polystyrene plate surfaces, such as those used for ELISA experiments, has been reported to lead to denaturation of CRP, leading to an increase in non-specific interactions of the altered CRP (termed neo-CRP) to ligands. (Potempa et al., 1987). It is likely that this phenomenon is responsible for reports of binding of surface-attached CRP to Factor H in a manner that is not inhibited by EDTA (i.e. Ca^{2+} independent) (Mold et al., 1999). A separate study indicates that this interaction is observed in mCRP but not pCRP. suggesting another potential interaction between CRP and the complement system apart from Classical Pathway (CP) activation following ligand binding with a reported anti-inflammatory effect (Molins et al., 2016)

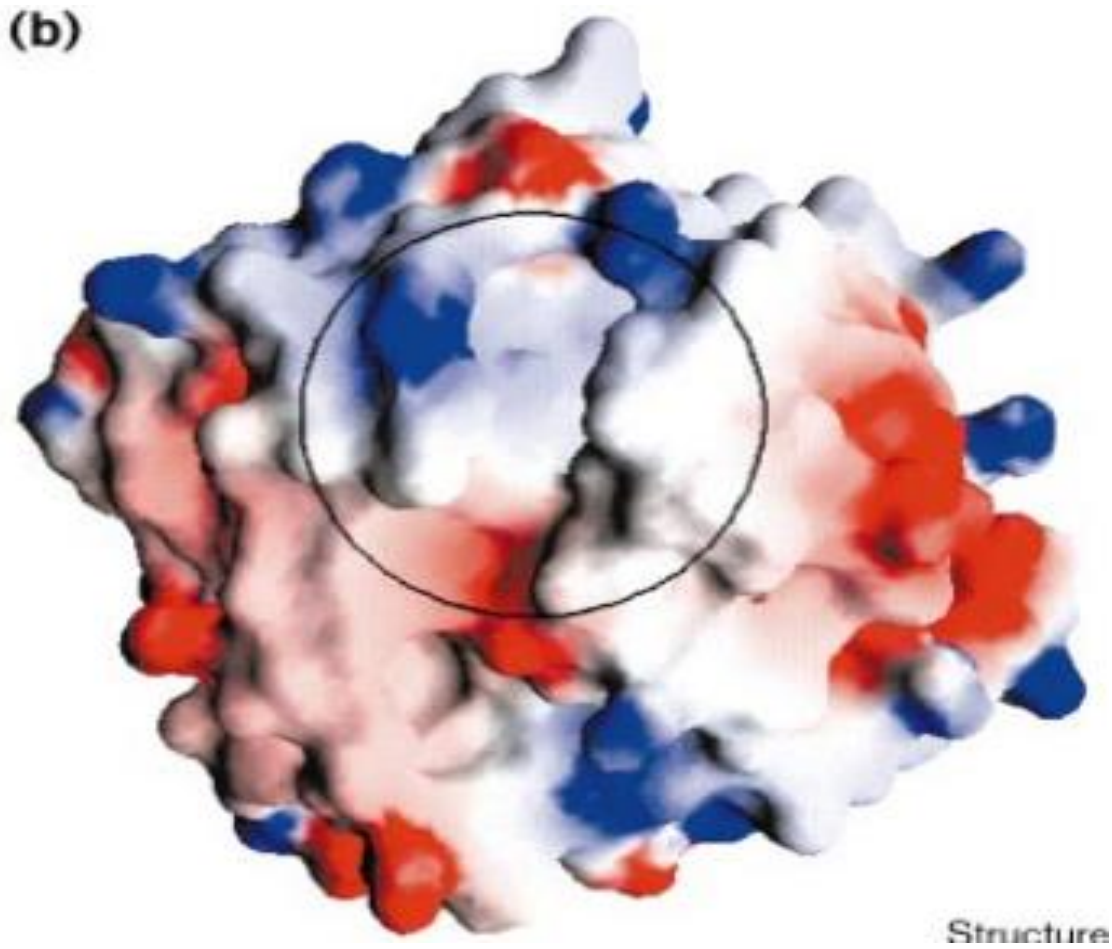

Figure 5: GRASP representation of the 'A' face of the CRP protomer and charge profile surrounding the PC-binding cleft (circled) (Thompson et al., 1999).

Blue: Positive charge
Red: Negative charge

1.2.1.5: Interactions with Complement

CRP has been shown to be capable of being an initiator molecule for complement activation via the classical pathway (CP), originally observed by the depletion of classical complement components by ligand-bound CRP. There is evidence that conformational change to CRP during a ligation event triggers CP activation. This has been observed in ligand-bound CRP, and to a lesser extent oligomerised (i.e. Aggregated) CRP. (Agrawal, 2005)

The C1q binding site on each CRP protomer is located in an extended, deep cleft, on the opposite of the PC-binding face. Binding appears dependent on a number of residues within this cleft. Tyr-175, Asp-112 and Glu-88 are essential contact residues for C1q, while Lys-114, His-38 and. Asn-158 on the neighbouring protomer appears to aid binding (Salazar et al., 2014). The interaction between C1q and CRP can be competitively inhibited in a similar manner to that of C1q-IgG, suggesting similar binding mechanisms between the two complement activation candidates to the initiator molecule C1q (Roumenina et al., 2006).

In addition to activating the classical complement pathway, it has been reported that CRP may inhibit the alternative pathway (AP) by interaction with the inhibitory molecule Factor H, inhibiting the formation of C3 convertase. CRP-mediated action on C4BP, a molecule that inhibits both the CP and LP, has been reported, providing a possible negative feedback mechanism by which CRP prevents excessive complement activation (Sjoberg et al., 2009, Sjoberg et al., 2006). While it should be noted that initial reports of this CRP-C4BP binding may be due to CRP denaturation after exposure to acidic conditions (pH 4.5), which has been reported to increase non-specific binding events. However, a separate study has reported the same phenomenon with native CRP using experimental methodology less likely to denature CRP, albeit at lower levels in comparison to modified CRP (Biro et al., 2007).

CRP binding has been shown to increase phagocytosis of opsonised cells by macrophages and neutrophils. Given its ability to activate the CP, it appears likely that this activity is partly due to complement deposition on cell surfaces, particularly on ligand-dense and subsequently highly CRP-coated microbes (e.g. *Pneumococcus* capsule surface).

It has been reported that CRP from rheumatoid arthritis patients have an increased association with complement degradation products (C3d and C4d), suggesting that certain conditions may lead to *in vivo* modifications of CRP that increase complement system interaction (Molenaar et al., 2001).

1.2.1.6: Cell surface CRP receptors

Recognition of both pentameric and monomeric CRP has been reported in the Fcγ receptor family (FcγR) (Table 1). FcγR are found on many immune cell types, such as monocytes, macrophages and PMN cells, with FcγRI having much higher CRP binding affinity than FcγRII/III (Bang et al., 2005). Binding of FcγR is also isoform dependent, suggesting varying cellular and physiological effects depending on the variant of CRP present. FcγR-mediated CRP activity is linked to immunoreceptor tyrosine-based activation motifs (ITAM) or immunoreceptor tyrosine-based inhibitory motifs (ITIM), with *in vitro* pre-treatment with FcγR inhibitors appearing to reduce CRP-mediated action.

CRP binding of ITAM-linked FcγRs causes conformational change of the linked intracellular domains, which then trigger a signalling cascade that then go on to mediate the effects associated with the signalling pathway. This typically begins with the phosphorylation and activation of a Src family tyrosine protein kinase (PKT), which goes to phosphorylate Syk tyrosine kinase, which is then responsible for the activation of multiple signalling molecules, including protein kinase C (PKC) and mitogen activating protein kinase (MAPK), as well as the release of secondary messengers such as diacylglycerol (DAG) and Ca^{2+}. Conversely, CRP binding to ITIM-linked FcγRIIB triggers a cascade that has been characterised by phosphatase activation (e.g. SHIP-1), causing the inhibition of activator signalling pathways, such as those described involving ITAM-linked FcγRs(Salazar et al., 2014).

CRP binding to lectin-like oxidized low density lipoprotein receptor-1 (LOX-1) has been reported, and has been linked to a number of pro-inflammatory effects, including complement activation and smoking-related vascular inflammation. Interestingly, CRP binding of LOX-1 receptors appears to upregulate LOX-1 expression, representing a possible positive feedback mechanism (Shih et al., 2009).

Receptor	Ligands	Location	Function
FcγRI (CD64)	pCRP	Monocytes	Induces release of cytokines
		Macrophages	Mediator of phagocytosis
FcγRIIa (CD32A)	pCRP	Monocytes	Induces release of cytokines
		Macrophages	Induces expression of LPL Mediator of phagocytosis
		Platelets	Inhibits binding of platelets to neutrophils
		PMN	Inhibits expression of CD62L
FcγRIIb (CD32B)	pCRP mCRP	Endothelial cells	Inhibits bradykinin- and insulin-mediated activation of eNOS
FcγRIII (CD16)	mCRP	Monocytes	Induces release of cytokines
		Macrophages	Induces expression of LPL
		Platelets	Promotes binding of neutrophils
		Endothelial cells	Induces synthesis of IL-8 and MCP-1 Induces expression of endothelial adhesion molecules
LOX-1	pCRP	Human aortic endothelial cells (*in vitro* models)	Increases human monocyte adhesion and LDL-ox uptake to endothelial cells

Table 1: Table of C-Reactive Protein Receptors according with their associated function and location. (Salazar et al., 2014)

1.2.2: Serum Amyloid P component (SAP)

1.2.2.1: Expression

SAP, also known as PTX2, is a ‘short’ pentraxins, sharing the characteristic homomeric pentamer structure seen in CRP. SAP is expressed constitutively in humans with little change in expression of serum/circulation concentration (Average 33 µg/ml in women, 43 µg/ml in during acute phase. In mice, however, SAP is an APP, while CRP conversely is not.

SAP is produced in the liver by hepatocytes, with slightly larger protomer subunits than CRP (25,462 Da vs 23,027 Da) resulting in an overall larger ultrastructure (127,310 Da vs 115,135 Da), with subunit consisting of 205 amino acid residues, containing glycosylated domains not seen in CRP (Debeer and Pepys, 1982, Pepys, 2018).

1.2.2.2: Structure

SAP protomers are non-covalently bound into a pentameric ring structure, with the central hole having a diameter of 20 angstroms and a depth of 35 angstroms. Interaction between the SAP is complex, involving the G, I and J strands of one protomer, and strand N and the strands between loops A-B, C-D, G-H and K-L of the adjacent protomer. Most of these interactions have been characterised as hydrogen bonding, salt bridging and hydrophobic group interaction. This pentameric structure and obscuration of many potential proteolytic enzyme binding sites contributes to SAP’s resistance to degradation. This is particularly true in the presence of calcium, which appears to confer resistance to cleavage by a number of proteolytic enzymes, including pronase and α-chymotrypsin (Du Clos, 2013).

The conformation of SAP when *in vivo* was the subject of debate although it is currently thought to be mainly pentameric *in vivo* (Hutchinson et al., 2000, Sorensen et al., 1995). SAP is sometimes observed to form decamers, although dissociation is observed when the pH is reduced to 5.5, suggesting that decameric structure formation is dependent on ionic interactions, possibly between carboxylate and imidazole groups. This is likely due to interactions

between individual SAP molecules. Aggregation can be inhibited by competition binding with PE and MOβDG, suggesting that SAP aggregation is dependent on the ligand/calcium binding site.

Of note, SAP contains carbohydrate modifications not seen in CRP in the form of a single oligosaccharide chain with the following sequence (Pepys et al., 1994):

Galβ4GlcNAcβ2Manα6(Galβ4GlcNAcβ2Manα3)-Manβ4GlcNAcβ4GlcNAc-ol

The oligosaccharide is attached to each protomer via N-glycosylation to Asn-32, in a β-strand located beneath the single a-helix opposite to the ligand and calcium-binding sites. Further analysis revealed that 70% of the oligosaccharide modifications on SAP structures contain two terminal sialic residues, approximately 25% are monosialylated and the remainder are neutral. The levels of sialylation appear to affect the speed of clearance of SAP from circulation in both human and mice models, with asialylated SAP being cleared much more rapidly (Poulsen et al., 2017). This is likely linked to the presence of asialglycoprotein receptors in liver hepatocytes, which have been suggested to have a role in regulating serum glycoprotein levels (Ashwell and Harford, 1982).

1.2.2.3: Ligand Binding and Specificity

SAP was first discovered as an unknown protein during early attempts to purify CRP via affinity chromatography. Unlike CRP, which bound to pneumococcal C-polysaccharide immobilised on agarose beads (i.e. Sepharose), this unknown protein appeared to bind in a calcium-dependent manner to the beads regardless of the ligand immobilised to it, unlike other serum proteins which washed away. Subsequent control experiments confirmed that this unknown pentraxin bound the plain, unsubstituted agarose, which could then be eluted in much the same manner for CRP affinity chromatography, with EDTA containing buffer (Pepys et al., 1977).

SAP binds to its specific ligands in a Ca^{2+} dependent manner, with differences in ligand specificity in comparison to CRP likely down to structural differences in the hydrophobic pocket. SAP exhibits binding specificity to phosphoethanolamine (PE), as well as β-D galactose, specifically the 4,6-cyclic

pyruvate acetal group it contains. Ligand and calcium-binding sites are arranged on the same 'effector' face of the SAP pentamer. SAP also appears to bind to chromatin and DNA, with DNA affinity being much higher in human SAP compared to mouse SAP. Of note, it has been speculated that human SAP's affinity for DNA is a factor in the lack of immunogenicity in DNA vaccination (Wang et al., 2012). This is supported by the effectiveness of DNA vaccines in different multiple animal models, including sheep, pigs, goat, horses, rabbit, cows and primates, where the vaccine's efficacy appears to correlate to the strength of binding of the particular species' SAP variant to DNA (Pepys, 2018). SAP has also been reported to bind to a number of polyanionic structures, such as heparin and bacteria surface-expressed carbohydrates, such as that found in *Streptococcus pyogenes* and *Neisseria meningitidis*, as well as LPS (de Haas, 1999).

Similar to CRP, SAP contains two Ca^{2+} binding sites (CBS), approximately 4.0-4.3 Angstroms apart. CBS1 consists of Asp-58, Asn-59, Glu-136 and Asp-138 side chains, as well as the carbonyl group of Gln-137. This arrangement of CBS residues coming from such disparate parts of the sequence is highly unusual, but is made possible due to a distortion in the E-strand, causing residues 136 and 138 to loop over 58-59. CBS2 is formed of Gln-148 and a pair of H_2O molecules. Binding of calcium to CBS1 appears to be less likely to affect the structural conformation of the protomer. With regard to ion binding avidity, it appears CBS2 binds to its target ion with lower avidity than the CBS1, with bound calcium far more likely to be displaced by analogous cations (e.g. cerium) and dissociate in calcium-free buffers. This 'loose' binding (compared to CBS1) is thought to be due to the position being more exposed and therefore more accessible to solvent, as well as the relatively few amino acid residues involved in calcium binding (Du Clos, 2013, Emsley et al., 1994).

SAP binding to phosphorylated (e.g. 6-phosphorylated mannose) and sulphated carbohydrates (e.g. 3-sulphated saccharides galactose, N-acetylgalactosamine and glucuronic acid). SAP binding to 6-mannose phosphate modified molecules is a characteristic shared with 6-mannose phosphate receptors, such as those responsible for enzyme transport in the lysosomal compartment, with binding to both inhibited by free mannose-6-phospahte. However, unlike the lysosomal receptors, SAP binding to the phosphorylated mannose moieties is inhibitable

by free galactose-6-phosphate, mannose-1-phosphate and glucose-6-phosphate (Loveless et al., 1992).

1.2.2.4: Antimicrobial action

Unlike CRP, SAP's function has been less well defined. SAP has long been thought to have an innate immune function against pathogenic challenge, due to its ability to bind to a variety of pathogen-derived molecules, such as *E. coli* PE (Kim et al., 2006) and Influenza A surface haemagglutinin (Andersen et al., 1997).

Phosphorylethanolamine (PE) is found on a variety of pathogen-associated molecules, forming modifications on *Escherichia coli* lipopolysaccharide (LPS) and *Neisseria meningitides* Lipooligosaccharide (LOS) (Takahashi et al., 2008a), with PE substitution being associated with antibody resistance and increased virulence respectively. There is conflicting evidence regarding the ability of SAP to activate the complement pathways (Section 1.2.2.7). In addition, there is evidence of SAP having an immune-modulatory effect in murine models, with the presence of SAP being associated with slower wound healing and resolution(Naik-Mathuria et al., 2008).

Part of the difficultly in discerning whether SAP has a protective role in host defence is SAP's indiscriminate tendency to confer resistance to proteolysis and phagocytosis to whatever macromolecule it binds (see below) In this way, many bacterial pathogens to which express SAP-binding surface markers appear to use it as a form of immune evasion, avoiding two major challenges to surviving in the host environment. For example, SAP-deficient mice have been shown to be more resistant to rough gram-negative bacterial infections, to which SAP binds, whilst simultaneously being more susceptible to smooth gram-negative bacteria, to which SAP does not bind (Noursadeghi et al., 2000, Du Clos, 2013) .

1.2.2.5: Wound resolution and anti-fibrosis

There is growing evidence that SAP has a role in regulating wound resolution. Studies on mice have shown that intradermal injections of SAP into wound sites

results in inhibition of monocyte differentiation into fibroblasts, reducing the rate of scar tissue formation (Loveless et al., 1992). When PBMCs were cultured in serum that was depleted of SAP, fibrocytes (i.e. inactive variant of fibroblast) rapidly appeared, indicating that SAP is the main endogenous inhibitor of fibrocyte differentiation in the blood.

SAP has been reported to have antifibrotic properties. Glycosylation of SAP is a feature not seen on CRP, and appears linked to SPA's ability to inhibit monocyte differentiation into fibrocytes. This is supported by evidence that desialylated SAP largely loses its ability to inhibit fibrocytes, while mutant CRP with an alanine residue substituted for asparagine becomes glycosylated gains the ability to inhibit fibrocyte differentiation. This action appears to be mediated by DC-SIGN, a C-type lectin receptor found on monocytes, supported by studies showing that small SAP- mimetic compounds blocking polysaccharide binding to DC-SIGN inhibits fibrocyte differentiation, with one such compound shown to be affective against a murine model of pulmonary fibrosis (Cox et al., 2015).

Wound dressing containing Ca^{2+} and agarose, which has binding affinity for SAP, has been shown to improve healing times for wounds of partial thickness in pigs, as well as full thickness wounds in mice. Of note, healing was more rapid in the pig model in comparison to commercially available dressings (e.g. Tielle, Intrasite). This is supported by clinical observations that survival rates for skin grafts improved in patients with lower SAP levels (Gomer et al., 2009).

In murine models of bleomycin-induced pulmonary fibrosis, injections of SAP reduced the number of fibrocytes detected in the lung and reduced fibrosis. Models of therapeutic dosing (i.e. SAP injections after inflammation and fibrosis is already present) also reduced symptoms of pulmonary fibrosis (Pilling et al., 2007). In addition, injection of SAP has been shown to models of other diseases linked to inappropriate fibrosis formation, including radiation-induced oral mucositis (Murray et al., 2010) and autoimmune encephalomyelitis (Ji et al., 2012).

1.2.2.6: Amyloid Fibril Formation

Amyloidosis occurs when normally soluble globular proteins have abnormal protein folding, causing them to aggregate into insoluble deposits in the form of cross β-sheet fibrils within extracellular compartments, causing tissue damage and a number of clinical conditions. Therapy that reduces the availability of the fibril precursor proteins has been linked to a reduction in amyloid deposition, this particular strategy is impractical in most forms of hereditary and acquired amyloidosis. Left untreated, most forms of amyloidosis are fatal to the patient. SAP has been implicated in several forms of amyloidosis, forming up approximately 14% of the dry mass of some amyloid deposits. However, the role of SAP in amyloid formation is poorly understood (Pepys et al., 2002).

Due to the classical pentraxins' resistance to proteolytic attack, it has been proposed that the integration of SAP prevents the breakdown of amyloid fibrils by proteolytic enzymes. This is supported by evidence in mouse models of systemic amyloidosis, where a targeted gene deletion of SAP results in a delay in amyloid deposition (Botto et al., 1997). In addition, *in vitro* models of amyloid fibrils experience rapid clearance by proteases and phagocytosis, which is not seen *in vivo* when amyloid fibrils are coated with SAP molecules. As circulating SAP does not confer degradation protection to amyloid fibrils, it appears that while SAP in itself is protease resistant, it is not a protease inhibitor *per se*, only conferring its protective qualities when deposited and bound to amyloid deposits (Tennent et al., 1995).

Treatment of models of amyloidosis with anti-SAP antibodies has been shown to be effective. The DESPIAD clinical trial is attempting SAP depleting treatments for Alzheimer's disease, a disease with amyloid formation being linked to neurological degradation. Separate to SAP's role in amyloid fibril persistence, SAP appears to have a degradative effect on neurological tissue, making depletion of SAP in the neurological compartment of particular interest for potential Alzheimer's disease therapy. (Al-Shawi et al., 2016, Pepys, 2018).

1.2.2.7: Interactions with Complement

SAP has been reported to activate complement, albeit at a more modest rate in comparison to CRP and PTX3. The role of SAP in complement activation is less

well studied than CRP. However, there is evidence of SAP aiding in complement mediated clearance of *Streptococcus pneumoniae*. This appears to be mediated by the classical pathway, with SAP-mediated complement deposition of *S.pneumoniae* increasing the efficiency of bacteria phagocytosis (Yuste et al., 2007) . However, separate studies have shown that SAP deposition on amyloid fibrils in mouse models, after most deposited SAP was removed by the palindromic molecule CPHPC, required subsequent binding of anti-SAP antibodies to residual SAP on the amyloid deposits in order to trigger complement mediated clearance of the amyloid fibrils, suggesting that SAP in itself does not contain the ability to interact with complement components in a direct manner (Bodin et al., 2010). This is reinforced findings in an analogous clinical trial, where the reduction in amyloidosis following anti-SAP antibody and CPHPC dosing resulted in reduction of liver stiffness and improvement of hepatic function (Richards et al., 2015).

It also appears that the ability of SAP to interact with complement components is dependent on immobilisation of SAP, with calcium-dependent C4 binding observed on SAP bound to sepharose beads either by direct conjugation, or indirectly with an anti-SAP antibody intermediary, with no indication of similar affinity in native-state SAP (de Beer et al., 1981). In addition, a separate study on SAP interactions with the complement components C1q and C4bp appear to indicate that binding events requires immobilisation of SAP, with no interactions observed in native, aggregated, or heparin sulphate-bound SAP. The same study also demonstrates competitive inhibition of C1q binding by collagen I, indication a shared binding site on the immobilised SAP. C1q and C4bp binding to SAP was independent of heparin, indicating multiple ligand binding sites on SAP (Sorensen et al., 1996).

1.3: Complement

1.3.1: The Complement System

The complement system is part of the innate immune system associated with a number of actions related to host defence against both exogenous (e.g. bacterial, parasitic) and endogenous (e.g. apoptotic cells) challenge, including opsonisation for phagocytosis by surface fixation by C3b, promotion of inflammation via the generation of anaphylatoxins C3a and C5a, and direct killing of pathogens via the formation of the Membrane Attack Complex (MAC), formed of C5b, C6, C7, C8 and C9. In addition, the deposition of C3d on antigen helps to activate the B cell co-receptor which greatly aids the activation and proliferation of B cells. The complement system consists of a series of zymogens (>20) found in circulation, where an activation event of a precursor molecule would trigger the conformational change required to activate the subsequent molecule, and so on. Synthesis of complement components can be mainly ascribed to liver hepatocytes, although extrahepatic expression of certain complement components has been reported. The importance of a functional complement system can be seen in a number to diseases and clinical symptoms relating to deficiencies in complement components.

There are three recognised pathways associated with the activation of the complement cascade: The Classical Pathway (CP) Alternative Pathway (AP) and Lectin Pathway (LP). All three pathways centre on the formation of C3 convertase, which leads to the activation and generation of downstream complement components responsible which go on to mediate the immune effects associated with complement activation (Dunkelberger and Song, 2010, Sjoberg et al., 2009) (Figure 5).

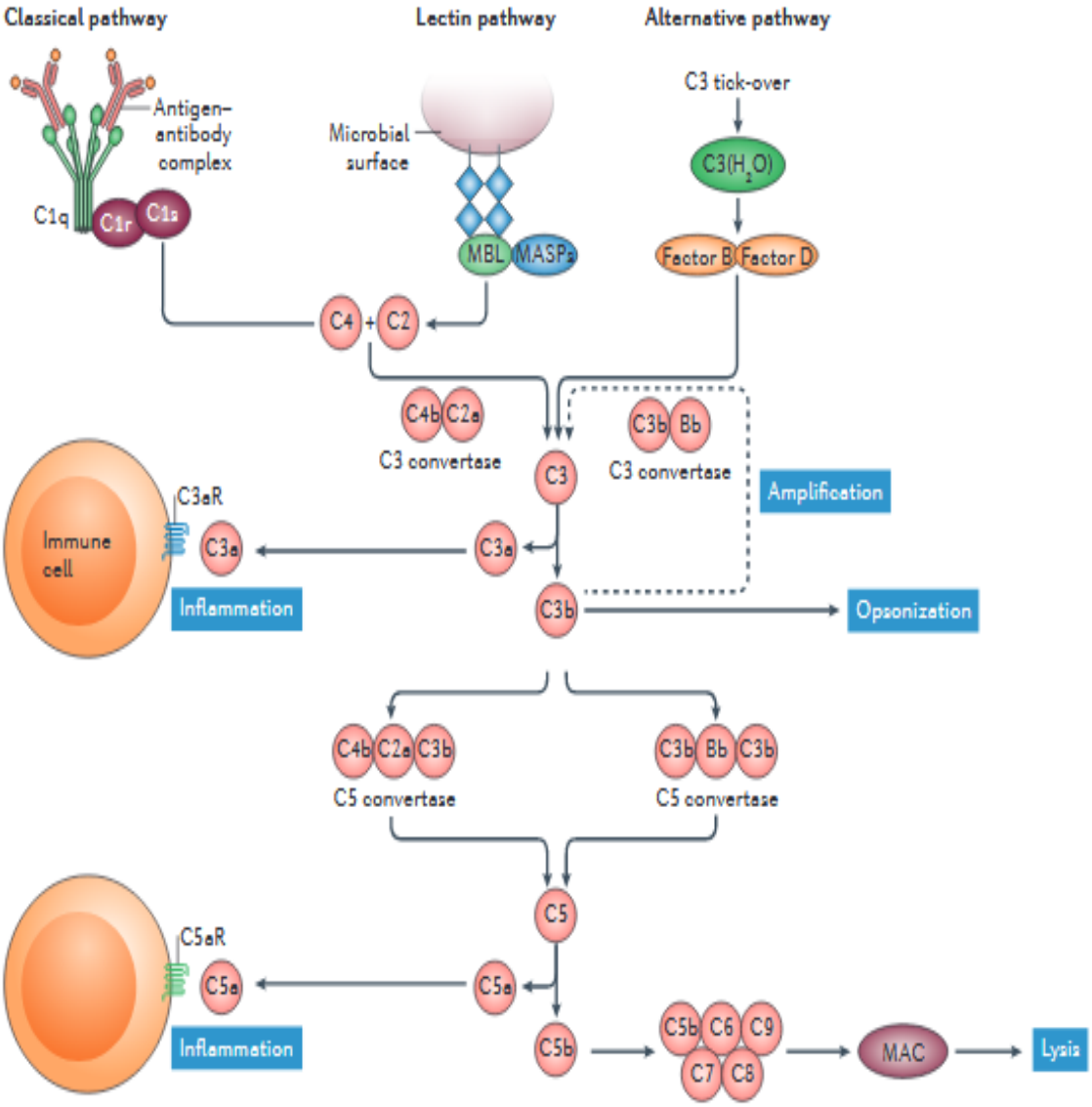

Figure 6: Flow diagram of the complement cascade in in relation to the three activation pathways (Trouw et al., 2017).

The complement cascade may be triggered via the Classical, Alternative and Lectin pathways. While each having specific activation requirements, all three pathways centre on the generation of C3 convertase, with generation of downstream complement mediators being responsible for inflammation, opsonisation and lysis.

1.3.2: The Classical Pathway

The CP is activated by the binding of its initiator molecule C1q to signalling molecules in complex with the target ligand, such as IgM, IgG and CRP. C1q in circulation is found bound to a pair of serine proteases (C1r and C1s) (Figure 7), with C1q binding triggering C1r activation, which in turn cleaves C1s, which is then responsible for the cleavage and activation of C4 and C2, the constituent components of a variant of C3 convertase (C4bC2a).

C1q does not have a hepatic origin, and is instead produced by a variety of cells types, such as epithelial cells and most notably in myeloid cells such as dendritic cells, monocytes and macrophages. In addition, unlike other complement proteins, C1q is not an acute phase protein, and is expressed constitutively by the above-mentioned cell types regardless of inflammatory state. In general, free C1q is found in tissues and as part of the C1 complex in circulation. C1q binds to the Fc region antigen-bound of IgG and IgM and initiates the generation of the C1 complex, and as such, C1q is an important component for classical pathway complement activation. C1q is also capable of binding to ligand-bound CRP, which also leads to the generation if the C1 complex(Kouser et al., 2015, Uday Kishore a, 2000). With conflicting reports on whether C1q bind to CRP via the collagen-rich 'stalk' region of C1q or the globular head regions in a similar manner to IgG and IgM. Evidence also exists of C1q binding to membrane proteins of *Klebsiella pneumonia* independent of intermediary opsonising molecules(Alberti et al., 1993).

In addition to its function as the CP initiator molecule, there is evidence that uptake of C1q by DCs and macrophages affects the maturation state of the cell, often leading to less inflammatory states(Castellano et al., 2007, Clarke et al., 2015, Sona et al., 2012). Dendritic cells matured in the presence of C1q have reduced expression of the co-stimulatory molecules CD80, CD83 and CD86, as well as lower expression of IL-6, TNF-α and IL-10 upon LPS stimulation(Castellano et al., 2007). It has been reported that C1q uptake reduces inflammasome activity in macrophages, limiting inflammatory action(Benoit et al., 2012).

C1q has a well-documented role in immune modulation and the clearance of apoptotic pathway and protein aggregates. The binding of C1q triggers the

phagocytosis of apoptotic cells, which in turn reduces the amount of inflammation caused upon cell death compared to that caused by the release of intracellular pro-inflammatory material upon cell death. Most notably, primary and secondary C1q deficiency has been linked to increased susceptibility to systemic lupus erythematous (SLE), which is characterised by the production of pathogenic autoantibodies against a variety of self-antigens, the formation of inappropriate immune complexes. While homozygous deficiency of the C1q gene is the strongest susceptibility factor in the development of SLE, the majority of cases are linked to secondary hypocomplementemia, often associated with the presence of anti-C1q autoantibodies (Benoit et al., 2012, Santer et al., 2012, Thanei and Trendelenburg, 2017). All of this highlights the key role that C1q play in tissue homeostasis while inflammation occurs. Complement pathway activation also has a number of downstream effects on the immune response, with evidence that C3 convertase products are required to promote an effective Th1 response (Arbore et al., 2016)

1.3.3: The Alternative Pathway

The AP could almost be considered a form of constitutive form of complement activation, in contrast to the CP and the LP which require binding of initiator molecules to target ligands to trigger activation. The AP is the result of background levels of spontaneous hydrolysis of the of an internal thioester bond within C3 generating $C3H_2O$, a functional analogue of the C3 convertase product C3b. This 'tick over' hydrolysis occurs at a rate of approximately 1% of total C3 per hour. Binding of factor B to $C3H_2O$ triggers the conformational change in factor B required for binding to and cleavage by the circulating protease factor D, producing $C3H_2OBb$, a variant of C3 convertase, which goes on to mediate the effects of complement system activation. As Both C3b (AP and LP generated) and $C3H_2O$ (AP generated) are capable of binding to the activated catalytic subunit of factor B (Bb) to form C3 convertase ($C3H_2OBb$ /C3bBb), this presents a model in which AP acts as an amplification of AP and LP activation (Thurman and Holers, 2006).

Regulation of the AP is largely dependent on the availability and concentration of essential and regulatory AP components. The activation and cleavage of

factor B by factor D is a Mg^{2+} dependent event. AP *in vitro* models using mouse serum and zymosan activation have demonstrated that factors B and D are essential components for efficient AP activation (Xu et al., 2001).

Properdin, a constitutively expressed glycoprotein, upregulates the AP by stabilising the $C3H_2OBb$ /C3bBb complex, whereas factor H downregulates the AP by enhancing the dissociation and proteolytic degradation of C3 convertase (Kouser et al., 2013). Both factor H and properdin have hepatic and extrahepatic synthesis sites, with extrahepatic release and synthesis allowing for potential localised AP regulation. Properdin concentrations can be increased by neutrophil release in response to TNF-α, *N*-formyl-methionine-leucine-phenylalanine (fMLP), C5a and IL-8 (Camous et al., 2011) or by release by endothelial cells in response to shear forces (Bongrazio et al., 2003) to trigger an increase in AP activation. Factor H release by keratinocytes (Timar et al., 2006) and endothelial cells (Brooimans et al., 1989) in response to IFN-γ likely represent mechanisms to downregulate the AP in order to prevent complement-mediated damage.

1.3.4: The Lectin Pathway

The LP greatly resembles the CP, with both pathways generating the same variant of C3 convertase, C4bC2a. However, the LP differs in ligand specificity and is independent of the CP initiator molecule C1q, being instead mediated by a number of lectins with carbohydrate-binding Pattern Recognition Receptors (PRR), expanding the scope of complement in host defence rather than being a redundant system. The LP may be activated by the Collectin mannose binding lectin (MBL), an analogue of the CP initiator molecule C1q, as well as ficolins (ficolin-1/M, ficolin-2/L and ficolin-3/H) (Roos et al., 2003, Fujita, 2002) (Figure 7). All initiator molecules exhibit lectin activity, and as such the LP is targeted towards unusual carbohydrate moieties that are designated as non-self, such as those found expressed by *Candida Albicans*, bacteria cell wall products such as those of *Streptococcus pneumoniae* and *Salmonella enterica*, and potentially in parasitic products, such as those expressed by *Leishmania*. There is evidence that the Collectin CL-11 is also capable of initiating LP activation, representing a

potential 5th LP initiator molecule (Ma et al., 2013, Nauser et al., 2018, Sandri et al., 2019).

MBL is synthesised in the liver and has a homotrimeric 'bouquet' basic structure similar to C1q and other collectins, such as Surface Protein A (SpA) and CL-11. Larger MBL oligomers are found in circulation formed of the basic trimer unit, including a dodecameric form (i.e. 4 x 3 polypeptide chains). Each MBL subunit has a 248 amino acid sequence and approximately 24 kDa, with the trimeric structure being stabilised by crosslinking of the cysteine-rich N-terminal regions, and ligand binding mediated via the C-type carbohydrate recognition domain (CRD) present on each subunit. Each polypeptide subunit also contains an α-helical 'neck' region, as well as a 'stalk' region with collagen-like structural properties. MBL binds to a variety of glycosylated ligands including mannose, glucose, fucose and N-acetyl-d-glucosamine. Similar to other collectins, ligand binding by MBL is Ca^{2+} dependent. In addition to being a LP initiator molecule, there is evidence that MBL may act as a direct opsonin for phagocytosis (van Asbeck et al., 2008, Garred et al., 2006, Auriti et al., 2017) (Figure 6).

Ficolins are related to collectins both in terms of structural characteristics and binding functionality, displaying similar carbohydrate-binding lectin activity and basic trimer structure. Unlike MBL, the basic ficolin trimer appears to be stabilised by collagen domain interactions, with higher order oligomers which can be hundreds of kilodaltons in size (4-8 x 3 subunits) formed via interactions between the N-terminal domains. Ficolin site of synthesis is highly subtype dependent, as is their ligand specificity, although in general reported ficolin specificity have been to more complex oligosaccharides rather that simple sugar groups such as mannose, or mannose-containing oligosaccharides (Table 2). Each ficolin polypeptide chain subunit is approximately 33-35 kDa in size and can be broadly divided into 4 domains that MBL subunits contain, with the exception that ficolin subunits bear a globular fibrinogen-like domain instead of MBL's CRD, which is responsible for the ficolin ligand binding (Ren et al., 2014, Bidula et al., 2019, Matsushita, 2013, Endoa et al., 2011).

MBL and Ficolin ligand binding leads to activation of a series of Mannose-Associated Serine Proteases (MASP-1, MASP-2 and MASP-3) (Heja et al.,

2012). MASP-2 acts in an analogous manner to the CP serine protease C1s in

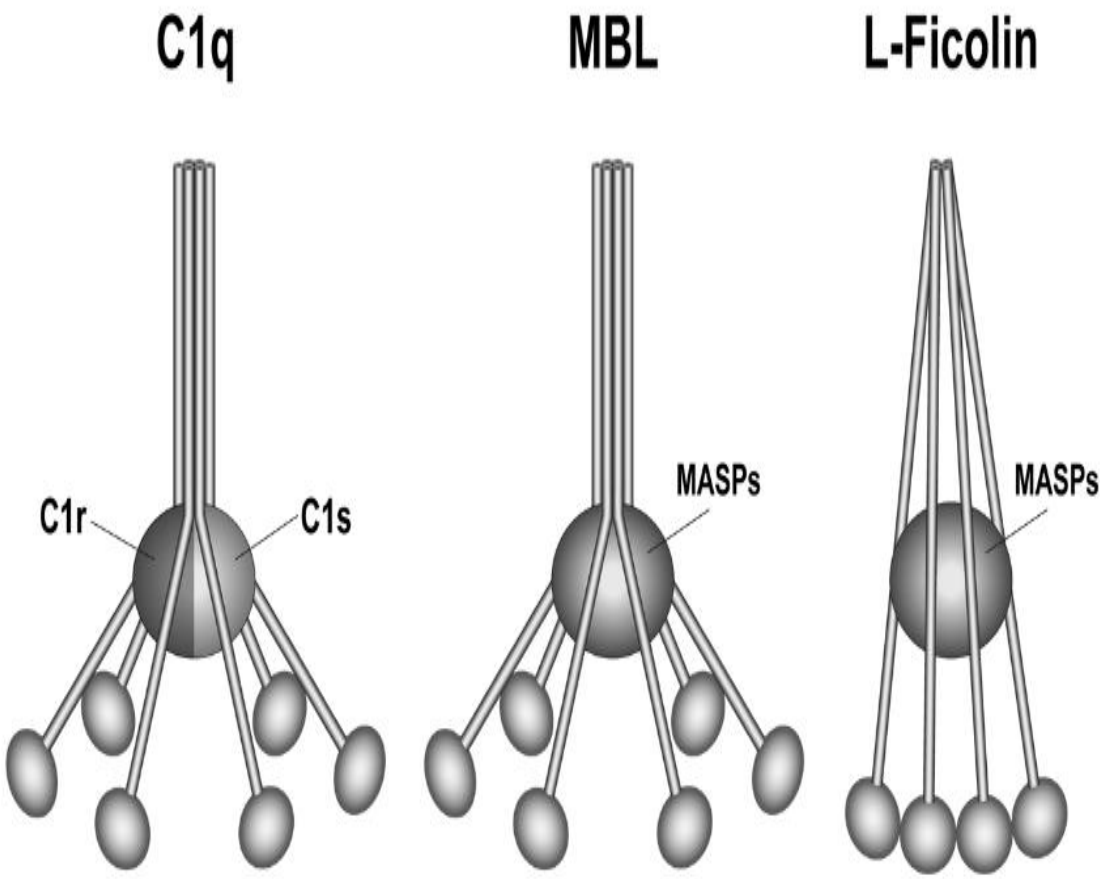

Figure 7: Structural comparison of C1q with MBL and Ficolin oligomers, and the location of associated serine proteases. (Ehrnthaller et al., 2011)

C1q and MBL share similar 'bouquet' structures, whereas Ficolins display a wider array due to trimer association occurring exclusively at the N-terminus. The LP initiator molecules (MBL and Ficolins) signal via MASPs, whereas the CP initiator C1q acts through C1r and C1s.

	Tissues of origin	Gene localization	Sugars	PAMPs	Endogenous/artificial ligands	Pathogen interactions
Human						
M-ficolin	Cell surface, serum	9q34	GlcNAc, GalNAc, LacNAc, SiaLacNAc, CysNAc, sialic acid, gangliosides	Ebola virus glycoprotein, chitin, β-1, 3-glucans	Acetylated human albumin CD43	*S. agalactiae*, *S. aureus*, *S. pneumoniae*, *S. mitis*, *E. coli*, IAV, *T. cruzi*, *Zaire Ebola virus*, *A. fumigatus*
L-ficolin	Serum	9q34	GlcNAc, GalNAc, ManNAc, CysNAc, GlyNAc, NeuNAc, acetylcholine, elastin	β-1, 3-glucans, N-glycans, HA, neuraminidase, teichoic acid, LPS	Acetylcholine, elastin, corticosteroids	*S. aureus*, *S. pyogenes*, *S. agalactiae*, *B. subtilis*, *S. typhimurium*, *E. coli*, *S. pneumoniae*, *L. monocytogenes*, *M. bovis* BCG, *M. tuberculosis*, *M. smegmatis*, *E. faecalis*, *A. fumigatus*, HCV, IAV, *T. cruzi*, *G. intestinalis*, *Leptospira biflexa*, *Pasteurella pneumotropica*
H-ficolin	Serum, bronchus, alveolus, bile	1p36.11	GlcNAc, GalNAc, fucose, glucose, acetylsalicylic acid, sialic acid, D-mannose, GlyNAc, CysNAc	LPS, PSA, Ag85	—	*S. typhimurium*, *S. minnesota*, *E. coli* O111, *Hafnia alvei*, *A. fumigatus*, IAV, *T. cruzi*, *G. intestinalis*, *P. pneumotropica*, *M. bovis* BCG, *M. kansasii*
Rodent						
Ficolin-A	Serum	2A3	GlcNAc, GalNAc	LPS	Fibrinogen	*S. pneumoniae*, *S. aureus*, *E. coli* O157:H7, *P. aeruginosa*, *C. neoformans*, *A. fumigatus*, *A. flavus*, *A. terreus*, *A. niger*
Ficolin-B	Peritoneal MØ	2A3	GlcNAc, GalNAc, LacNAc, SiaLacNAc, LDL, NeuNAc	—	LDL, fetuin	Nk

Table 2: Table of human and rodent ficolins according to site of expression, ligand specificity and target pathogens. (Bidula et al., 2019)

binding and cleaving C4 and C2 to provide the base components required to generate the same variant of C3 convertase (C4bC2a) (Vorup-Jensen et al., 2000, Chen and Wallis, 2004, Chen and Wallis, 2001) and appears to be essential for LP function, as demonstrated by *in vitro* experiments with MASP-2 depleted human serum (Moller-Kristensen et al., 2007) and MASP-2 deficient mice (Schwaeble et al., 2011). The exact function of MASP-1 and MASP-3 are less well defined. MASP-1 has approximately 10 times the circulating concentration of MASP-2, and appears to be capable of cleaving C2 but not C4, making it a potential supportive element to LP activation, with MASP-1 addback restoring the partial reduction in LP activity observed in MASP1/3$^{-/-}$ knockout mouse serum *in vitro* experiments (Ambrus et al., 2003, Takahashi et al., 2008b). MASP-3 has been linked to binding and activation of factor D, a key regulator of the AP, representing a possible link between the lectin and alternative complement pathways (Dobo et al., 2016), as well as a possible down regulator of MASP-2 mediated LP activation (Dahl et al., 2001).

1.4: *Leishmania*

1.4.1: Leishmaniasis

Leishmaniasis is a zoonotic disease caused by the *Leishmania* genus of protozoan parasites. It affects diverse mammalian species and is transmitted by certain species of female sandfly (Members of the subfamily *Phlebotominae*) via feeding. Disease presentation takes the form of cutaneous, mucosal and visceral leishmaniasis, displaying a spectrum of clinical symptoms. Leishmaniasis is a major neglected tropical disease, with 1.5 to 2 million new cases each year distributed across 98 endemically effected countries, including South America, Sub-Saharan Africa and the Indian subcontinent, resulting in approximately 50,000 fatalities where children make up a disproportionately high number. Leishmania epidemics occur in affected regions regularly: In Bihar, India, 1977, an outbreak of visceral leishmaniasis resulted in 70,000 fatalities, with another outbreak occurring in 1991 (Mukhopadhyay and Mandal, 2006). Of particular concern is leishmaniasis as an opportunistic infection, such as in HIV positive or otherwise immunocompromised patients. *Leishmania* is also relevant as a veterinary pathogen, being an efficient infective agent in multiple mammalian species, with dogs being recognised as a major reservoir of disease in South America and endemically the Southwestern region of Europe (Cecilio et al., 2014).

1.4.2: Life cycle

Leishmania initial infection of the mammalian host by the sandfly vector consists of three components: Metacyclic promastigotes, sandfly saliva and promastigote secretory gel (PSG). Metacyclic promastigotes differentiate from leptomonad promastigote in the sandfly foregut, characterised by high motility and capability of establishing infection in the mammalian host. Sandfly saliva contribution to infection is linked to anticoagulation, allowing the sandfly to probe and feed from the blood pool so that inoculation can occur in the first place. Experimental models also implicate sandfly saliva in the ‘Trojan Horse’ model of *Leishmania* infection of macrophages via phagocytosis of short-lived,

infected neutrophils, suggesting that sandfly saliva increases chemokine-mediated phagocytosis of infected neutrophils (van Zandbergen et al., 2004, Prates et al., 2011).

The *Leishmania* parasite has a complex, digenetic life cycle, existing as a series of motile, flagellated promastigotes in the digestive tract of the sandfly vector, and as non-motile, intracellular amastigotes in the mammalian host, chiefly within the parasitophorous vacuole of the macrophage within which the parasite persists and replicates (Figure 7). There is also evidence of *Leishmania* uptake by short-lived neutrophils, using them as an intermediary 'Trojan horse' before being taken up into the macrophage (Laskay et al., 2003, van Zandbergen et al., 2004).

Leishmania morphology changes dramatically according to the changes in its' local environment when moving between the mammalian and arthropod (i.e. sandflies, *Phlebotomus* in the old world, *Lutzomyia* and in the new world) hosts. In the sandfly gut environment, ingested parasites rapidly change into flagellated, motile promastigote stage parasites. When introduced to the mammalian circulation during bloodmeal feeding attempts, promastigotes are phagocytosed by macrophages, triggering their change into non-flagellated, non-motile amastigote stage parasites that replicate in the phagolysosome (Killick-Kendrick, 1990).

Upon uptake of infected macrophages, amastigote stages are encapsulated along with the rest of the bloodmeal with a peritrophic membrane, a chitin-rich membrane produced by the sandfly. There the amastigotes transform into procyclic promastigotes, with amastigotes disappearing within 48 hours of the bloodmeal. Procyclic promastigotes undergo their first replicative cycle within the sandfly gut environment, known as the bloodmeal phase. Shortly after, non-replicative nectomonad and leptomonad stage parasites are detected, with nectomonad stages implicated in escape from the peritrophic membrane through secretion of chitinase. This escape allows continuation of the infection, as any the bloodmeal would eventually be excreted as part of the sandflies' normal digestive process. Nectomonad stage parasites transform into leptomonad stage parasites, with migrate further to the anterior pole of the sandfly gut environment. Leptomonad stage parasites begin the production and

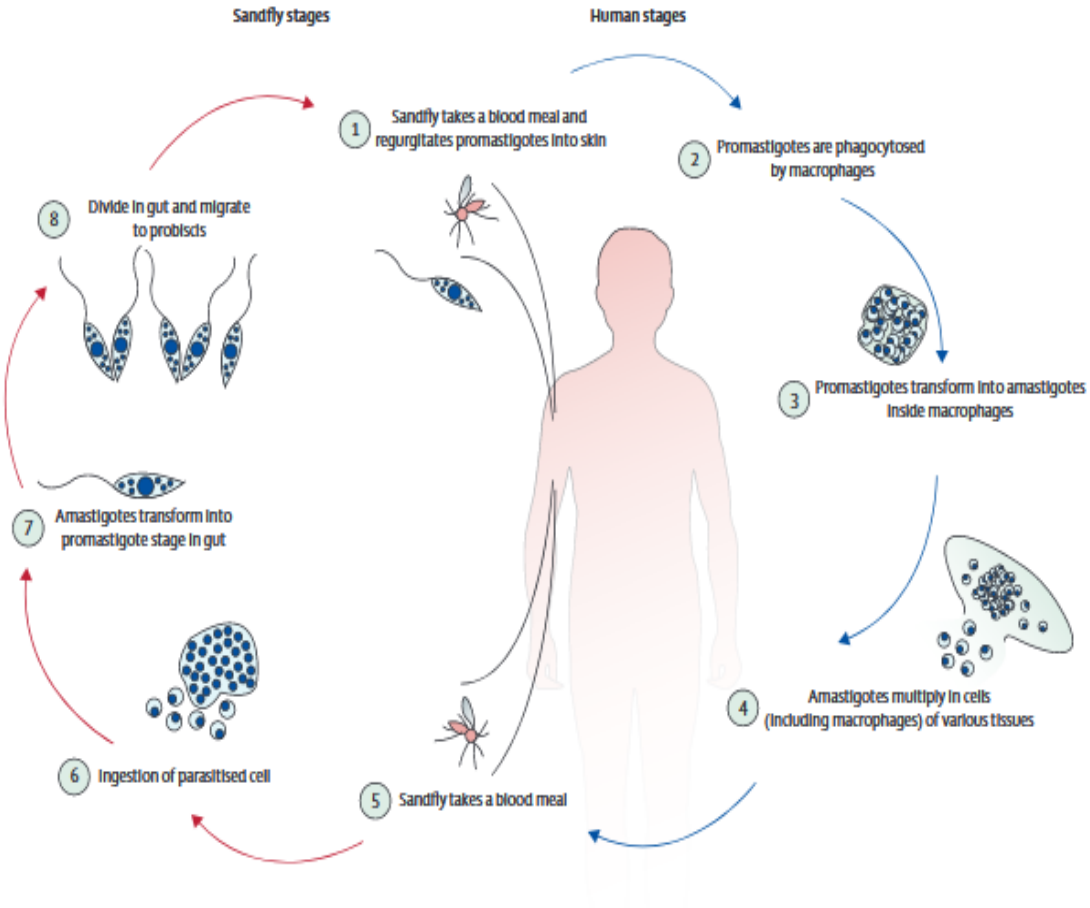

Figure 8: Illustration of the life cycle of *Leishmania* species parasites within human and sandfly hosts (Reithinger et al., 2007).

secretion of proteophosphoglycans, with forms the PSG matrix. Leptomonad stage parasites then undergo a replicative phase (i.e. sugarmeal phase), with parasite densities of 10^{10} – 10^{11}/ml being observed. It is from this reservoir of leptomonads that metacyclic promastigotes differentiate from, forming a replicative reservoir population to maintain sufficient numbers of infective stage-parasites to promote infection (Rogers et al., 2002, Gossage et al., 2003).

Metacyclic promastigotes within the sandfly vector has been reported to be largely PSG-associated, with approximately 75% of the total population being associated with the gel matrix in *L.mexicana*-infected *L.longipapis.* Within the PSG plug, there appears to be a localisation of metacyclic promastigotes to the anterior pole of the gel matrix, with 58% of PSG metacyclic promastigotes found in proximal to the stomodeal valve (Rogers et al., 2002). This localised concentration of infective-stage parasites to the site of PSG and bloodmeal mixing, and subsequent regurgitation into the feeding site, may serve to promote infection of the mammalian host.

1.4.3: Clinical Symptoms

Visceral leishmaniasis (VL), also known as kala-azar is the most clinically severe manifestation of leishmaniasis, characterised by irregular episodes of pyrexia, cachexia, anaemia, splenomegaly and hepatomegaly. It is commonly associated with *L.donovani* and *L.infantum* infection. There are an estimated 50,000 to 90,000 new cases each year, the majority of which are localised to Southeast Asia, East Africa and Brazil (Postigo, 2020).

Mucosal leishmaniasis (ML) is characterised by parasite invasion of mucosal tissue, with partial or total destruction of mucous membranes of the oropharynx and nose. Complications associated with ML include obstructions of the larynx, sepsis from secondary infection, starvation due to difficulty of feeding and pneumonia. Disfiguration of the midfacial region is common in ML, along with the stigma associated with it. Bolivia, Brazil, Ethiopia and Peru account for around 90% of all mucocutaneous leishmaniasis cases (Postigo, 2020).

Cutaneous leishmaniasis (CtL) is the most common clinical manifestation of leishmaniasis, with approximately 600,000 to 1000,000 new case per year. CtL manifests as skin lesions an ulceration, affecting exposed regions of the body that are susceptible to sandfly bites. CtL can result in scarring as well as disability, along with the stigma common to bearers of visible disfiguration. Afghanistan, Algeria, Brazil, Colombia, Iran (Islamic Republic of), Iraq and the Syrian Arab Republic account 95% of CtL cases(Postigo, 2020). Diffuse cutaneous leishmaniasis (DCtL) is a subset of CtL characterised by multiple non-ulcerating skin modules, high parasite load and a relatively anergic host immune response to infection. DCtL is particularly associated with HIV co-infection, where compromised immune function may play a role in DCtL development, as well as infection by *L.aethiopica*. although DCtL cases have been attributed to other *Leishmania* species (e.g. *L.panamensis*) as well (Van der Auwera and Dujardin, 2015).

Leishmania is capable of remaining dormant after initial infection in the form of post Kala-Azar dermal leishmaniasis (PKDL), a cutaneous disease manifestation, typically on the upper body after a patient recovers from diffuse, (VL), with *L.donovani* being the common causative agent. PKDL manifests anywhere from months to years after initial infection, with prevalence among VL

survivors ranging from 50% in Sudan and 5-10% in India. PKDL susceptibility factors are currently unknown, but there is some evidence that PKDL manifestation is due to immune dysregulation. PKDL typically manifests as a papular or nodular rash of the face arms and upper trunk, likely caused by a reactivation of dormant parasites in the skin compartment. The relative localisation of the symptoms to the upper body might suggest that the trigger for PKDL is related to UV light exposure (Zijlstra, 2016).

Classification of *Leishmania* species to clinical manifestations is not straightforward, with the symptoms being as much a result of the host immune response to the pathogen as the parasite's infection strategy. This can be seen from immunocompromised patients infected with *Leishmania* strains typically associated with cutaneous leishmaniasis instead experiencing more severe, visceral leishmaniasis symptoms(Gupta et al., 2013).

1.4.4: Treatment and therapeutic strategies

Current *Leishmania* treatment options have several deficiencies. Pentavalent antimonial compounds have been the benchmark for anti-leishmanial therapy, with sodium stibogluconate being commonly used for systemic treatment of leishmaniasis since the 1940s. However, increasing microbial resistance against drugs of this class have reduced their efficacy, and may be linked to reports to parasite reactivation. In India alone, 60% of *Leishmania* cases are classed as antimonial resistant, with the heavy metal toxicity associated with antimonial drugs meaning that increasing the dosage would be of questionable net therapeutic value. Increasingly, there are reports of immunocompromised patients failing to respond to antimonial treatment and failure to clear leishmaniasis, leading to a re-establishment of infection once therapy ended(Ashford, 2020).

The macrolide antibiotic amphotericin B in deoxycholate preparation is often used as an alternative treatment, and while efficacious with low microbial resistance, has a high level of toxicity, due to amphotericin B's avidity to cholesterol (the host equivalent of the ergosterol target) domains on mammalian host cells. Liposomal preparations of amphotericin B, which is approved by the FDA as only one of two anti-*Leishmania* treatment compounds has been shown

to be effective at treating leishmaniasis with reduced toxicity, and has been used to successfully treat antimonial-resistant leishmaniasis in HIV co-infected patients, Despite the increased safety for patients, the increased cost of liposomal amphotericin B in comparison to other treatments options is likely to put it out of the reach of many of the developing regions afflicted(Ashford, 2020).

Azole-class drugs (e.g. ketoconazole, itraconazole, and fluconazole) have been used for the treatment of leishmaniasis, though reports of its efficacy have been mixed, with itraconazole appearing to be was ineffective against VL caused by *L.panamensis* and ketoconazole only demonstrating relatively modest effects against *L.mexicana* and *L.panamensis* infection (Ashford, 2020).

Pentamidine often used as a second-line treatment option, despite not being official approved by the FDA for leishmaniasis treatment. However, it has a high toxicity profile, with reported side effects including vascular collapse and damage to pancreatic β-cells, causing inappropriate release of insulin, leading to hypoglycaemia and type 1 diabetes-like symptoms (Ashford, 2020).

Miltefosine, both as a standalone therapy and as part of a combination therapy alongside amphotericin B or paromycin, has been trialled successfully for leishmaniasis treatment, and at the moment the only orally available treatment option(Ashford, 2020).

Leishmaniasis treatment presents a particular challenge in cases with HIV coinfection. Co-infection exacerbates the clinical manifestations of both pathogens, being linked to the establishment of *Leishmania* infection in multiple organs and tissues (i.e. VL) and decreased latency period for HIV, both of which directly correlate to increased mortality and morbidity in co-infection patients. In addition, coinfected patients are more likely to have more severe symptoms even if the *Leishmania* species in question is not associated with VL (Ashford, 2020).

1.4.5: Vaccination

Vaccination for *Leishmania*, especially given the limitations and side effects of available treatment options, has been subject of extensive research as part of

the wider anti-*Leishmania* strategy. However, vaccine development has been hampered by several issues, including the lack of an animal model that accurately reflects *Leishmania* infection in humans, the genetic diversity and heterogeneity of the target populations, and *Leishmania* immune evasions strategies.

The value of resistance to *Leishmania* in endemic areas has long been recognised, with early observations that healed skin lesions, a visible sign of previous CtL infection, correlated with resistance to subsequent infection. Further research has validated this, with previously infected individuals demonstrating an effective immunological response against subsequent challenge, suggesting the possibility of a vaccine against *Leishmania* (Sundar and Singh, 2014). Leishmanisation, a form of variolation where *Leishmania* parasites are administered to a discrete skin site on the patient to produce a typically self-resolving cutaneous lesion, has been traditionally practiced in several areas where the disease is endemic, and was first subjected to a vaccine study in the 1940s. Trials in several locations, including Asia, the now defunct Soviet Union and the Middle East, produced 100% protective efficacy. However, this practice had several side effects common to using live, virulent pathogens, including incidence of more severe Leishmaniasis symptoms, including diffuse spread of cutaneous lesions, as well as contraindication to several other vaccines, causing immunosuppression and consequently reduced protective efficacy against diphtheria, tetanus and pertussis (Modabber, 1995).

The first trial performed in Brazil using killed parasite as a vaccine candidate demonstrated comparatively good immunogenicity and safety profile in comparison to leishmaniasation, but resulted in poor protective efficacy (Mayrink et al., 1979). BCG in combination with killed *L.major* or *L.amazonensis* parasites for vaccination against CtL produced promising results, conferring 95% protection in individuals. Despite the ease and low cost of production, there are issues including questions regarding reproducibility of the results, as well as lack of standardisation in the cultured parasites used, making registration of the potential vaccine candidate difficult (Convit et al., 1987).

An attempt to generate avirulent *Leishmania* parasite strain by knockout of reductase thymidylate synthase gene (DHFR-TS) in a strain of *L.major*

conferred significant protection in mouse models but failed to do so in non-human primates (Breton et al., 2005). More recently, parasites treated with Amotosalen, a DNA and RNA crosslinker, and controlled doses of UV radiation to produce KBMA (Killed but Metabolically Active) candidates have conferred protection in mouse models against *L.infantum*. This candidate also has the advantage of inability to replicate. (Bruhn et al., 2012).

Leish-111f, a recombinant polyprotein vaccine with three immunogenic components (TSA: Thiol Specific Antioxidant, LmSTI1: *Leishmania major* Stress-Inducible Protein 1, LeIF: *Leishmania* Elongation Initiation Factor), has been shown to be safe and efficacious in protection against both visceral and cutaneous Leishmaniasis in both animal models (mice and nonhuman primates) as well as humans in clinical trials performed worldwide (USA, Peru, Brazil and India) (Coler et al., 2002, Rhea N. Coler, 2007).

Promising potential candidates for use in veterinary use include Leishmune, a canid vaccine combination of *L.donovani* FML antigen and saponin adjuvant that has been shown to be efficacious against veterinary VL (Parra et al., 2007), and Leish-Tec, a combination of *L.donovani* A2 protein and adenovirus licensed for used in canids(Grimaldi et al., 2017, Parra et al., 2007).

While no DNA vaccines for humans have thus far been approved for human use, a DNA vaccine against West Nile virus for use in horses has been cleared for use (Davis et al., 2001), representing a successful POC example of DNA vaccines in mammals. An initial attempt to develop a DNA vaccine for *Leishmania* protection targeted GP63 and Hsp70 production for protection against murine models of VL in BALB/c mice, resulting in reduced hepatic and splenic parasite loads with increased levels of Th1 cytokines as well as reduced IL-1 and IL-10 (Salehi-Sangani et al., 2019).

1.4.6: Vector Control

Targeting of the arthropod sandfly vector to tackle endemic leishmaniasis have been thus far unsuccessful. Widespread spraying of insecticide s (e.g. DDT) may reduce *Leishmania* transmission in the short term, but reduces herd immunity to the parasite, such that epidemics of a more severe nature occur

once spraying of pesticides stops (Claborn, 2010), in addition to having a severe environmental impact.

Vector control of *Leishmania* is also complicated by humans not being the exclusive hosts of *Leishmania* species, with each species being capable of establishing intracellular, amastigote infection in multiple mammalian species, generating a reservoir for future infection. In addition, there is evidence that disease reservoirs are present in humans in the form of residual, dormant parasites post-infection, such as in cases of PKDL, make it difficult to eliminate endemic leishmaniasis.

While insecticide-impregnated bed nets have been used in an attempt to reduce sandfly feeding and transmission events, a study conducted in Nepal and India suggests that this measure did not significantly affect the frequency of bites by *Phelbotomus argentipes*, the natural vector for *L.donovani* (Gidwani et al., 2011).

1.4.7: Immune response against *Leishmania* infection

The vulnerability of *Leishmania* parasites appears to be stage dependent. In vitro experiments have shown that cultured, log phase promastigotes are vulnerable to lysis in normal human serum, whereas infective stage promastigotes in many *Leishmania* species are resistant (Franke et al., 1985). It has been suggested the this is due to differences in the expression of cell surface markers between the two promastigote stages rather than a lack of complement activation by metacyclic promastigotes (Puentes et al., 1988). *In vitro* experiments have shown that *Leishmania* strains responsible for mainly cutaneous disease tend to be more vulnerable to complement lysis via alternative pathway activation in comparison to strains responsible for the more severe visceral, diffuse disease, suggesting that complement lysis may have a role in limiting infection to the relatively benign skin infection (Mosser et al., 1986).

Similar to other intracellular parasite, successful clearance of *Leishmania* infection is often associated with Th1 responses, while Th2 responses are implicated in parasite *Leishmania* survival and replication within the host

(Heinzel et al., 1989). This dichotomy can be seen in studies of *Leishmania* phagocytosis of macrophages, which are capable of both killing the parasite, as well as being the site of amastigote differentiation and survival. The priming of the local immune environment by Th-1 type cytokines, such as IFN-γ and TNF-α, is associated with cell mediated immunity and a pro-inflammatory response. This appears to drive the maturation of conventionally activated macrophages (CAM), with generation of intracellular cytotoxic elements (e.g. reactive oxygen species, NO by iNOS induction) leading to parasite destruction in the phagolysosome. Th-2 cytokine in the local environment, such as IL-4, IL-5 and IL-13, on the other hand, is associated with humoral immunity, and drives alternatively activated macrophage (AAM) development. Arginase-1 activity in AAMs have been implicated in providing polyamines required for *Leishmania* amastigote nutrition. In this manner, AAMs can be seen as not only passively providing a safe haven against extracellular antimicrobial factors, but also being subverted to promote parasite survival (Rogers et al., 2009). The role of Th1/Th2 cytokine polarity in disease outcome can be seen in studies of *L.major* infection in susceptible BALB/c mice, where a switch of the Th2 biased CD4+ cell to a Th1 phenotype by inhibition of the lysosomal cysteine protease cathepsin B resulted in parasite clearance (Maekawa et al., 1998). In addition, the shift from the usual resistant, Th1 biased response to a Th2 phenotype during pregnancy in otherwise resistant C57BL/6 mice appears to lead to impairment of resistance to *L.major* infection, resulting in increased cutaneous lesion size, higher parasite loads and lack of disease resolution (Krishnan et al., 2020). The plasticity of CD4+ T cells has been demonstrated by transformation of polarized Th1 or Th2 cells to the opposite phenotype by exposure to T-cell modulatory cytokine factors, providing a potential insight into modulation of host immunity for therapeutic and vaccination purposes against leishmaniasis. There is also evidence that IL-12 is essential in developing effective antiparasitic responses. With homologous knockouts of either the P35 or P40 subunits in otherwise resistant mice demonstrating similar or increased parasite load following *L.major* infection compared to vulnerable BALB/c mice correlated with the production of a Th2, IL-4 dominated response, whereas WT resistant mice produced a Th1, IFN-γ dominated response. Similarly, several studies have

shown that treatment of resistant mice with antibodies specific for IL-12 increased susceptibility to infection.

Dendritic cells in determining the outcome of *Leishmania* infection via MHCII determines the activation of CD4+ T helper cells. This, alongside the cytokines signalling present at the time of presentation, determines differentiation into Th1 or Th2 type maturation states, which go on to influence the immune environment though their own cytokine signalling pathway (Feijo et al., 2016).

While Th1 responses are strongly associated with disease resolution and parasite clearance, there is evidence that downregulation of Th1 response that enables some parasite persistence may be important in the development of long-term immunity. Several studies have indicated that acute infection, whether it is brought on by reduced IL-10 or low parasite numbers, results in an ineffective memory response and consequently a lack of protection against reinfection. Indeed, in the case of *L.braziliensis*, infection has been observed to trigger a strong induction of not just a strong Th1 response but also a simultaneous increase in IL-10, inhibition of which causes an increased frequency in TNF-α producing monocytes. This indicates that, while seemingly contradictory, the development of regulatory immune cell populations that allow some parasite persistence alongside Th1 type responses associated with clearance is essential for the development of long-term protective immunity to leishmaniasis usually seen in previously infected individuals (Antonelli et al., 2004). It has been speculated that the short-term persistence (as opposed to more rapid clearance) of whole parasites and their associated immunogenic factors is essential in the development of effector memory (TEM) and central memory T-cells (TCM), conferring long-term resistance *Leishmania* to reinfection. In animal models, transfer of TCM cells from previously infected mice to naïve ones conferred protection to leishmaniasis. Interestingly, TCMs were taken from animals that were infected months before harvesting of TCMs, indicating that TCM population is capable of enduring in the absence of live parasites. Given that TEM cells appear to require live parasites in order to maintain their population, it suggests that Th1-biased TCMs, generated in the presence of a sufficiently long-term initial infection, is the basis for protective immunity to leishmaniasis. While it should be noted that the memory response in animals with transplanted TCMs was weaker than that observed in animals

that previously been infected, this may be a reflection in a relatively low population of TCMs in transplanted animals, and the lag time inherent in differentiating Th1 effector cells from TCMs (Gollob et al., 2005).

The influence of the immune response profile to *Leishmania* infection can also be seen in the animal models used to study leishmaniasis. In general, C57BL mice, which have a strong bias towards a Th1 type response, are known to be resistant to *Leishmania* infection, as well as to other intracellular pathogens. On the other hand, BALB/C mice, which are geared towards Th2 type response to challenge, are more vulnerable to models of infection for *Leishmania*. However, more recent studies challenge the relatively simplistic view that Th1 promotes resistance and Th2 is associated with vulnerability to infection (McMahon-Pratt and Alexander, 2004).

PKDL, a reestablishment of CtL often associated with *L.infantum* infection from dormant parasites from previous cases of VL, has a unique immunological profile in comparison to that of *Leishmania* caused by direct infection. Following anti-*Leishmania*l therapy PKDL patients do not have diffuse, systemic infection, and do not have the characteristic clinical symptoms that accompany VL, such as splenomegaly and hepatomegaly. However, dormant parasites appear to be harboured in the skin, which suggests a dichotomy of immune responses or an imbalance of distribution of the initial antileishmanial compounds in the viscera versus the skin, leading to a lack of sterilising clearance. Cytokine profiles in PKDL patients reveals that while systemic immune response adopts a Th1, IFN-γ type response, the skin compartment has high levels of IL-10 suggesting a Th2 type response. (Zijlstra, 2016).

The importance of DCs can be seen in CtL caused by *L.major*. C57BL mice have self-healing lesions when challenged with *L.major*, in contrast to Batf3$^{-/-}$ mice (C57BL background), which experience increased lesion size as well as increased parasite burden. Batf3 encodes the Jun dimerization protein p21SNFT, a transcriptional repressor of AP-1-mediated proteins that is essential to CD8α+ cDCs as well as CD103+ dDCs, leading to a decrease in DC cross presentation, as well as reduction in IL-12 production. Batf3$^{-/-}$ mice are also shown to have reduced IFN-γ secretion, as well as increased Th2 and Th17 cytokine levels. This is reflected in an increased level of anti-*Leishmania*

antibodies, with humoral immunity being a sign of a Th2-biased response (Ashok et al., 2014).

Evidence from infection of animal models suggest that complement has a role in *Leishmania* resistance at initiation of infection. Early studies found that rabbit serum contained a component that was inhibitory to *in vitro* growth of *L.donovani, L.tropica* and *L.enriettii*. The component was heat inactivated above temperatures of 56 ^{o}C, suggesting that it has a complement mediated event (Gettner, 1969). Other in vivo experiments in complement depleted and non-depleted BALB/C mice in *L.amazonensis* infection studies have shown that complement depleted mice have an increased parasite load and a reduced inflammatory response to parasite infection challenge. In addition, the increased parasite load in complement depleted mice at the initial site of inoculation persisted long term (30 days after challenge), suggesting a role for complement in the control of CtL in particular (Laurenti et al., 2004).

Studies regarding the primary complement pathway activated by *Leishmania* is mixed. While some studies claim *Leishmania* parasites activate the classical complement pathway, *in vitro* experiments demonstrating complement mediated lysis of promastigotes independent of specific antibodies suggest that alternative pathway activation has role in host defence against leishmaniasis.

However, if parasites are not lysed, some evidence suggests that complement interactions with *Leishmania* increases the infectivity of the parasite. *L.donovani* promastigotes that have been fixed by surface C3bi following incubation with complement containing serum experience a higher level of uptake my resident murine macrophages, likely through the CR3 receptor, in comparison to promastigotes incubated in a similar manner in serum-free solution (Ueno and Wilson, 2012). However, a similar experiment of *L.donovani* infection of human monocyte-derived macrophages suggests that this is not due to the C3bi-binding site on the CR3 receptor (Wilson and Pearson, 1988).

In addition, there appears to be no difference in survival rates following uptake between the two groups. There is also evidence that ligation of CR1 and CR3 receptors does not efficiently trigger oxidative burst mechanisms (Wright and Silverstein, 1983), providing a potentially relatively safe method of entry for *Leishmania* promastigotes. However, *in vitro* experiments of *L.amazonensis*

infection of macrophages reveal efficient binding and uptake even in the absence of serum, with the introduction of complement only leading to a minor increase in parasite uptake (Laurenti et al., 2004, Mukbel, 2005), suggesting that this might not be an essential entry strategy across all *Leishmania* species .

Studies have shown that the presence of dead parasites at the inoculation site may be essential to successful *Leishmania* infection. Models of *L.major* infection *in vitro* with purified, parasites identified as 'non-apoptotic' did not establish successful infection of phagocytes in comparison with 'apoptotic' (van Zandbergen et al., 2006). It has been proposed that the exposure of phosphatidylserine on the disrupted cell membranes on apoptotic parasites may be the mechanism behind this phenomenon, supported by studies on CtL in C57BL/6 mice by intradermal injection of *L.amazonensis*, where resistance to infection is observed in mice administered with anti-PS antibodies after *Leishmania* challenge (Wanderley et al., 2013, Wanderley et al., 2009).

Better understanding of the effect of *Leishmania* interactions with the host immune system including entry strategy into macrophages, methods of modulating the host cytokine profile to favour parasite survival and alteration of host immune cell activation would be key in the development of potential new therapeutic interventions and vaccinations against leishmaniasis.

1.4.8: Immune evasion and modulation by *Leishmania* parasites

The most obvious strategy for *Leishmania* immune evasion in the mammalian host is its rapid invasion of phagocytic cells in order to evade extracellular antimicrobial factors. In doing so, as with other intracellular pathogens, *Leishmania* trades relative safety against humoral and complement mediated immune factors for vulnerability against cell-mediated, intracellular killing mechanisms, such as the oxidative burst and CD8+ mediated T cell apoptosis. There is evidence that *Leishmania* actively downregulates IL-12, which is necessary for Th1 type activation and cell mediated immunity (Rub et al., 2009, Srivastava et al., 2011).

While macrophages, being the potential site for both parasite elimination or replication, are the main cell type of interest in many *Leishmania* studies, multiple studies have highlighted the importance of neutrophils to the establishment of infection in the mammalian host, particularly regarding early modulation of the local immune environment. Several studies have shown that it is neutrophils, rather than mononuclear cells, that are recruited in the early stages of *Leishmania* transmission. In natural infection models of C57Bl/6 mice *with L.major*, neutrophils are the predominant cell type recruited two hours after challenge (Peters et al., 2008). This is supported by observations of *in vivo* models of leishmaniasis, with intradermal infection models of BALB/c mice with *L.infantum* (Ribeiro-Gomes et al., 2012) as well as subcutaneous infection with *L.major* (Muller et al., 2001) and *L.amazonensis* (Pompeu et al., 1991) eliciting high levels of neutrophil recruitment to the site of infection. Challenge of with *L.donovani* and *L.major* into the murine pouch inflammation model showed that neutrophils were the main inflammatory cell type recruited following infection(Matte and Olivier, 2002) Of note, *L.major* extracellular vesicles introduced into the murine pouch has been shown to elicit a similar response that appears independent of the metalloprotease GP63 (Hassani et al., 2014), perhaps highlighting the importance in other *Leishmania* surface markers in neutrophil recruitment. Early neutrophil recruitment to the inoculation site has also been noted in other animal models, with intradermal injection of *L.donovani* in hamsters similarly showing both PMN and mononuclear phagocyte recruitment within the first 24 hours of challenge, with promastigotes being found intracellular of populations. Of interest, histology 48 hours after challenge revealed that parasites which had transformed to the mammalian infective amastigote stage were found exclusively within macrophages (Wilson et al., 1987), perhaps indicative of the ‘Trojan Horse’ strategy.

This idea suggests phagocytosis of *Leishmania* promastigotes by neutrophils trigger a number of mechanisms by which they promote ‘silent’ entry to enhance parasite survival in the phagolysosome compartment of the macrophage.

While early recruitment of neutrophils to the sandfly feeding site likely is attributable to the repair and sterilisation response triggered by simple mechanical damage that occurs during when the sandfly mouthpart lacerates the dermis during feeding attempts, there is evidence that *Leishmania* parasites

directly recruit neutrophils to the wound site in later stages, with *in vitro* incubation of L. major parasites with human PMNs stimulating IL-8 release (Laufs et al., 2002), This likely amplifies the effect of early IL-8 release by endothelial cells in response to challenge, forming an amplification loop that further recruits neutrophils to the feeding site, as well as stimulating their phagocytic activity, increasing parasite uptake (Scapini et al., 2000). The anaphylatoxin C5a has also been shown to contribute directly to neutrophil recruitment to the wound site, possibly highlighting a role for complement in early neutrophil recruitment (Ehrengruber et al., 1994). It should be noted that the effects of C3a in acute inflammation are less well defined, with some reports suggesting an immunomodulatory effect that acts to prevent neutrophil-mediated pathologies (Coulthard and Woodruff, 2015). While neutrophils are commonly associated with antimicrobial activity, including intracellular oxidative burst mechanism and the release of neutrophil extracellular traps (NETs), there is evidence that intracellular *Leishmania* inhibit fusion of the phagosome and the lysosome, promoting parasite survival (Mollinedo et al., 2010). In addition, *Leishmania* phagocytosis by neutrophils appears to delay cell apoptosis by activation of caspase-3 (Aga et al., 2002), enabling early immune evasion by extending the lifespan of its host cell and allowing later phagocytosis by mononuclear phagocytes.

L.major-infected neutrophils have been shown to release macrophage chemotactic factor MIP-1, increasing recruitment of the *Leishmania* host cell. Immunomodulation of macrophage maturation state also occurs, with phagocytosis of *L.major*-infected PMNs having been shown to induce increased TGF-β expression by macrophages (van Zandbergen et al., 2004), which has been associated with silent entry into macrophages for both *L.major* (van Zandbergen et al., 2004) and *L.amazonensis* (Afonso et al., 2008). Elevated levels of IL-10 and reduced levels of IL-12 triggered by macrophage clearance of apoptotic neutrophils has also been linked to parasite persistence and macrophage regulatory phenotype development (Filardy et al., 2010),

DCs are also a key component of the Trojan Horse strategy. DC phagocytosis of *Leishmania*-infected neutrophils appears to inhibit early DC priming of an effective anti-leishmanial response (Ribeiro-Gomes et al., 2012), as well as

inhibiting DC maturation and hence their ability to cross-present antigens for T-cell activation (Ribeiro-Gomes et al., 2015).

It has been suggested that part of the *Leishmania* survival strategy involves the exposure of phosphatidylserine (PS), a cell membrane component that would be exposed during the membrane disruption associated with neutrophil apoptosis, triggering phagocytic uptake via PRR recognition on macrophages. PS was also found to be absent in multiple *Leishmania* species, including *L.major, L.donovani, L. mexicana, L. amazonensis, L. tropica, L. guyanensis,* and *L. shawi*, suggesting that *Leishmania* species parasites as a whole would be reliant on triggering apoptosis of host cells in order to take advantage of this mechanism of entry (Weingartner et al., 2012).

In addition to the 'Trojan Horse' strategy, a 'Trojan Rabbit' model of macrophage invasion has also been proposed, wherein the parasite escapes the apoptotic neutrophil transiently before phagocytosis by the host cell. The importance of neutrophils in successful *Leishmania* infection is the subject of debate, with neutrophil depletions in mouse models giving mixed results with regard to the success of the infection (Ritter et al., 2009).

Leishmania immunomodulatory effects ascribed to specific products will be discussed in greater detail below (Section 1.5).

1.5: *Leishmania* phosphoglycan products

In addition to LPG, *Leishmania* also produces a variety of proteophosphoglycans (PPGs), many of which may play a role in parasite persistence and virulence. Many of these PPGs share similar proteoglycan structures and moieties to LPG, as shown by the cross-reactivity of many antibodies between LPG and many other PPGs such as filamentous PPG (fPPG) and secreted acid phosphatase (ScAP). These PPGs have high carbohydrate contents, which form upwards of 70% of their molecular weight. The exact function of these PPGs is currently unknown, but promastigote secretory gel (PSG) injected with or without saliva in murine studies, simulating the mammalian infection event, promotes CtL infection, suggesting that PSG may be a virulence factor (Rogers et al., 2004, Rogers et al., 2010).

A common feature of *Leishmania* infection is the obstruction of the sandfly vector's thoracic midgut and mouthparts. This consists of free-moving *Leishmania* promastigotes embedded in a three-dimensional matrix consisting of (PSG). Studies have shown that the main component of PSG is filamentous proteophosphoglycan (fPPG), a mucin-like, PPG rich molecule. Secreted acid phosphatase (ScAP), while not a primary component of PSG, is present among promastigote stage secretory products, and is named for its enzymatic activity at acidic conditions. (Ilg, 2000b)

1.5.1: Lipophosphoglycan (LPG)

1.5.1.1: Expression

LPG is arguably the most well-studied of *Leishmania*'s glycosylated products, and the major glycoconjugate expressed on the parasites' membrane. With 1 -3 x 10^6 copies expressed per cell in promastigote-stage parasites, LPG forms a thick glycocalyx surrounding the parasite, which is then downregulated in amastigote stage parasites, with *L.major* experiencing a 500 to 1500-fold decrease in surface LPG, and *L.donovani* and *L.mexicana* amastigotes having no detectable LPG at all. It has been demonstrated that LPG may have a role in concealing more immunogenic epitopes present on the cell surface. LPG is a

developmentally regulated molecule, with differences occurring in the number and type of side-chain substitutions, as well as the number of phosphorylated disaccharide repeats present, directly correlating to size and length of LPG, with metacyclogenesis causing a doubling in LPG length of Indian strain *L.donovani* parasites. This increase in LPG length is also observed in *L.major*, with procyclic LPG containing an average of 14 repeat units and metacyclic stage parasites containing 30 (McConville et al., 1992). This modification of LPG also affects LPG-mediated attachment of the parasite to lectins expressed on the sandfly gut surface, having implications for parasite migration and motility with the sandfly gut environment (Guimaraes et al., 2018).

As a heavily glycosylated glycolipid, LPG is found on the *Leishmania* surface but is also released, potentially either as a free glycolipid or in association with proteins such as albumin found in culture media, and thereby has an intrinsic ability to thereby associate with neighbouring cells and proteins.

1.5.1.2: Structure

LPG structurally consists of four components: a lysoalkyl phosphinositol anchor which inserts into the parasite cell membrane, a highly conserved, hexasaccharide region linked to the anchor by N-acetylglucosamine, phosphorylated disaccharide repeats (Gal-Man-PO_4), and a neutrally charged, mannosylated oligosaccharide end-cap. Aside from the Gal-Man-PO_4 repeat region, LPG is structurally conserved between species and stages, and as such it is variations in this region which is the topic of most study and discussion in regard to LPG.

The disaccharide chain has been observed to form a helical structure, with the length of the LPG molecule being directly related to the number of disaccharide-repeats in a given LPG molecule, this spring like structure has been hypothesised to be able to expand and contract in length, from between 90-160 Angstroms for an LPG molecule containing 16 repeating disaccharide units. This number can vary between developmental stages as well as between different species, which will be discussed below. In addition to differences in length, LPG has also been reported to have side chain modifications, with the

extent and type to substitutions present being stage and species dependent as well.

1.5.1.3: Stage-specific variations

LPG length varies greatly between developmental stages, with later-stage promastigotes expressing longer LPG molecules than those preceding it. Though the length of LPG may vary, it appears that LPG in highly expressed in all promastigote stages, forming a glycocalyx surrounding the parasite. In contrast, the transformation into amastigotes is associated with a sharp downregulation of LPG.

Metacyclogenesis appears to be linked to an increase in phosphorylated disaccharide repeats (Figure 8), which may affect parasite attachment to the sandfly midgut. In *L.major*, it has been shown that β-linked galactose side chain substitutions on procyclic stage parasites contains affinity for a β-galactose-binding lectin widely expressed in on the midgut surface of *Phlebotomus papatasi*, the natural vector for *L.major*. B-linked galactose side chain substitutions are downregulated substantially in metacyclic stage parasites and replaced with arabinopyranose and glucose residues (Guimaraes et al., 2018). This likely has implications in parasite survival and infection of both the arthropod and mammalian vectors. On one hand, the lack of midgut attachment likely allows selective ejection of the mammalian injective-stage parasites during feeding attempts by the sandfly, whereas procyclic promastigotes are retained in the sandfly midgut and protected from exposure to mammalian serum components to which it is vulnerable, or being carried by shear forces in the to the hindgut, where they would be vulnerable to the sandfly's digestive enzymes.

Changes in LPG length can also influence parasite attachment to the midgut. In Sudanese strain *L.donovani*, the loss of midgut binding ability during metacyclogenesis does not appear to be related to side chain substitutions , but instead the concealment of α-mannose and β-galactose substitutions due to conformation change of LPG related to its elongation causing a 'hairpin' turn in its phosphorylated disaccharide chain (Sacks et al., 1995).

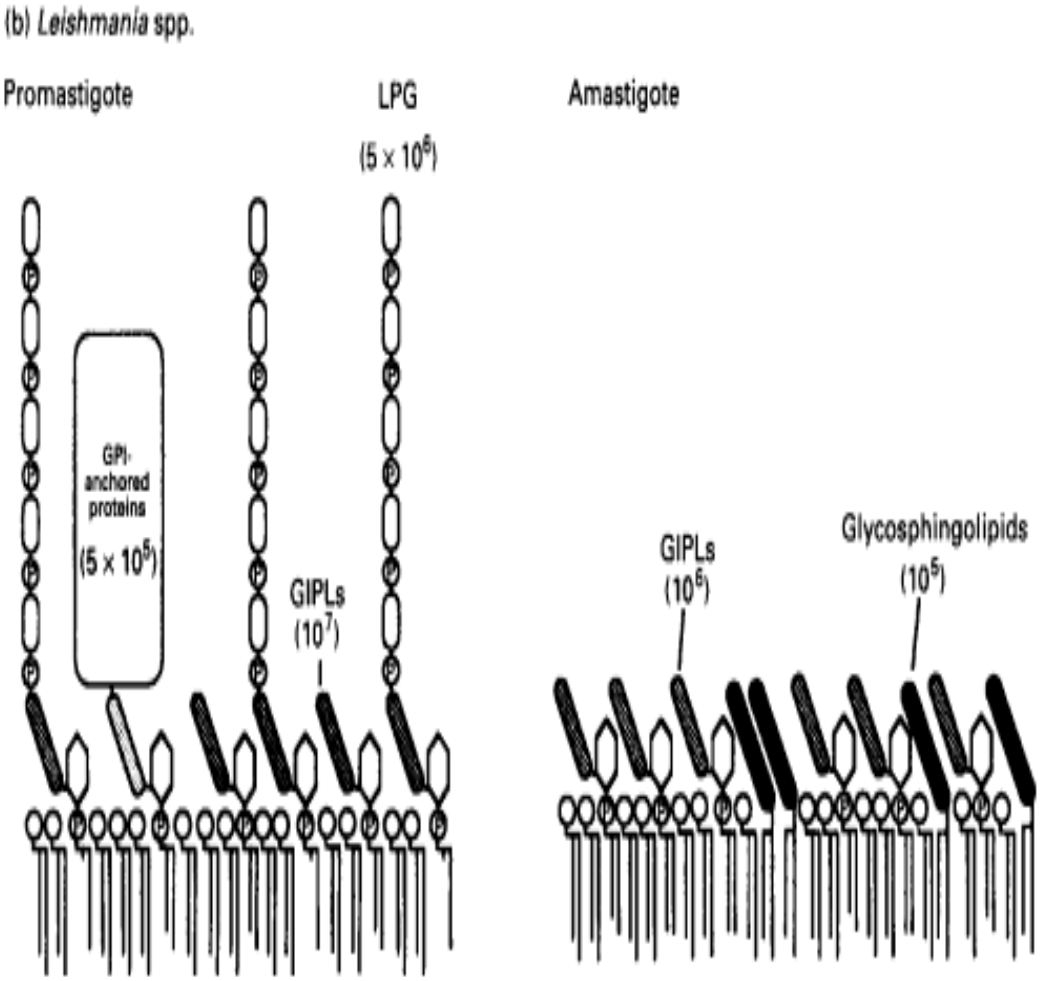

Figure 9: Differential expression of cell membrane surface markers between promastigote and amastigote stage *Leishmania*. (McConville and Ferguson, 1993)

LPG is highly expressed in promastigotes, forming a glycocalyx surrounding the parasite and obscuring other cell surface markers. LPG is then greatly downregulated in amastigote stage parasites, being virtually undetectable in most *Leishmania* species.

Substantial changes in LPG structure during metacyclogenesis has also been observed in other *Leishmania* species. Indian strain *L.donovani*, with procyclic stage promastigotes containing β1,3 glucose side chains substitutions in both the end cap and the phosphorylated disaccharide repeat structures allowing midgut binding to *Phlebotomus argentipes*, its natural vector. Metacyclogenesis is associated with a doubling in LPG length and the loss of the side chains substitutions responsible for midgut binding (Mahoney et al., 1999).

1.5.1.4: Species specific variations

LPG from different species have variations relating to the Gal-Man-PO_4 side chain substitutions and length. It is likely that these are adaptations to promote attachment to receptors expressed on the sandfly midgut, as well as having an influence on their infection strategies in the mammalian host environment (Figure 9).

Group I LPG (e.g. *L.donovani*) have no substitutions to their side chains.

Group II LPG (e.g. *L.mexicana, L. tropica, Lmajor*) have side chain modification branches from the galactose C3 position, which does not disrupt the helical structure of the glycosylated LPG structure. Levels of substation vary within Group II LPG species, with *L.mexicana* LPG exhibiting 20% substitution and *L.tropica* exhibiting virtually complete substitution of side chains. Group II LPG side chain oligosaccharide substitutions are often capped with arabinose residues.

Group III LPG (e.g. *L.aethiopica*) have side chain modifications attached to the C2 position of the mannose component of the disaccharide repeat.

It should be noted that it would be premature to assume that substitutions of LPG's disaccharide repeats would be reflected in the parasite's other glycosylated products (e.g. fPPG and ScAP).

LPG has a role in parasite attachment to the sandfly gut wall through an interaction with galectins expressed on the gut wall surface. This likely has implications in successful colonisation and infection of the appropriate sandfly vector for a given *Leishmania* species: Notably, *phlebotomis papatasi*, the natural arthropod vector for *Leishmania* major, expresses a gut surface lectin capable of binding the β-linked galactose modifications found on *L.major* procyclic LPG, promoting adherence of non-infective stage parasites and preventing their expulsion into the mammalian host, where they would be vulnerable to complement-mediated lysis.

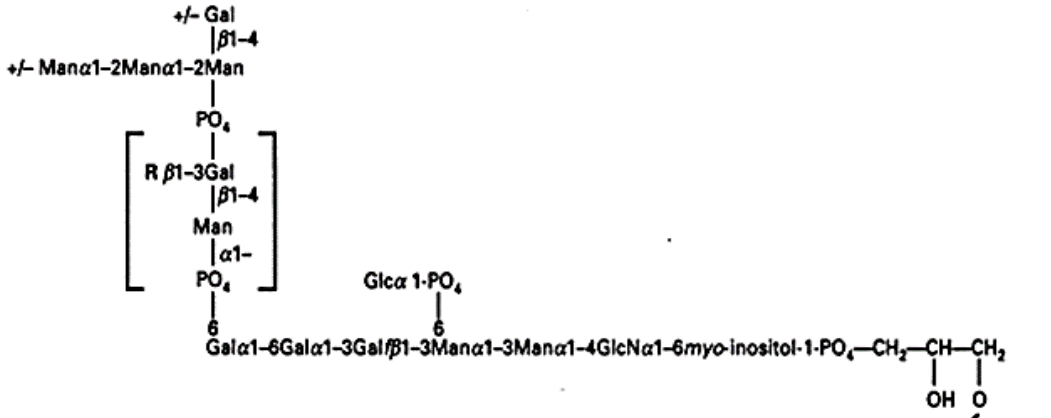

R	*L. donovani* LP	*L. mexicana* LP	*L. major* LP	*L. major* MP	*L. major* A
H	+++	+++	+	++	+++
Glc	–	++	–	–	+
Glcβ1-3Gal	–	–	+	+	+
Gal	–	–	+++	++	++
Galβ1-3Gal	–	–	++	+	+
Galβ1-3Galβ1-3Gal	–	–	+	+	+
Galβ1-3(Galβ1-3)$_{4-10}$Gal	–	–	+	–	+
Arapβ1-2Gal	–	–	+	+++	–
Arapβ1-2Galβ1-3Gal	–	–	+	+	–
Arapβ1-2Galβ1-3Galβ1-3Gal	–	–	+	+	–
n	16	30	14	30	36

Figure 10: Stage and species dependent side-chain modifications in *Leishmania* LPG (McConville and Ferguson, 1993).

Above: LPG consists of four regions: a lysoalkyl phosphinositol anchor, a highly conserved hexasaccharide region linked to the anchor by N-acetylglucosamine, phosphorylated disaccharide repeats (Gal-Man-PO_4), and a neutrally charged, mannosylated oligosaccharide end-cap.
Below: Table of side-chain substitutions type and frequency found in LPG from different species and life cycle stages.

LP: log phase promastigotes
MP: Metacyclic Phase promastigotes
A: Amastigotes
+++: >50%
++: 10-50%
+ < 10%

1.5.2: Filamentous Proteophosphoglycan (fPPG)

1.5.2.1: Expression

fPPG is expressed as part of the glycome of all observed *Leishmania* species, released from the flagellar pocket of promastigote stage parasites. When grown in culture medium, the synthesis and release of PSG, of which fPPG is the primary component, corresponds to late log phase/early stationary phase promastigotes, roughly corresponding to leptomonad-stage parasites (Ilg et al., 1996). In addition, PSG extracted from *L.mexicana* infected sandflies with mature infections have been found to predominantly leptomonad stage parasites (Rogers et al., 2002). While this may tentatively suggest leptomonad promastigotes are responsible for PSG formation, there has yet to be a definitive analysis of differential levels of fPPG expression between promastigote stages at the time of this writing.

While there is evidence that *L.major* and *L.mexicana* fPPG is encoded by exceptionally large members (>23kBa) of a multigene family with DNA repeats which appear to translate into polypeptide chains rich in Serine, Proline and Alanine residues, the projected PPG molecule would be predicted to be approximately 2 μm long. fPPG molecules have been observed that are three times this length, but it is unknown what mechanisms allow the larger molecule to be assembled (Ilg, 2000b).

1.5.2.2: Structure

fPPG is a large, filamentous molecule, reaching 3–6nm in diameter and up to 6μm in length, sharing similar structural characteristics to mammalian mucins. It is a heavily glycosylated molecule, with carbohydrates forming approximately three quarters of its molecular mass: Structural analysis of *L.major* fPPG derived from culture supernatant reveals a molecular mass that is 75.6% carbohydrate, 20% phosphate and 4.4% amino acids per weight respectively. Unusually, greater that 50% of the amino acid residues found in fPPG consist of serine, with the remainder consisting of alanine or proline residues. Approximately 84-90% of serine residues in fPPG are phosphoglycosylated, consisting of 6Gal(β1,4) Man (α1-) PO_4)- repeats capped in mannose-

containing oligosaccharides in a similar manner to other *Leishmania* glycosylated products, such as LPG and ScAP. The high level of phosphoglycosylation appears to make fPPG particularly proteinase resistant, possibly through stearic hinderance. Both N and O-linked glycans have been found on fPPG, although since most of the phosphoglycosylation modifications are associated with serine, it would appear that the latter is the dominant form of glycosylation present on fPPG (Ilg et al., 1996).

fPPG is highly viscous even at low concentrations in solutions, with gelation observed at 5-10 mg/ml and above (Figure 10). While the exact chemical interactions responsible for this gelation is unknown, it would not be unreasonable to assume that they are similar to that seen in the structurally similar mammalian mucins, where hydrogen bonding, calcium bridging, disulphide linkages and non-mucin factors have been implicated in gel assembly (Bansil and Turner, 2006). It is possible that fPPG, as well as other *Leishmania* glycosylated products, contains species-specific side chain substitutions similar to those observed in LPG, but this has not been confirmed at the time of this writing. fPPG *Leishmania* promastigotes in culture form aggregates which are structurally identical to PSG extracted from infected sandfly midguts (Stierhof et al., 1999).

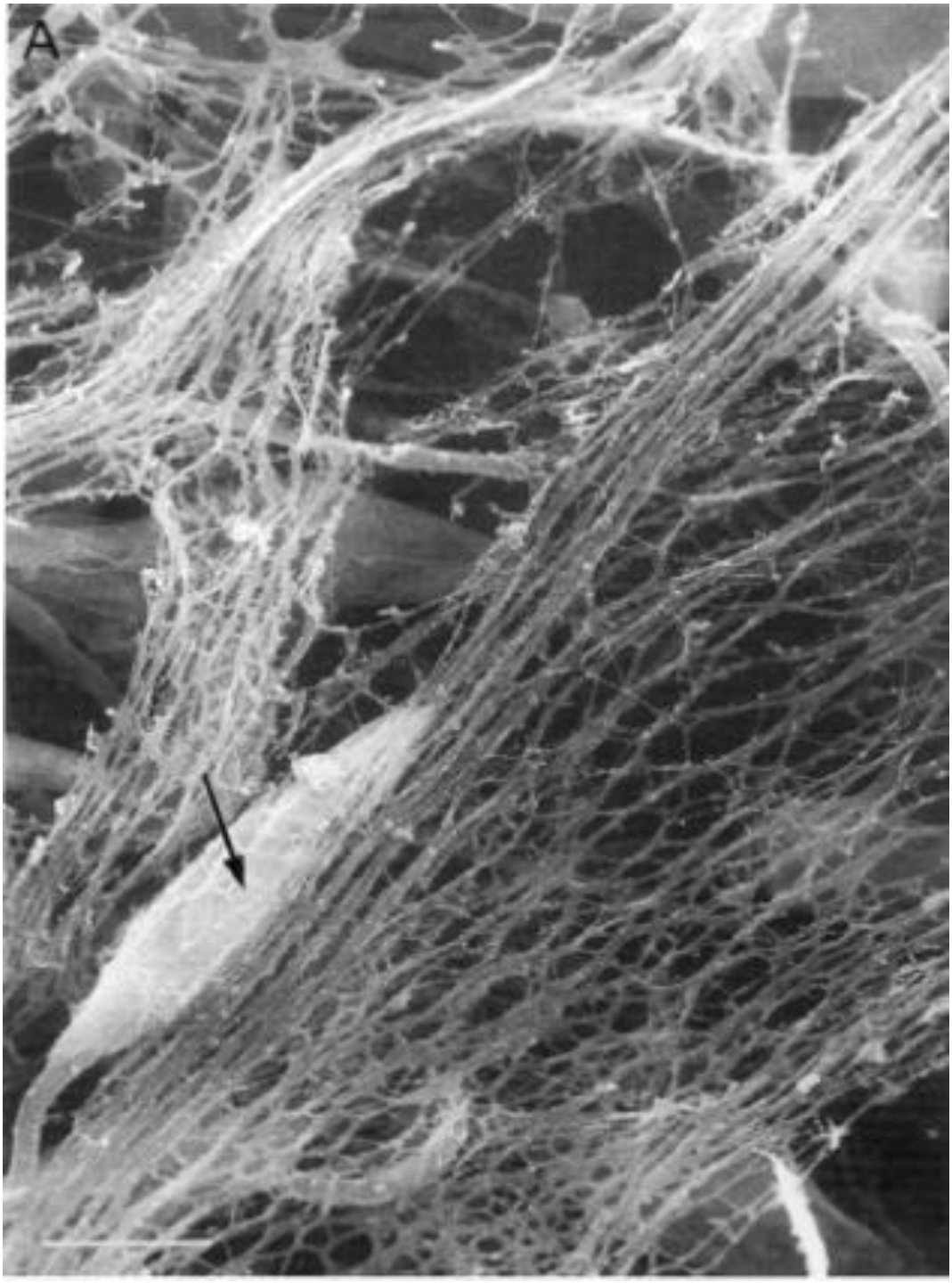

Figure 11: Image of *L.mexicana* PSG three-dimensional structure using Scanning Electron Microscopy (SEM) (Stierhof et al., 1999)

SEM of PSG reveals a complex gel matrix formed of interwoven fPPG strands. Image also captures a promastigote-stage *Leishmania* parasite embedded within the PSG matrix, indicated by the arrow (→).

1.5.2.3: Function: Promoting survival in Sandfly gut lumen

One of the challenges *Leishmania* faces in attempting to establish infection in the sandfly vector is secreted anti-microbial factors in the gut environment. These include proteolytic trypsins and chymotrypsins (Ramalho-Ortigao et al., 2007, Dostalova et al., 2011), with at least one example demonstrated to be upregulated in response to bloodmeal (Telleria et al., 2010). Other examples of other potentially anti-leishmanial candidates found in the midgut include metallocarboxypeptidases, alanyl aminopeptidases and astacin-like metalloproteases (Oliveira et al., 2009).

In vitro experiments with *L.major* mutants deficient in both LPG and PPG ($LPG2^{-/-}$) and LPG only ($LPG1^{-/-}$) in sand fly infections appear to point towards a role for PPG in survival during bloodmeal digestion. Further *in vitro* experiments using sandfly midgut lysates suggest that PPG rather than LPG confers protection to *Leishmania* parasites against sandfly digestive enzymes. Even in LPG deficient mutants, PPG appears to bind passively to the parasite cell surface to exert its protective effects (Svárovská et al., 2010, Sacks et al., 2000).

1.5.2.4: Function: Promoting mammalian infection via sandfly gut obstruction

Obstruction of the digestive tract, extending from the anterior midgut to the stomodeal valve in infected sandflies, has been observed in multiple combinations of *Leishmania* parasite and arthropod vector (Figure 11). In *L.infantum* infected *Lutzomiya longipapis* sandflies, PSG can be observed 2/3 days after initial infection, coinciding with the peak in leptomonad stage parasites, which are derived from nectomonad stage parasite following their migration to the anterior midgut. The concentration of PSG in *Lutzomiya longipapis* has been estimated at 1 g/ml, with fPPG purified from culture supernatants aggregating at concentrations between 5-10 mg/ml (Rogers, 2012). This ease of gelation, particularly in a volume as confined as that of a sandfly digestive tract (approximately 10 nl), likely contributes to the formation of PSG. This appears to be a common feature of established infection in the sandfly vector (Ilg et al., 1999, Ilg et al., 1996).

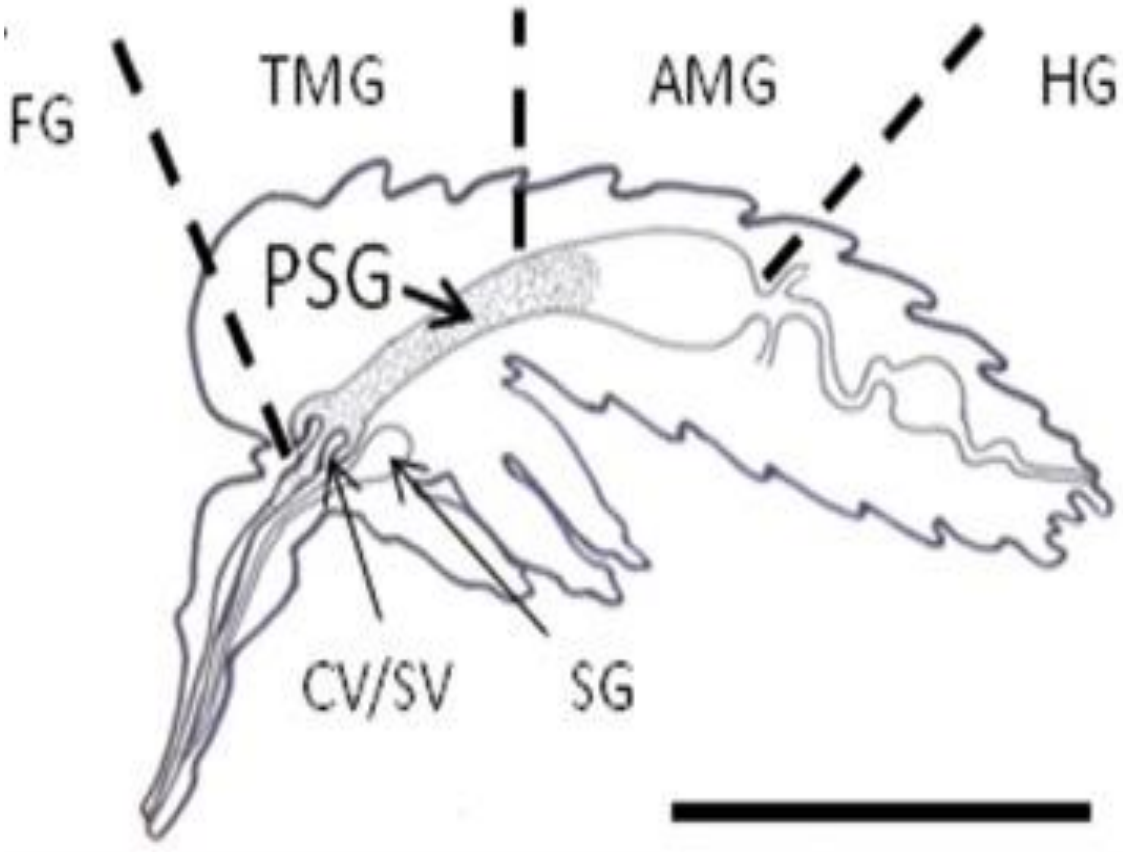

Figure 12: Location of PSG obstruction in *Leishmania* infected sandflies digestive tract (Rogers, 2012).

Location of PSG is indicated by the arrow (→), with the extent of the blockage highlighted in grey. Scale bar (—) = 10 µm

FG: Foregut
TMG: Tegmental midgut
AMG: Anterior midgut
HG: Hindgut
CV/SV: Cibarial valve/ Stomodeal valve
SG: Salivary glands
PSG: Promastigote secretory gel

It has been suggested that PSG obstruction of the sandfly gut changes sandfly feeding behaviour, with increased probing attempts observed in infected sandflies compared to healthy ones. It is estimated that 87% of infected sandflies are only capable of receiving a partial bloodmeal, and must feed multiple times in order to satisfy its nutritional requirements. This increase in probing and feeding attempts has been suggested to increased transmission events (Rogers et al., 2002). This is supported by observations in hamster infection models with *L.donovani* and *Phlebotomus chinensis* sandflies that have shown that incomplete or unsuccessful feeding attempts are more likely facilitate *Leishmania* transmission than successful ones (Chung et al., 1950, Killick-Kendrick et al., 1977).

Mechanical obstruction of the sandfly gut has been linked to multiple mechanisms implicated in increased chance of infection of the mammalian host. PSG appears to increase the difficulty for the sandfly attempting to draw up the bloodmeal, which results in regurgitation events as the sandfly attempts to alleviate the obstruction. This works in combination with the damage and distension of the stomodeal valve in infected sandflies, which has been reported in *L.major*-infected *p.papatasi* (Schlein et al., 1992) as well as *L.mexicana*-infected *L.longipapis* (Rogers et al., 2002), where the PSG works in tandem with parasite-derived chitinases to modify the sandfly physiology, resulting in greater deposition of PSG and promastigotes into the feeding site due to the sandfly being unable to prevent reflux of midgut contents during feeding (Figure 12).

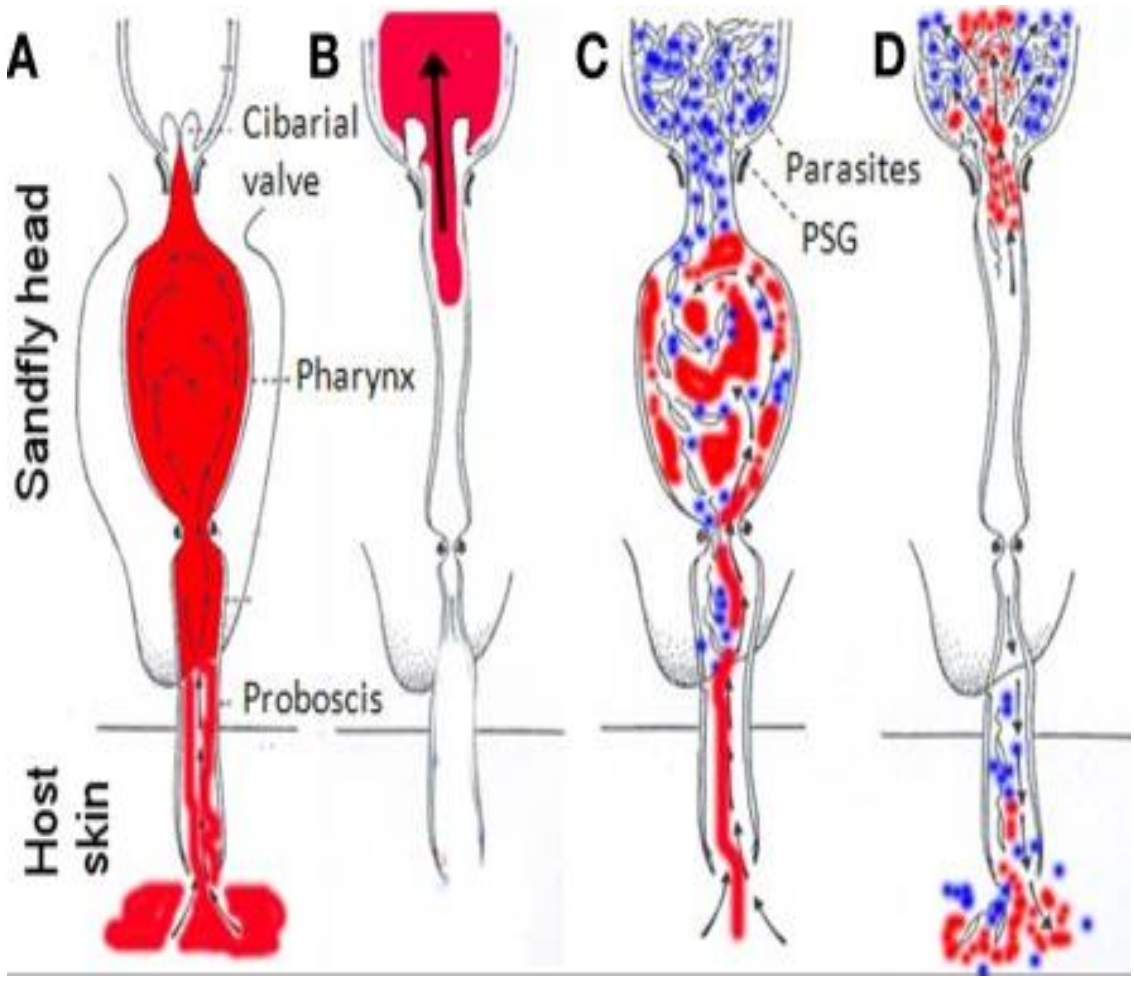

Figure 13: Regurgitation Model of *Leishmania* Infection (Rogers, 2012)

A, B: When a healthy sandfly takes in a bloodmeal, it gets drawn up via the proboscis and pharynx (A) and past the one-way cibarial/stomodeal valve into the midgut (B), where it is subsequently digested.

C, D: In infected sandflies, promastigotes are attached to the anterior midgut and PSG forms a blockage, distending the stomodeal valve and obstructing the pharynx and midgut. During feeding attempts, this allows mixing of the soluble PSG and the parasites embedded within in with the bloodmeal (C), which is then regurgitated into the skin of the mammalian host by backflow, causing the initial infection (D).

1.5.2.5: Function: Modulation of macrophages

Macrophages play a pivotal role in potential infection of the mammalian host, being capable of either elimination of *Leishmania* or the site of amastigote differentiation and replication, both of which take place within the parasitophorous vacuole. As previously discussed (Section 1.4.7), the outcome of *Leishmania* infection is influenced by the profile of cytokines influencing the immune environment, including macrophage development.

iNOS activity is associated with classically activated macrophages (CAM) whose maturation state is stimulated by Th1 cytokines TNF-α and IFN-γ, whereas arginase-1 induction is associated with alternatively activated macrophages (AAM), whose maturation state is stimulated by the Th2 cytokines IL-4, IL-10, IL-13 and IL-21 (Wang et al., 2019). Induction of a CAM-type maturation state is associated with parasite clearance, the generation of nitric oxide (NO) and antimicrobial activity. AAM induction, on the other hand appears to favour parasite survival and replication, as arginase-1 generates the polyamines urea and ornithine from L-arginine hydrolysis, a key nutritional requirement for intracellular *Leishmania* growth. It has been demonstrated in multiple models of protection that IFN-γ-generated response at the local environment is a key component of resistance to leishmaniasis (Kima and Soong, 2013).

It has been shown that sandfly bites trigger a strong delayed-type hypersensitivity (DTH) reaction in murine models of CtL (Dhaliwal and Liew, 1987), characterised by the infiltration of Th1 driving, proinflammatory cells into the local environment, which would prime macrophages towards anti-*Leishmania* activity. There is *in vitro* evidence in BALB/c mice that PSG uptake into macrophage inhibits this affect, driving host cells towards a CAM maturation state and stimulating arginase activity leading as well as increasing parasite burden, with arginase inhibition by N^{ω}-hydroxy-nor-Arginine (nor-NOHA) significantly reducing this effect. The ability of PSG to modulate macrophage activity appears to be linked to its carbohydrate structures, as de-glycosylated PSG treatment on *in vitro* macrophages failed to significantly increase arginase activity regardless of the activation or infection state of the macrophages in question. (Rogers et al., 2009).

.

1.5.3: Secreted Acid Phosphatase (ScAP)

1.5.3.1: Expression

Similar to fPPG, ScAP is a promastigote PPG product released from the parasite flagellar pocket. It is unknown whether ScAP expression is particular to a certain stage of promastigote development, but studies with *L.mexicana* would suggest that ScAP is not the predominant component of PSG (Stierhof et al., 1999), Although ScAP secretion into the culture medium has been detected in all species apart from *L.major (Lovelace and Gottlieb, 1986)*. ScAP concentration in the open flagellar pocket is up to a 1000-fold higher than in the culture medium, with release appearing from this open compartment being a slow process (Figure 13). It has been suggested that this due to the increase in concentration-dependent viscosity from the release of PPGs from a relatively small compartment (Ilg, 2000b).

It should be noted that *L.donovani* amastigotes in culture have been observed to produce and release a secreted acid phosphatase (Bates et al., 1989). This is in contrast to *L.mexicana* amastigotes, with no ScAP detected neither in culture nor in infected mouse tissue (Ilg et al., 1995).

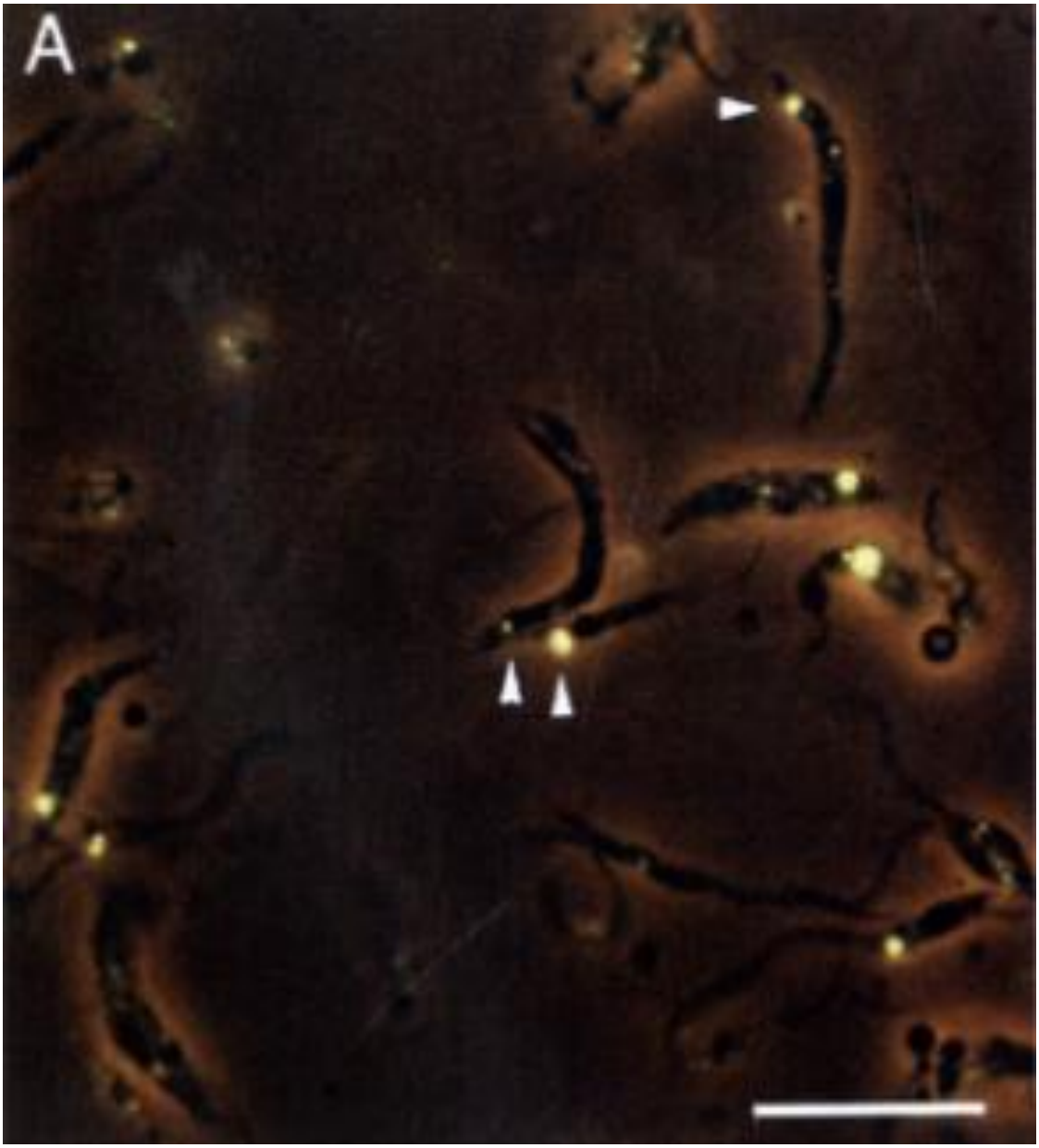

Figure 14: Microscopy of *L.mexicana* promastigotes from infected *Lutzomiya longipalpis* midguts, with additional phase contrast illumination (Stierhof et al., 1999).

Smear was probed with labelled with anti-ScAP, with a strong fluorescent signal at the flagellar pocket providing indication of ScAP localisation.

1.5.3.2: Structure

ScAP structure varies greatly between species, which will be discussed in detail in following sections. Common to ScAP from all species is a heavily glycosylated product with a serine-rich polypeptide backbone. Several studies have shown that ScAP contains the same Gal-Man-PO_4 modifications seen in LPG. This was demonstrated by binding experiments showing affinity of purified ScAP from *L.mexicana (Ilg et al., 1991a)* and *L.tropica* (Bates et al., 1990) product to monoclonal antibodies specific to LPG moieties, as well as analysis of *L.donovani* ScAP after various chemical cleavage methods (Bates et al., 1990). Experiments demonstrating a reduction in molecular mass in purified ScAP following N-Glycanase treatment demonstrates that suggest that N-linked Glycans are present in ScAP. O-Glycan linkages have also reported in *L.mexicana* ScAP, with O-linked glycans accounting for the majority (93%) of protein glycosylation (Figure 14)(Ilg et al., 1994).

L.donovani ScAP has been shown to be monomeric and/or oligomeric, in contrast to *L.mexicana* ScAP, which exhibits a filamentous structure. In addition, ScAP composition per molecular weight appears to vary between species as well, with *L.donovani* containing a much lower carbohydrate and higher protein content (57% protein, 28.5% carbohydrate, 14.5% phosphate) in comparison to *L.mexicana* ScAP (13.3% protein, 74.4% carbohydrate, 12.3% phosphate). These structural differences are reflected across other *Leishmania* species as well, with Old World *Leishmania* species (e.g. *L.tropica, L.aethiopica*) having mono/oligomeric ScAP expression in a similar manner to *L.donovani*, and New World *Leishmania* species (e.g. *L.amazonensis*) having polymeric, filamentous ScAP resembling that of *L.mexicana* (Ilg et al., 1991b, Stierhof et al., 1994), suggesting that the differences in ScAP structures could be the result of evolutionary divergence brought about by geographical isolation.

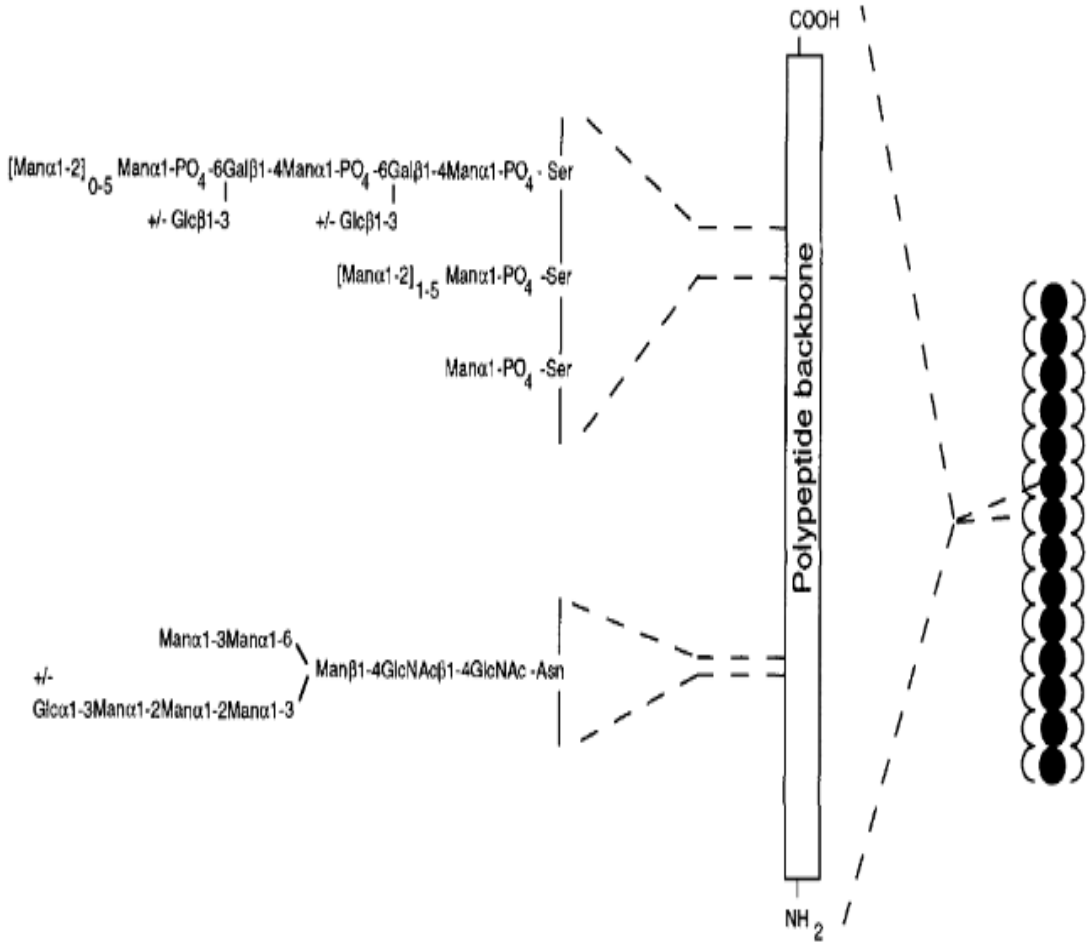

s

Figure 15: Comparison of O and N-linked glycosylation in *L.mexicana* ScAP (Ilg et al., 1994)

Both N and O-linked glycans are present in ScAP, with the former covalently linked to asparagine residues (Asn) and the latter covalently linked to serine residues (Ser) in the polypeptide backbone. The glycan motifs attached are illustrated above. Due to both the types of glycan groups associated with O-glycosylation and the abundance of serine residues in ScAP, O-linked glycosylation is responsible for the majority of phosphoglycan modifications in ScAP.

1.5.3.3: *L.mexicana* ScAP

ScAP derived from *L.mexicana* has a linear, bottlebrush structure (Figure 15). Studies on *L. mexicana* ScAP revealed a complex of two different glycoproteins (100 & 200 kDa). ScAP1 is more highly expressed that ScAP2 in the *L.mexicana* exoglycome, and are expressed from genes *lmsap1* and *lmsap2* respectively. The two genes are identical, aside from the length of a serine/Threonine-rich repeating domain near the C-terminus, which is 32 amino acid residues long in ScAP1 and 383 amino acid residues long in ScAP2 (T Ilg, 1991). It is these Ser/Thr motifs which are the target for phosphoglycosylation, and therefore the relative abundance of these residues is likely to influence the composition of ScAP (Wiese et al., 1995).

The pattern of phosphoglycosylation differs between ScAP1 & 2, with ScAP1 exhibiting approximately 40% of serine residues directly capped with α1-2-oligomannosidase (i.e. no Gal-Man-PO_4 repeats) and the remaining serine residues having a high level of modification with a single disaccharide repeat only. In contrast, ScAP2 has been show to contain a high proportion of serine residues which are modified with multiple disaccharide repeats. This is reflected in the length of the polymeric filament extending from the polypeptide backbone C-terminus, which is approximately 15-20 nm in ScAP1, but may be greater than 100 nm in length in ScAP2 (Ilg et al., 1991b).

.

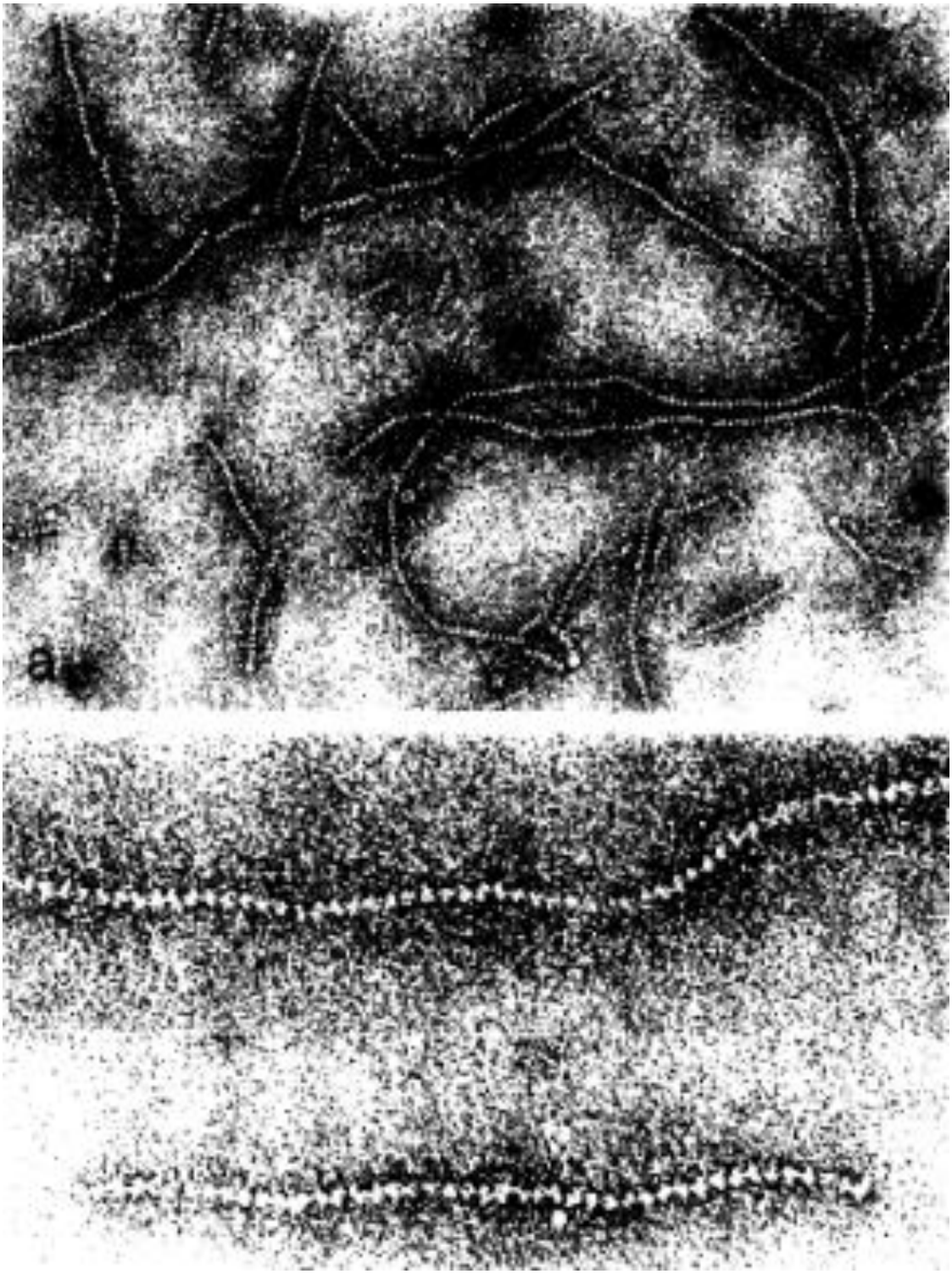

Figure 16: Imaging of *L.mexicana* ScAP (T Ilg, 1991)

L.mexicana ScAP was negatively stained with 1% aqueous uranyl acetate, with electron micrograph images taken at low (above) and high (below) magnification, exhibiting the linear, bottlebrush structure and the string-of-pearls polypeptide backbone.

1.5.3.4: *L.donovani* ScAP

L.donovani ScAP has been shown to be monomeric or oligomeric, and approximately 110 and 130 kDa in size, with gene products of approximately 95 and 107 kDa (i.e. pre-phosphoglycosylation). Studies on *L.donovani* ScAP have revealed peptides with serine/threonine-rich C-terminus regions which are heavily glycosylated (Mukhopadhyay and Mandal, 2006).

While both N and O-linked glycans are present, it is O-linked glycans which account for the majority of phosphoglycan modifications in *L.donovani* ScAP. This commonly takes the form of repeated 6Gal(β1,4) Man (α1-) PO_4 motifs, covalently bound by phosphodiester linkages to serine residues, with on average of 32 phosphorylated disaccharide repeats per modified serine. Amino acid sequence analysis suggests that phosphoglycosylation modifications appears to be highly targeted to specific serine residues. In addition, no modification of threonine residues has been observed (Lippert et al., 1999, Mukhopadhyay and Mandal, 2006).

1.5.3.5: ScAP: Function

While ScAP is secreted by and is present in all promastigote-stage *Leishmania* parasites with the exception of *L.major*, it has been determined to not be the main constituent of PSG, with the function of PSG obstruction of the infected sandfly digestive tractive and its associated effects more appropriately ascribed to fPPG instead (Stierhof et al., 1999).

The exact function of ScAP and the possible relevance of its enzymatic activity is unknown. It has been suggested that *L.donovani* ScAP may have a role in promastigote nutrition within the sandfly gut environment, due to it having a broad substrate specificity and resistance to proteases present in the digestive tract (Joshi et al., 2004). This could be a similar mechanism to that of another unicellular parasite, *Plasmodium falciparum*, which appears to produce its own ScAP in order to scavenge phosphate ions from host nutrients within the intracellular environment (Muller et al., 2010).

It has been reported that ScAP acts on parasite-derived protein kinase C (PKC) to increase parasite interaction with macrophages in ScAP-expressing

Leishmania species, facilitating invasion of the host cell. This was demonstrated by reduction of *Leishmania*-macrophage interaction in the presence of a sodium tartrate, a ScAP inhibitor, for *L.amazonensis*, but not in *Lmajor*, which expresses no ScAP (Meyer-Fernandes, July 1995).

L.mexicana mutants that do not synthesise ScAP (lmsap1/2 gene knockout) are identical to the WT strain in terms of *in vitro* growth, host cell invasion and differentiation from promastigote to amastigote-stage parasites, they lose their ability to establish progressive leishmaniasis in BALB/c mice, suggesting that ScAP is an essential virulence factor for mammalian infection (Wiese, 1998).

1.6: Innate Immune recognition of *Leishmania*

While the role of innate immunity in *Leishmania* infection has been studied, particularly within the context of relevant cell populations and their respective roles in disease resolution or immune evasion, the recognition of *Leishmania* antigens by acellular innate immune proteins, such as the classical pentraxins (CRP and SAP) and the complement system, and their resulting immunological consequences is currently not well understood. While earlier work observed a binding event of CRP to a *Leishmania* 'excreted factor' (Eilam et al., 1985), it remains an underreported field of study, particularly in light of the likely importance of the early immune response to the determination of leishmaniasis outcome.

The Raynes group (Department of Infection Biology, Faculty of Infectious and Tropical Diseases, London School of Hygiene and Tropical Medicine, United Kingdom) has made strides in elucidating the interactions between *Leishmania* products and innate immune proteins, with a particular emphasis on CRP. Initial work demonstrated binding of CRP to an atypical, non-PC ligand present on *L.donovani* LPG, as well as tentatively suggesting binding to ScAP, in a manner that was inhibited by EDTA (Culley et al., 1996). Further investigation of this phenomenon using synthetic analogues of LPG glycosylated regions determined that CRP binding was due to multiple, individually weak interactions to phosphorylated carbohydrate moieties present on LPG, with CRP binding avidity increasing when the increase in ligand length allowed multiple CRP subunit binding (Culley et al., 2000).

The potential relevance of these binding events was observed, with CRP binding to *L.donovani* metacyclic promastigotes increasing macrophage uptake (Culley et al., 1996), with subsequent work demonstrating that CRP-mediated uptake of *L.donovani* did not appear to be associated macrophage activation or parasite elimination, suggesting a potential mechanisms for silent entry into the host cell (Bodman-Smith et al., 2002a). This is in contrast to other examples of CRP opsonisation of other pathogens, such as *S.pneumoniae*, where the mechanism is strongly associated with innate resistance to infection (Simons et al., 2014).

Outside of the Raynes group, there have some reports into the interaction of acellular innate immune proteins with *Leishmania*. *In vitro* experiments with *L.chagasi* suggest that monocyte uptake of MBL-opsonised promastigotes could generate a VL-associated phenotype (Santos et al., 2001). It has also been suggested that GP63 is a virulence factor for *L.amazonensis* in murine models of infection, associated with reduction in complement-mediated lysis and an inhibition of Th1-type responses (Thiakaki et al., 2006). This is supported by findings derived from *L.major* infection of BALB/c mice, suggesting a role for GP63 in mammalian infection (Joshi et al., 1998).

The relatively narrow range of *Leishmania* species, ligands and innate immune proteins observed in existing studies suggests a need to further investigate the role of acellular components in *Leishmania* infection.

1.7: Hypothesis and aims

We hypothesise that *Leishmania* glycosylated products, such as fPPG, ScAP and LPG, are able to modulate the local innate immune environment in order to encourage *Leishmania* infection, survival and replication within the mammalian host. We propose that they exert some of their influence via interactions with the classical pentraxins CRP and SAP. This may be through the complement cascade to manipulate the downstream effects, including the modulation of dendritic cell and macrophage maturation states, recruitment of host cells and complement exhaustion. Alternatively, binding of these proteins to the *Leishmania* ligand may alter other functions of these important parasite virulence factors. We believe that increased understanding of these the innate immune interactions with these ligands will contribute to optimising vaccine and anti-parasitic therapeutics against leishmaniasis, as well as explore the potential of these immune-modulators as therapeutics against a variety of autoimmune conditions, such as rheumatoid arthritis, asthma and Systemic Lupus erythematous (SLE).

Initially, we aimed to establish the binding characteristics of a number of carbohydrate ligands, namely *Leishmania* promastigote secretory products (fPPG, ScAP and LPG), as well as other PC, PE and mannose-containing ligands, (PCBSA, PEC, Mannan), to innate immune mediators (CRP, SAP, MBL). This includes establishing the nature of the interaction, such as determination of calcium-dependency and specific binding site, as well as exclusion of possible cross-reactivity of *Leishmania* ligands in the form of impurities (e.g. establish that binding of pentraxins to *Leishmania* PSG is independent of LPG, a well-established CRP ligand). We also aimed to determine whether the interactions were common to all or specific to one or a few *Leishmania sp*.

When formation of the *Leishmania* ligand to the innate immune mediatior was demonstrated, we then investigated the ability of the complex to trigger the complement cascade, as well as determine the pathway/s activated, by binding of the complex to complement pathway initiator molecules (e.g. C1q for CP,

MBL for LP) and generation of C3 convertase downstream products (e.g. C3d, C3bi), in the absence and presence of selective pathway inihibitors.

When binding capactity of *Leishmania* ligands to pentraxins was demonstrated with ELISA and LB techniques, surface plasmon resonance (SPR) was used in order to determine the binding kinetic and affinity properties between the in a real-time and label-free environment, with novel immobilisation techniques used in order to better mimic *in vivo* antigen presentation, as well as overcome the inherent difficulties encountered with large, glycosylated molecules in SPR experiments.

CHAPTER 2

Materials and methods

2.1: Buffers

All buffers were made up using ultrapure distilled H_2O (Merck Milli-Q® Water Purification Systems), and were further purified just prior to use by vacuum filtration (Thermo Scientific Nalgene 291-4520 Bottletop Filters, 0.2um, Surfactant-Free Cellulose Acetate) into sterilised containers for SPR experiments.

2.2: ELISA

ELISA experiments were performed on 96 well microtitre plates, chosen in accordance to the hydrophobicity of the ligand of interest in order to optimise attachment to the surface.

Blocking of non-specific binding sites on the plate surface was achieved by incubation of BSA (2% w/v) and Tween 20 (0.05% v/v) in Phosphate-buffered Saline (PBS: 1.8 mM KH_2PO_4, 10 mM Na_2HPO_4, 137 mM NaCl, 2.7mM KCl, pH 7.4) for two hours at room temperature.

In between incubation stages, plates were washed thrice in HEPES-buffered saline (HBS: 20mM HEPES, 150mM NaCl, pH 7.4) with 0.5M $CaCl_2$, (HBSC), and Tween 20 (HBSCT: 0.05% v/v).

3,3′,5,5′-Tetramethylbenzidine (TMB, 0.1mg/ml) in phosphate-citrate buffer (0.05M, pH 5.0) with hydrogen peroxide (0.006% v/v) was added following HRP-conjugated antibody incubation stage, and the subsequent colour change reaction was stopped with H_2SO_4 (2 M, 15 µl). The plate was read at wavelength 450nm with subtraction of the reference wavelength at 405nm (Titertek Multiskan MCC/340).

2.3: SDS-PAGE

1-dimensional SDS-PAGE was performed under denaturing conditions with a discontinuous buffer system in accordance to a well-established, existing protocol (Laemmli, 1970).

Material of interest was separated using a Mini-PROTEAN Tetra Cell system (Bio-Rad Laboratories, USA) according to manufacturer's instructions.

1.5 mm thickness, 10-well polyacrylamide gels (66 µl volume/well) were hand-cast within glass cassettes (Mini-PROTEAN® Tetra Cell Casting Module #1658021, Bio-Rad). Resolving gels were made according to the following recipe:

12.5% Resolving gel

16.7 ml	40% w/v Acrylamide (Bis-acrylamide ratio 19:1, Severn Biotech Ltd.)
10 ml	1.5M Tris-HCl, pH 8.8
400 µl	10% w/v Sodium Dodecyl Sulphate (SDS: VWR Chemicals BDH)
75 µl	10% w/v Ammonium Persulphate (APS: Sigma-Aldrich)
12.8 ml	dH_2O

6% Resolving gel

4.5 ml	40% w/v Acrylamide
7.5 ml	1.5M Tris-HCl, pH 8.8
200 µl	10% w/v SDS
150 µl	10% w/v APS
17.8 ml	dH_2O

20 µl of N,N,N′,N′-Tetramethylethylenediamine (TEMED: Sigma-Aldrich) was added immediately prior to pouring in order to initiate polymerisation. The solution was degassed and poured using a Pasteur pipette to the desired width, after which dH_2O was carefully layered above with care taken to prevent homogenisation. Once set (approximately 30 minutes at room temperature), the dH_2O was removed and the resolving gel was overlaid with a stacking gel solution:

4% Stacking gel

2.67 ml	40% w/v Acrylamide
5.0 ml	0.5M Tris-HCl, pH 6.8
133 µl	10% w/v SDS
100 µl	10% w/v APS
12 ml	dH_2O

Polymerisation was initiated with 20 µl of TEMED solution immediately prior to pouring. Once degassed, the solution was poured via a Pasteur pipette with care taken to avoid air pocket formation. Well-combs were then inserted and the gel was left to set (approximately 30 minutes at room temperature).

Polyacrylamide gels were immersed in running buffer (25mM Tris, 192mM glycine, 0.1% w/v SDS). Samples were prepared by mixing with 2x sample buffer (65.8 mM Tris-HCl, 26.3% w/v glycerol, 1% w/v SDS, 0.01% w/v bromophenol blue, pH 6.8) at a 1:1 ratio and boiling for 2 minutes. Samples were deposited in wells via micropipette alongside commercially available, pre-stained molecular weight markers. Electrophoresis under constant current (25 mA/gel) was performed for approximately 1 hour.

2.4: Western and ligand blotting

Material was transferred from polyacrylamide gels following SDS-PAGE onto Polyvinylidene difluoride (PVDF: Immobilon-P, Millipore) membranes using a semi-dry blotting method (V20-SDB, Scie-Plas Ltd). PVDF membranes were activated by soaking in absolute methanol for 1 minute, and transferred into blotting buffer (20mM Tris-HCl, 192mM glycine, 20% v/v methanol) for 5 minutes. A cassette was assembled in the semi-dry blotting apparatus using Whatman filter paper pre-soaked in blotting buffer, in the following order:

Cathode - 4x filter papers - PVDF membrane - Polyacrylamide gel - 4 x filter papers – anode

Care was taken to prevent air pockets being trapped during cassette assembly to ensure full transfer. Blotting was performed at a constant voltage (11V) for 1.5 hours. The cassette was then disassembled, and the PVDF membranes blocked in PBS with BSA (2% w/v) and Tween 20 (0.05% v/v) at 2^0C overnight.

Membranes were then washed in TBS with Tween 20 (TBST: 0.05% v/v) three times for 5 minutes each cycle on a tube roller (Benchmark Scientific), prior to the addition of probing antibody or ligand in TBST with BSA (1%). Each probing step was performed by incubation of the PVDF membrane with the probing agent for 1 hour at room temperature on a tube roller, with washing of the membrane in TBST between each incubation as described above.

PVDF membranes probed with fluorescent agents were imaged and analysed on an Odyssey® CLx Imaging System (Li-Cor).

PVDF membranes probed with alkaline phosphatase-conjugated agents were incubated in a chromogenic substrate:

BCIP/NBT solution

32 µl	50 mg/ml 5-Bromo-4-chloro-3-indolyl phosphate (BCIP) in 100% v/v Dimethylformamide (DMF)
60 µl	50 mg/ml 4-Nitrotetrazolium Blue chloride (NBT) in 70% v/v DMF
10 ml	100mM Tris-HCl, 150mM NaCl, 1mM $MgCl_2$, pH 9.0

PVDF membranes were incubated in the NBT/BCIP substrate until sufficient colorimetric change was achieved, after which the reaction was stopped by washing in dH_2O three times, for 5 minutes each cycle on the tube roller.

2.5: Protein gel staining

Following SDS-PAGE, polyacrylamide gels were placed on an orbital shaker washed three times for 5 minutes each cycle in dH_2O in order to remove SDS. The gel was then incubated in a Coomassie Blue staining solution for 30 minutes:

Coomassie Blue solution

1g	Coomassie Brilliant Blue R-250 (Thermo Scientific)
500 ml	Methanol
100 ml	Glacial acetic acid
400 ml	dH_2O

The gel was then washed in de-staining solution (40% v/v methanol, 10% v/v glacial acetic acid, 50% v/v dH_2O) on an orbital shaker until bands were apparent against the background. The gel was then washed in dH_2O as described above and imaged with a UVP Gel Documentation system with a white light/ultraviolet transilluminator (Analytik Jena US LLC).

2.6: Carbohydrate quantification assay

Quantification of highly glycosylated material was based on an existing protocol (Masuko et al., 2005), with the entire assay being performed in a fume hood due to safety considerations. In short, carbohydrate products were hydrolysed by exposure to strong acidic conditions, with the concentration-dependent colorimetric change being elicited by the addition of phenol.

The assay was performed on acid-stable, polystyrene plates (Nunc-Immuno™ MicroWell™ 96 well solid plates, Sigma-Aldrich). A standard curve was produced using serially diluted, known concentrations of most common component monosaccharide of the material in question. The investigated material was serially diluted in dH_2O and added in replicate alongside (n=4 technical replicates).

150 µl of concentrated H_2SO_4 was added per well, mixed by pipetting and left to incubate at room temperature for 30 minutes to hydrolyse the material. 30 µl of phenol (5% w/v) was added per well. The plate was then sealed and incubated at 90^0C for 30 minutes in a water bath.

The colorimetric change was measured by absorbance at 490nm wavelength (Titertek Multiskan MCC/340).

2.7: Serum

2.7.1: Extraction

Whole blood was obtained from healthy donors under informed consent at London School of Hygiene and Tropical Medicine by the on-site phlebotomist (Carolyn Stanley, LSHTM, UK). This was covered by ethical approval (10672/RR/3680). Whole blood was collected in sterile tubes with no additive, and allowed to clot at for 30 minutes at 2 ^{o}C, followed by centrifugation at 2000g for 10 minutes at 2 ^{o}C. The serum supernatant was collected immediately after by pipetting and stored at -80^{o}C in 200 µl aliquots.

.

2.7.2: Serum depletion of pentraxins

2.7.2.1: Affinity chromatography

Whole serum was depleted of SAP, CRP or both by affinity chromatography. In short, serum was passed through a column containing solid-phase ligand to CRP, SAP or both, with the elute being collected and stored for use. Both individual (Approximately 2.5 ml per donor) and pooled (Approximately 15 ml) serum was subjected to each depletion condition (CRP-depleted, SAP-depleted, or CRP and SAP-depleted), with some whole serum retained for assessment purposes. Depletion was performed at 2 ^{o}C to reduce complement activation, and serum was stored at -80^{o}C in 200 µl aliquots.

For CRP depletion, serum was flowed through a gravity-fed column of Chicken anti-CRP IgG antibody (5ml, Econo-Pac® Chromatography Column, Bio-Rad) equilibrated in salt-containing Tris-buffered saline (Equilibration buffer: 20mM Tris-HCl, 100mM NaCl, pH 7.5).

For SAP depletion, serum was flowed through a gravity-fed column of murine anti-SAP IgG antibody (5.4D, 5ml, Econo-Pac® Chromatography Column, Bio-Rad) equilibrated in equilibration buffer.

For depletion of both CRP and SAP, serum was flowed through a gravity-fed column of phosphoethanolamine (PE-conjugated Sepharose, 5ml, Econo-Pac® Chromatography Column, Bio-Rad), equilibrated in equilibration buffer.

2.7.2.2: Magnetic bead depletion of CRP

Magnetic beads (Mobitec, 100 µl) were washed into Glycine buffer (0.1M, pH 8.3). N-(3-Dimethylaminopropyl)-N′-ethylcarbodiimide (EDC: 10 µl, 10 mg/ml) was added to the beads and left to incubate at room temperature on a rocker for 5 minutes. Chicken anti-CRP IgG antibody (1mg/ml, 25 µl,) was added and left to incubate and cross-link overnight at room temperature. Blocking of remaining active cross-linking sites was achieved by incubation in Phosphate-buffered saline (PBS: 1.8 mM KH_2PO_4, 10 mM Na_2HPO_4, 137 mM NaCl, 2.7mM KCl, pH 7.4) with BSA (1% w/v) for 1 hr at room temperature. The beads were then washed into HEPES-buffered saline (HBS: 20mM HEPES, 150mM NaCl, pH 7.4) with 0.5mM $CaCl_2$ (HBSC) and stored at 4^{o}C. Whole serum (100 µl) was vortexed with the anti-CRP beads for 30 seconds and allowed to incubate at 2 ^{o}C immediately prior to experiments..

2.7.3: Determination of pentraxin concentration

Serum concentration of CRP or SAP was determined by sandwich ELISA with antibody specific to the pentraxin in question immobilised to the plate surface. A standard curve against which absorbance values from investigated serums was generated by incubation alongside with varying dilutions of commercially available standard sera with known concentrations of CRP or SAP.

2.7.3.1: CRP-detection ELISA

Sheep anti-CRP antibody (1:4000, The Binding Site) in sodium-bicarbonate buffer (0.1 M, pH 8.3) was coated onto 96 well microtiter plates (Nunc MaxiSorp® flat-bottom, Invitrogen, Thermo Fisher Scientific). Commercially available CRP-Standard serum (MyBioSource Inc.) was added in serial dilutions to produce a standard curve, along with several dilutions of serum with unknown CRP levels in HBSC with BSA (HBSC-BSA: 1% w/v). For CRP

detection, the plate was incubated with primary antibody rabbit anti-CRP (Dako, 1:800) in HBSC-BSA, followed by HRP conjugated Goat anti-rabbit IgG (1:3000) dilution in HBSC-BSA.

2.67.3.2: SAP-detection ELISA

Rabbit Anti-SAP antibody (1:400, Calbiochem) in PBS was coated onto 96 well microtiter plates (Nunc MaxiSorp® flat-bottom, Invitrogen, Thermo Fisher Scientific) SAP-Standard serum was added in serial dilutions (1:2000 top dilution, doubling dilutions) to produce a standard curve, along with of serum with unknown SAP levels (1:3200 dilution) In HBSC-BSA. For SAP detection, the plate was incubated with murine anti-SAP antibody culture supernatant (5.4A, 1:20) in HBSC-BSA, followed by HRP conjugated Goat anti-mouse IgG at a (1:3000) in HBSC-BSA.

2.8: Pentraxins

2.8.1: Purification

CRP and SAP were purified from donated human plasma using affinity Ca^{2+} dependent affinity chromatography, followed by Ion exchange chromatography. In short, the donated plasma was passed through a phosphoethanolamine (for SAP purification) or phosphorylcholine (for CRP purification) and eluted using Ethylenediaminetetraacetic acid (EDTA)-containing buffer.

2.8.1.1: Ca^{2+} dependent affinity chromatography

For CRP affinity binding, activated, carboxylated Sepharose beads (CH-Sepharose 4B, Sigma-Aldrich) were coupled to p-aminophenylphosphorylcholine as per the manufacturer's protocol using EDC. For SAP affinity chromatography, activated, carboxylated Sepharose beads were coupled to phosphoethanolamine (PE) as per the manufacturer's protocol.

PE/PC-Sepharose beads were then equilibrated into TBSC, and packed into a column (25 ml, XK26 column, GE Healthcare). Acute-phase plasma was passed through the column at 1 ml/min at room temperature. Unbound protein was then washed off with 250 ml of TBSC. Material bound to the PE/PC-Sepharose beads were then eluted with TBS with EDTA (TBSE: 10mM) at 1 ml/min, with elute being collected in in 5 ml fractions (Biotech RediFrac Fraction Collector, Pharmacia). Fractions were read on a spectrophotometer (Optical density at 280 nm wavelength) to estimate protein content, with fractions of high material concentration being retained and pooled for further purification.

2.8.1.2: Anion Exchange Chromatography

DEAE-52, a positively-charged resin, was packed into a column (10 ml DEAE-52, XK16 column, GE Healthcare) and equilibrated in TBS. Pooled fractions from the previous stage (approximately 30 ml) were diluted in dH_2O (2:1 v/v) and passed through the column at 1 ml/min, with unbound protein being washed off with TBS (60 ml). Material was eluted from the column using a linear

gradient from equilibration buffer into high ionic strength TBS (20mM Tris-HCl, 500mM NaCl, pH 7.5) at 1 ml/min. Fractions were collected (Biotech RediFrac Fraction Collector, Pharmacia). Fractions were read on a spectrophotometer (Optical density at 280 nm wavelength) to estimate protein content, with fractions of high material concentration being retained and pooled. Purified protein was dialysed into TBS to remove excess salt.

2.8.2: Biotinylation

2.8.2.1: CRP-biotin

Biotinylation of CRP was performed by John Raynes (Department of Infection Biology, London School of Hygiene and Tropical Medicine, United Kingdom) and donated for experimental use.

Purified CRP (1mg/ml) was dialysed into PBS. 6 µl of an NHS-ester activated biotinylation reagent conjugated to a 30.5 Angstrom long chain spacer (10mM, Biotin-LC-LC-NHS, Cayman Chemicals) in Dimethyl Sulfoxide (DMSO) was added per ml of CRP and incubated at room temperature for 1 hour. A relatively low ratio of label to CRP was used in order to avoid excessive biotinylation and potential obstruction of binding activity.

Material was then dialysed with dialysis tubing (Spectrum™ Spectra/Por™ 1 RC Dialysis Membrane Tubing: 6000 to 8000 Dalton Molecular Weight Cut-Off) into PBS overnight at 24^{o}C. The material was diluted into HBSC, re-purified via Ca^{2+} dependent affinity chromatography on a phosphorylcholine-Sepharose column, and eluted with HBS with EDTA (HBSE: 10mM) in a similar manner to unmodified CRP purification (Section 2.8.1.1).

The concentration was determined by absorbance spectrophotometry at 280 nM wavelength (NanoDrop™ 1000 Spectrophotometer, Thermo Fisher Scientific) and purity and identity validated by Coomassie blue staining (Section 2.5) and Western blotting (Section 2.4) after SDS-PAGE (Section 2.3). Material was then dialysed into TBSC at pH 8.0, aliquoted and stored at -80^{0}C.

2.8.2.2: SAP-biotin

Purified SAP (1 mg) was dialysed into a variant of PBS at pH 7.6 with 0.5M NaCl. Sodium metaperiodate was added to a final concentration of 2 mM in solution, and incubated on ice within a dark container to prevent photodegradation for 3 minutes. The solution was then was passed through a gel filtration column (PD10, GE Healthcare) equilibrated in PBS at pH 7.2 in order to remove excess periodate. Biotin LC hydrazide (Cayman Chemicals) was added to a final concentration of 5mM in solution, and left to incubate at 2 hours at room temperature.

Material was then dialysed with dialysis tubing (Spectrum™ Spectra/Por™ 1 RC dialysis membrane tubing: 6000 to 8000 Dalton molecular weight cut-off) into Tris-buffered-saline (10mM Tris-HCl, 0.15M NaCl, pH 8.0) overnight at 2^{o}C. The material was repurified via Ca^{2+} dependent affinity chromatography on a phosphoethanolamine-sepharose column, and eluted with TBSE at pH 8.0, in a similar manner to unmodified SAP purification (Section 2.8.1.1).

The concentration was determined by absorbance spectrophotometry at 280 nM wavelength (NanoDrop™ 1000 Spectrophotometer, Thermo Fisher Scientific) and validated by Coomassie blue staining and Western blotting after SDS-PAGE. Material was then dialysed into TBSC at pH 8.0, aliquoted and stored at -80^{o}C.

2.9: Pentraxin ligands

2.9.1: Phosphorylcholine-conjugated bovine serum albumin (PCBSA)

Endotoxin-free Bovine Serum Albumin was dissolved in Na_2HPO_4 (50 mM, pH 4.5) at a concentration of 20 mg/ml. An equal volume of the crosslinker 1-ethyl-3 (3-dimethylaminopropyl) carbodiimide (EDC, 1% w/v) and para-amino phenyl phosphorylcholine (4 mg/ml) was added, and the solution left to incubate at room temperature overnight. The solution was dialysed for 2 hours in dialysis tubing (Spectrum™ Spectra/Por™ 1 RC Dialysis Membrane Tubing: 6000 to 8000 Dalton Molecular Weight Cut-Off) against 500ml of PBS at room temperature. Conjugated PCBSA (100mg) was separated by size-exclusion chromatography by gravity-flow through a gel filtration column (Sepharose® CL-4B, 85cm x 2.2 cm column) equilibrated in PBS into monomeric and polymeric products. PCBSA concentration was determined by absorbance spectrophotometry at 280 nM wavelength (NanoDrop™ 1000 Spectrophotometer, Thermo Fisher Scientific) to estimate protein concentration.

Monomeric and polymeric PCBSA fractions were subjected to SDS-PAGE (Section 2.3) on polyacrylamide gels (4% acrylamide stacking gel layer 12.5% Resolving gel layer). The Molecular weight standards used was Precision Plus Kaleidoscope (Bio-Rad). Gels were subsequently stained with Coomassie blue (Section 2.5) or subjected to Western Blotting (Section 2.4) For CRP binding and detection, membranes were incubated in TBSCT with BSA (1% w/v), Tween 20 (0.05% v/v), 0.5mM $CaCl_2$ plus either 5µg/ml CRP. CRP was detected with a combination of rabbit α-CRP (Dako, 1:1000) followed by IRDye® 800CW goat anti-rabbit IgG (Li-Cor) or biotinylated α-CRP followed by IRDye® 680RD Streptavidin (Li-Cor).

2.9.2: Phosphoethanolamine cellulose (PEC)

2.9.2.1: Generation

Creation of the PEC-overexpressing form of *Escherichia Coli* was done by Lynette Cegelski (Department of Chemistry, Stanford University, Stanford, CA 94305, USA) (Thongsomboon et al., 2018) who kindly donated the K-12 non-pathogenic (CL1) strain .

K-12 strain AR-3110csg *Escherichia Coli* was grown in Luria-Bertani culture overnight. Colonies were formed by spotting 5 µl of culture onto agar plates containing YESCA media (10g caramino acid, 1g yeast extract, 20g agar), transformed into a PEC-overexpressing form with plasmid PMMB956, and selected for by resistance to ampicillin (100 µM), which was supplemented into the YESCA media when it reaches 50^{o}C. A colony from the ampicillin plate was chosen and spread over YESCA plates containing 250 µM Isopropyl β-D-1-thiogalactopyranoside (IPTG), and left to grow at 25^{o}C until smooth colonies were visible.

2.9.2.2: Purification

Purification of PEC was performed by John Raynes (Department of Infection Biology, London School of Hygiene and Tropical Medicine, United Kingdom).

Colonies and biofilm were scraped off the agar plates, suspended in Tris-buffered saline (10mM, 7.4), and homogenised in a Polytron homogeniser (Shear for 1 minute, 2 minutes rest, 5 cycles). Solution was centrifuged (5000g, 10 minutes 4^{o}C), with the supernatant being retained. This was repeated twice more, with the pellet being resuspended in TBS, and the supernatant being retained and pooled each time. The pooled supernatant was dialysed overnight in Spectrum™ Tubing, 100 kDa molecular weight cut-off (Spectra/Por™ Biotech) into distilled H_2O overnight. Material was then freeze-thawed and centrifuged (10000g, 4^{o}C, 20 minutes). The pellet was resuspended in 4% (w/v) SDS overnight, then washed in PBS three times by centrifugation.

Quantification was done using the phenol-sulphuric acid assay previously described using glucose as a standard (Section 2.6).

2.10: Promastigote Secretory Gel (PSG)

Semi-purified PSG was obtained from Matthew Rogers (Department of Infection Biology, London School of Hygiene and Tropical Medicine, United Kingdom). Late log/early-stationary phase promastigote cultures were established using parasites stored in liquid nitrogen (10^8 cells: Wild type *L. mexicana* M379*, L.major* LV39*, L.tropica* K27*, L.aethiopica* LV100*, L.panamensis, L.amazonensis* M2269*, L.infantum* IPT1 and *Ldonovani* LV9*.* PSG was semi-purified using anion exchange chromatography followed by ultracentrifugation.

2.10.1: Generation

Culturing of *Leishmania* parasites was performed by Matthew Rogers (Department of Infection Biology, London School of Hygiene and Tropical Medicine, United Kingdom).

Promastigote cultures were established using parasites stored in liquid nitrogen (10^8 cells: *L mexicana* (M379 WT, LPG1$^{-/-}$, LPG2$^{-/-}$, ScAPKO, ScAPAB), Late log/early-stationary phase *L.mexicana* promastigotes were grown up in culture media by and the supernatant collected by Matthew Rogers (Department of Infection Biology, London School of Hygiene and Tropical Medicine, United Kingdom). Further description of the *L.mexicana* mutant strains were provided later (Section 3.2.4: LPG1$^{-/-}$ & LPG2$^{-/-}$. Section 3.2.5: ScAPKO & ScAPAB).

2.10.2: Purification

2.10.2.1: Anion Exchange Chromatography

The culture supernatant (approximately 250ml) was flowed through a column (XK16, GE Healthcare) of DEAE-52, a positively charged resin (10 ml), equilibrated in a low ionic strength Tris-buffered saline (Equilibration Buffer: 20mM Tris-HCl, 100mM NaCl, pH 7.5) at a rate of 2 ml/min. The column as then washed with 200 ml of equilibration buffer to remove unbound protein at a rate of 120ml/hr. Material bound to DEAE-52 was eluted from the column using a

high ionic strength Tris-buffered saline (500mM NaCl, 20mM Tris-HCl, pH 7.5) at a rate of 60ml/h. Fractions (3ml) were collected in bijou tubes (Biotech RediFrac fraction collector, Pharmacia). Fractions were read on a spectrophotometer (optical density at 280 nm wavelength) to estimate protein content, with fractions of high material concentration being retained and pooled for further purification.

2.10.2.2: Hydrophobic Interaction chromatography

Retained, PSG-containing fractions from anion exchange chromatography were pooled and adjusted to 1M ammonium sulphate via dilution with concentrated ammonium sulphate solution (10M NH_2SO_4, 1:9 v/v ratio relative to material). The material was then flowed through a column (Econo-Pac® chromatography column, Bio-Rad) of Hydrophobic Interaction media (5 ml, Octyl−Sepharose® 4 Fast Flow, Sigma-Aldrich) that has been equilibrated in ammonium sulphate and EDTA-containing Tris-buffered saline (20mM Tris-HCl, 1M NH_2SO_4, 5 mM EDTA, pH 7.5). This was followed by low ionic strength Tris-buffered saline (10 ml, 20mM Tris-HCl, 100mM NaCl, pH 7.5), Tris-buffered saline (20 ml, 20mM Tris-HCl, pH 7.5) and Propan-1-ol (20%, 70% v/v). Fractions were collected and pooled according to their buffer type in bijou tubes (Biotech RediFrac Fraction Collector, Pharmacia). Fractions were read on a spectrophotometer (Optical density at 280 nm wavelength) to estimate protein content, with fractions of high material concentration being retained and pooled for further purification.

2.10.2.3: Ultracentrifugation

Following sequential anion exchange and hydrophobic interaction chromatography, material was ultra-centrifuged at 42,000 RPM (Beckman-Coulter Optima L-90K, Beckman-Coulter type 90 rotor, 100000G, 4^{o}C in vacuum in Quick-Seal®, Polypropylene 13.5 ml tubes, no brake). The supernatant was decanted and the pellet was re-suspended in distilled H_2O. PSG material was stored at -80^{o}C in 20 µl aliquots.

2.10.3: Quantification and Verification

Quantification was done using the phenol-sulphuric acid assay previously described using mannose as a standard (Section 2.6), in addition to weighing of purified product following lyophilisation with a nitrogen evaporator.

PSG was subjected to SDS-PAGE (Section 2.3) on polyacrylamide gels (4% Stacking gel layer, 6% Resolving gel layer) with an extended stacking gel layer for better resolution of large molecular products (approximately 20 mm). The Molecular weight standards used was Color Prestained Protein Standard, Broad Range (10-250 kDa, New England Biolabs).

Monoclonal antibodies LT6 and LT15, which were specific for the repeating phosphorylated disaccharide Gal-Man-PO_4 common to *Leishmania* glycosylated products, was kindly donated by Thomas Ilg (Max Planck Institute for Biology, Tubingen, Germany) in the form of hybridoma supernatants. Ligand blotting was performed as previously described (Section 2.4). Membranes were incubated in TBSC with Tween 20 (TBSCT: 0.05% v/v) and BSA (1% w/v), plus the murine LT6 antibody (1:4 dilution). LT6 binding was detected with an alkaline phosphatase conjugated goat anti-mouse antibody (Goat Anti-Mouse IgG-AP Conjugate #1706520, Bio-Rad, 1:1000).

2.10.4: Biotinylation

L.mexicana WT PSG was dissolved in dH_2O to a concentration at 1 mg/ml, and mixed with an equal volume of carbonate buffer (50mM, pH 9.6). 1µl of NHS-LC biotin (75mM in 100% DMSO, EZ-Link™ NHS-LC-Biotin, Thermo Scientific) was added and left to incubate at room temperature for 10 minutes, after which the addition step was repeated once more. The solution was left to incubate at room temperature for one hour, after which the reaction was stopped with excess ethanolamine (1M).

In order to separate PSG-biotin from the excess unreacted and/or hydrolysed biotin molecules, the solution was subjected to anion exchange chromatography. The solution was gravity-flowed through a mini-column (Poly-

Prep® Chromatography Column, Bio-Rad) packed with the positively charged resin DEAE-52 (1ml) equilibrated in equilibration buffer (20mM Tris-HCl, 100mM NaCl, pH 7.5). The Column was washed with 10 ml of equilibration buffer to remove unbound material. PSG-biotin was eluted from the column using 5 ml of high ionic strength Tris-buffered saline (20mM Tris-HCl, 500mM NaCl, pH 7.5). The elute was collected, dialysed with dialysis tubing (Spectrum™ Spectra/Por™ 1 RC Dialysis Membrane Tubing: 6000 to 8000 Dalton Molecular Weight Cut-Off) into Tris-buffered saline (10mM Tris-HCl, 7.4) to remove excess salt and stored at -80^{o}C in 20 µl aliquots.

Quantitation of PSG-biotin was performed in the same manner as for unmodified PSG (section 2.9.3).

To ensure CRP binding capacity of PSG was not affected by biotinylation, a CRP-binding ELISA was performed (Section 2.2). *L.mexicana* PSG and PSG-biotin (biotin (2.0-0 µg/ml) in PBS was coated onto 96 well microtiter plates (Immulon™ 2 HB 96-Well Microtiter EIA Plate, ImmunoChemistry Technologies, LLC). CRP (2.0 µg/ml) in HBSC-BSA was added and the plates were incubated at room temperature for 1 hour. For CRP detection, the plate was incubated with primary antibody rabbit anti-CRP (Dako,1:800) in HBSC-BSA, followed by HRP conjugated Goat anti-rabbit IgG (1:3000) in HBSC-BSA.

2.11: Lipophosphoglycan

2.11.1: Generation

L.mexicana parasites were grow in culture to metacyclic and nectomonad stages, centrifuged, and the supernatant decanted by Matthew Rogers (Department of Immune Biology, London School of Hygiene and Tropical Medicine). Cell pellets were donated for LPG purification and stored at -80ºC.

2.11.2: Purification

LPG was purified from *L.mexicana* promastigote cell pellets by a solvent extraction method adapted from an existing protocol (Mcconville et al., 1987).

Cell pellets were pooled into solvent-resistant centrifuge tubes (Nalgene™ Oak Ridge High-Speed Centrifuge Tubes, Thermo Scientific). Initial delipidation of the was achieved by resuspension of pellets in 5 ml of chloroform-methanol solution (1:2 v/v ratio), followed by 5 minutes of bath sonication (5 minutes) and 10 minutes of centrifugation (PK120 Centrifuge, ALC) at 2200g. This was performed twice with the supernatant decanted and the pellet being retained.

The pellet was further delipidated by suspension in 5 ml of Chloroform-methanol-water solution (5:10:4 v/v ratio), followed by 5 minutes of bath sonication and 10 minutes of centrifugation at 3000g, with the supernatant being decanted. This was performed thrice with the supernatant decanted and the pellet being retained.

The pellet was then dried in a nitrogen evaporator (37ºC), resuspended in butanol (9%, 0.5 ml), bath sonicated (5 minutes) and centrifuged (Max. speed, 15 minutes). This was performed twice, with the LPG containing supernatant fractions being pooled, dried in a nitrogen evaporator (37ºC) and resuspended in dH_2O. LPG was stored at -80ºC in 20 µl aliquots.

2.11.3: Quantification and verification

LPG was quantified via a phenol-sulphuric acid assay (Section 2.6), with mannose (Sigma-Aldrich) used to produce the standard.

LPG was subjected to SDS-PAGE (Section 2.3) on polyacrylamide gels (4% Stacking gel layer, 12.5% Resolving gel layer). The Molecular weight standards used was Color Prestained Protein Standard, Broad Range (10-250 kDa, New England Biolabs).

Western Blotting was performed with the murine LT6 antibody previously described (Section 2.10.3, 1:4 dilution). LT6 binding was detected with an alkaline phosphatase conjugated goat anti-mouse antibody (goat anti-mouse IgG-AP conjugate #1706520, Bio-Rad, 1:1000).

2.11.4: Biotinylation

L.mexicana LPG from nectomonad or metacyclic stage promastigotes was dissolved in sodium acetate buffer (0.1M CH_3COONa, pH 5.5) to a concentration of 2mg/ml. LPG was oxidised by addition of sodium-meta-periodate (in sodium acetate buffer, pH 5.5) to a concentration of 20mM of the oxidising agent, followed by incubation for 30 minutes at 4^{o}C, with the container wrapped in foil to prevent photodegradation. Excess periodate was removed by dialysis in dialysis tubing (Spectrum™ Spectra/Por™ 3 RC Dialysis Membrane Tubing, 3500 Dalton molecular weight cut off) into PBS.

An NHS-ester activated biotinylation reagent conjugated to a long chain spacer (EZ-Link™ NHS-LC-biotin, Thermo Fisher Scientific) in DMSO was added to a final concentration of 50mM to provide an approximately 10-fold excess of the biotinylating agent, followed by incubation for 40 minutes at room temperature. Excess biotin removed by dialysis (Spectrum™ Spectra/Por™ 3 RC dialysis membrane tubing 3500 Dalton MWCO) into PBS LPG-biotin was stored at -80^{o}C in 20 µl aliquots.

2.12: Pentraxin binding to *Leishmania* PSG

2.12.1: Western/ligand blot and protein gel staining

PSG and PCBSA was subjected to SDS-PAGE as previously described (Section 2.3) on a 4% Stacking gel layer in combination with a 6% and 12.5% Resolving gel layer for PSG and PCBSA respectively. PSG was subjected to SDS-PAGE on polyacrylamide gels with an extended stacking gel layer for better resolution of large molecular products (approximately 20 mm). The molecular weight standards used were Color Prestained Protein Standard, broad range (10-250 kDa, New England Biolabs) for PSG imaging and Precision Plus Kaleidoscope (Bio-Rad) for PCBSA imaging.

Gels were then stained with Coomassie blue (Section 2.5) or transferred to PVDF membranes for Ligand blotting (Section 2.4).

For CRP binding and detection, membranes were incubated with CRP (5µg/ml). CRP binding to immobilised CRP was detected with a combination of rabbit α-CRP (Dako, 1:1000) followed by IRDye® 800CW Goat anti-Rabbit IgG (Li-Cor) or biotinylated anti-CRP followed by IRDye® 680RD Streptavidin (Li-Cor). SAP binding to immobilised PSG was detected with biotinylated anti-SAP (1:1000, generated in-house by the Raynes Laboratory) followed by IRDye® 680RD Streptavidin (Li-Cor).

2.12.2: PSG-pentraxin ELISA

PSG (0-3 µg/ml) in PBS was coated onto 96 well microtiter plates (Immulon™ 2 HB 96-Well Microtiter EIA Plate, ImmunoChemistry Technologies, LLC) (Section 2.2).

CRP (0-3 µg/ml) in HBSC-BSA was added and the plates were incubated at room temperature for 1 hour. For inhibition assays, PC chloride-calcium salt (10mM, Sigma-Aldrich) or EDTA (10mM) was added at the CRP incubation stage. For CRP detection, the plate was incubated with primary antibody rabbit anti-CRP (Dako: 1:800) dilution followed by HRP-conjugated Goat anti-rabbit IgG at a (Bio-Rad, 1:3000) dilution in HBSC-BSA.

SAP (0-3 µg/ml) in HBSC-BSA was added and the plates were incubated at room temperature for 1 hour. For SAP detection, the plate was incubated with murine anti-SAP antibody (5.4A, 1:20) followed by HRP conjugated Goat anti-mouse IgG (Bio-Rad, 1:3000) in HBSC-BSA.

2.13: Complement assays

2.13.1: C1q capture assay

We adapted an existing immune complex capture assay(Ahmed et al., 2016) in order to investigate the complexes formed between CRP and different CRP ligands, including PSG and PC-containing molecules (Section 2.2).

Purified C1q (Calbiochem, 10µg/ml0 was coated onto 96 well microtiter plates (Immulon 4 HBX, Thermo Fisher Scientific) at 4ºC overnight. Plates were incubated with BSA (3% w/v) and Tween 20 (0.05% v/v) in PBS for non-specific site blocking at room temperature for 2 hours.

Serum was diluted (1:20v/v) with CRP (1µg/ml) and BSA (1% w/v) in veronal-buffered saline (VBS) with 0.15mM $CaCl_2$ and 0.5mM $MgCl_2$, with or without EDTA (10mM). CRP ligand (PSG, PCBSA) was added at a range of concentrations (3-0 µg/ml), and the plate was incubated at room temperature for 1 hour. Detection step was performed with a sheep anti-CRP conjugated with horseradish peroxidase (1:2000).

2.13.2: C1q binding assay

The ligand was immobilised onto an appropriate 96 well microtiter plate surface (e.g. polyvinyl surface for hydrophobic LPG attachment) (Section 2.2).

CRP and SAP depleted serum was diluted at (1:30) with SAP or CRP at a range of concentrations (2.0 - 0 µg/ml) in HBSC-BSA. The plate was incubated at room temperature for 1 hour.

C1q binding was detected with a biotinylated anti-C1q antibody generated in-house (John Raynes, Department of Immune Biology, LSHTM, UK) and HRP-conjugated streptavidin (1:15000) (MyBioSource).

2.13.3: C3d Deposition assay

To assess C3 convertase formation, an existing protocol to detect the C3 convertase downstream product C3d was adapted (Ahmed et al., 2016). *L.infantum* PSG (4 µg/ml) and PCBSA (0.4 µg/ml) was diluted in PBS and immobilised on 96 well microtiter plates (Immulon™ 2 HB 96-Well Microtiter EIA Plate, ImmunoChemistry Technologies, LLC) (Section 2.2). Ligand concentration was chosen to allow equivalent CRP binding as determined by previous CRP-ligand ELISA (Section 2.12.2).

In order to prevent complement activation until the start of the experiment, all serum additions were done with the reagents, serum and microtiter plate on ice (0^{o}C). Donor serum was added to the wells (1:100 dilution) in GVBSCaMg (VBS with 0.2% v/v gelatin, 0.15mM $CaCl_2$ and 0.5mM $MgCl_2$), with or without additional purified CRP (0.4 µg/ml). C3d deposition with or without purified CRP was also analysed in the presence or absence of the non-specific ion chelator EDTA (10mM), and the specific calcium chelator EGTA (10mM) plus 0.5mM $MgCl_2$.

Plates were brought up to a uniform temperature at the same time in a water bath (37^{o}C, 30 second immersion) and were left in an incubator (37^{o}C) for 20 minutes, with undeposited complement components rapidly washed out of the wells in order to stop the reaction.

For C3d detection, plates were incubated with primary biotinylated anti-C3d antibody (1:1000) followed by HRP conjugated streptavidin (1:15000) in HBSC-BSA.

2.13.4: C3bi Deposition assay

L.mexicana PSG (2 µg/ml) was diluted in PBS and immobilised on 96 well microtiter plates (Immulon™ 2 HB 96-Well Microtiter EIA Plate, ImmunoChemistry Technologies, LLC). Ligand concentration was chosen to allow equivalent CRP binding as determined by the previous CRP-ligand ELISA (Section 2.12.2).

In order to prevent complement activation until the start of the experiment, all serum additions were done with the reagents, serum and microtiter plate on ice (0^{o}C). Donor serum was added to the wells (1:100 dilution) in GVBSCaMg (VBS with 0.2% v/v gelatin, 0.15mM $CaCl_2$ and 0.5mM $MgCl_2$), with or without additional purified CRP (0.4 µg/ml). C3d deposition with or without purified CRP was also analysed in the presence or absence of the non-specific ion chelator EDTA (10mM), and the specific calcium chelator EGTA (10mM) plus 0.5mM $MgCl_2$.

Plates were brought up to a uniform temperature at the same time in a water bath (37^{o}C, 30 second immersion) and were left in an incubator (37^{o}C) for 20 minutes, with undeposited complement components rapidly washed out of the wells in order to stop the reaction.

For C3bi detection, the plate was incubated with primary biotinylated anti-C3bi mouse antibody (Cedarlane, 1:1000) followed by horseradish peroxidase-conjugated streptavidin (1:15000) in HBSC-BSA.

2.14: PSG-MBL binding ELISA

PSG (*L. aethiopica, L.donovani, L.infantum, L.panamensis, Lmajor, L.mexicana, L.tropica,* and *L.amazonenesis*, 2.0 µg/ml in PBS) and mannan (Sigma-Aldrich: 2.0 µg/ml in PBS) was coated onto 96 well microtiter plates (Immulon™ 2 HB 96-Well Microtiter EIA Plate, ImmunoChemistry Technologies, LLC) (Section 2.2) overnight at 4^{o}C.

Various concentrations of MBL (2.0 – 0 µg/ml) were added in HBSC-BSA, and the plate was incubated at room temperature for 1 hour. For Ca^{2+} dependency ELISA EDTA (10mM) was added at the MBL incubation stage.

For MBL detection, the plates were incubated with primary antibody biotinylated rabbit anti-MBL (1:1000, Dako), followed by HRP-conjugated streptavidin (1:15000) dilution in HBSC-BSA.

2.15: Characterisation of LPG interactions with pentraxins

2.15.1: SDS-PAGE, western and ligand blotting

SDS-PAGE and semi-dry blotting of *L.mexicana* LPG from nectomonad and metacyclic-stage parasites was performed in the same manner as previously described (Section 2.3).

Ligand blotting was performed as previously described (Section 2.4).

CRP binding was assessed by incubation of PVDF membranes with CRP-biotin (Section 2.8.2.1, 5 µg/ml), followed by alkaline phosphatase-conjugated streptavidin (STAR6B, Bio-Rad, 1:3000) in HBSC-BSA.

SAP binding was assessed by incubation of PVDF membranes with SAP-biotin (Section 2.8.2.2, 5 µg/ml), detected by alkaline phosphatase-conjugated streptavidin (STAR6B, Bio-Rad, 1:3000) in HBSC-BSA.

2.15.2: LPG-pentraxin ELISA

Metacyclic and Nectomonad-stage *L.mexicana* LPG (1.0 µg/ml) was coated onto 96 well microtiter plates (Corning™ 96-Well Clear PVC Assay Microplates) (Section 2.2).

For assessment of direct binding of pentraxin to LPH, CRP or SAP (2.0 – 0 µg/ml) was deposited in HBSC-BSA, and the plate was incubated at room temperature for 1 hour.

For specific binding site and Ca^{2+}dependency assessment, Gal-Man-PO_4 specific antibody LT6 (1:10) or EDTA (10mM) was added at the CRP incubation stage respectively.

For CRP-SAP cross-inhibition ELISA, the detected ligand, CRP or SAP (0.5 µg/ml) was added to wells in the presence of varying concentrations of the competing pentraxin (20-0 µg/ml) in HBSC-BSA

For CRP detection, the plate was incubated with rabbit anti-CRP antibody (Dako, 1:1000), followed by HRP conjugated Goat anti-rabbit IgG (Bio-Rad, 1:3000) in HBSC-BSA. For SAP detection, the plate was incubated with primary antibody murine anti-SAP antibody (5.4D, 1:1000) followed by Donkey anti-mouse IgG (Bio-Rad, 1:3000) in HBSC-BSA.

2.16: LPG-PSG ELISA

Metacyclic and Nectomonad-stage *L.mexicana* LPG (1.0 µg/ml) was coated onto 96 well microtiter plates (Corning™ 96-Well Clear PVC Assay Microplates) (Section 2.2).

L.mexicana PSG-biotin (0.5 µg/ml) was incubated with immobilised LPG in the presence of varying concentrations of CRP (0 – 10 µg/ml) in HBSC-BSA, in the presence of 0.5mM $CaCl_2$ or 10mM EDTA.

PSG-biotin binding was detected by incubation with HRP-conjugated streptavidin (1:15000 dilution) in HBSC-BSA

2.17: Surface plasmon resonance analysis of pentraxin interaction with PSG

2.17.1: PSG immobilisation

In order to optimise coupling of the ligand to the chip surface, pH scouting of *L.mexicana* WT PSG (10 µg/ml) in acetate buffer (5mM: pH 4.0, 4.5, 5.0 and 5.5) was performed, with pH 5.0 being chosen for the ligand immobilisation method described below.

2.17.1.1: Amine coupling of PSG

Surface Plasmon Resonance was performed on a BIACORE 3000 (GE Healthcare) equipped with a research-grade C1 sensor chip (Biacore). *L.mexicana* WT PSG was immobilized via amine coupling of amines likely in the protein component of PSG to the carboxyl on the C1 surface. Flow cells were activated for 7 min with a 1:1 mixture of 0.1 M NHS (N-hydroxysuccinimide) and fresh 0.1 M EDC (3-(N,N-dimethylamino) propyl-N-ethylcarbodiimide) at a flow rate of 5 µl/min. The ligand, *L.mexicana* WT PSG (50 µg/ml) in acetate buffer (5mM, pH 5.0) was flowed over (5 µl/min) and immobilized on the test flow cell (500 RU). Control flow cell was left blank and both surfaces were blocked with a 7 min injection of ethanolamine (1M, pH 8.3).

2.17.1.2: Analysis of pentraxin binding

CRP or SAP in HBSPC (10 mM HEPES, 150 mM NaCl, 0.005% v/v P20, 0.5mM $CaCl_2$, pH 7.4) was injected over the two flow cells (20 µg/ml) at various flow rates 5, 10 and 20 µl/min) at a temperature of 25°C. The complex was allowed to associate for 300s and dissociate 1200s.

The surfaces were regenerated with a 10s injection of EDTA-containing HEPES buffer (HSBPE: 10 mM HEPES, 150 mM NaCl, 0.005% P20, 0.5mM EDTA, pH 7.4). Data was collected at a rate of 1 Hz. The data were fit to a simple 1:1 interaction model using the global data analysis option available within BiaEvaluation 3.1 software.

2.17.2: Desthiobiotin attachment for regenerable surface

A method by which would allow for selective regeneration (i.e. removal of fluid-phase analyte from immobilised, solid-phase ligand) and stripping (i.e. removal of ligand from chip surface) was devised by John Raynes (Department of Infection Biology, Faculty of Infectious and Tropical Diseases, London School of Hygiene and Tropical Medicine, UK).

In short, desthiobiotin was directly coupled to the chip surface, allowing for subsequent coupling to avidin-type molecules (e.g. streptavidin, neutravidin, ultravidin). As desthiobiotin binds to avidins with lower avidity in comparison to biotinylated molecules, this allows for indirect coupling of biotinylated ligands to the chip surface via the avidin spacer which can be selectively removed with guanidine thiocyanate (6M) between analysis. The desthiobiotin-coupled surface was left chemically intact, allowing for sequential reapplication of the avidin spacer and desired biotinylated ligand. Neutravidin was chosen as the avidin spacer due to the reduced nonspecific binding associated with the lack of RYD site and reduced glycosylation in comparison to other candidates. In addition, neutravidin has a near-neutral isoelectric point, optimising ligand coupling.

2.17.2.1: Amine coupling of desthiobiotin

Surface Plasmon Resonance was performed on a BIACORE 3000 (GE Healthcare) equipped with a research-grade C30M sensor chip (Xantec). This was a carboxylated hydrophilic polymer suitable for high molecular weight ligands. Chosen flow cell surfaces were activated for 7 min with a 1:1 mixture of 0.1 M NHS (N-hydroxysuccinimide) and 0.1 M EDC (3-(N, N-dimethylamino) propyl-N-ethylcarbodiimide) at a flow rate of 5 µl/min. Aminodesthiobiotin (20mM in DMSO) was diluted to 0.5mM in sodium maleate buffer (10mM, pH 6.8), and flowed over the surface at 2 ul/min for 30 min (150 RU). Excess activated surface NHS was deactivated by addition of 1M ethanolamine (pH 8.3, 5 ul/min, 420s) All capture and test stages were performed at 25^{o}C

2.17.2.2: Analysis of PSG binding to captured CRP-biotin

Neutravidin (10 µg/ml) in calcium-containing HEPES buffer (HBSPC: 10 mM HEPES, 0.5 mM CaCl, 150 mM NaCl, 0.005% P20, pH 7.4) was injected at injected at 10 µl/min for 1 minute (150 RU) on both test and control flow cell. The ligand, CRP-biotin (10 µg/ml) in in HBSPC was immobilized on test flow cell alone (150 RU).

PSG analyte at a range of concentrations (0.16 - 20 µg/ml) in HBSPC was injected over the two flow cells at various flow rates at a temperature of 25°C. The complex was allowed to associate for up to 300s and dissociate for up to 1200s.

The surfaces were regenerated to remove calcium-dependent pentraxin binding with a 10s injection of EDTA-containing HEPES buffer (HSBPE: 10 mM HEPES, 150 mM NaCl, 0.005% P20, 0.5mM EDTA, pH 7.4). Data was collected at a rate of 1 Hz. The data was fitted to a simple 1:1 interaction model using the global data analysis option available within BiaEvaluation 3.1 software.

2.17.2.3: Analysis of CRP binding to captured PSG

Desthiobiotin was amine-coupled to the surface of a C30M chip and this was then loaded with neutravidin as described previously (Section 2.17.2.1). The ligand*, L.mexicana* PSG-biotin (20 µg/ml) in sodium acetate buffer (10 mM, pH 5.0) was flowed over the test surface but not control flow cell (300 RU).

CRP analyte at a range of concentrations (0.16 - 20 µg/ml) in HBSPC was injected over the two flow cells (30 µl/min) at a temperature of 25°C. The complex was allowed to associate for 300s and dissociate 600s.

The surfaces were regenerated with a 10s injection of EDTA-containing HEPES buffer (HSBPE: 10 mM HEPES, 150 mM NaCl, 0.005% P20, 0.5mM EDTA, pH 7.4). Data was collected at a rate of 1 Hz. The data was fitted to a simple 1:1 interaction model using the global data analysis option available within BiaEvaluation 3.1 software.

2.17.2.4: Indirect assay of CRP binding

It was observed that PSG bound to the CRP bound to CRP-biotin ligand had a negligible rate of dissociation. Therefore, the ability of the now immobilised PSG to subsequently bind CRP analyte flowed over the surface was investigated.

PSG was captured on CRP-biotin in the test flow cell (8-16 RU) in the manner described previously (Section 2.17.2.2), with the reference flow cell containing CRP-biotin only. CRP analyte at a range of concentrations (0.1 – 6.4 µg/ml) in HBSPC was injected over the two flow cells (20 µl/min) at a temperature of 25°C. The complex was allowed to associate for between 180-300s and dissociate for 300-600s.

The surfaces were regenerated with a 10s injection of EDTA-containing HEPES buffer (HSBPE: 10 mM HEPES, 150 mM NaCl, 0.005% P20, 0.5mM EDTA, pH 7.4), with PSG ligand being reapplied on the surface after each run. Data was collected at a rate of 1 Hz. The data was fitted to a simple 1:1 interaction model using the global data analysis option available within BiaEvaluation 3.1 software.

2.18: Surface plasmon resonance analysis of pentraxin interaction with LPG

Several methods were used to immobilised LPG on the chip surface in order to observe its interaction with pentraxins. In short, the initial attempt used aldehyde coupling of oxidised LPG to a hydrazine-derivatised chip. Subsequently, a method was devised in which LPG was immobilised to a hydrophobic alkyl chip surface, with the aim to capture the molecule via the GPI anchor in order to immobilise LPG in an orientation resembling that observed in the *Leishmania* cell membrane.

2.18.1: Aldehyde coupling of PSG

This experiment was performed and designed by John Raynes (Department of Infection Biology, London School of Hygiene and Tropical Medicine, UK) using material derived from Jan-Hendrik Schroeder (Department of Inflammation Biology, King's College London, UK). The protocol was adapted from the Biacore manual for aldehyde coupling.

LPG was treated with sodium metaperiodate at (10mM, pH5.5) in the dark for 30 mins, and subsequently dialysed overnight to remove excess metaperiodate. The surfaces of flow cells one and two were activated for 7 min with a 1:1 mixture of 0.1 M NHS (N-hydroxysuccinimide) and 0.4 M EDC (3-(N, N-dimethylamino) propyl-N-ethylcarbodiimide) at a flow rate of 5 µl/min. The surface was then treated with 5mM carbohydrazide in dH_2O at 10ul/min for 7 mins. The surface-reactive NHS groups were then reacted with 1M ethanolamine pH 8.3 in order to block any remaining reactive sites. LPG was added for in the test flow cell and control flow cell was left blank. Both flow cells were then offered 10mM cyanoborohydride in sodium acetate buffer (0.1M, pH 4.0) for 20 mins at 2 ul/min to stabilise the LPG bound to the surface and remove reactive hydrazide.

2.18.2: Hydrophobic attachment to alkyl surface

A hydrophobic planar alkyl surface (Xantec HPP) was pre-washed with the non-ionic surfactant octyl β-glucoside (40mM, 10 µl/min, 600s) in order to remove any residual contaminants. Thereafter all buffers and samples were free of detergent.

The ligand *L.mexicana* LPG from metacyclic or nectomonad-stage parasites (50 µg/ml) in HBSC (10 mM HEPES, 150 mM NaCl, 0.5mM $CaCl_2$ pH 7.4) was then flowed over (2 µl/min) and immobilised on the surface at a lower (Figure 78-79, Both 25 RU) or higher (Figure 80-81: metacyclic LPG 290 RU, Figure 82-83: nectomonad LPG 250 RU) surface density) on test flow cell, with flow cell 1 left blank as a reference.

CRP at a range of concentrations (0.02 – 40 µg/ml) in HBSC was flowed over both flow cells (30 µl/min) at a temperature of 25°C. The complex was allowed to associate for 180s and dissociate for 300s. CRP background binding to the hydrophobic surface was minimal.

The surfaces were regenerated with a 10s injection of EDTA-containing HEPES buffer (HBSE: 10 mM HEPES, 150 mM NaCl, 0.5mM EDTA, pH 7.4). Data was collected at a rate of 1 Hz. The data was fitted to a simple 1:1 interaction model using the global data analysis option available within BiaEvaluation 3.1 software.

2.18.3: Analysis of pentraxin binding

The ligand, *L.mexicana* LPG (nectomonad and metacyclic) was flowed over and immobilized on flow cell 2 (205 RU). Flow cell 1 was left blank to serve as a reference surface. Both surfaces were blocked with a 7 min injection of ethanolamine (1M, pH 8.3).

CRP analyte at a range of concentrations (0.16 – 40 µg/ml) in HBSPC (10 mM HEPES, 150 mM NaCl, 0.005% v/v P20, 0.5mM $CaCl_2$, pH 7.4) was flowed over both flow cells (20 µl/min) at a temperature of 25°C. The complex was allowed to associate for 180s and dissociate for 270s.

The surfaces were regenerated with a 10s injection of EDTA-containing HEPES buffer (HSBPE: 10 mM HEPES, 150 mM NaCl, 0.005% P20, 0.5mM EDTA, pH 7.4). Data was collected at a rate of 1 Hz. The data was fitted to a simple 1:1 interaction model using the global data analysis option available within BiaEvaluation 3.1 software.

2.19: Statistical analysis

Student's *t* tests were performed using Prism software (version 7.03) and Microsoft Excel (Office 2019) for data analysis.

The number of replicates used per experiment was indicated in the figure legends.

Unless otherwise indicated, figures in which the number of replicates was not specified were chosen examples that best represent the consistent data obtained from multiple repeats. This was done for experimental models where it would be impractical to present all of the available data (e.g. Western Blots; Surface Plasmon Resonance).

CHAPTER 3

Results

3.1: Material generation, purification and quantification

3.1.1: Generation of Generation of the CRP ligand PCBSA

PCBSA was generated in order to provide a positive control for CRP binding as well as complement activation, as it has been previously been shown to activate the classical complement pathway in a similar manner to other PC-containing molecules from pathogens, such as *Streptococcus pneumoniae* cell wall polysaccharide (CWPS)(Ahmed et al., 2016). PC was crosslinked to BSA using EDC/NHS carbodiimide coupling (Section 2.9.1). After cross linking the material was purified by size exclusion chromatography since complexes were also generated other than the monomeric PCBSA (i.e. PC-containing molecules with multiple BSA residues). Monomeric molecules and larger undesired conjugated molecules were separated by size exclusion chromatography, with collated fractions subjected to SDS-PAGE (Figure 16). Coomassie blue staining of SDS-PAGE gels of these fractions also revealed two distinct populations of PCBSA generated (Figure 17B), with the smaller, monomeric ligand (approximately 65 kDa) being found in fractions corresponding to the second peak, and larger multimeric conjugated molecules corresponding to the first peak . Ligand blotting with purified CRP showed that both populations were capable of CRP binding (Figure 17B).

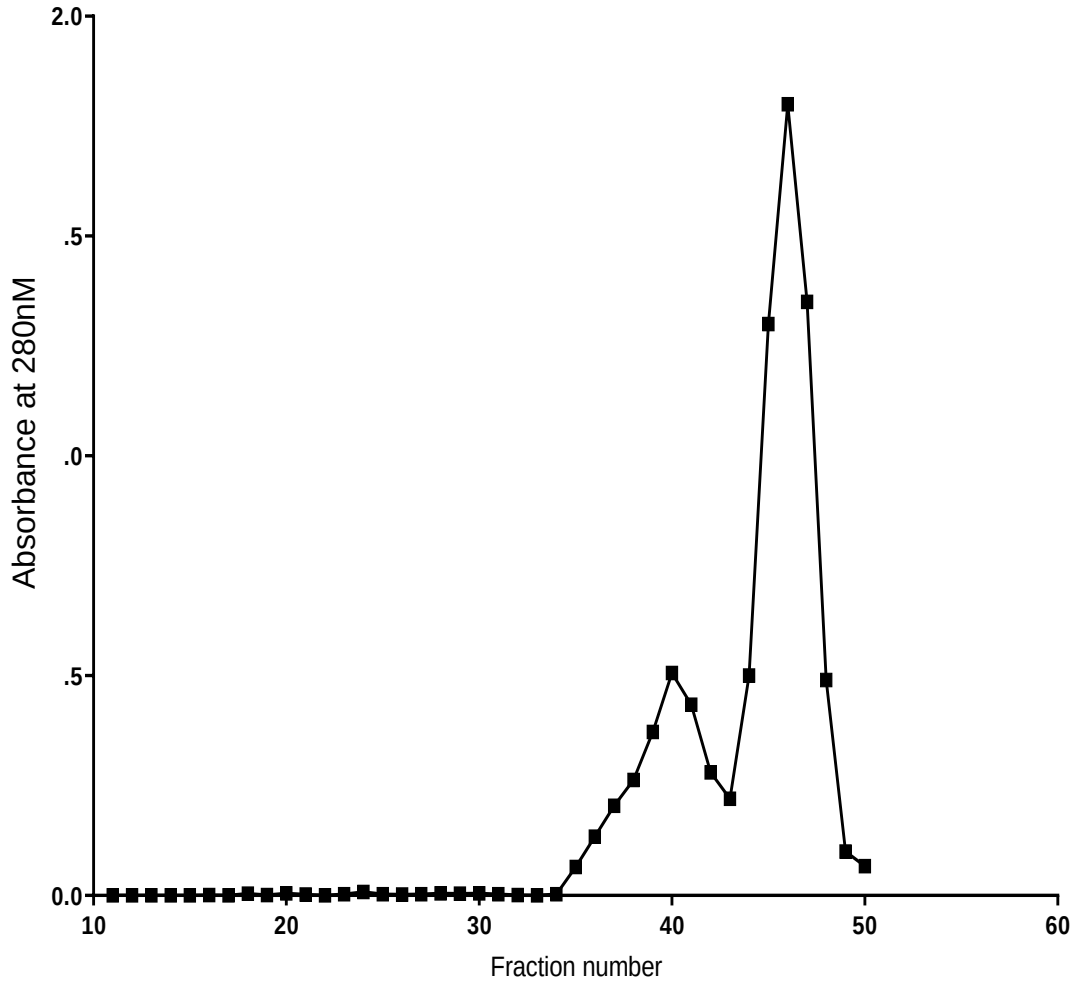

Figure 17: PC-BSA conjugation produces two ligands of different molecular weights.

Fractions (5 ml) were collected from size-exclusion chromatography (Equal volumes of GE Healthcare S200 & S300 media, 85 x 22 mm column), exhibiting two distinct peaks in spectrophotometer absorbance (A280 wavelength), The first (39-41) and second (45-47) peaks were pooled separately.

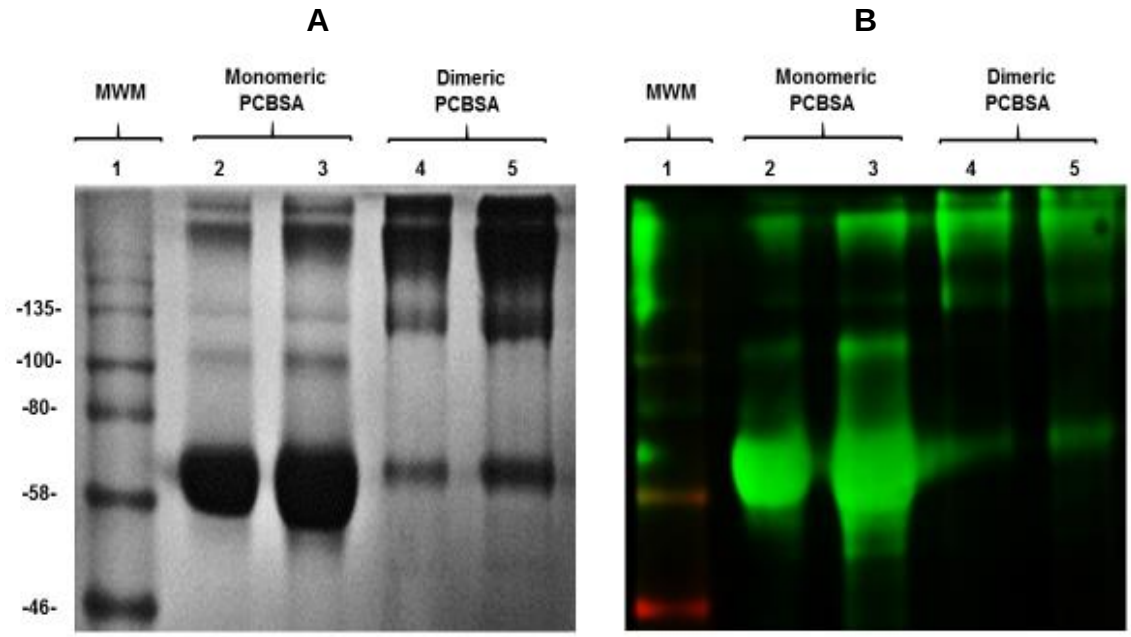

Figure 18: Protein gel staining and ligand blot analysis of PCBSA.

A: SDS-PAGE of PCBSA monomeric and dimeric fractions from size-exclusion chromatography, stained with Coomassie Blue. Monomeric PCBSA has a molecular weight of 66.5 kDa, with multimeric PCBSA being considerably larger. While either fraction contains both forms of PCBSA, monomeric BSA was far more prevalent in its given fraction.
B: NIR imaging of PCBSA ligand blot, using purified CRP and a fluorescent anti-CRP detection system. This confirmed CRP binding to both monomeric and dimeric PCBSA. The red colouration in the lower molecular weight markers was likely due to natural fluorescence of the protein used to form the ladder.

1: Molecular weight marker, 2: 10µg Monomeric PCBSA, 3: 20µg Monomeric PCBSA, 4: 20µg Polymeric PCBSA, 5: 40µg Polymeric PCBSA

3.1.2: Purification of SAP ligand PEC

Phosphoethanolamine cellulose (PEC), produced as a part of the biofilm of *Escherichia coli*, was expressed in culture by John Raynes (Department of Infection Biology, London School of Hygiene and Tropical Medicine, United Kingdom). As a phosphoethanolamine ligand, PEC was extracted to be used as a positive control for SAP binding (Section 2.9.2). As PEC was composed mostly of carbohydrate structures, a carbohydrate quantification assay was performed for quantification purposes (Section 2.6). The standard curve was generated with known concentrations of the cellulose main monosaccharide component, glucose, with the absorbance values of PEC dilutions read against it in order to estimate the concentration (Figure 18). This work was performed by the author.

The insolubility of cellulose in aqueous solution and lack of protein structures made validation by SDS-PAGE and Western blotting unsuitable. Multiple ELISA experiments, however, indicated that PEC has SAP binding capacity.

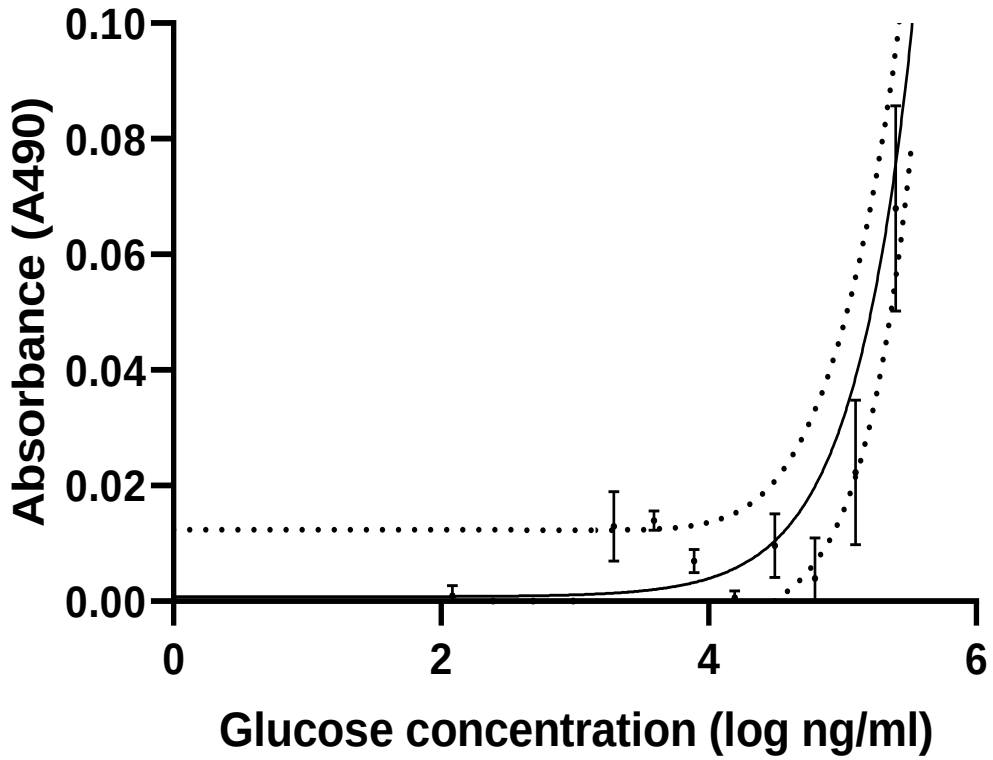

Dilution factor	Absorbance (490 nm)	Carbohydrate concentration (log ng/ml)	PEC concentration estimate (mg/ml)
5	0.029	4.9733	0.4702
10	0.019	4.7778	0.5995

Figure 19: Quantification of PEC using Phenol-H_2SO_4 assay.

A standard curve for PEC quantification was generated using serial dilution of glucose (D+, 2.0-0 mg/ml, n=3 technical replicates), represented by the solid line, allowing extrapolation of carbohydrate concentration for a given absorbance value measured at 490nm wavelength absorbance. The absorbance from different dilutions of PE cellulose (1:5 and 1:10) was used to estimate the concentration of the original PE cellulose aliquot. Dotted line indicates confidence bands (95% confidence interval).

(PEC concentration) = (carbohydrate content at given dilution factor) x (Dilution factor)

3.1.3: Purification of PSG

Promastigote secretory gel (PSG) from multiple *Leishmania* species (*L.aethiopica*, *donovani*, *panamensis*, *major*, *tropica*, *infantum*, *mexicana* and *amazonensis*) was purified or donated by Jan-Hendrik Schroeder and Matthew Rogers (LSHTM).

PSG was also derived from wild-type and mutant (ScAPKO, ScAPAB, LPG1$^{-/-}$ and LPG2$^{-/-}$). *L.mexicana* promastigote supernatant was further purified by sequential anion exchange chromatography (Figure 19), hydrophobic interaction chromatography (Figure 20) and ultracentrifugation (Ilg et al., 1996). In particular, hydrophobic interaction chromatography allows for selective removal of potential glycolipid contaminants, such as LPG and GP63, due to their increased strength of their hydrophobic interactions to the media (i.e. Octyl Sepharose) trapping them on the beads during PSG elution stages. Fractions collected during chromatography stages were quantified on a spectrophotometer (absorbance at 280nm wavelength), with fractions of high concentration being collected, pooled and put through for subsequent stage of purification.

During hydrophobic interaction chromatography, the majority of PSG material was collected with the application of high salt wash buffer (20mM Tris-HCl, 100mM NaCl). Less hydrophobic contaminants not bound strongly to the octyl-sepharose media were eluted in prior, less ionic buffers (Fractions 1-5), while more hydrophobic material, such as LPG and GP63, remained bound to the column until subsequent elution using 50% Propan-1-ol (Fractions 21-25), allowing for effective isolation and purification of PSG.

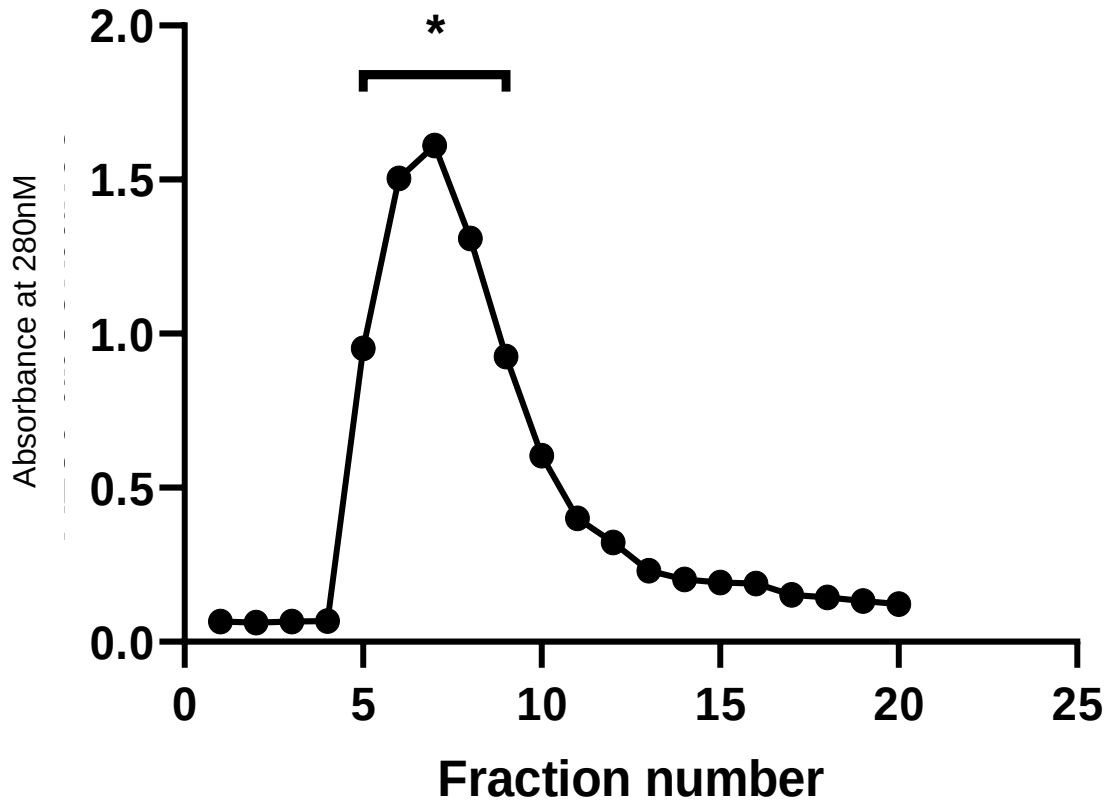

Figure 20: Anion Exchange chromatography of PSG.

Promastigote culture supernatant (WT Metacyclic stage *L.mexicana* parasites) was passed through an anion exchange chromatography column (10 ml, DEAE-52, XK16 column, 10 ml, equilibrated in 100mM NaCl, 20mM Tris-HCl, pH 7.5), and material was eluted from the column using a high salt wash buffer (500mM NaCl, 20mM Tris-HCl, pH 7.5, 60ml/h). Fractions were collected and read on a spectrophotometer (Optical density at 280 nm wavelength). * = Retained fractions.

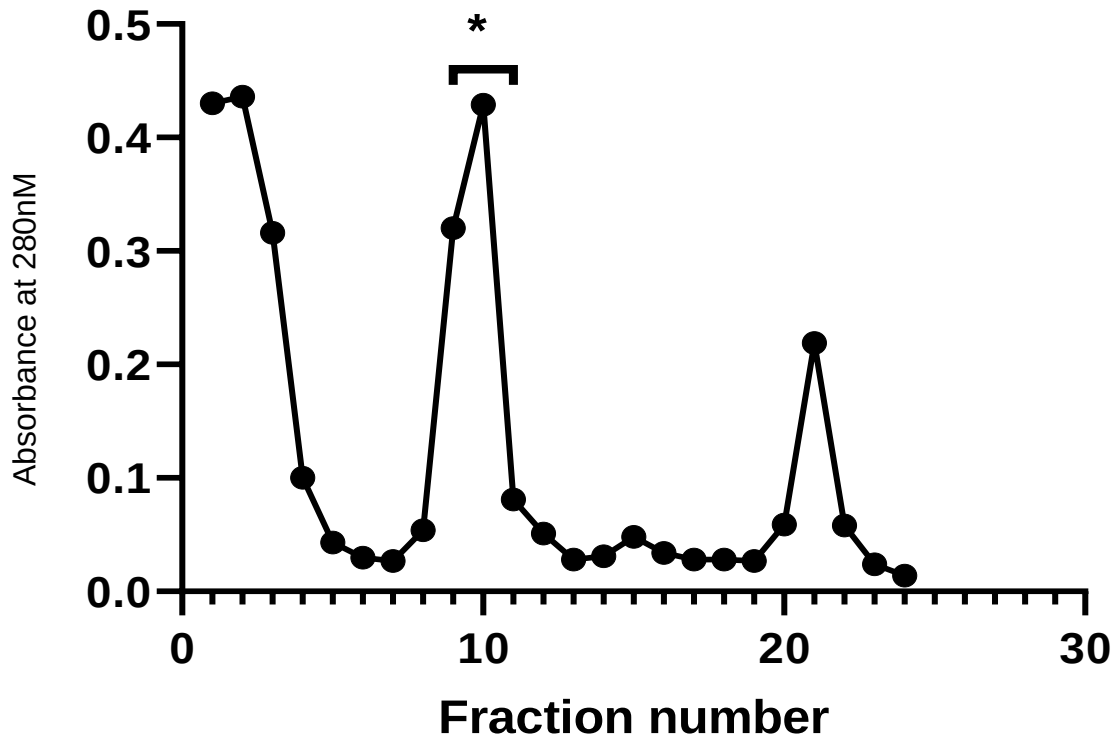

Figure 21: Hydrophobic Interaction chromatography of PSG.

Fractions retained from anion exchange chromatography (Figure 21) were pooled, adjusted to 1M ammonium sulphate, and flowed through a hydrophobic interaction chromatography column (Octyl-sepharose, 5 ml, equilibrated in 1M ammonium sulphate, 20mM Tris-HCl, 5 mM EDTA, fraction 1-5). Adsorbed material was eluted in the same buffer followed by 25 ml of equilibration buffer (fractions 6-10), 25 ml of 20mM Tris-HCl with 100mM NaCl (fractions 11-15), 25 ml of 20mM Tris-HCl (fractions 16-20) and 25 ml of 50% Propan-1-ol (fractions 21-25). Fractions were collected and pooled according to their buffer type. * = Retained fractions.

3.1.4: Purification of CRP and SAP from serum

CRP (Figure 21) and SAP (Figure 22) were purified from donated human plasma using affinity calcium-dependent affinity chromatography, followed by Ion exchange chromatography. Plasma was passed through a phosphoethanolamine (for SAP purification) or phosphorylcholine (for CRP purification)-containing column and eluted using EDTA buffer. The Elution was dialysed into TBS with 0.1M NaCl. The elution was then passed over a column of DEAE-cellulose and eluted with TBS wash buffer with gradually increasing NaCl concentration (100-500mM) (Section 2.8.1).

Material was subjected to SDS-PAGE (Section 2.4) and Coomassie blue protein gel staining (Section 2.5) for verification via molecular weight identification.

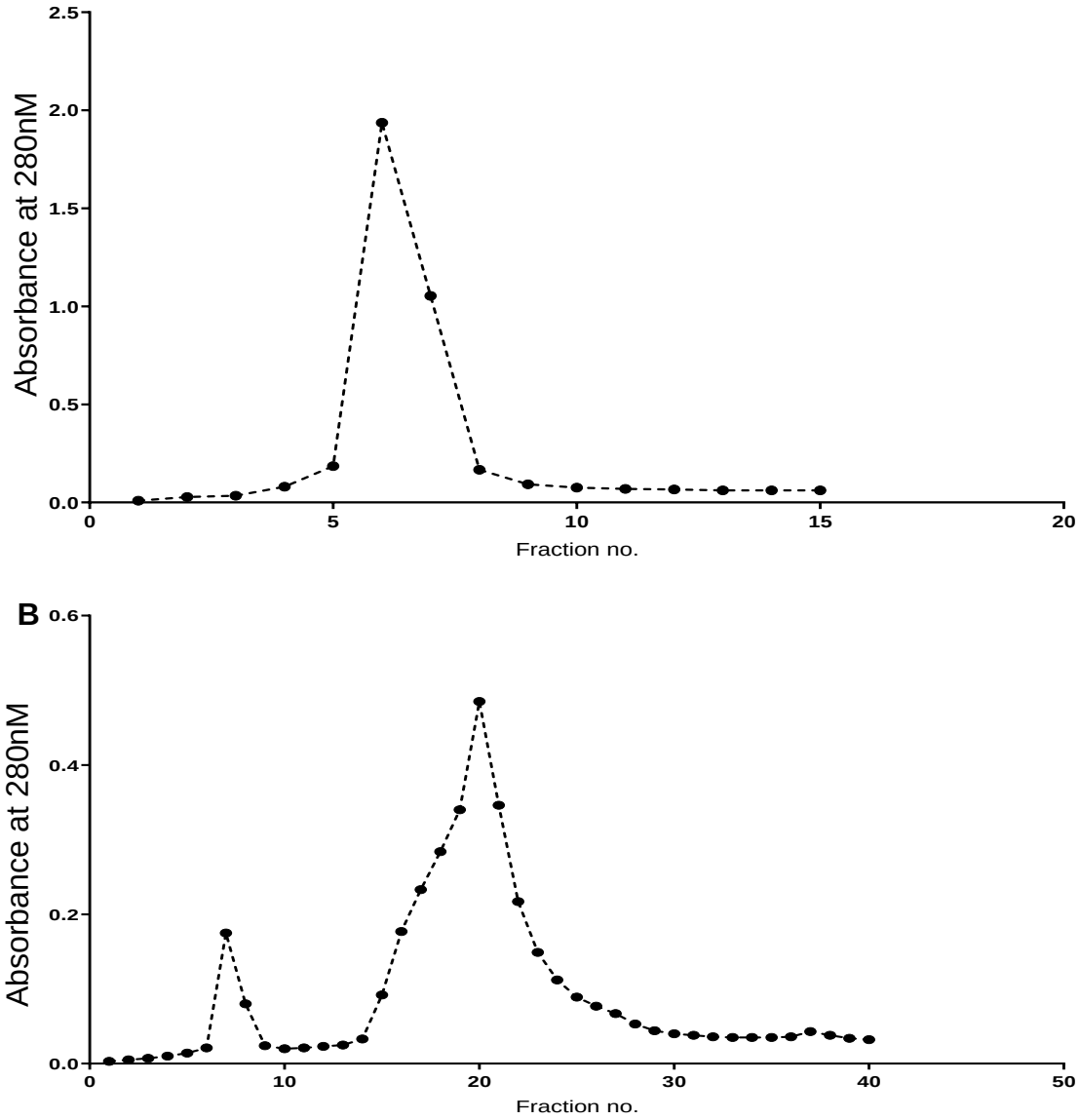

Figure 22: Purification of CRP by sequential calcium-dependent PC-sepharose affinity chromatography (A) and anion exchange chromatography (B).

A: Human plasma was passed through an affinity chromatography column containing the CRP ligand PC immobilised onto Sepharose beads (25ml, XK16 column, equilibrated in 100mM NaCl, 20mM Tris-HCl, pH 7.5). Material was eluted with EDTA buffer (10mM EDTA, 100mM NaCl, 20mM Tris-HCl, pH 7.5). Fractions were collected and read on a spectrophotometer (Optical density at 280 nm wavelength) with fractions corresponding to the peak in protein concentration (Fractions 6-7) being pooled and retained for anion exchange chromatography (see below).
B: Pooled fractions were passed through an anion exchange chromatography column (10 ml, DEAE-52, XK16 column, equilibrated in 100mM NaCl, 20mM Tris-HCl, pH 7.5), and material was eluted from the column using a high salt wash buffer (500mM NaCl, 20mM Tris-HCl, pH 7.5, 60ml/h). Fractions were collected and read on a spectrophotometer (Optical density at 280 nm wavelength) with fractions corresponding to the peak in protein concentration (Fractions 18-22) being pooled and dialysed into Tris-buffered saline (20mM, pH7.4)

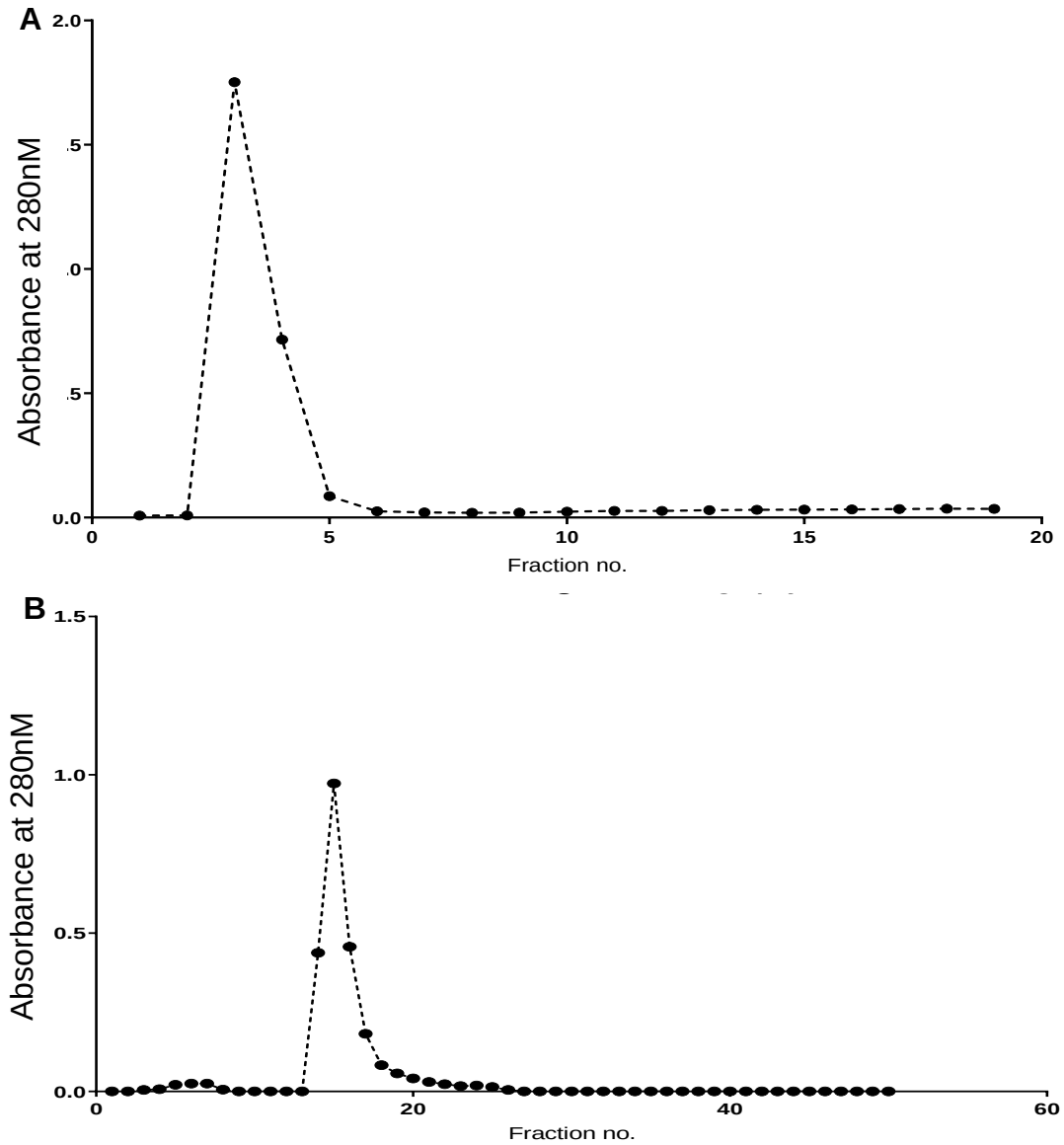

Figure 23: Purification of SAP by sequential calcium-dependent PE-sepharose affinity chromatography (A) and anion exchange chromatography (B).

A: Human plasma was passed through an affinity chromatography column containing the SAP ligand PE -sepharose beads (25ml, XK16 column, equilibrated in 100mM NaCl, 20mM Tris-HCl, pH 7.5). Material was eluted with EDTA buffer (40ml, fractions 0-8, 10mM EDTA, 100mM NaCl, 20mM Tris-HCl, pH 7.5). Fractions were collected and read on a spectrophotometer (Optical density at 280 nm wavelength) with fractions corresponding to the peak in protein concentration (Fractions 3-4) being pooled ad retained for Anion exchange chromatography.
B: Pooled fractions were passed through an anion exchange chromatography column (10 ml, DEAE-52, XK16 column, equilibrated in 100mM NaCl, 20mM Tris-HCl, pH 7.5), and material was eluted from the column using a high salt wash buffer (500mM NaCl, 20mM Tris-HCl, pH 7.5, 60ml/h). Fractions were collected and read on a spectrophotometer (Optical density at 280 nm wavelength) with fractions corresponding to the peak in protein concentration (Fractions 14-16) being pooled and dialysed into Tris-buffered saline (20mM, pH7.4)

3.1.5: Purification of Biotinylated of CRP and SAP

Biotinylated CRP and SAP was repurified from either a phosphorylcholine (PC) or phosphoethanolamine (PE)-conjugated sepharose column respectively, in order to ensure the material still maintained active ligand binding sites and also remove excess biotin (Section 2.8.2). Material was then subjected to SDS-PAGE, transferred onto PVDF membranes via semidry blotting, and probed with alkaline-phosphatase conjugated streptavidin in order to validate material purity and identity via molecular weight estimation (Section 2.4). CRP-biotin containing lanes reveal a single band of approximately 25 kDa molecular weight, and SAP-biotin lanes reveal a band of approximately 28 kDa. This would correspond with the molecular weight of CRP and SAP monomers, with the additional molecular weight attributable to the addition of biotin moieties. The CRP bands display greater intensity than those for SAP for a given concentration (e.g. Bands 4 and 5 for CRP and SAP respectively), suggesting a reduced level of biotinylation in recovered SAP versus recovered CRP (Figure 23).

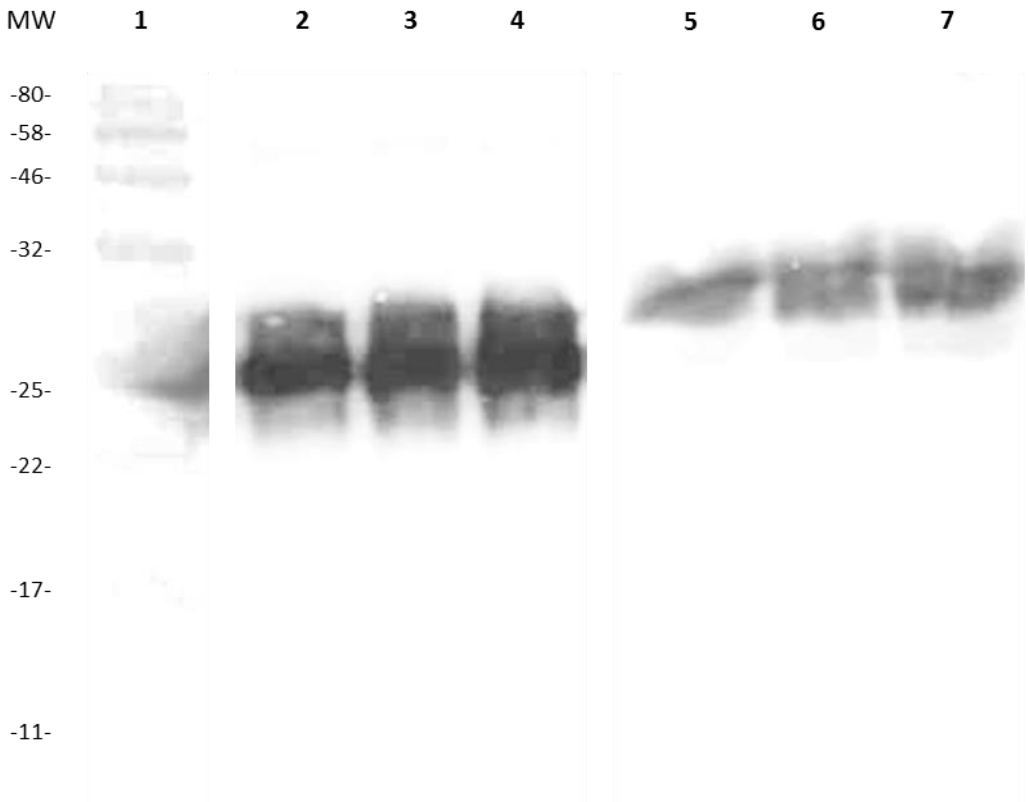

Figure 24: Western blot analysis of biotinylated CRP and SAP.

Biotinylated CRP and SAP was subjected to SDS-PAGE, transferred to PVDF membranes and probed with alkaline phosphatase conjugated streptavidin. This was done to ensure that biotinylation was successful and that cross-contamination was absent.

Lanes 1: Molecular weight marker, 2: 5 µg CRP-biotin. 3: 7.5 µg CRP-biotin, 4: 10 µg CRP-biotin, 5: 10 µg SAP-biotin, 6: 15 µg SAP-biotin, 7: 20 µg SAP-biotin

3.1.6: Serum depletion of SAP and CRP by affinity chromatography

Serum depleted of SAP, CRP or both by affinity chromatography (Section 2.7.2.1) had the level of pentraxin quantified by ELISA against serial dilutions of pentraxin standard serum (i.e. concentration of CRP or SAP known) in order to determine the efficacy of the depletion process. The results reveal that different levels of CRP varied widely between donor samples. Pooled serum depleted of both CRP and SAP by a phosphoethanolamine column showed >90% depletion of both pentraxins. Only serum depleted to an acceptable level (85% depletion or more) of one or the other pentraxin using CRP or SAP specific IgG conjugated columns was used for subsequent experiments.

Calculation of CRP (Figure 24) and SAP (Figure 25) levels in serum before and after depletion by affinity chromatography was performed by sandwich ELISA against a commercial CRP or SAP standard serum. A table of CRP and SAP pentraxin concentration was generated per donor.

A

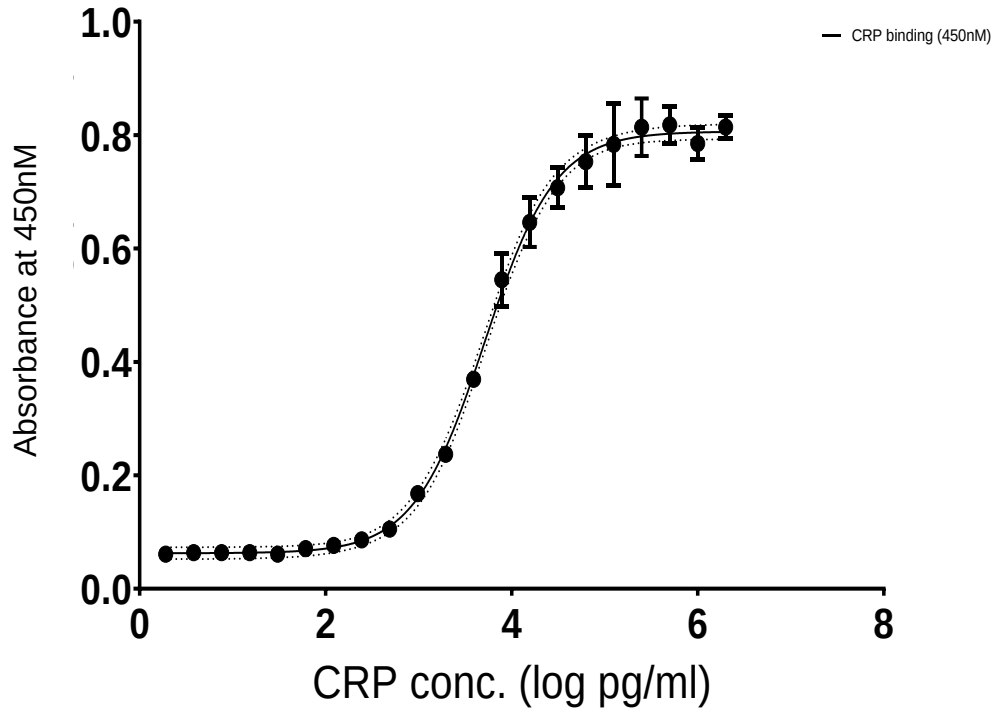

B

Donor	Whole or depleted serum	CRP conc. (ng/ml)	Original: Collected volume	Depletion percentage (%)
284F	**Whole**	18.62	0.98	82.47
	Depleted	2.88		
606F	**Whole**	1.55	0.92	87.63
	Depleted	0.07		
734F	**Whole**	6.03	0.92	56.19
	Depleted	2.14		
670F	**Whole**	1.55	0.89	36.41
	Depleted	0.81		
682F	**Whole**	1.55	0.95	59.35
	Depleted	0.55		
22	**Whole**	13.49	0.96	72.17
	Depleted	3.24		
Pool	**Whole**	10.23	0.93	92.48
	Depleted	0.07		

Figure 25: Standard curve generated using CRP-standardised serum (A) and table of serum CRP concentrations before and after affinity chromatography depletion (B).
Serum (1:100 dilution) from individual donors was passed through a column of anti-CRP IgG-conjugated beads depleting for CRP only, while pooled serum was passed through a phosphoethanolamine column for CRP and SAP double depletion. CRP in serum was quantified by ELISA, with a reference curve (A) being generated using CRP-standard serum, against which CRP concentration in serum pre and post depletion was determined (B). Dotted line indicates confidence bands (95% confidence interval).

A

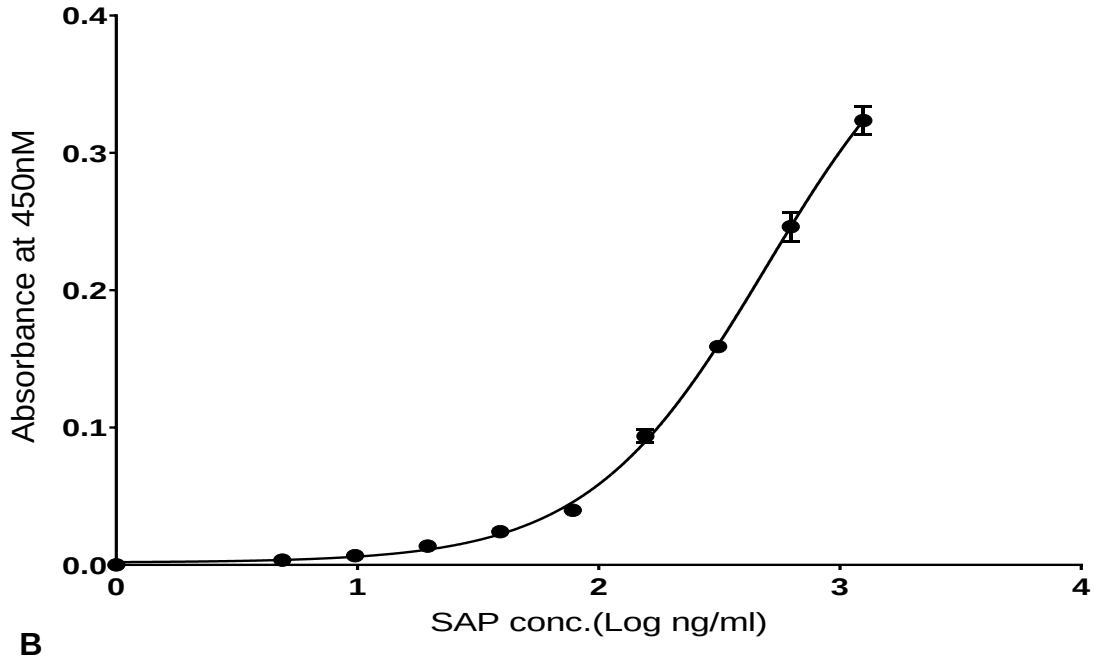

B

Donor	Whole or depleted serum	SAP Conc. (ng/ml)	Original: Collected volume	Depletion percentage (%)
284F	**Whole**	102.33	0.88	46.77
	Depleted	42.66		
606F	**Whole**	54.95	0.92	68.87
	Depleted	12.88		
734F	**Whole**	102.33	0.98	74.23
	Depleted	24.55		
670F	**Whole**	371.54	1.00	87.41
	Depleted	46.77		
682F	**Whole**	83.18	0.96	56.34
	Depleted	33.11		
22	**Whole**	125.89	0.98	87.20
	Depleted	13.49		
Pool	**Whole**	93.33	0.93	92.08
	Depleted	1.00		

Figure 26: Standard curve generated using SAP-standardised serum (A) and table of serum SAP concentrations before and after affinity chromatography depletion (B).
Serum (1:100 dilution) from individual donors was passed through a column of anti-SAP IgG-conjugated beads depleting for SAP only, while pooled serum was passed through a phosphoethanolamine column for CRP and SAP double depletion. SAP concentration in serum was quantified by ELISA, with a reference curve (A) being generated using SAP-standard serum, against which SAP concentration in serum pre and post depletion was determined (B).

3.1.7: Depletion of CRP from serum using Magnetic beads

Serum depleted via affinity chromatography columns with immobilised PC were shown to have complement activated by the process (results not shown), making them unsuitable for complement deposition and binding experiments. An alternative method of on-the-spot CRP depletion was devised, using chicken anti-CRP IgG conjugated magnetic beads due to chicken antibody having minimal human complement activation capacity. Whole serum was vortexed with the beads for 10 seconds and kept at 2 ^{o}C and used for complement deposition C3d ELISA against whole serum (Section 2.7.2.2). Results showed significantly less complement deposition and activation in CRP-depleted serum with both PCBSA and *L.mexicana* PSG ligands, validating the method for studying CRP-driven classical complement activation. Importantly, the purification process did not result in background C3d deposition in control conditions (EDTA) seen because of prior activation. This activation was dependent on the presence of calcium, as it C3d generation was ablated by EDTA (0.5mM). There was a small but significant amount of C3d generated by PSG in the presence of EGTA, suggesting that there was alternative pathway activation present with PSG, but not PCBSA (Figure 26).

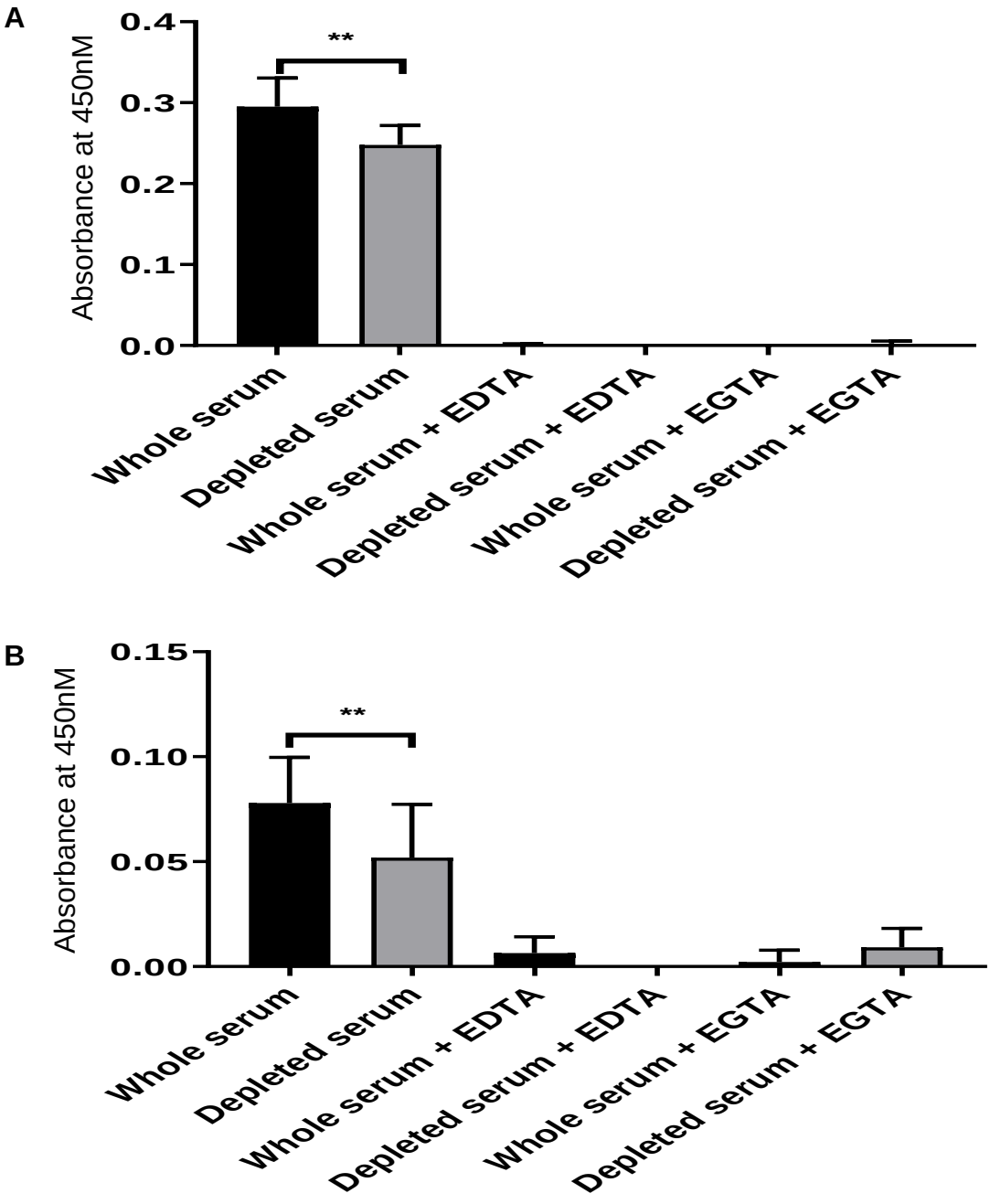

Figure 27: M-bead depletion of CRP in serum shows significant reduced complement activation.

C3d generation, which directly correlates to C3 convertase formation and complement activation, was significantly increased in the presence of purified CRP (0.4 µg/ml) in both ligands. Dose response of complement in whole or CRP depleted serum (1:100, donor 463M) by immobilised PCBSA (A: 0.4 µg/ml) *or L. mexicana* PSG (B: 4 µg/ml). Detection was achieved with Biotinylated anti-C3d, HRP conjugated streptavidin and TMB substrate (OD 450nm). n=6 technical replicates. Error bars represent standard deviation. *: $P \leq 0.05$, **: $P \leq 0.005$

3.1.8: Quantification of LPG using carbohydrate assay was more accurate than weight estimation of lyophilised LPG

LPG was quantified using a modified existing assay (Section 2.6), based on the principal of quantifiable colorimetric change (490nM) when carbohydrate was oxidised and treated with phenol(Albalasmeh et al., 2013). Mannose was used to generate a standard curve, being a major carbohydrate constituent of LPG, as well as having the same absorbance value per weight to the other common saccharide component of LPG, galactose. Absorbance data from different dilutions of *L.mexicana* nectomonad and leptomonad stage LPG were read again the standard curve in order to determine the concentration of LPG in solution (Figure 27A).

An initial attempt was made to quantify LPG by weight following lyophilisation, (i.e. dry weight estimate). This was compared against quantification results from the carbohydrate assay previously described. The reasonably similar factorial differences (i.e. Dry weight estimate/carbohydrates acid assay estimate) per life cycle stage suggested that quantification of LPG was consistent (Figure 27B).

Due to the inherent inaccuracy of dry weight estimation following lyophilisation of relatively small quantities of LPG in comparison to equipment limitation (i.e. the accuracy of the laboratory weighing scale), all quantification estimates for LPG were subsequently made using the carbohydrate assay.

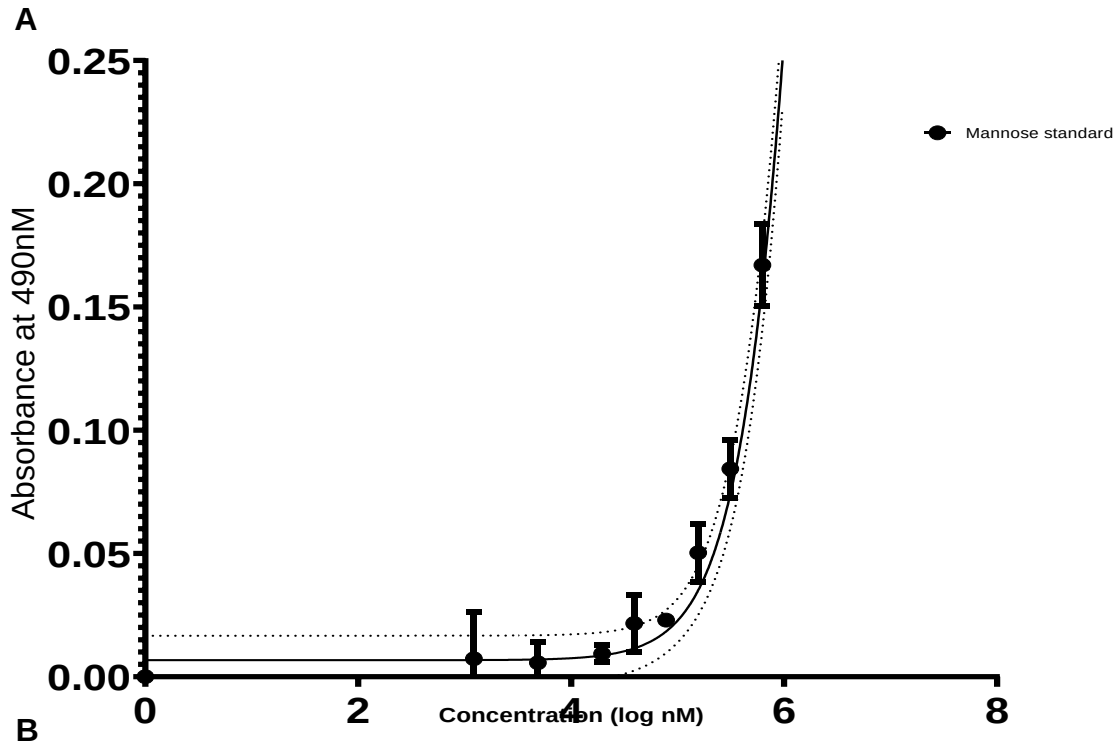

	Dry weight estimate (mg/ml)	Phenol-Sulphuric acid assay (mg/ml)	Factoral difference (DW/AW)
Metacyclic	0.500	0.060	8.343
	0.250	0.028	8.776
	0.125	0.012	10.145
Nectomonad	0.500	0.043	11.543
	0.250	0.017	14.699
	0.125	0.008	15.180

Figure 28: Quantification of LPG via carbohydrate assay against a mannose standard.

A reference curve (A) was generated using serial dilutions of known concentrations of mannose (0 – 0.1 mg/ml), which was then oxidised with concentrated sulphuric acid. Colorimetric change was triggered by the addition of 5% phenol and absorbance was recorded at 490 nm wavelength. Dotted line indicates confidence bands (95% confidence interval). Concentration of metacyclic and nectomonad LPG was estimated (B) by interpolation of LPG absorbance values on the standard curve (AW: Phenol-sulphuric acid assay) and weighing of lyophilised product (DW: “Dry weight estimate).

3.1.9: PSG is a heterogeneous material (fPPG and ScAP)

In order to characterise the molecular weight of *L.mexicana* PSG material that had repeating phosphorylated disaccharide, L.mexicana WT, ScAPKO and ScAPAB PSG was subjected to SDS-PAGE on 8% polyacrylamide gels with a 6% stacking gel layer, transferred onto PVDF membranes. The stacking gel layer was extended and of relatively low density in order to better visualise high molecular weight components, such as fPPG, which were unlikely to be able to migrate into the resolving gel. Western blotting was performed with LT6, a murine antibody shown to be specific to the Galactose-Mannose-PO_4 disaccharide repeats common to many *Leishmania* products (Section 2.3).

The results indicate several large, glycosylated molecules, which appear as diffuse bands due to the variability of molecular weight and charge on highly glycosylated products (Figure 28). Previous studies would suggest that this would consist of filamentous proteophosphoglycan (fPPG), as well as two variants of secreted acid phosphatase (ScAP1 and ScAP2)(Ilg, 2000b) .

Native *L.mexicana* PSG obtained from sandfly midgut dissection shows a similar high molecular weight pattern, with the relatively weak signal attributable to the relatively small amounts of material run as compared to the cultured PSG (Figure 29). The relative lack of high molecular weight material appearing near the top of the resolving gel in the native versus cultured PSG could be indicative of the different relative levels of fPPG and ScAP in the sandfly gut environment compared to culture supernatant. 2.5 µl of native (I.e. extracted from sandfly gut) PSG was used per lane during SDS-PAGE. As a single infected sandfly contains approximately 1-1.5 µl PSG, this would be the PSG contents of approximately 2 infected sandfly guts.

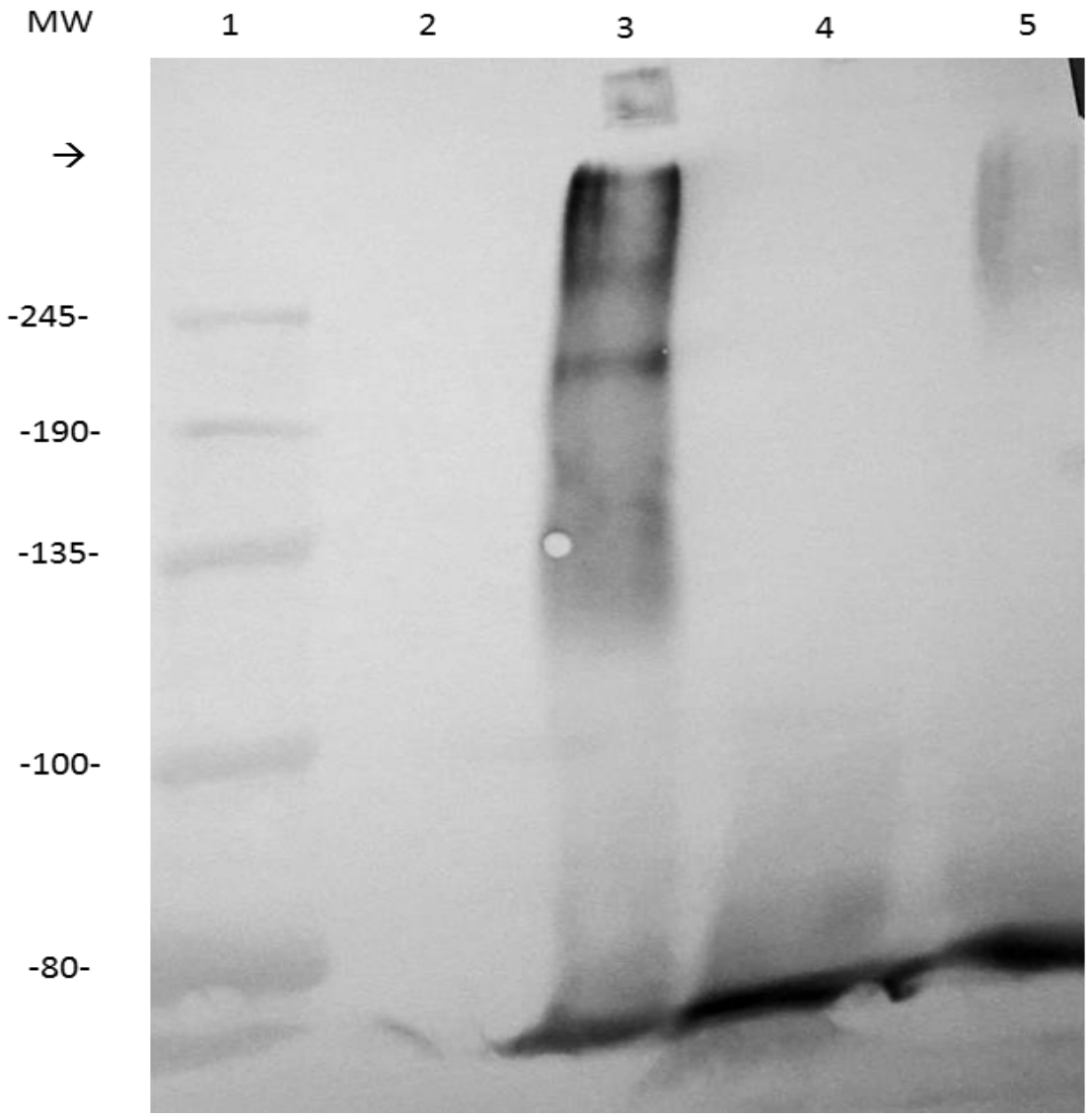

Figure 29: LT6 binding *L.mexicana* PSG from culture supernatants.

Purified PSG (*L.mexicana* WT, ScAPKO and ScAPAB) on 6% SDS-PAGE gels and transferred onto a PVDF membrane. Blots were incubated with LT6 supernatant (1:4), an antibody specific for Gal-Man- PO_4 repeats found in *Leishmania* glycosylated products. This was followed by alkaline phosphatase conjugated goat anti-mouse antibody. Precipitate deposition on the membrane indicates presence of material containing the phosphorylated repeating disaccharide. MW: Molecular weight, -->: Stacking/resolving gel border, 1: Molecular weight standard, 2: Blank, 3: Wild-type *L.mexicana* PSG, 4: SAPKO *L.mexicana* PSG, 5: SAPAB *L. mexicana* PSG

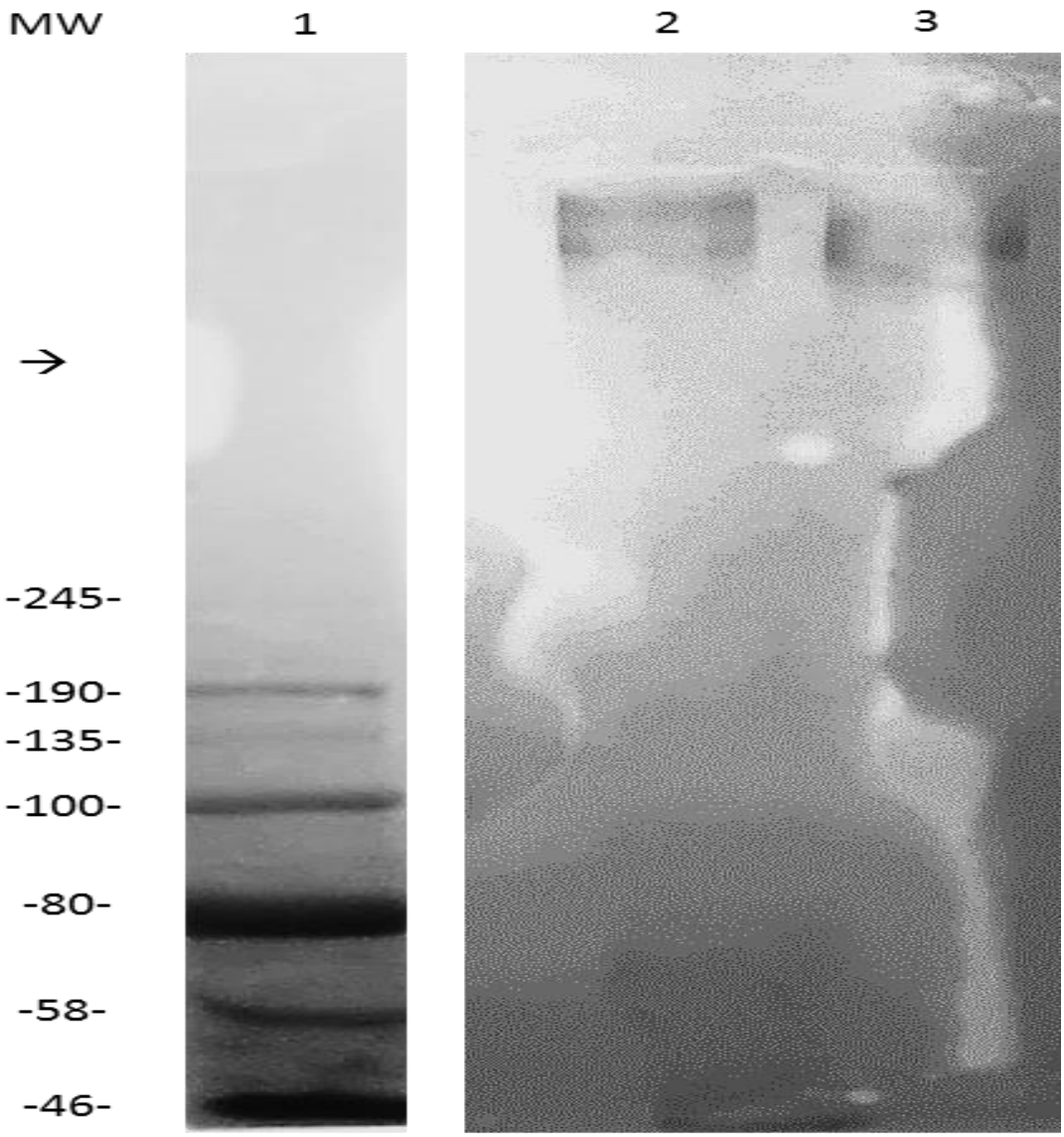

Figure 30: LT6 binding to native *L.mexicana* PSG.

Purified PSG (*L.mexicana* WT, SAPKO and SAPAB) on 6% SDS-PAGE gels and transferred onto a PVDF membrane. Blots were incubated with LT6 supernatant (1:4), an antibody specific for Gal-Man-PO_4 repeats found in *Leishmania* glycosylated products. This was followed by alkaline phosphatase conjugated goat anti-mouse antibody. Precipitate deposition on the membrane indicates presence of material containing the phosphorylated repeating disaccharide. 1: Marker, 2: 2.5 µl Native WT PSG, 3: 2.5 µl Native ScAPKO PSG

3.2: Characterisation of CRP binding to *Leishmania* PSG

3.2.1: Binding of CRP to PSG is affected by the PC binding site

CRP was known to have both calcium-dependent and independent binding sites, and as such an attempt was made to determine which binding site was responsible for interaction to PSG. A dose response ELISA of CRP binding to *L.mexicana* PSG purified from *Leishmania* culture supernatant (Section 2.10.2) in the presence or absence of PC chloride-calcium salt (10mM) was performed (Section 2.12.2).

PC inhibits CRP-PSG binding in a competitive manner, with the reduction in binding being gradually overcome by increasing levels of CRP. This would suggest that PC and PSG share the same binding site on the effector face of CRP, with binding of PC to CRP sterically inhibiting PSG binding, and vice versa (Figure 30).

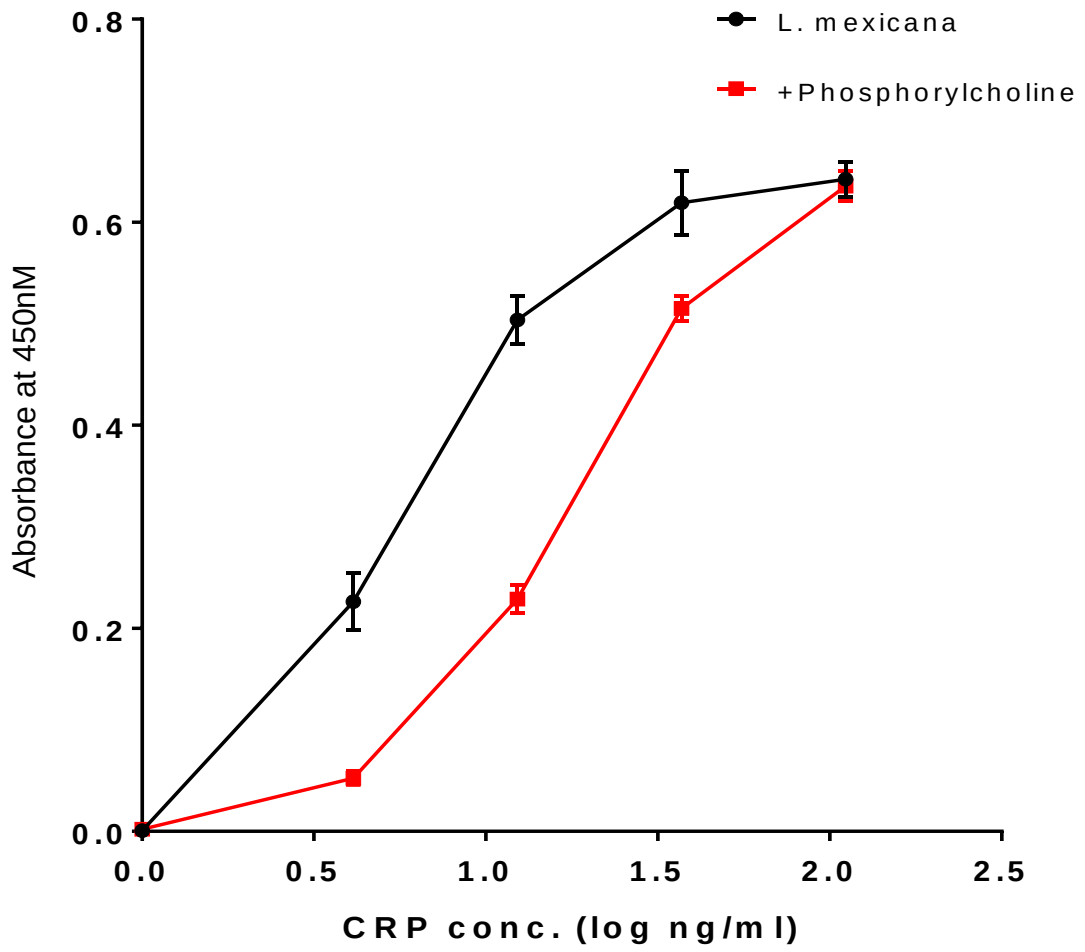

Figure 31: PC inhibits CRP binding of PSG.

Dose-Response of binding of purified CRP (0 - 1.0 µg/ml) to immobilised PSG *L.mexicana* wild-type PSG (0.3 µg/ml). Binding was observed in the presence and absence of PC calcium-chloride salt (10mM). CRP binding was detected using rabbit anti-CRP antibody, HRP-conjugated goat anti rabbit antibody and TMB substrate (OD 450nm). n=3 technical replicates. Error bars represent standard deviation.

3.2.2: CRP binding to PSG is calcium-dependent and magnesium-independent

CRP has been shown to bind to ligands in both a calcium-dependent and independent manner. In order to characterise the ion dependency, if any, of CRP binding to PSG, a dose-response ELISA of CRP-biotin binding to PSG in the presence of calcium, ethylenediaminetetraacetic (EDTA) or ethylene glycol-bis (β-aminoethyl ether)-N,N,N′,N′-tetraacetic acid (EGTA) was performed. Experiments were also performed in the absence or presence of CRP-depleted serum in order to determine the influence of other circulatory components on the binding event (Figure 31). Binding was not observed in the presence of EDTA (calcium and magnesium chelating) in the absence of any divalent cations; or in EGTA (calcium chelating) with the presence of Mg^{2+}, indicating the dependency of the binding event to calcium, but not other divalent cations.

Following this, varying quantities of *L.mexicana* PSG was subjected to SDS-PAGE (Section 2.3) and ligand blotting with CRP (Section 2.12.1), in the presence of Ca^{2+} or EDTA (Figure 32), revealing dose responsive binding of CRP to PSG in the form of varying colorimetric intensity proportional to the quantity of PSG per well, which was completely ablated in the presence of EDTA.

ELISA of CRP binding to PSG (Section 2.12.2) from multiple other species in the presence of Ca^{2+} or EDTA showing near complete ablation of CRP binding to PSG in the presence of EDTA would suggest that this does not appear to be an outstanding characteristic of *L.mexicana* PSG (Figure 33).

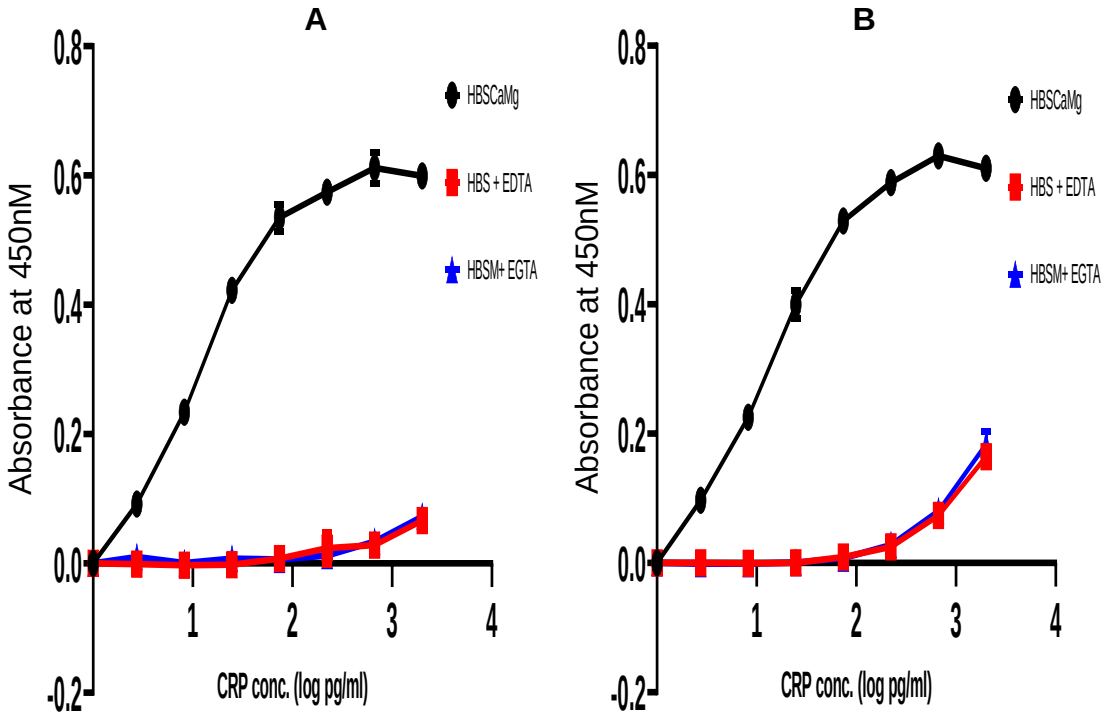

Figure 32: PSG binding to CRP is dependent on calcium and independent of magnesium

Dose-Response of binding of biotin-conjugated CRP (0 - 2.0 µg/ml) to immobilised *L.mexicana* wild-type PSG (1 µg/ml). Binding was observed in the presence of Ca^{2+} and Mg^{2+} (Both 0.5mM), EDTA (10mM) or EGTA with Mg^{2+} (10mM and 0.5mM respectively), and in the presence (B) or absence (A) of CRP-depleted serum (1:20). CRP binding was detected using HRP-conjugated Streptavidin (1:15000) and TMB substrate (OD 450nm). n=3 technical replicates. Error bars represent standard deviation.

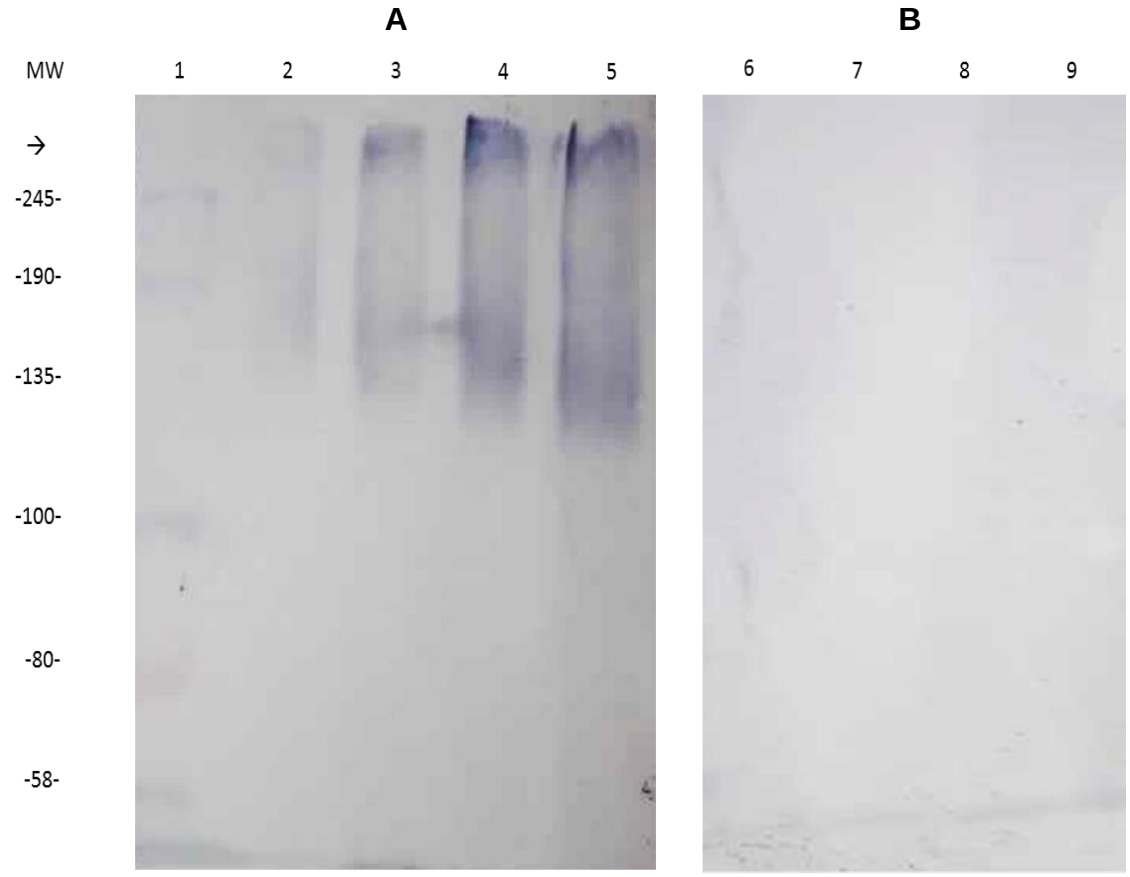

Figure 33: CRP binding to WT PSG is dose and Ca^{2+} dependent

Purified Wild-type *L. mexicana* PSG (1, 2, 3 and 4 µg) was run on 6% SDS-PAGE gels and transferred onto a PVDF membrane. Blots were incubated with CRP-biotin (1 µg/ml) in the presence (0.5.mM $CaCl_2$, Lanes 1-5) and absence (0.5mM EDTA, lanes 6-9) of calcium. This was followed by alkaline phosphatase-conjugated streptavidin (1:1000). Precipitate deposition on the membrane indicated CRP binding to PSG components.

MW: Molecular weight. →: Stacking/resolving gel border. 1: Molecular weight standard. 2,6: 1 µg Wild-type L. mexicana PSG. 3,7: 2 µg Wild-type L. mexicana PSG. 4,8: 3 µg Wild-type L. mexicana PSG. 5,9: 4 µg Wild-type L. mexicana PSG.

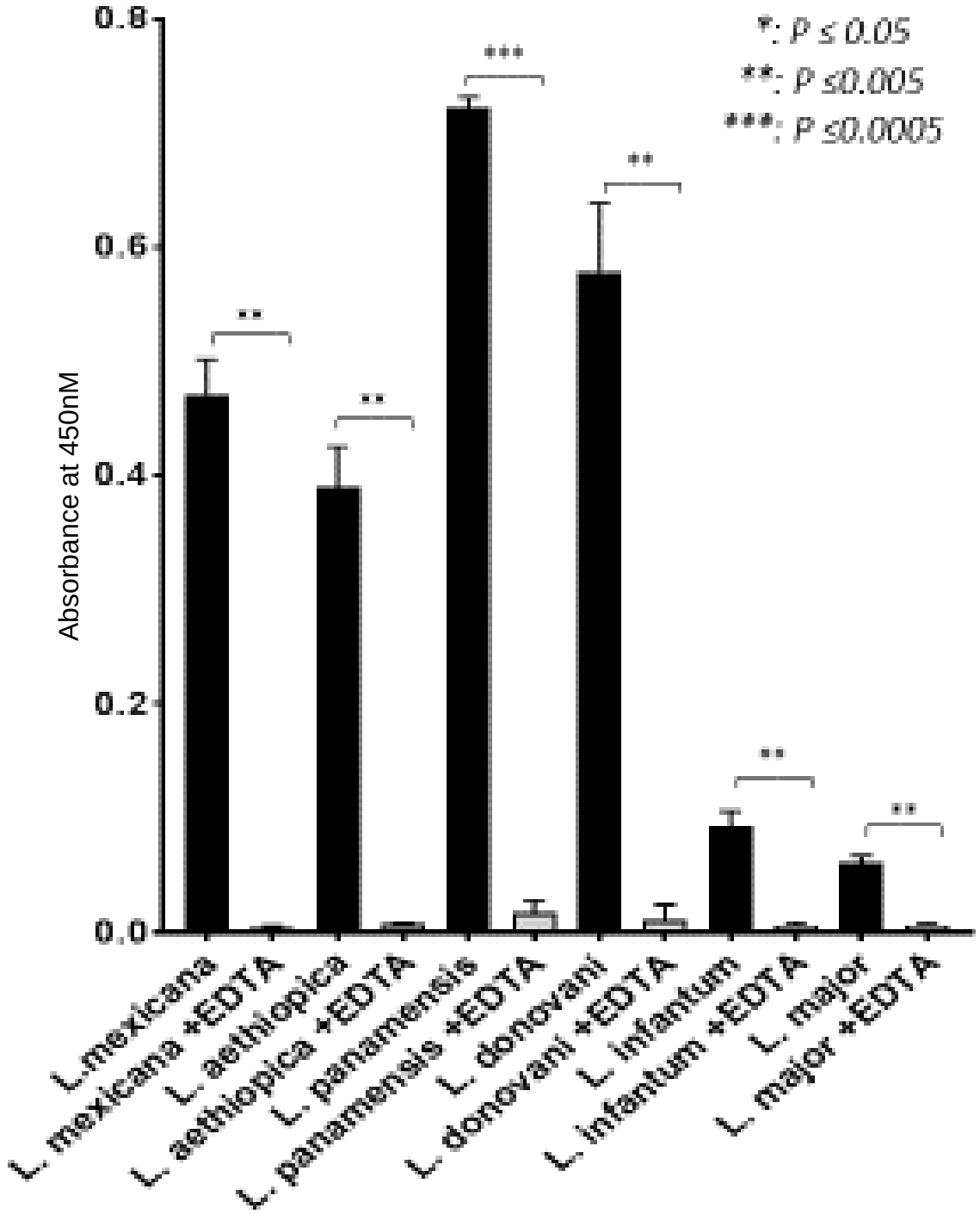

Figure 34: CRP binding of PSG from different species is also a calcium-dependent interaction

EDTA (10mM) inhibited binding of purified CRP (1µg/ml) to immobilised PSG from different *Leishmania* species (0.3 µg/ml, *L.mexicana, L.aethiopica, L.panamensis, L.donovani, L.infantum* and *L.major* PSG). CRP binding was detected using rabbit anti-CRP antibody, HRP-conjugated goat anti-rabbit antibody and TMB substrate (OD 450nm) as previously described (Section 2.12.2). n=3 technical replicates. Error bars represent standard deviation.

3.2.3: PSG from different *Leishmania* species have widely varying CRP binding capacities

In order to ascertain the PSG binding capacity of different *Leishmania* species, ELISA (Section 2.12.2) and Western blotting (Section 2.12.1) of PSG with CRP was performed. ELISA allowed a dose-response binding of CRP to PSG in both orientations (Figure 34). The order of CRP binding capacity between different *Leishmania* species' PSG was consistent in both orientations of binding (i.e. whether it was CRP immobilised and PSG in fluid phase or vice versa), giving confidence to the results.

PSG material of the same quantity from multiple species was subjected to SDS-PAGE, transferred onto PVDF membranes and probed using fluorescent antibodies (Section 2.12.1) emitting in the near-infrared (NIR) spectrum, with the varying fluorescence intensities visible indicating differences in CRP binding capacity between the PSG purified from different species' culture supernatants (Figure 35). While ligand blotting was a semi-quantitative technique, the results appeared to broadly correspond with observations from the ELISA experiments, *with L.panamensis, L.mexicana* and *L.tropica* generating a strong, moderate and weak signal respectively. Fluorescence intensity also appears to change in a dose-responsive manner when varying quantities PSG derived from the same species was subjected to SDS-PAGE and ligand blotting (Figure 36).

ELISA of CRP binding to immobilised PSG from *L.aethiopica* and *L.donovani* in the absence or presence of PC chloride-calcium salt (10mM) would suggest that similar to *L.mexicana* (Figure 30), CRP binding to PSG was mediated by the PC binding site (Figure 37).

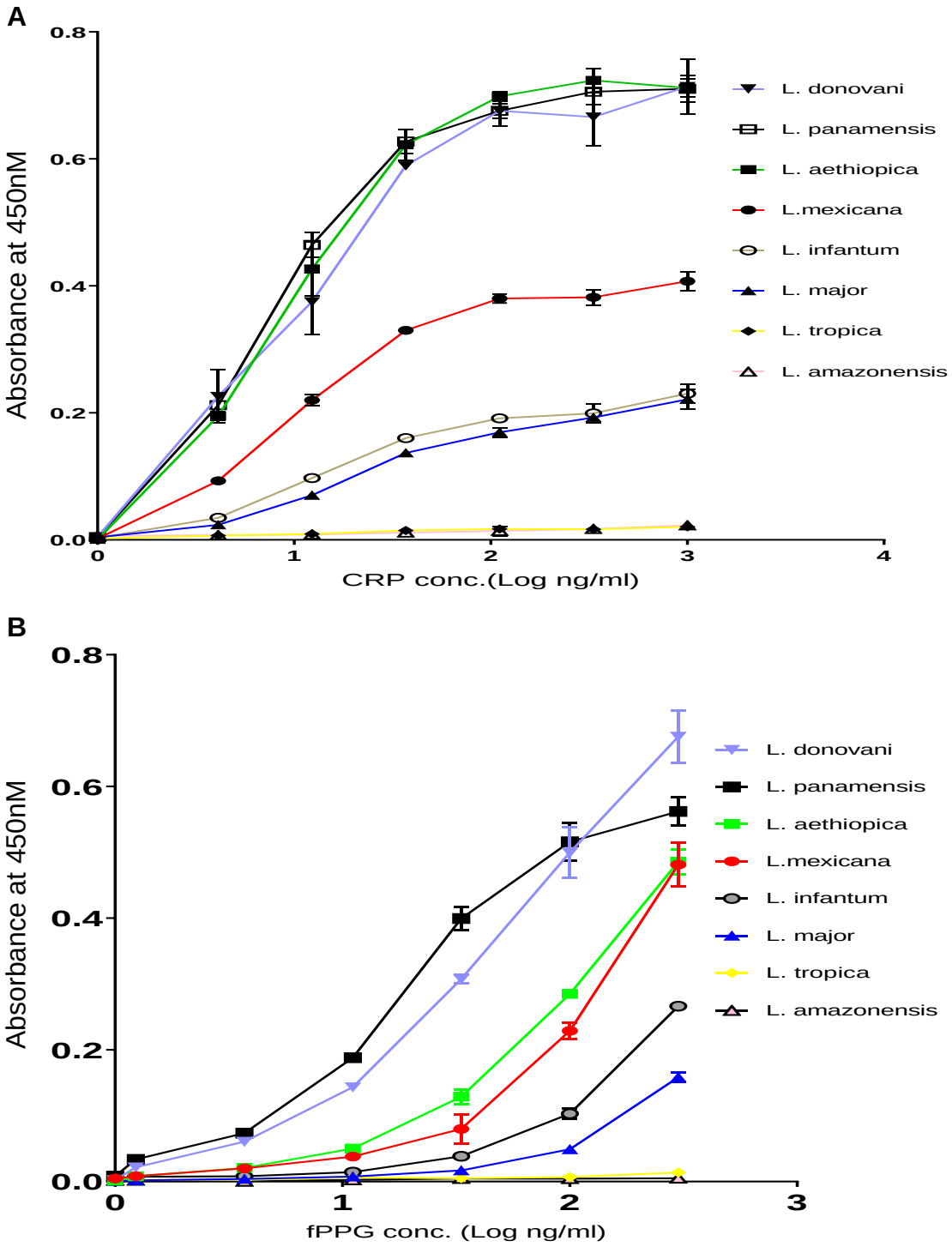

Figure 35: PSG from different *Leishmania* species exhibit widely varying CRP binding capacities.

Dose-Response of binding of purified CRP (0 - 1.0 µg/ml) to immobilised PSG from different *Leishmania* species (0.3 µg/ml). **B:** Dose-Response of binding of purified CRP (1.0 µg/ml) to immobilised PSG from different *Leishmania* species (0 - 0.3 µg/ml). In both **A&B**, CRP binding was detected using rabbit anti-CRP antibody, HRP-conjugated goat anti rabbit antibody and TMB substrate (OD 450nm). n=3 technical replicates. Error bars represent standard deviation.

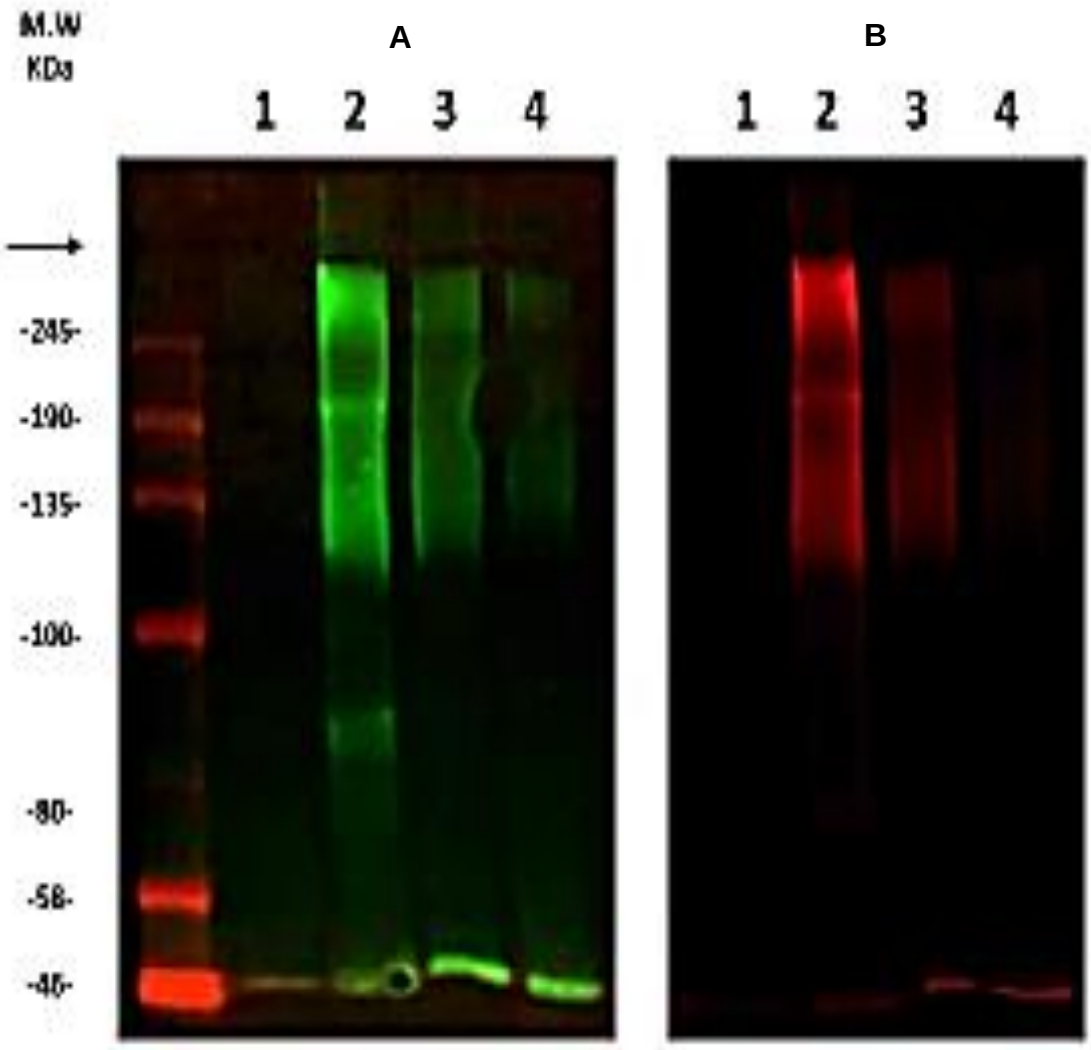

Figure 36: Different *Leishmania* species produce varying levels of CRP binding components.

PSG from different *Leishmania* species were probed on the same blot, with the difference in fluorescence intensity indicating a difference in CRP binding capacity and supporting the data from CRP binding ELISA. CRP (5 µg/ml CRP in TBS, 1% BSA, 0.5mM Tween 20 and 5mM $CaCl_2$) binding to PSG (3 µg PSG per lane) was detected with two systems to verify data. Fluorescent NIR images (Left=IR800; Right=IR680) of CRP binding to PSG from different *Leishmania* species.

1= L. tropica, 2= L. infantum, 3 = L.panamensis, 4 = L.donovani.

A: Ligand blotting with purified human CRP, with Rabbit anti-CRP and fluorescent IRDye® 800CW Goat anti-Rabbit IgG.
B: Ligand blotting with purified human CRP, biotinylated α-CRP and IRDye® 680RD Streptavidin.

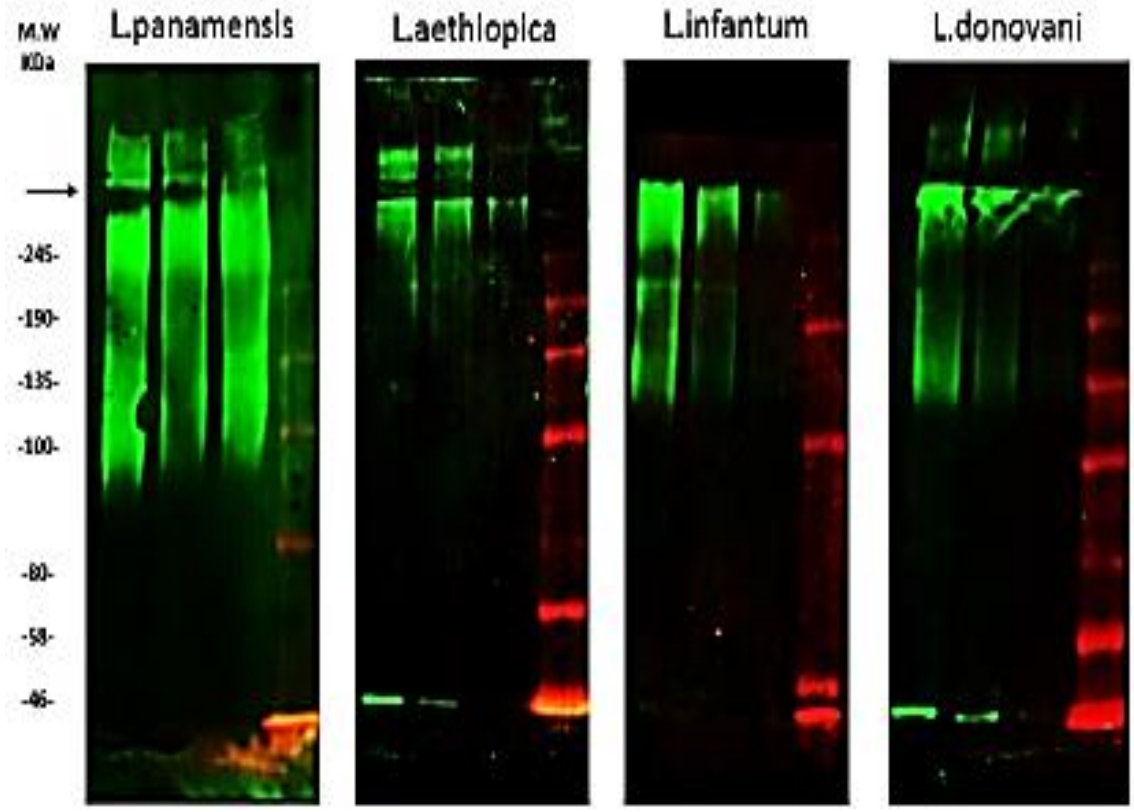

Figure 37: Different *Leishmania* species produce high-molecular weight PSG components that bind to CRP

CRP to bind to large molecule components of PSG above 100 kDa. NIR fluorescent ligand blot images (IR800 dye) of CRP (5 µg/ml CRP in TBS, 1% BSA, 0.5mM Tween 20 and 0.5mM $CaCl_2$) binding to PSG (1.5, 3.0 and 4.5 µg PSG per lane, from right to left) from different *Leishmania* species (*L.panamensis, L.aethiopica, L.infantum* and *L.donovani*).

Ligand blotting with purified human CRP, Rabbit anti-CRP and fluorescent IRDye® 800CW Goat anti-Rabbit IgG.

MW: Molecualr weight. →: Stacking-resolving gel border.

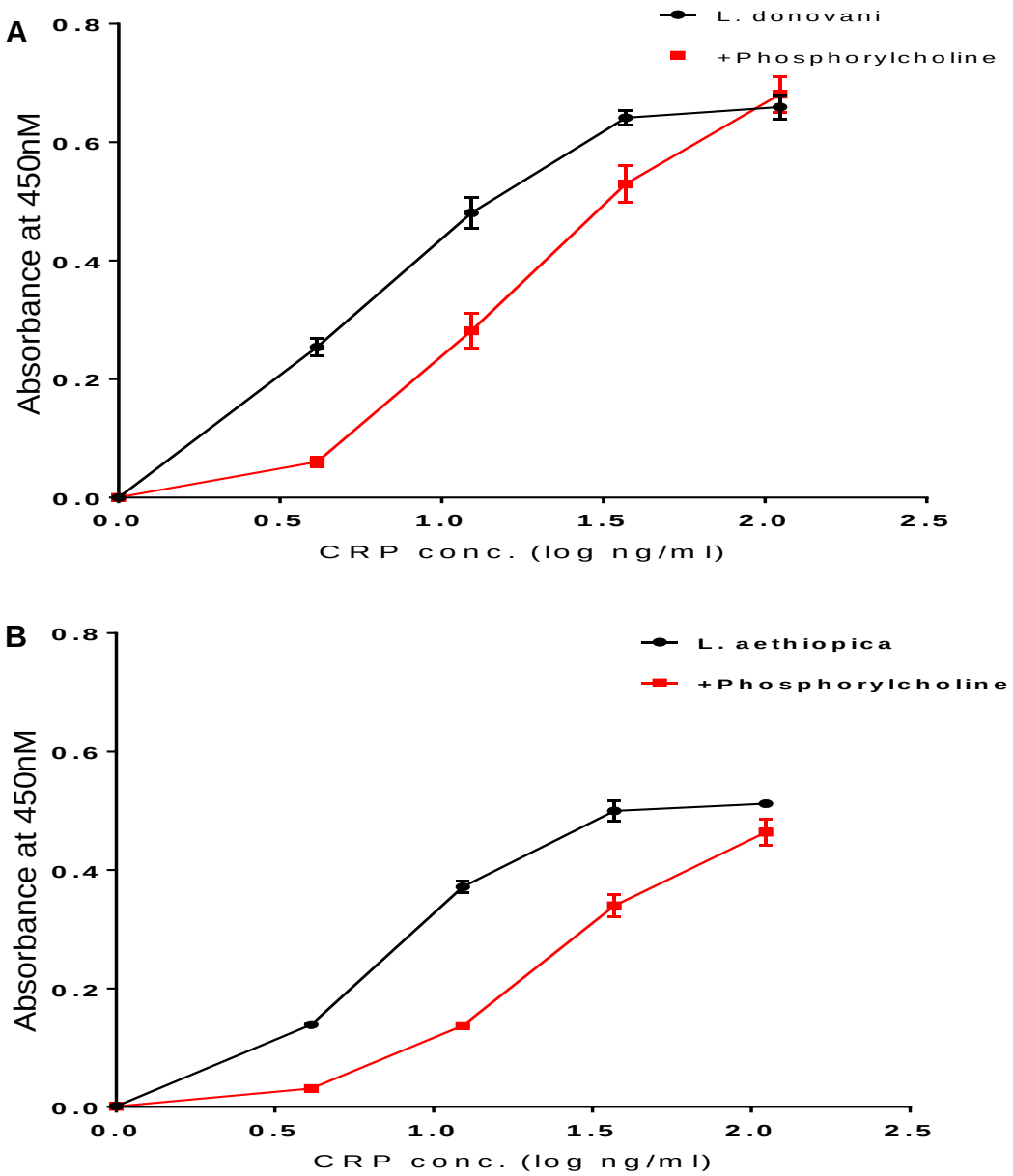

Figure 38: PC inhibits CRP binding of PSG in multiple species

Dose-Response of binding of purified CRP (0 - 1.0 µg/ml) to immobilised PSG from **A:** *L.donovani*, and **B:** *L. aethiopica* (0.3 µg/ml). Binding was observed in the presence and absence of PC chloride-calcium salt (10mM) in different *Leishmania* species. CRP binding was detected using rabbit anti-CRP antibody, HRP-conjugated goat anti rabbit antibody and TMB substrate (OD 450nm). n=3 technical replicates. Error bars represent standard deviation.

3.2.4: CRP binding to PSG is not dependent on LPG

While precautions taken by the additional hydrophobic interaction chromatography step during the precaution to remove glycolipid contaminants from PSG (Figure 20), we needed to ascertain if CRP binding was due to residual LPG in the material, especially in light of LPG being a CRP ligand. Low molecular weight bands were seen in some blots and glycolipids such as LPG can run aberrantly on SDS gels. *L. mexicana* LPG1$^{-/-}$ mutant, which lacks a putative b-galactofuranosyl (b-Galf) transferase within the Golgi apparatus responsible for adding al b-Galf residue to the LPG conserved phosphorylated heptasaccharide region, has been shown to express PPGs as per the WT parasite, but does not express a functional LPG ligand (Ilg, 2000a). *L.mexicana* LPG2$^{-/-}$ mutant expresses neither PPG or LPG, with downregulation of PG synthesis as well as mannose end cap structures. (Ilg et al., 2001).

Dose-response ELISA was performed on immobilised WT, LPG1$^{-/-}$ and LPG2$^{-/-}$ *L.mexicana* PSG with varying concentrations of CRP, in the absence or presence of whole serum, in order to determine the influence of other serum components on the binding interaction (Section 2.12.2). While virtually no CRP binding was detected for the LPG2$^{-/-}$ mutant, CRP binding affinity and capacity towards LPG1$^{-/-}$ appeared virtually identical to that of WT PSG across a range of CRP concentrations, suggesting low or negligible levels of LPG in *L.mexicana* WT PSG purified from culture supernatant (Figure 38). Of note, this ELISA experiment was repeated using rCRP, with very similar results (not shown).

Wild type (WT) and LPG1$^{-/-}$ *L. mexicana* PSG was subjected to SDS-PAGE and transferred onto PVDF membranes. Ligand blotting with CRP (Section 2.12.1) showed similar binding to PSG between WT and LPG1$^{-/-}$ PSG, indicating that CRP was binding primarily to PSG components, and not LPG contaminants in PSG preparations. However, the distinct band seen at running front of WT PSG but not in LPG1^{-} PSG could be indicative of free LPG in PSG preparations, although positive identification of this artefact was complicated by the similarity in ligand moieties between LPG and PSG (Figure 39A). Blotting for *Leishmania* product carbohydrate domains (galactose-mannose-phosphate disaccharide

repeats) with specific antibody LT6 suggests that WT and LPG1$^{-/-}$ (labelled ‘KO’ within figure) *L.mexicana* PSG have similar proteophosphoglycan compositions (Figure 39B). An additional SDS-PAGE and Western Blot of WT, LPG1$^{-/-}$ and LPG2$^{-/-}$ *L.mexicana* PSG of the same quantity that was probed with CRP (Figure 40) appears to show similar levels of CRP binding with regard to the molecular weight of the smear pattern, as well as fluorescence intensity, between WT and LPG1$^{-/-}$ PSG, while detecting no binding in the LPG2$^{-/-}$, supporting the results of the previous ELISA (Figure 38).

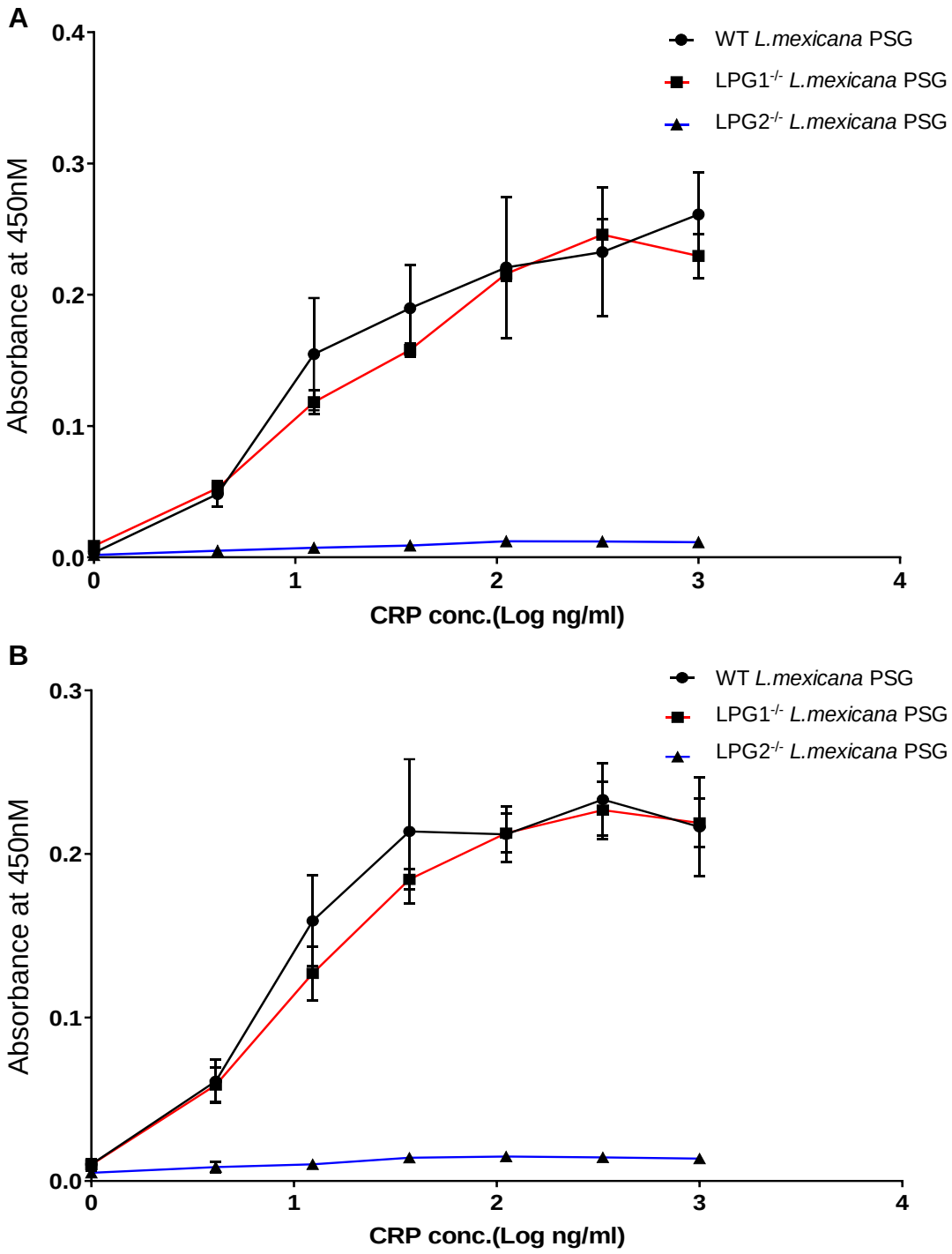

Figure 39: CRP binding of PSG is independent of LPG

Dose-Response of binding of purified CRP (0 - 1.0 µg/ml) to immobilised *L.mexicana* PSG (WT, LPG1$^{-/-}$ & LPG2$^{-/-}$: 0.3 µg/ml) in the absence (A) and presence (B) of CRP-depleted serum (1:60). In both A&B, CRP binding was detected using rabbit anti-CRP antibody, HRP-conjugated goat anti rabbit antibody and TMB substrate (OD 450nm). n=3 technical replicates. Error bars represent standard deviation.

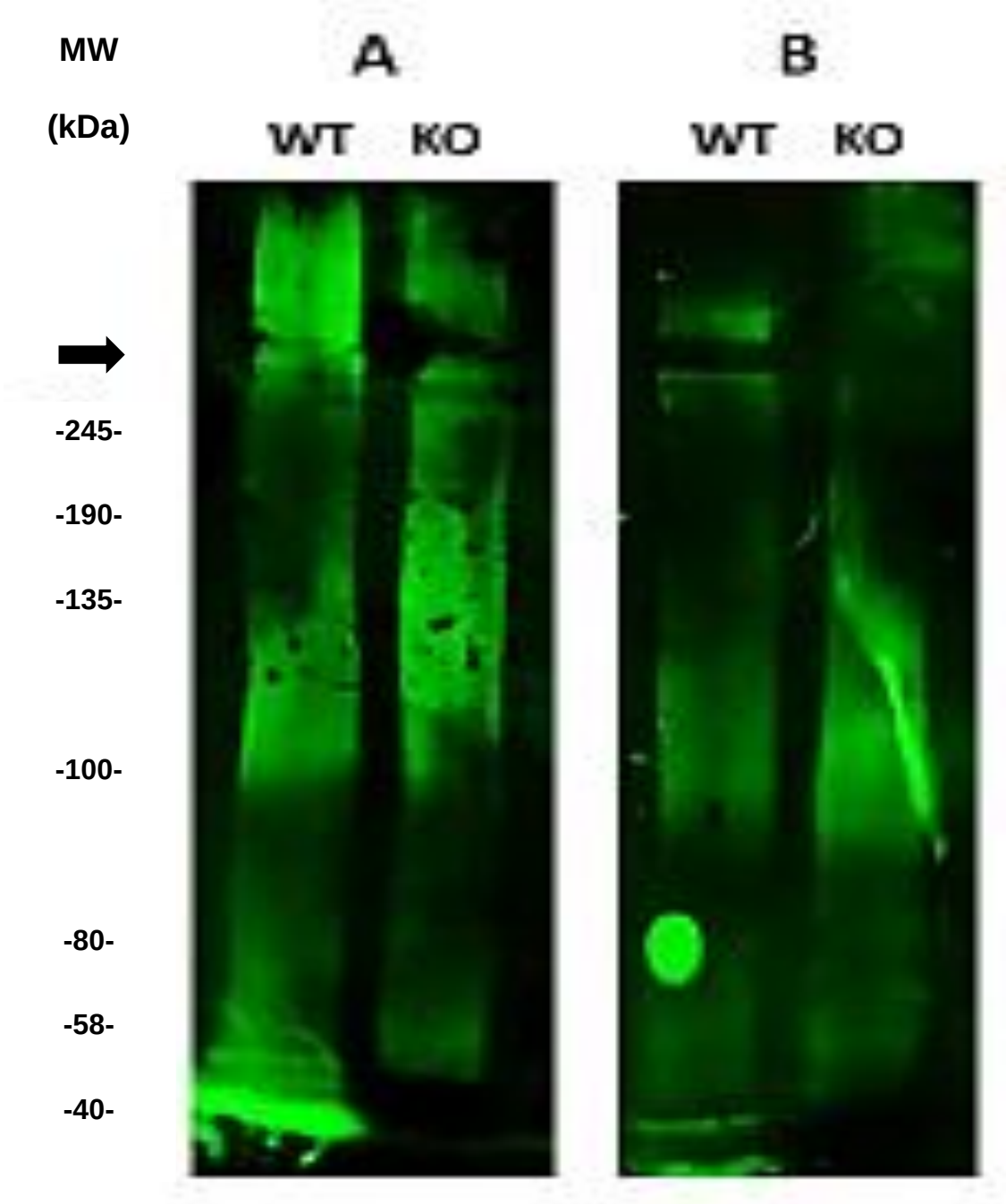

Figure 40: CRP binding to PSG is not dependent on LPG.

NIR fluorescent imaging of WT (Wild-type) and LPG1$^{-/-}$ (KO: LPG-deficient) *L.mexicana* PSG. The similarity in the fluorescent smear between the WT and KO indicates that CRP was not binding to PSG-associated LPG
A: Ligand-blotting with purified CRP, Rabbit anti-CRP and fluorescent IRDye® 800CW Goat anti-Rabbit IgG.
B: Detection of *Leishmania* phosphoglycan repeats (common to fPPG, ScAP and LPG) with specific murine antibody LT6 and IRDye® 800CW Donkey anti-Mouse IgG.

MW: Molecular weight. →: Stacking-resolving gel layer border.

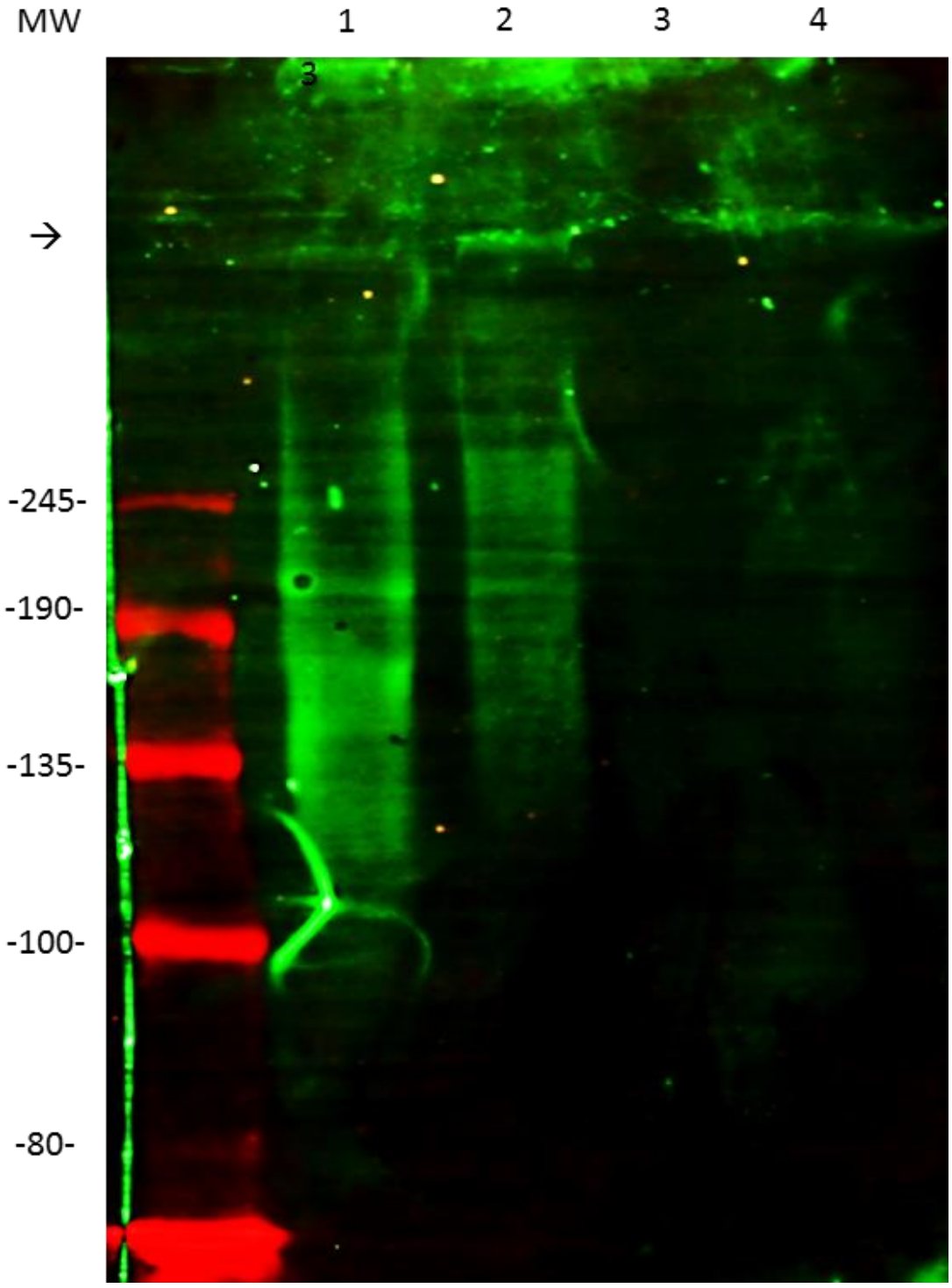

Figure 41: CRP binding to PSG is not dependent on LPG and corresponds to PG synthesis in *Leishmania* PSG.

NIR fluorescent image of WT (Wild type), LPG1$^{-/-}$(LPG-deficient) and LPG2$^{-/-}$ (LPG and PPG deficient) *L.mexicana* PSG. Ligand blotting with purified CRP, Rabbit anti-CRP and fluorescent IRDye® 800CW Goat anti-Rabbit IgG.

1=WT; 2=LPG1$^{-/-;}$ 3=LPG2$^{-/-}$; 4=Blank.
MW: Molecular weight →=Stacking-resolving gel layer border

3.2.5: Secreted acid phosphatase is responsible for the majority of CRP binding capacity in *L.mexicana* PSG

While fPPG had been previously reported to be the primary constituent of PSG as found as a blockage within the infected sandfly gut, *Leishmania* promastigotes have also been shown to express PG product, namely ScAP. As such, it was possible that WT PSG material was heterogenous in nature, with fPPG, ScAP1 (~100kDa) and ScAP2 (~200kDa) as its constituents, particularly since no studies have been made regarding differential expression of PGs *in vivo* versus the culture supernatant. *L.mexicana* mutants had been generated previously with different ScAP expression profiles, namely ScAPKO which expresses no ScAP whatsoever (i.e. fPPG only) due to knockout of both the lmSAP1 and lmSAP2 genes, and ScAPAB, a partial addback mutant which expresses the larger but more lowly expressed 200 kDa ScAP2 molecule (i.e. fPPG and ScAP2).(Ilg, 2000b)

ELISA of immobilised *L.mexicana* WT, ScAPKO and ScAPAB with a dose-response of varying concentrations of CRP in the presence or absence of whole serum was performed (Section 2.12.2). ScAPKO PSG exhibited greatly decreased CRP binding capacity compared to WT PSG. SAPAB, which expressed the larger 200 kDa ScAP2 variant, exhibited a partial rescue of CRP binding capacity, suggesting that ScAP1 constitutes the majority of the CRP binding capacity of PSG purified from culture supernatant (Figure 41).

An ELISA was also performed on WT and ScAPKO *L.mexicana* PSG in the presence of Ca^{2+} or the Ca^{2+}-chelating agent EDTA (Figure 42). In the presence of Ca^{2+}, ScAPKO PSG was again shown to have greatly reduced CRP binding capacity in comparison to WT PSG. Of note, there appeared to be no significant difference in CRP binding when comparing WT in the presence of EDTA and ScAPKO in the presence of Ca^{2+}. It was unknown if this could indicate the presence of Ca^{2+} independent CRP binding that was specific to fPPG and does not occur in ScAP, or simply a reflection of the background signal and/or the limitations of the detection method and protocol.

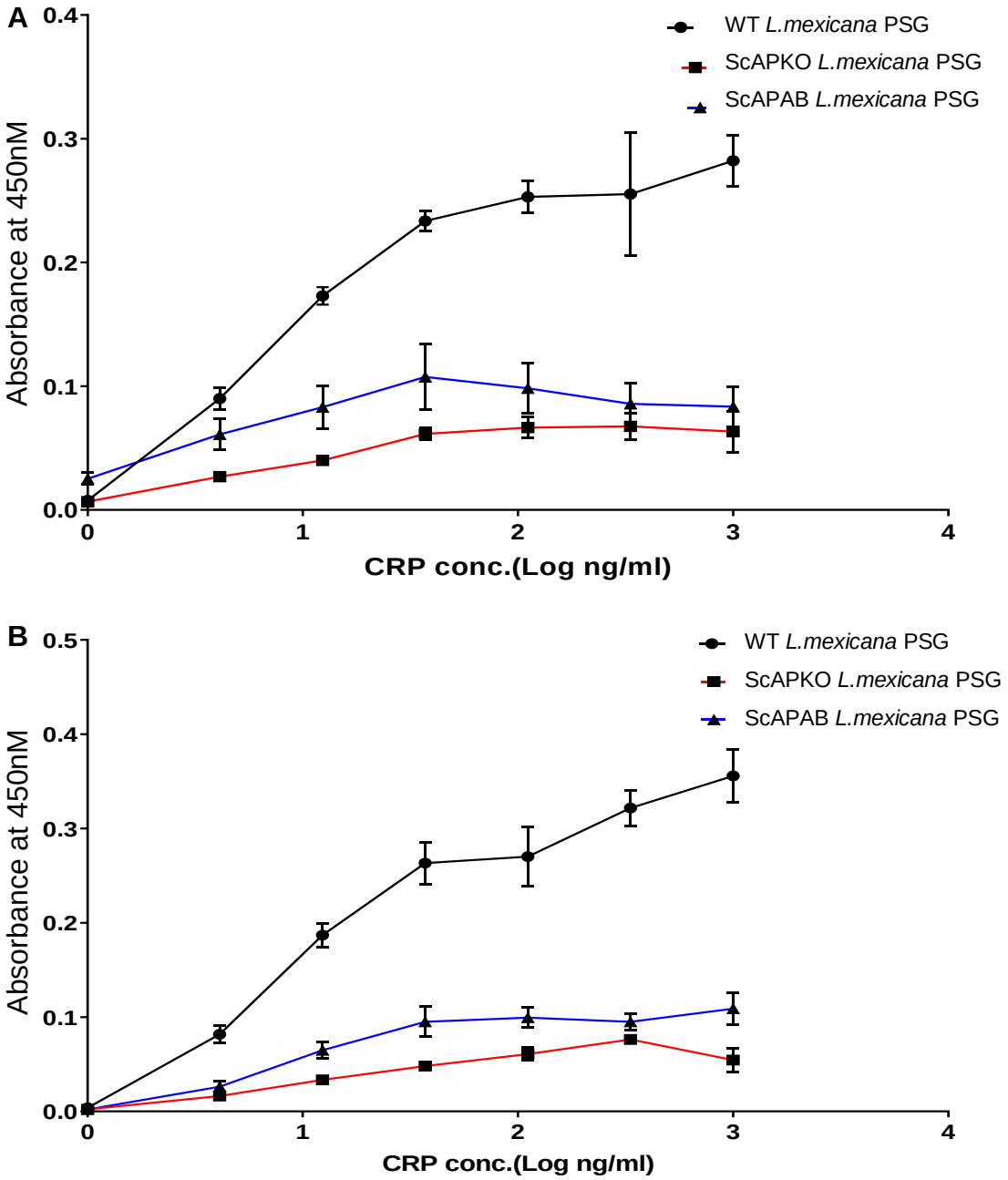

Figure 42: ScAP provides the majority of CRP binding capacity in PSG.

Dose-Response of binding of purified CRP (0 - 1.0 µg/ml) to immobilised *L.mexicana* PSG (WT, ScAPKO & ScAPAB: 0.3 µg/ml) in the absence (A) and presence (B) of CRP-depleted serum (1:60). In both **A&B**, CRP binding was detected using rabbit anti-CRP antibody, HRP-conjugated goat anti rabbit antibody and TMB substrate (OD 450nm). n=3 technical replicates. Error bars represent standard deviation.

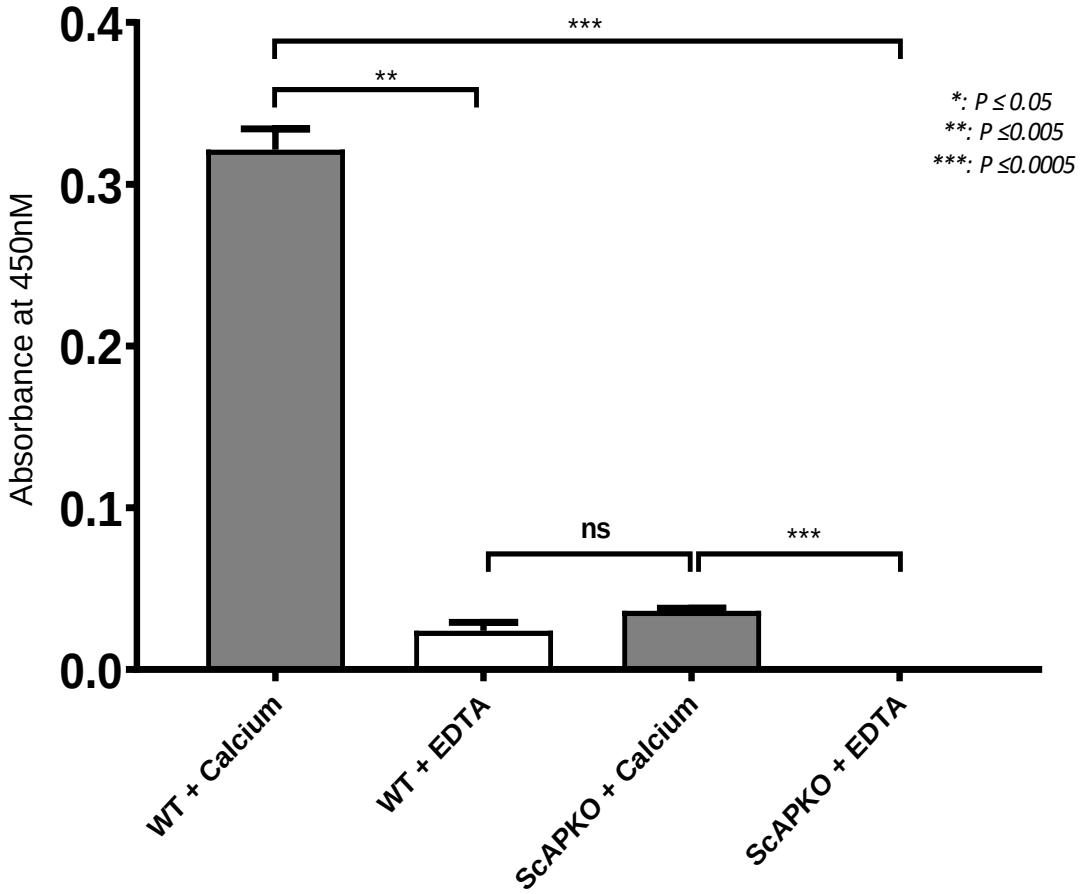

Figure 43: ScAP provides the majority of CRP binding capacity in PSG.

Binding of CRP-biotin (1.0 µg/ml) to immobilised *L.mexicana* PSG (WT & ScAPKO: 1.0 µg/ml) in calcium-containing buffer (0.5 mM) or EDTA-containing buffer (10mM)

CRP-biotin binding was detected by HRP-conjugated streptavidin. n=3 technical replicates. Error bars represent standard deviation. *: P ≤0.05, **: P ≤0.005, ***: P ≤0.0005, ns: Not significant.

3.3: Investigation of complement activation potential by CRP-PSG complex

3.3.1 PSG-CRP complex is capable of binding C1q

CRP has been identified as an activator of the classical complement pathway (Salazar et al., 2014). As PSG had been identified as a major component of material injected into the mammalian host during feeding attempts by *Leishmania*-infected sandflies (alongside sandfly saliva and infective metacyclic promastigotes) and we had demonstrated the ability of CRP to bind to PSG in a dose and Ca^{2+} dependent manner, we investigated the ability of PSG to activate complement, which would have a role in modulation of the local immune environment and subsequently have the potential to directly influence the survival and replication of *Leishmania*, particularly in the early stages of mammalian infection.

Key to the potential of PSG to activate the classical complement pathway via CRP would be the ability of the PSG-CRP complex to bind to the initiator molecule C1q, which would be contingent on calcium-dependent ligand binding triggering the conformational change necessary in CRP to allow C1q binding. ELISA with immobilised C1q and incubation with a fixed concentration of CRP and varying concentrations of PSG from multiple species was performed (Section 2.13.1) in order to investigate to potential of CRP-PSG complexes to bind to C1q (Figure 43). Unbound CRP exhibited no binding to C1q, with increasing concentrations of PSG (presumably increasing the number of CRP-PSG complexes) causing a dose-responsive change to CRP captured on the surface, indicating that PSG binding to CRP was able to trigger the conformational change required for C1q binding. Of interest, the ranking order of CRP-PSG complex binding did not appear to directly correspond to that of the CRP binding capacity between different *Leishmania* species previously shown (Section 3.2.3), suggesting that CRP binding of PSG may not be a directorrelate of the conformational change in CRP that allows C1q binding.

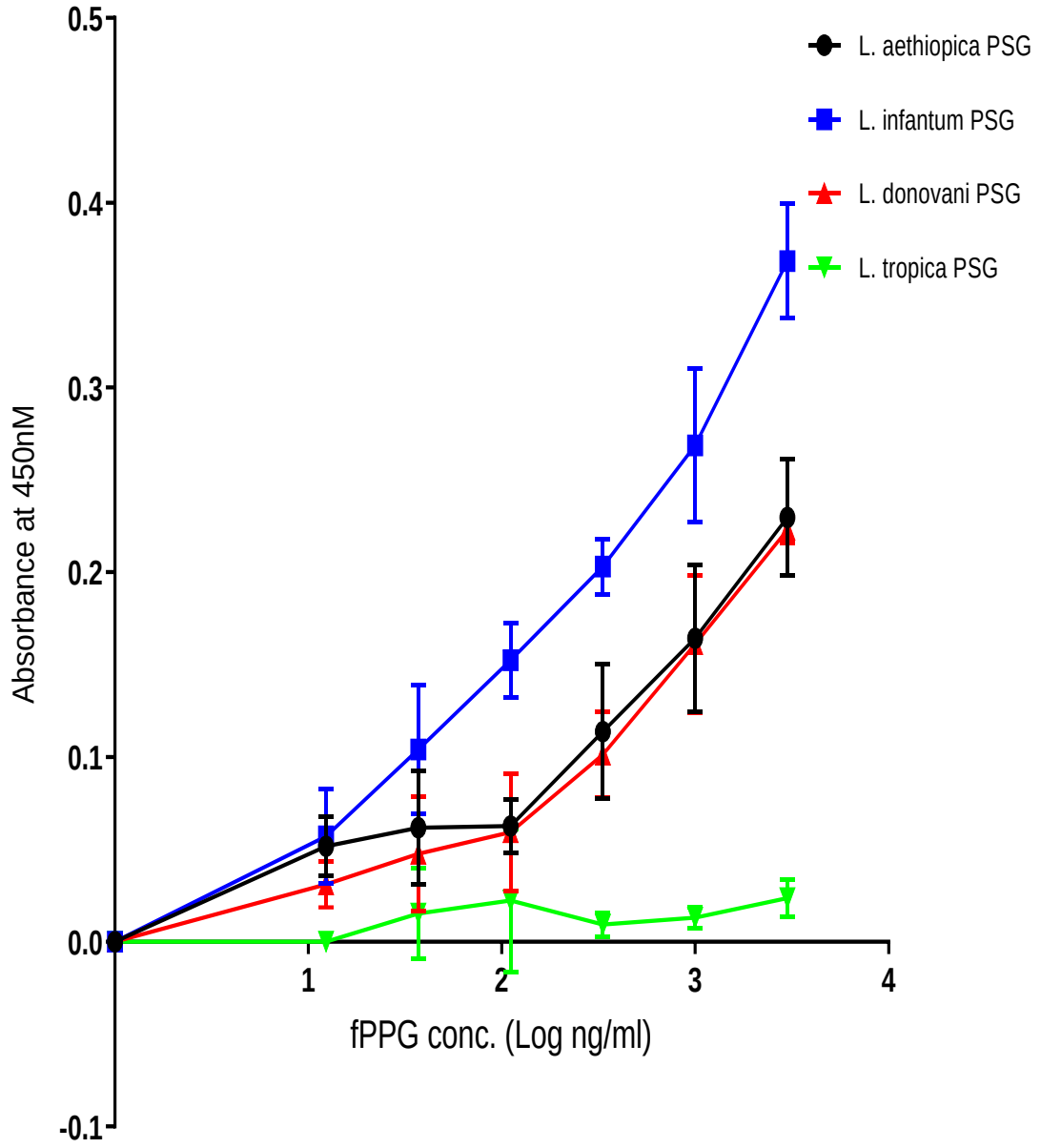

Figure 44: PSG-CRP complexes are capable of binding to C1q.

The order of binding capacity of C1q to CRP-PSG complexes does not correspond with PSG's CRP binding capacity. This could suggest that the binding of PSG to CRP does not directly correlate to the conformational change of CRP to allow subsequent CRP binding. Dose-response curves of PSG-CRP complex (1 µg/ml CRP, 0-3µg/ml) fPPG binding to immobilised C1q (10µg/ml). Error bars represent standard deviation)

L.tropica PSG that displayed little CRP binding capacity also showed no ability to induce the CRP-c1q interaction.

ELISA with immobilised C1q and incubation with a fixed concentration of CRP and PSG from multiple species as well as the positive control CRP ligand PCBSA was performed, either in the presence of Ca^{2+}or the Ca^{2+} chelating agent EDTA (Figure 44). Binding of the CRP-PSG complex to immobilised C1q was significantly reduced by calcium depletion in all instances.

ELISA with immobilised C1q and incubation with a fixed concentration of CRP and varying concentrations of *L.aethiopica* PSG in the presence of varying background levels of PC chloride-calcium salt was performed, PC inhibited binding of C1q to the PSG-CRP complex in a competitive and concentration dependent manner. This suggests that PC in itself, while capable of binding to CRP, was unable to trigger the conformational change in CRP required for C1q binding (Figure 45).

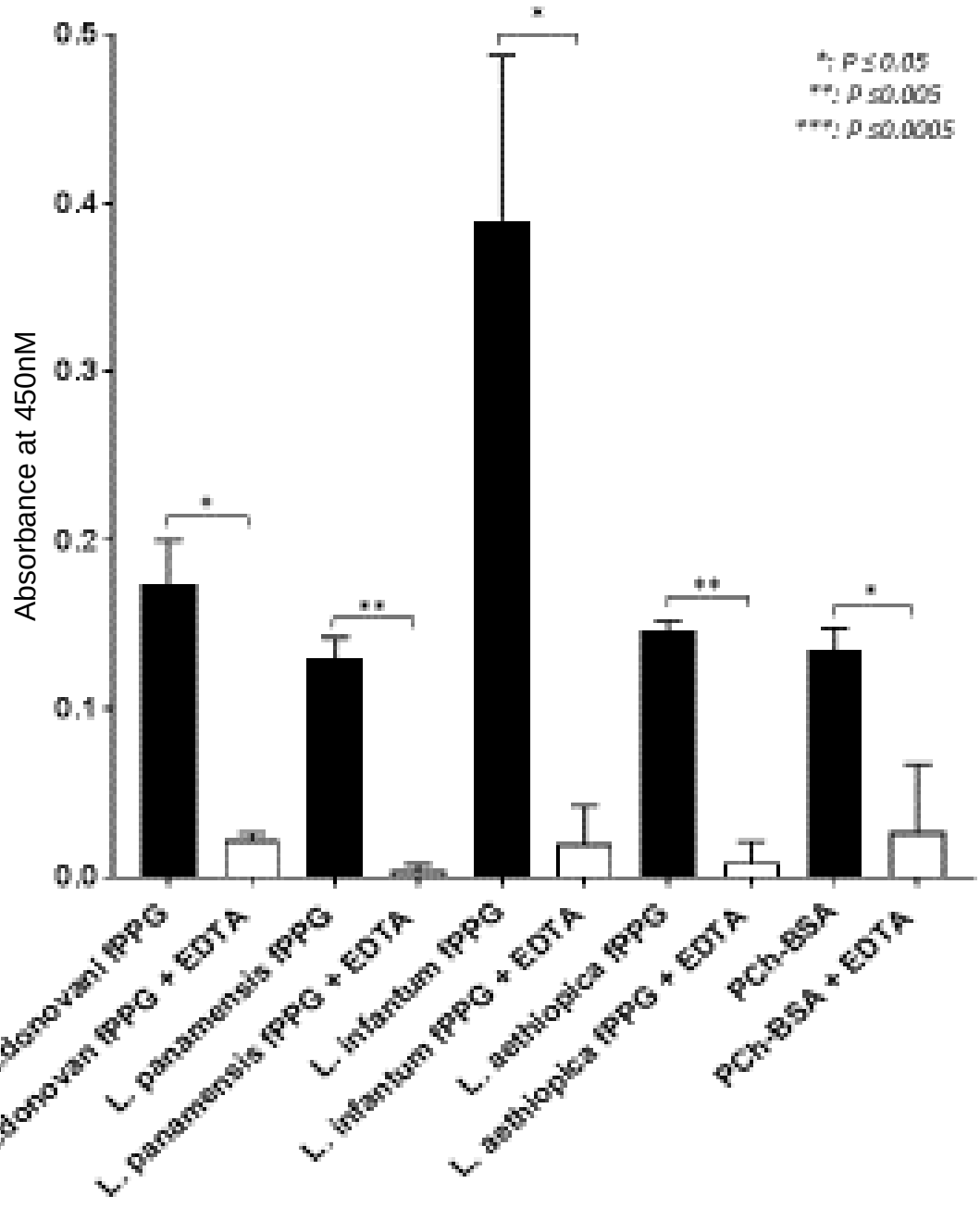

Figure 45: C1q binding of PSG-CRP complex is Ca^{2+} dependent.

C1q binding to CRP-PSG complex was ablated by EDTA, indicating that it was a calcium-dependent interaction. We have previously shown that CRP binding to PSG was also calcium-dependent, which suggests that it was the disruption of PSG-CRP binding leading to the lack of conformational change in CRP necessary for C1q binding. Histogram of ligand-CRP complex binding to immobilised C1q in the presence and absence of EDTA (3 µg/ml fPPG, 1 µg/ml CRP, 10µg/ml C1q, +/-10mM EDTA, n=3.) *: P ≤0.05, **: P ≤0.005, ***: P ≤0.0005, ns: Not significant

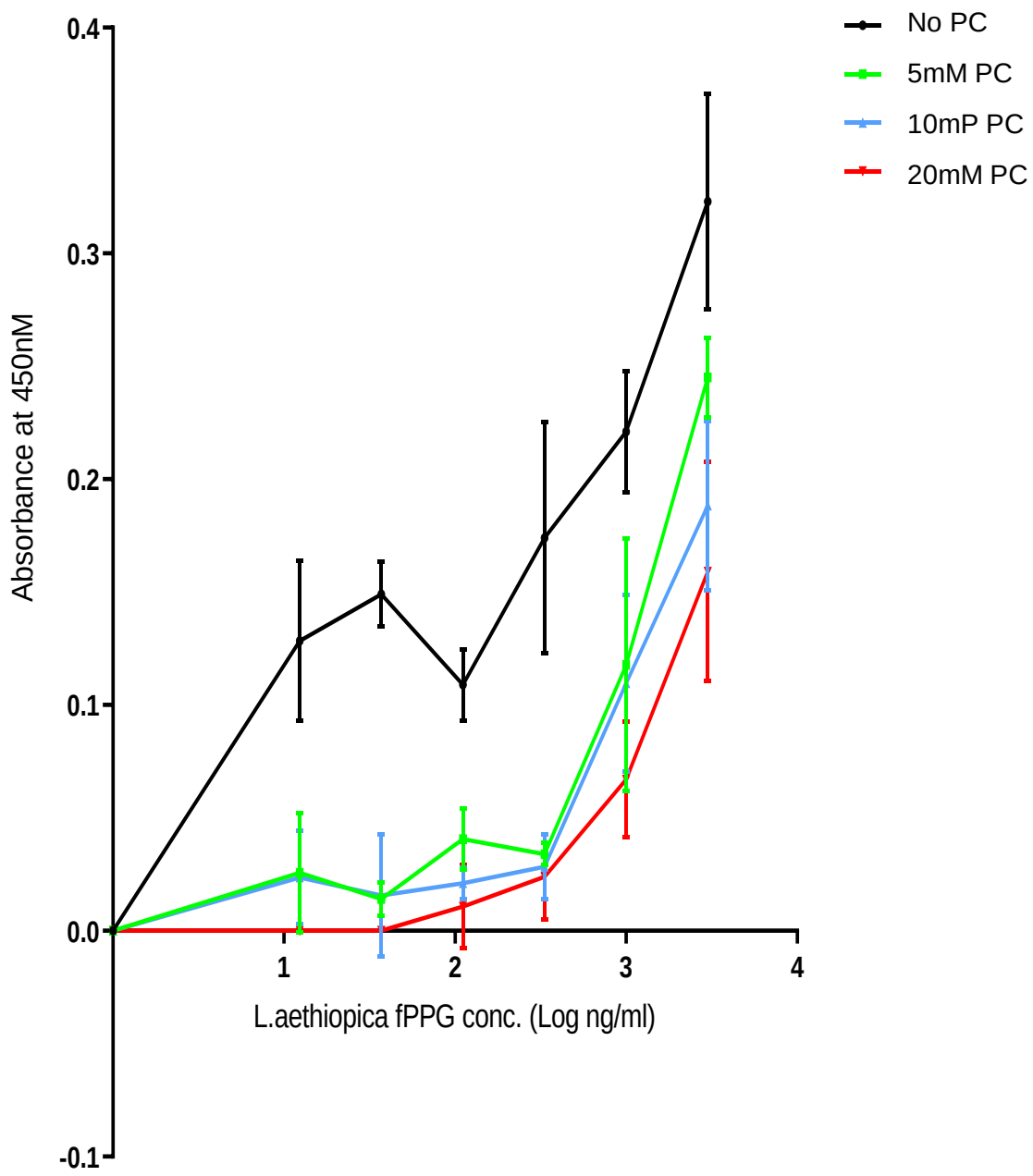

Figure 46: PC inhibits C1q binding of *L.aethiopica* PSG-CRP complex.

PC acts as a competitive inhibitor to PSG for CRP binding sites, suggesting a shared binding site between the two ligands. Dose-response curve of CRP-PSG complex (0-3 µg/ml *L. aethiopica* PSG, 1 µg/ml CRP) binding to immobilised C1q (10 µg/ml) in the absence and presence of varying concentrations of PC (5mM, 10mM, 20mM). n=3 technical replicates. Error bars represent standard deviation

3.3.2: PSG-CRP complex activates to classical complement pathway to generate C3 convertase

C3d and C3bi were chosen as markers for C3 convertase formation, with both candidates being relatively stable intermediary products of C3 degradation.

Complement activation experiments were performed using an ELISA with *L.mexicana* PSG immobilised to the microtitre plate, which was then incubated with whole serum, in the presence or absence of additional purified CRP, in the presence of Ca^{2+} and Mg^{2+}, EDTA, or EGTA and Mg^{2+}, with incubation being stopped at different time points and measuring C3bi. Incubation with EDTA would ablate both the classical (CP) and alternative (AP) pathways, as they were Ca^{2+} and Mg^{2+} dependent respectively, with the Ca^{2+} specific chelator EGTA + Mg^{2+} selectively leaving the alternative pathway intact. A time-course ELISA measuring C3bi deposition at different points in time was performed in order to determine when the reaction should be stopped in subsequent experiments (Section 2.13.4). It was determined that 20 minutes was the optimal incubation period for the experimental model, as well as demonstrating that *L,mexicana* PSG experiences statically significant activation of the classical complement pathway via the addition of CRP (Figure 46). Data from an individual assayed for C3bi was shown, indicating that CRP was capable of activating C3 convertase formation when bound to PSG and that this was largely due to CP activation (Figure 47).

For assay of C3d deposition a time-course was also performed to determine optimal C3d detection (not shown). Ligand concentration was chosen according to previous CRP-binding assay in order to provide a similar amount of CRP binding capacity between ligands (PCBSA: 0.4 µg/ml, *L. infantum* PSG: 4.0 µg/ml) (Section 2.13.3). The addition of CRP (0.4µg/ml) to serum already present (1:100 dilution) was shown to significantly increase C3d generation in a single individual, suggesting that both PCBSA and PSG were activators of CRP-mediated, classical complement pathway (Figure 48). Assays from multiple individual sera showed a significant increase in C3d generation with the addition of purified CRP in both PCBSA and PSG. The lack of C3 formation in the presence of EDTA would suggest that complement pathway activation was

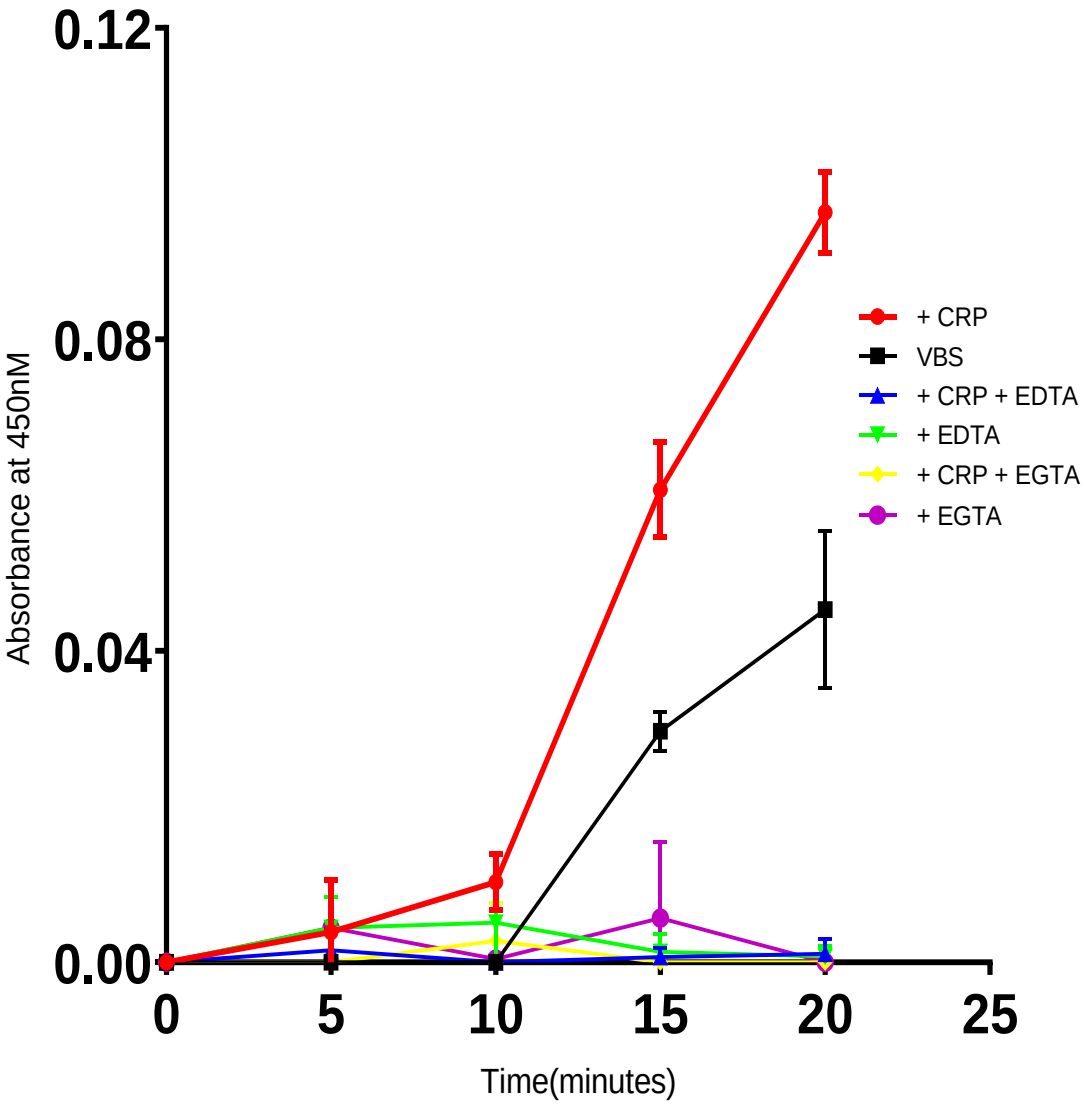

Figure 47: Complement activation by *L.mexicana* PSG is time sensitive.

C3bi generation was a marker for classical complement activation. Dose-response of generated C3bi following complement activation of serum components (1:100 dilution) by immobilised *L. mexicana* PSG (2 µg/ml) in the presence and absence of additional purified CRP (0.4 µg/ml), EDTA (5mM) and EGTA (5mM). The complement generation was stopped at different time points (5, 10, 15 and 20 minutes) by washing out complement components. n = 6. Error bars represent standard deviation.

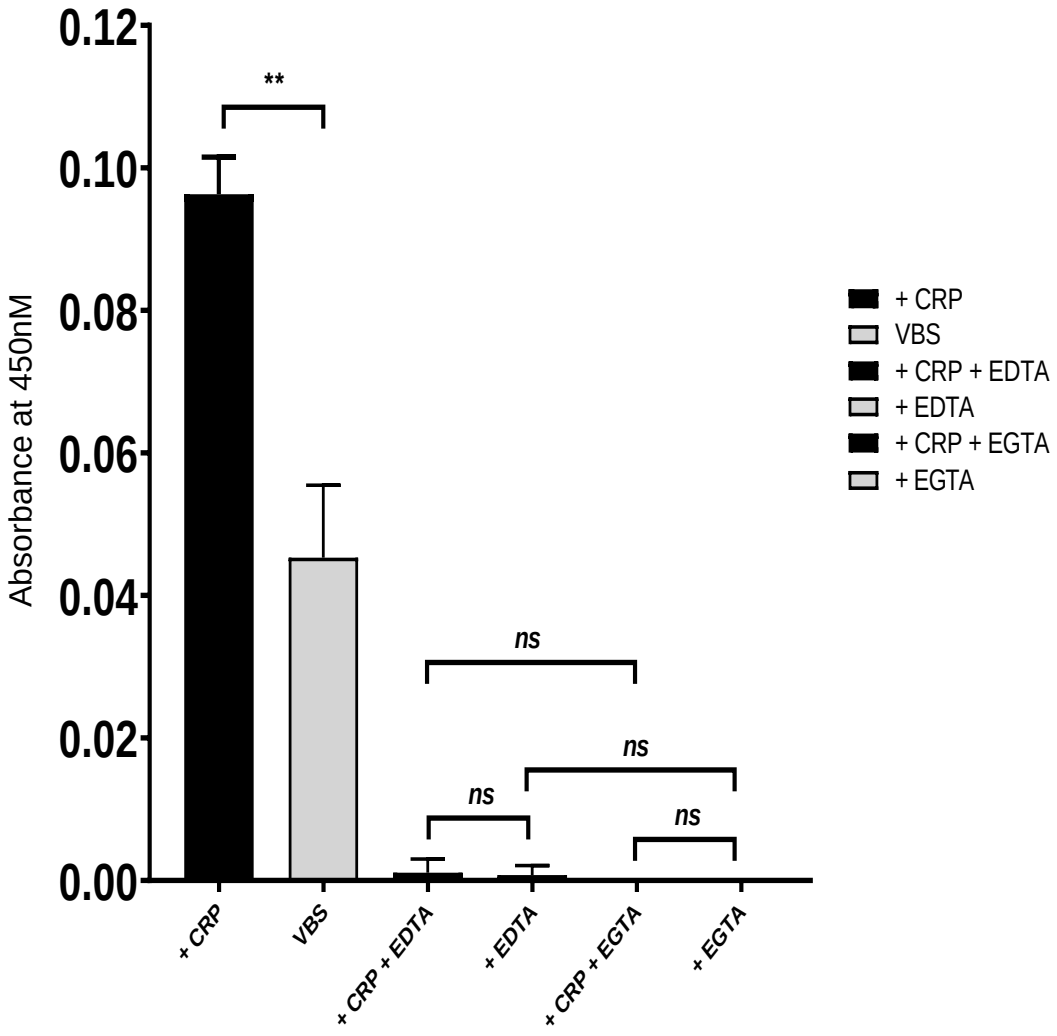

Figure 48: *L.mexicana* PSG activates the classical complement pathway and was increased by CRP binding.

C3bi generation was a marker for classical complement activation. Dose-response of generated C3bi following complement activation of serum components (1:100 dilution) by immobilised *L. mexicana* PSG (2 µg/ml) in the presence and absence of additional purified CRP (0.4 µg/ml), EDTA (5mM) and EGTA (5mM). n = 6. Error bars represent standard deviation. *: P ≤ 0.05, **, P ≤ 0.005, ns: Not significant.

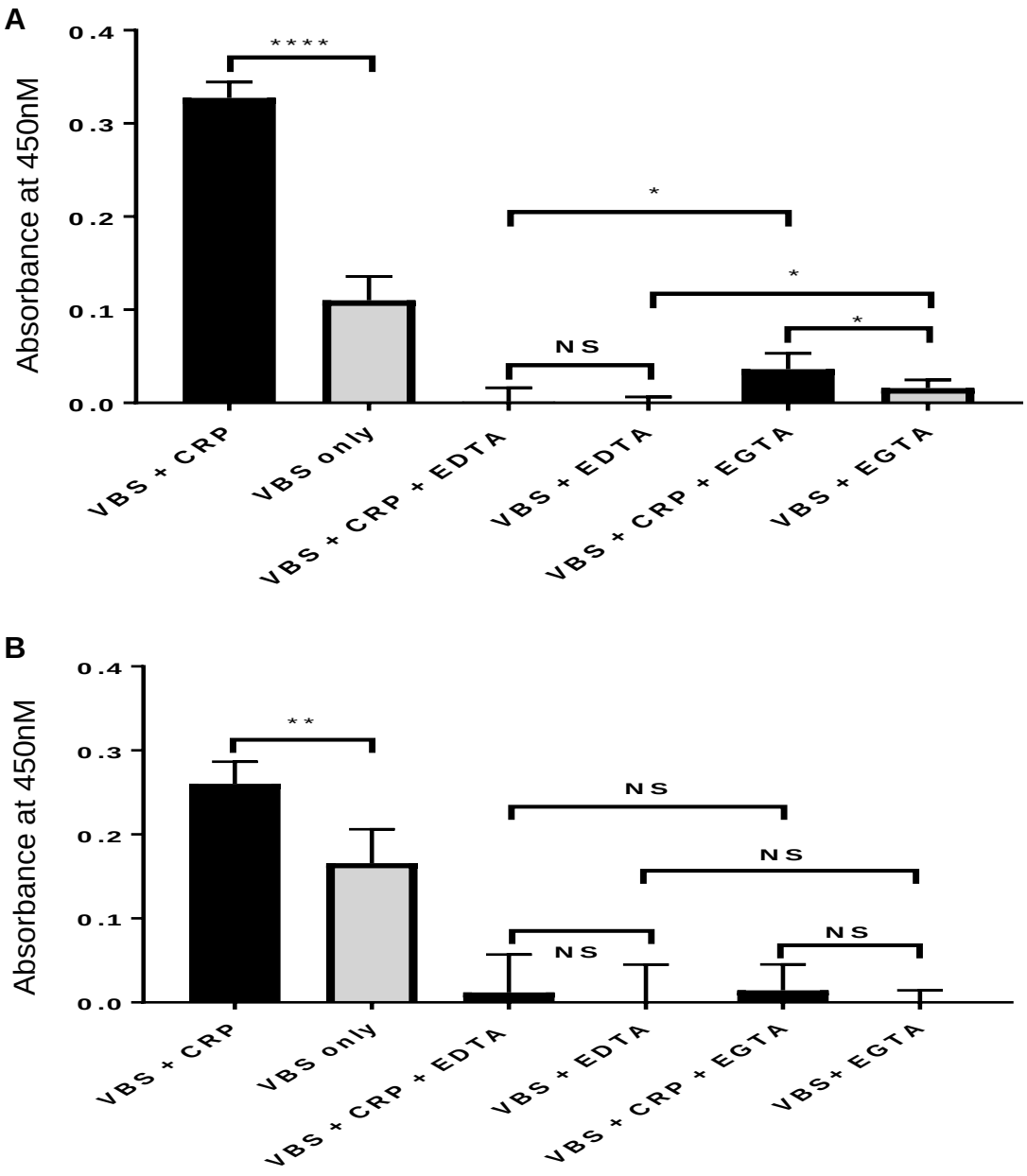

Figure 49: PSG activates complement primarily via the classical pathway.

Dose response of complement in serum (1:100, donor 463M) by immobilised PCBSA (A: 0.4 µg/ml) or *L. infantum* PSG (B: 4 µg/ml) in the presence and absence of additional purified CRP (0.4 µg/ml), EDTA (0.5mM) and EGTA (0.5mM). Detection was achieved with biotinylated anti-C3d, HRP conjugated streptavidin and TMB substrate (OD 450nm). n=6. Error bars represent standard deviation. *: P ≤ 0.05, **, P ≤ 0.005, ns: Not significant.

calcium and magnesium-dependent, which would implicate the CP and AP respectively. When calcium was selectively chelated by EGTA, there was a small but statistically significant increase in C3d generation with PSG (Figure 49A), but not with PCBSA (Figure 49B). This would suggest a minor role in alternative pathway activation in PSG. It should be noted that alternative activation in PSG appeared to be relatively minor compared to classical complement activation, as seen in the magnitude of difference in C3d formation in the presence and absence of EGTA, both in the presence and absence of additional purified CRP (Figure 48). It was possible that residual C3d generation in the absence of purified CRP could be due to classical complement pathway activation by residual CRP, IgG or IgM in the diluted serum. Measurement of complement generation with another complement activation marker, C3bi, supports the data obtained from C3d generation.

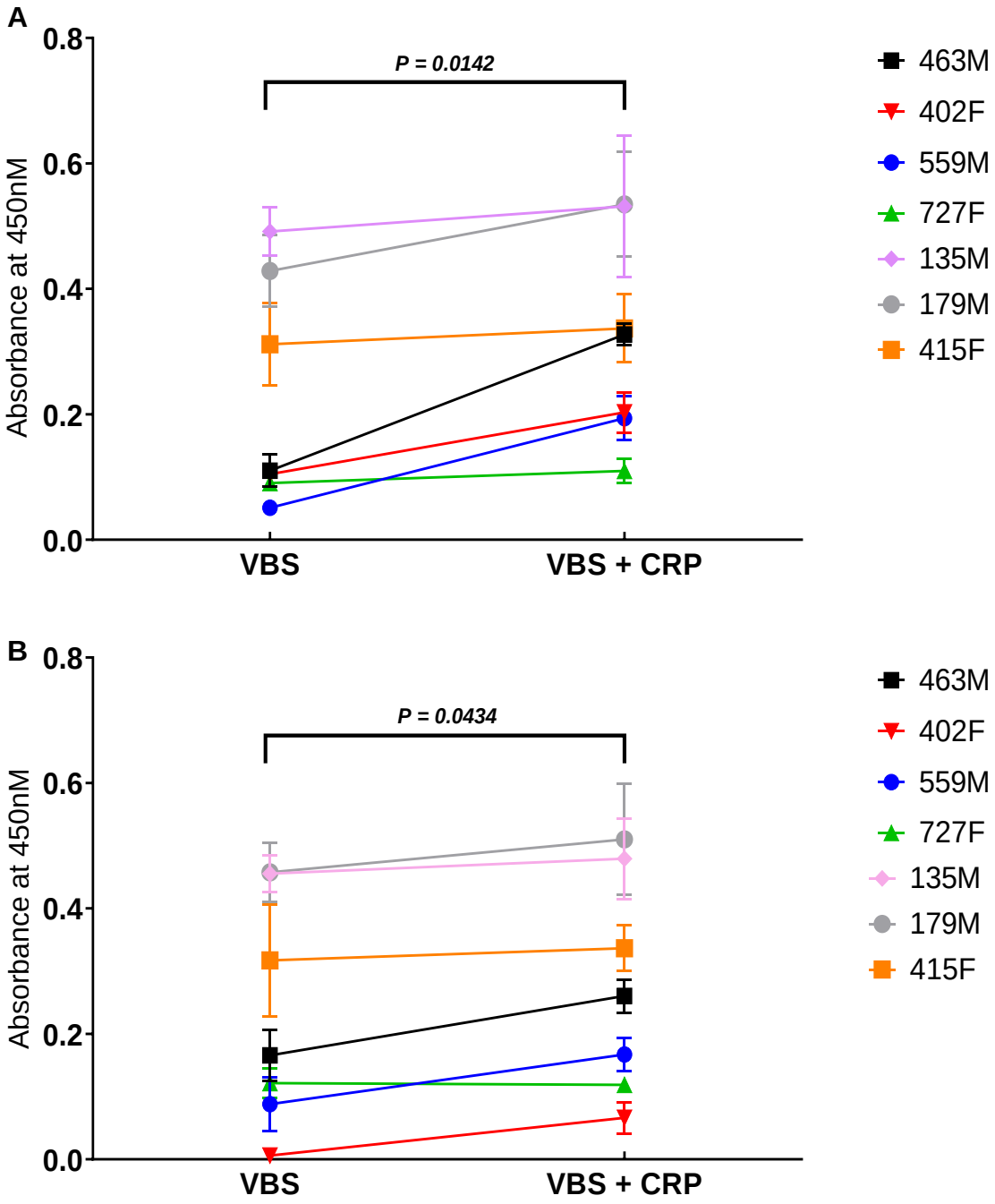

Figure 50: PSG and PCBSA activates classical complement pathway activation via CRP.

C3d generation, which directly correlates to C3 convertase formation, had an increasing trend in the presence of purified CRP (0.4 µg/ml) with different serum donors (463M, 402F, 559M & 727F). Dose-response of generated C3d following complement activation of serum components (1:100 dilution) by immobilised **A:** *L. infantum* PSG (4 µg/ml) or **B:** PCBSA (0.4 µg/ml)) in the presence and absence of additional purified CRP (0.4 µg/ml). n=7 biological replicates. P = P-value

3.3.3: PSG-CRP complex classical pathway activation is not due to LPG contamination

In order to confirm that the previous C3 convertase generation seen in previous C3bi and C3d deposition ELISAs was due to PPG components ELISA was performed as before measuring C3d deposition (Section 2.13.3) with immobilised *L.mexicana* LPG1$^{-/-}$ and LPG2$^{-/-}$. (Figure 50).

PSG derived from LPG1$^{-/-}$ mutant parasites, which maintains normal PPG (i.e. fPPG and ScAP) synthesis but does not express LPG, was capable of generating statistically significant complement generation with the addition of CRP, whereas PSG derived from LPG2$^{-/-}$ mutant, which does not synthesise any PG molecules (i.e. no fPPG, ScAP and LPG) does not, suggesting that, at least for this particular preparation, PSG and not LPG in the *Leishmania* exoglycome was the key component for CRP-driven classical complement pathway activation. This activation was dependent on the presence of calcium, as C3d generation was ablated by EDTA (0.5mM). It should be noted that this was observed from a single serum donor, and that further investigation would be required to determine the veracity of this phenomenon.

Both LPG1$^{-/-}$ and LPG2$^{-/-}$ PSG appear to have minor alternative pathway activation, as suggested by the relatively low C3d deposition observed in the presence of EGTA and Mg^{2+}, with the majority of complement activation accounted by the classical pathway.

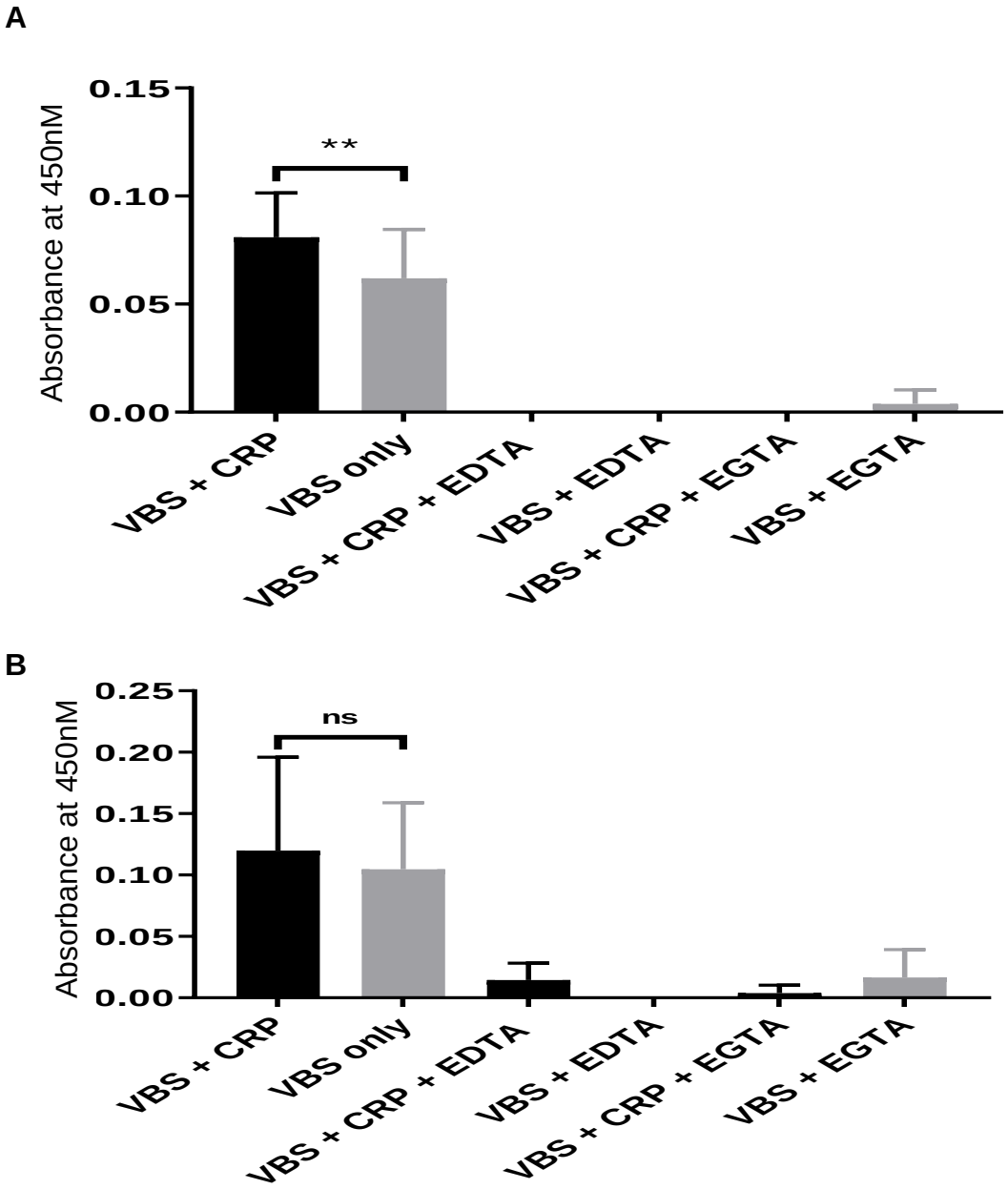

Figure 51: PSG causes a statistically significant increase in classical complement activation as measured by C3d deposition.

Response of complement actvation in serum (1:100, donor 463M) by immobilised LPG1$^{-/-}$(A) or LPG2$^{-/-}$(B) *L. mexicana* PSG (4 µg/ml) in the presence and absence of additional purified CRP (0.4 µg/ml), EDTA (0.5mM) and EGTA (0.5mM). Detection was achieved with biotinylated anti-C3d, HRP conjugated streptavidin and TMB substrate (OD 450nm). n=6 technical replicates. Error bars represent standard deviation. *: P ≤ 0.05, **, P ≤ 0.005, ns: Not significant.

3.4: Investigation of potential PSG interaction with the Lectin Pathway of complement activation

3.4.1: PSG is capable of binding to Mannose Binding Lectin

As highly glycosylated molecules with a large proportion of mannose-containing moieties it seems possible that PSG may be the target of host immune receptors targeting pathogen-derived carbohydrate markers. There was evidence of complement activation in serum that could be classical or lectin mediated that might be induced by endogenous CRP or other innate serum proteins. The lectin pathway (LP) may contribute to the complement cascade when activated by binding of initiator molecules (e.g. MBL, CL-11, ficolins) to sugars found on glycosylated ligands (e.g. mannose and glucose)(Ali et al., 2012). In order to investigate potential activation of the lectin pathway by PSG, PSG binding of the Lectin pathway initiator molecule MBL was assessed.

ELISA was performed measuring the binding of a Lectin Pathway initiator molecule, Mannose-Binding Lectin (MBL), to immobilised PSG from a variety of *Leishmania* species, as well as mannan, which served as a positive control for ligand binding in the absence or presence of whole serum (Section 2.14). ELISA results showed that MBL was indeed capable of binding to PSG, fulfilling an initial requirement for potential activation of the Lectin Pathway. PSG derived from different *Leishmania* species exhibited varying binding capacities for MBL. The lack of correlation of the binding capacity hierarchy for MBL, CRP (Figure 34) and SAP (Figure 53) would suggest binding of different epitopes on PSG. The serum and purified MBL seemed to show a similar capacity for binding of *Leishmania* species. *L.donovani* and *L.panamensis* were capable of binding more MBL, with *L.mexicana* PSG demonstrating low MBL binding capacity (Figure 51).

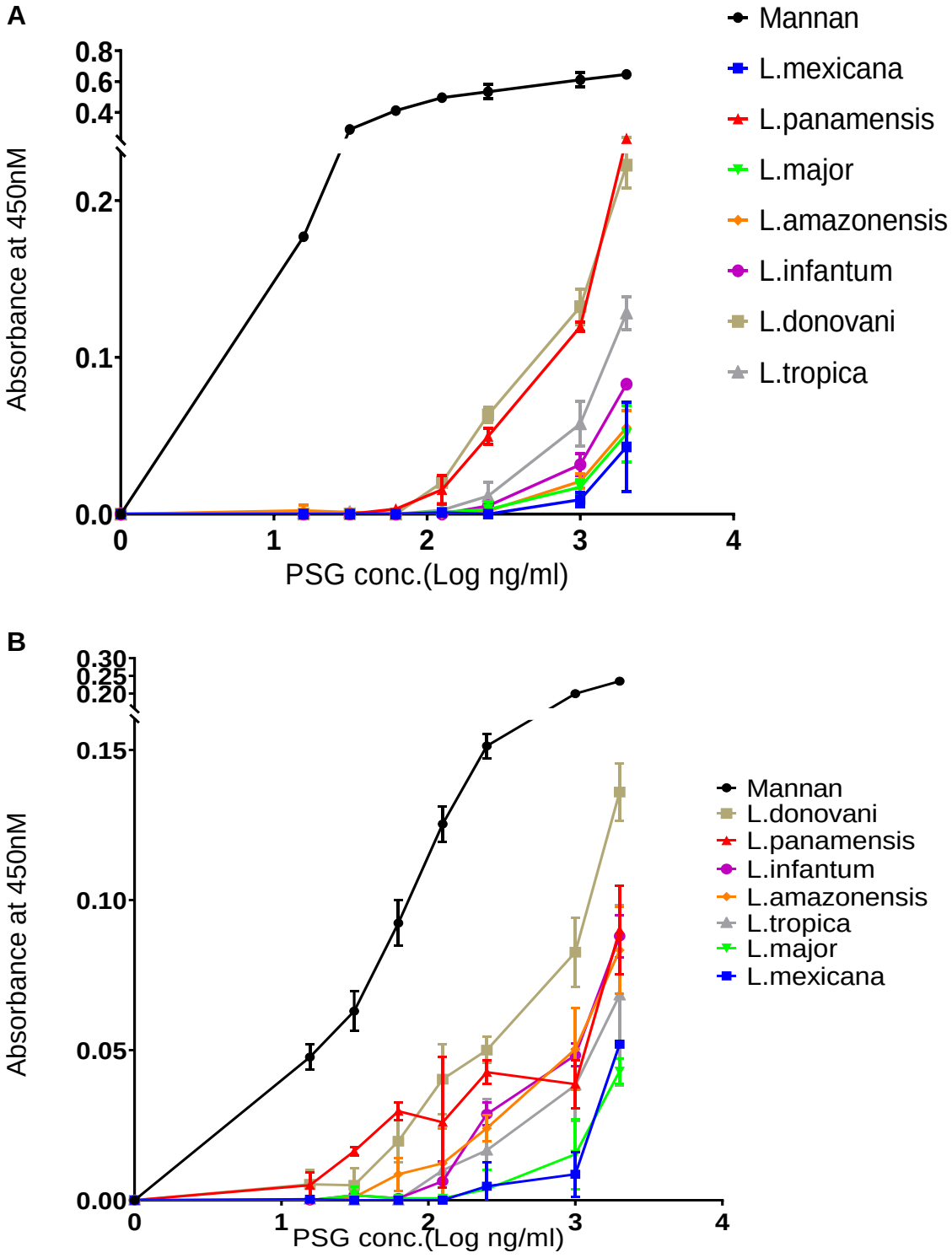

Figure 52: PSG from different *Leishmania* species exhibit widely varying MBL binding capacities.

Dose-Response of binding of purified MBL (A, 0.2 µg/ml) or MBL in serum (B, 1:20 dilution) to immobilised PSG from different *Leishmania* species (2.0 - 0 µg/ml). In both **A&B**, MBL binding was detected using biotin-conjugated rabbit anti-MBL antibody, HRP-conjugated streptavidin and TMB substrate (OD 450nm). n=3 technical replicates. Error bars represent standard deviation.

An attempt to determine lectin pathway complement activation by selectively inhibiting it using sodium polyanethole sulfonate (0.4 µg/ml) (Palarasah et al., 2011) in a complement generation ELISA measuring C3d deposition was unsuccessful, as ascertained by complete lack of inhibition of complement activation by the lectin pathway positive control ligand, mannan (not shown).

3.4.2: MBL binding of PSG appears to be independent to the presence of Ca^{2+}

MBL binding to a variety of pathogenic molecules has been previously shown to be a Ca^{2+} dependent interaction (van Asbeck et al., 2008). In order to investigate the potential of PSG to activate the Lectin Pathway in a similar manner to existing models, it was necessary to further characterise MBL binding to PSG.

ELISA was performed with varying concentrations of immobilised *L.aethiopica* PSG or Mannan incubated with MBL, in the presence of Ca^{2+} or EDTA (Section 2.14). While *L.aethiopica* PSG experiences as decrease in MBL binding in the presence of EDTA, this phenomenon was significantly muted in comparison to MBL binding to Mannan, which experiences almost complete ablation to binding when Ca^{2+} was removed, even at high concentrations of the immobilised ligand (Figure 52). This could signify a novel MBL binding mechanism to PSG that was Ca^{2+} independent.

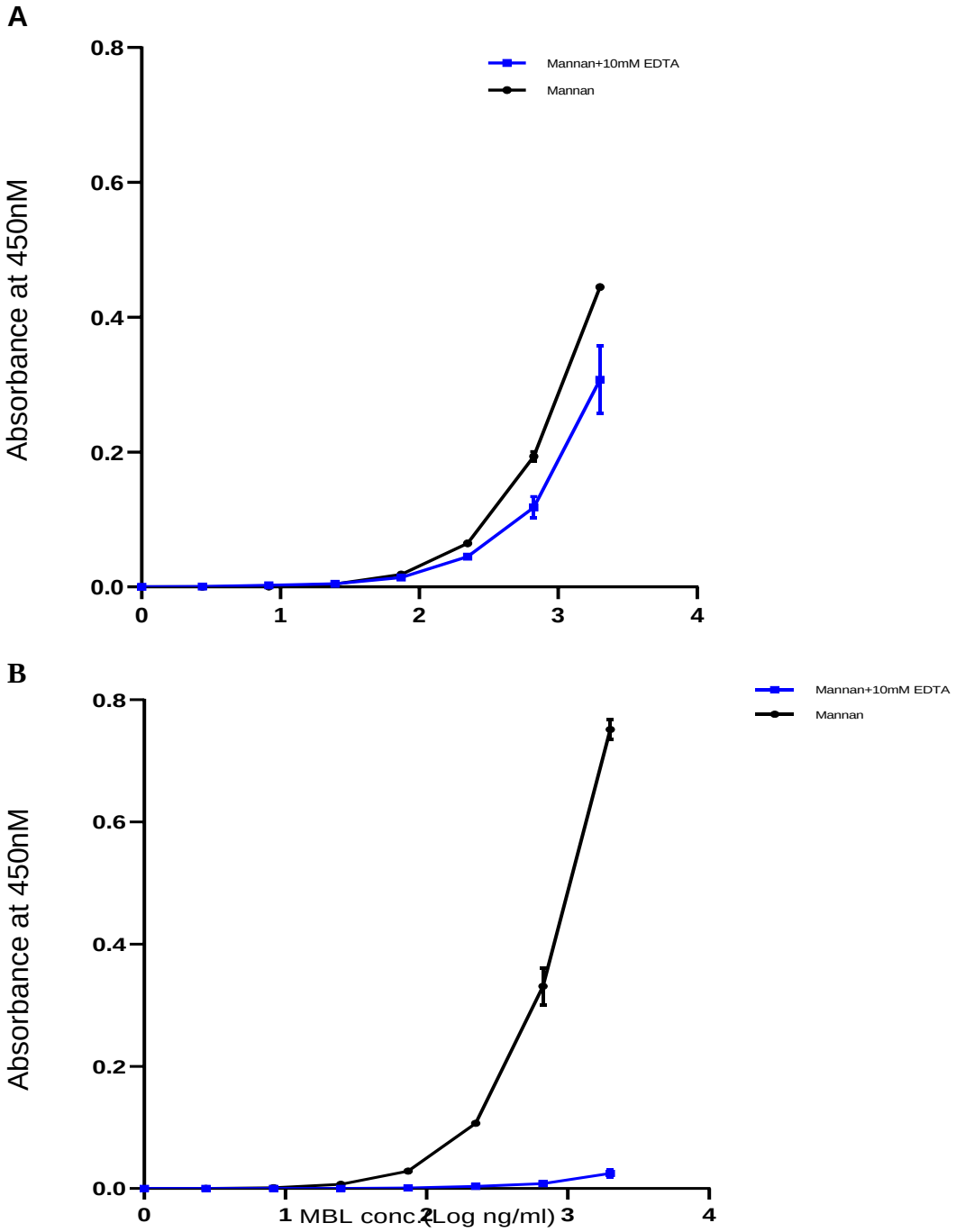

Figure 53: MBL binding of PSG is not entirely calcium-dependent.

Dose-Response of binding of purified MBL (0.2 µg/ml) to immobilised *L. aethiopica* PSG (A, 2.0 - 0 µg/ml) or mannose (B, 2.0 - 0 µg/ml) in the presence of calcium (0.5mM) or EDTA (10mM) containing HEPES buffer. In both **A&B**, CRP binding was detected using biotin-conjugated rabbit anti-MBL antibody, HRP-conjugated streptavidin and TMB substrate (OD 450nm). n=3 technical replicates. Error bars represent standard deviation.

3.5: Investigating interaction of SAP with Leishmania PSG

3.5.1: PSG from different *Leishmania* species have varying SAP binding capacities

Despite not being an acute phase protein in humans, SAP had been shown to experience multiple fold increases in circulating concentration in several other species as part of the acute phase response. In addition, humans have a high constitutive circulating level of SAP of approximately 30 µsg/ml in plasma, as well as a variety of immune relevant functions that have been reported, despite being not as clearly profiled an immune protein as CRP (Poulsen et al., 2017). As such, effort was made to investigate the interaction of SAP with *Leishmania* PSG. Initially, direct binding of purified SAP to PSG was investigated.

To detect SAP binding, ELISA was performed with immobilised PSG from different *Leishmania* species incubated with varying concentrations of purified SAP in the presence of human serum from healthy individuals (Section 2.12.2). SAP exhibited binding to PSG in a dose-responsive manner, with the widely varying half-maximal values between the different *Leishmania* species indicates that PSG has varying binding capacities for SAP (Figure 53). The difference in order of PSG binding capacities to CRP and SAP between different *Leishmania* species suggests that SAP binds to a different component of PSG compared to CRP (Figure 34) or to MBL (Figure 51). *L panamensis* and *L. aethiopica* showed approximately 100-fold more capacity for SAP binding than the others and they exhibit saturation of binding which suggests a specific binding event.

PSG was subjected to SDS-PAGE, transferred onto PVDF membrane and ligand blotted with SAP (Section 2.12.1), with detection using fluorescent anti-SAP antibodies. Probing with SAP ligand blotting method indicated that SAP appears to bind to much lower molecular weight components than CRP does, with a distinct band at 80 kDa and a fainter band at 100kDa. There appeared to be varying levels of expression of these components between different

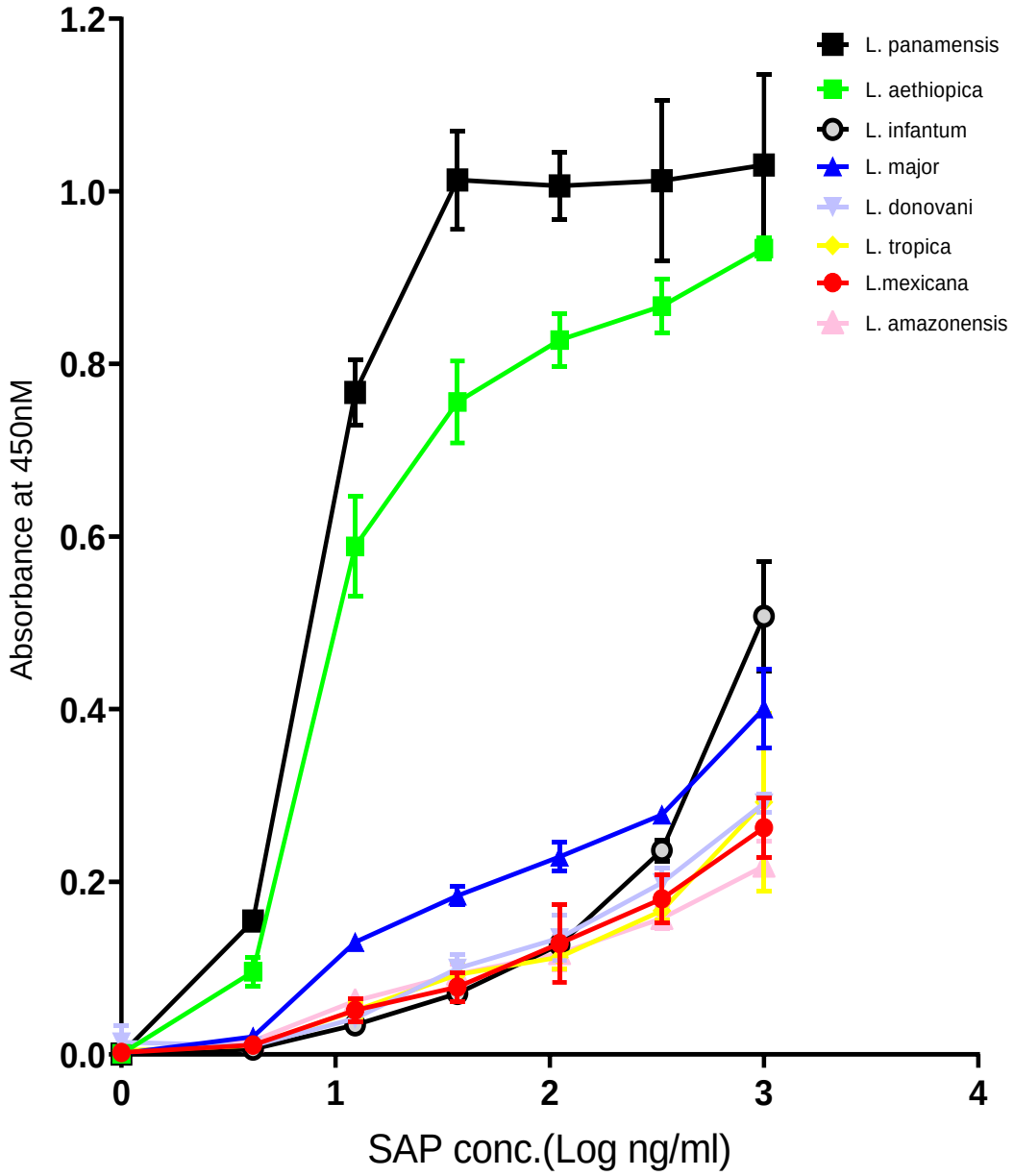

Figure 54: PSG from different *Leishmania* species exhibit widely varying SAP binding capacity and is dependent on serum components; SAP binds to different PSG component than CRP

SAP binding was detected using monoclonal murine anti-SAP antibody, HRP-conjugated Goat anti-mouse antibody and TMB substrate (OD 450nm). n=3 technical replicates. Error bars represent standard deviation.

Leishmania species. NIR fluorescent imaging of *L. tropica* and *L. infantum* ligand blots. (Figure 54). The pattern of binding would suggest that SAP binds to different components of PSG of approximately 80 kDa and 100 kDa molecular weight, as opposed to CRP where a similar SDS-PAGE/ Western Blotting experiment revealed binding to much higher molecular weight products (Figure 35-36). The lack of SAP binding of higher molecular weight components in the same ‘smear’ pattern in the resolving gel layer or larger components trapped in the stacking gel layer would tentatively suggest that SAP does not bind to fPPG or ScAP.

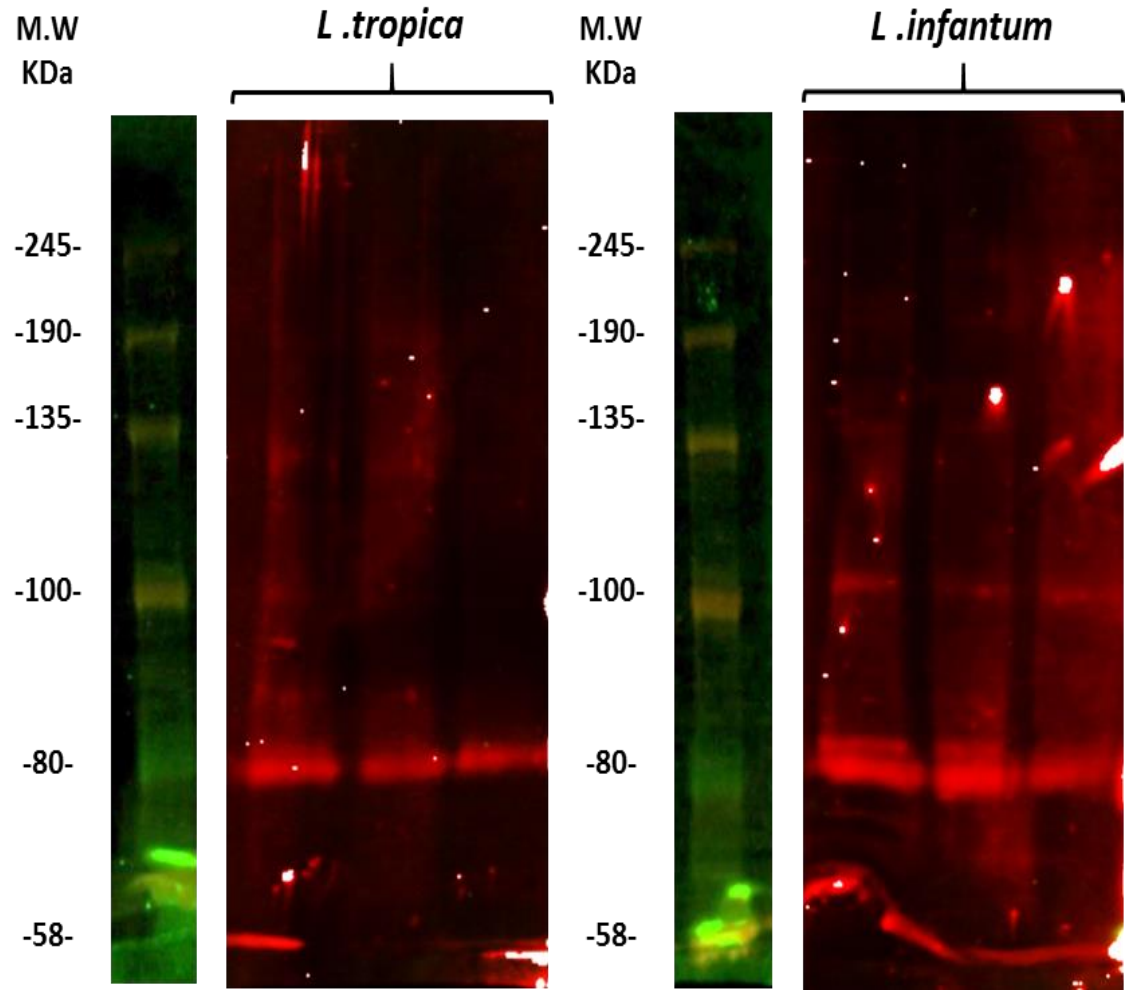

Figure 55: SAP binds to different components in PSG compared to CRP.

Fluorescent probing was done with purified SAP in the presence of serum, monoclonal murine biotinylated anti-SAP 5.4A and IRDye® 680RD Streptavidin. Images were captured using a LI-COR Odyssey CLx system.

3.5.2: fPPG has a higher SAP binding capacity than ScAP for a given quantity of material

As PSG was itself a heterogenous material, being formed of fPPG and ScAP, effort was undertaken to determine whether different PSG components have varying levels of SAP binding capacity. ELISA of SAP binding to *L.mexicana* PSG WT, LPG1$^{-/-}$, LPG2$^{-/-}$, ScAPKO and ScAPAB was performed in order to elucidate this (Section 2.12.2). While not a particularly strong binder of SAP, previous studies have indicated that *L.mexicana* was a good model for sandfly infection.

SAP detection ELISA of immobilised WT, LPG1$^{-/-}$ and LPG2$^{-/-}$ *L.mexicana* PSG incubated with varying concentrations of SAP was performed (Figure 55). Interestingly, SAP binding between the WT and mutant PSG appears virtually identical across a range of concentrations, suggesting that SAP binding previously observed was not due to glycolipid contamination. In addition, the binding observed in LPG2$^{-/-}$ material would suggest that PSG may not be a major component of SAP binding at all.

In order to determine if fPPG and ScAP have differential SAP binding capacities, SAP detection ELISA of immobilised WT, ScAPKO and ScAPAB *L.mexicana* PSG incubated with varying concentrations of SAP was performed (Figure 56). ScAPKO *L.mexicana* PSG displayed greater SAP binding capacity in the mutants (ScAPKO > ScAPAB > WT). Assuming high levels of proteophosphoglycan purity in the material used, this would suggest that fPPG may have a greater SAP binding capacity per weight compared to ScAP, due to the higher proportion of fPPG in the mutants (ScAPKO: fPPG only, ScAPAB: fPPG and ScAP2) compared to WT PSG (fPPG, ScAP1 and ScAP2).

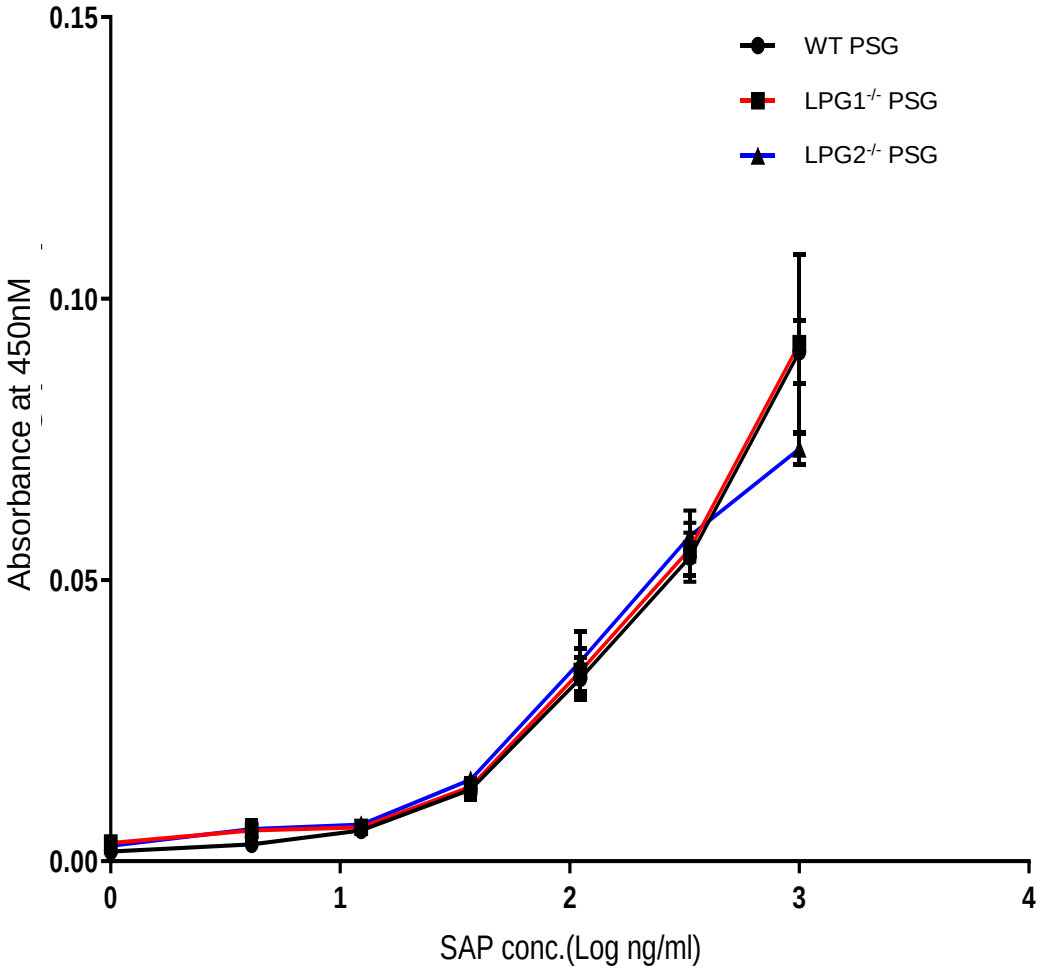

Figure 56: SAP binding of PSG is not LPG-dependent.

Dose-Response of binding of purified SAP (0 - 1.0 µg/ml) to immobilised *L.mexicana* PSG (WT, LPG1$^{-/-}$ & LPG2$^{-/-}$: 0.3 µg/ml). SAP binding was detected using mouse anti-SAP antibody (5.4D), HRP-conjugated goat anti-rabbit antibody and TMB substrate (OD 450nm). n=4 technical replicates. Error bars represent standard deviation.

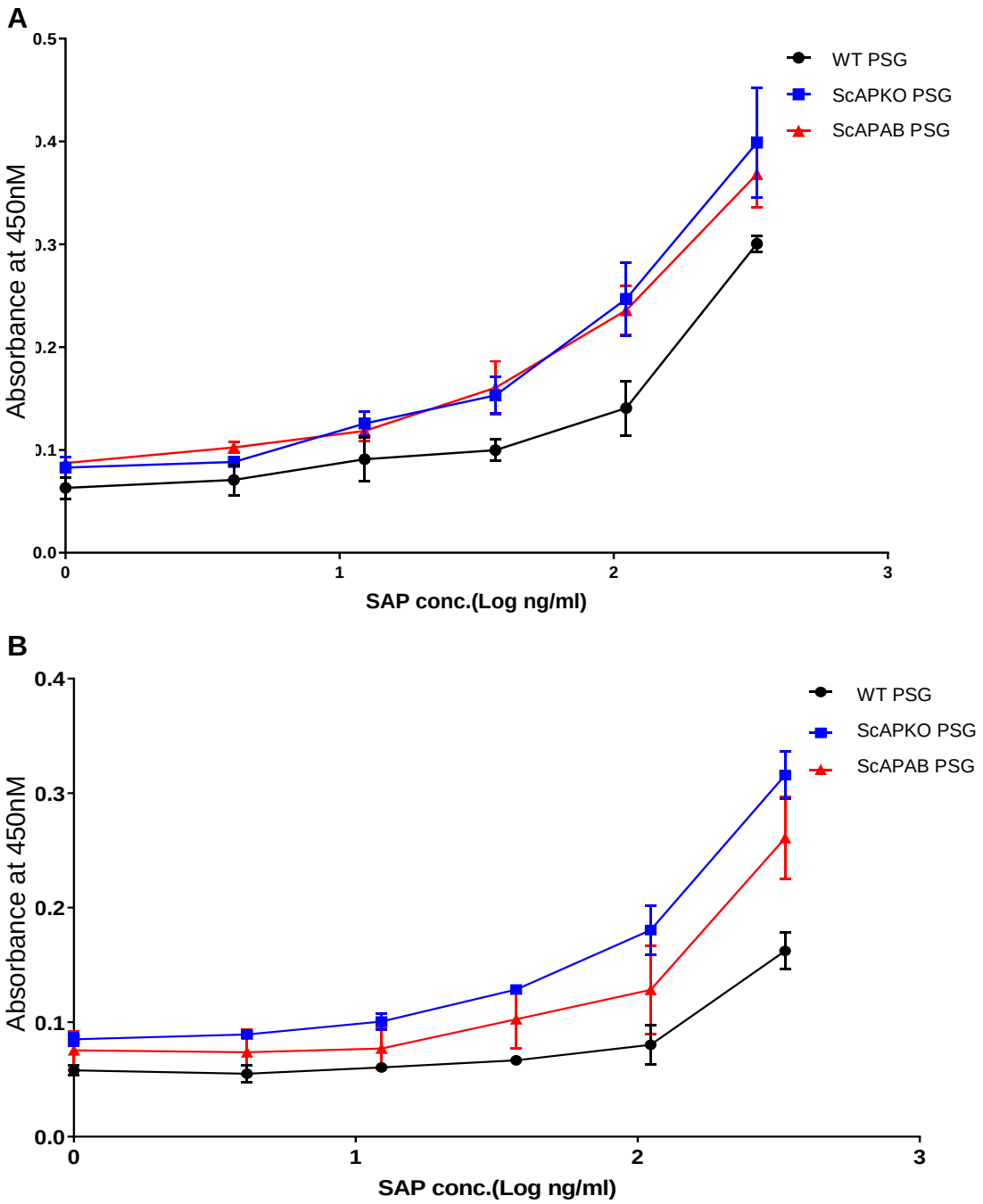

Figure 57: fPPG provides the majority of SAP binding capacity in PSG.

Dose-Response of binding of purified SAP (0 - 1.0 µg/ml) to immobilised *L.mexicana* PSG (WT, ScAPKO & ScAPAB: 0.3 µg/ml) in the absence (A) and presence (B) of SAP-depleted serum (1:60). In both **A&B**, SAP binding was detected using mouse anti-SAP antibody (5.4D), HRP-conjugated goat anti-rabbit antibody and TMB substrate (OD 450nm). n=4 technical replicates. Error bars represent standard deviation.

3.6: Characterisation of LPG interactions with CRP

3.6.1: *Leishmania* promastigotes produce LPG of different sizes at different life cycle stages

LPG was perhaps the most well-studied of the *Leishmania* virulence factors and was heavily expressed in promastigote stage parasites, forming a glycocalyx surrounding the parasite. Due to the relative abundance and availability of membrane-bound LPG during early stages of infection, it would be reasonable to investigate possible innate immune interactions of LPG, including to the pentraxins SAP and CRP (Culley et al., 1996).

LPG expression was previously reported be stage-dependent, with metacyclic LPG being longer and larger than those from nectomonad stage parasites by reason of the increase number of phosphorylated disaccharide repeats previously mentioned (Ilg, 2000b). In order to validate that LPG was purified from the appropriate promastigote stages for subsequent experiments, LPG purified from nectomonad and metacyclic stage *L.mexicana* promastigotes was subjected to SDS-PAGE, transferred onto PVDF membranes and Western blotted with LT6, a murine antibody specific for Gal-Man-PO_4 repeats common to *Leishmania* glycosylated products (Section 2.15.1). Western blotting revealed a broad band pattern, with a molecular weight of approximately 50 kDa and 70 kDa for nectomonad and metacyclic LPG respectively (Figure 57). This would correspond with existing literature, which suggests that metacyclic LPG was larger due to an increased number of the phosphorylated disaccharide repeats.

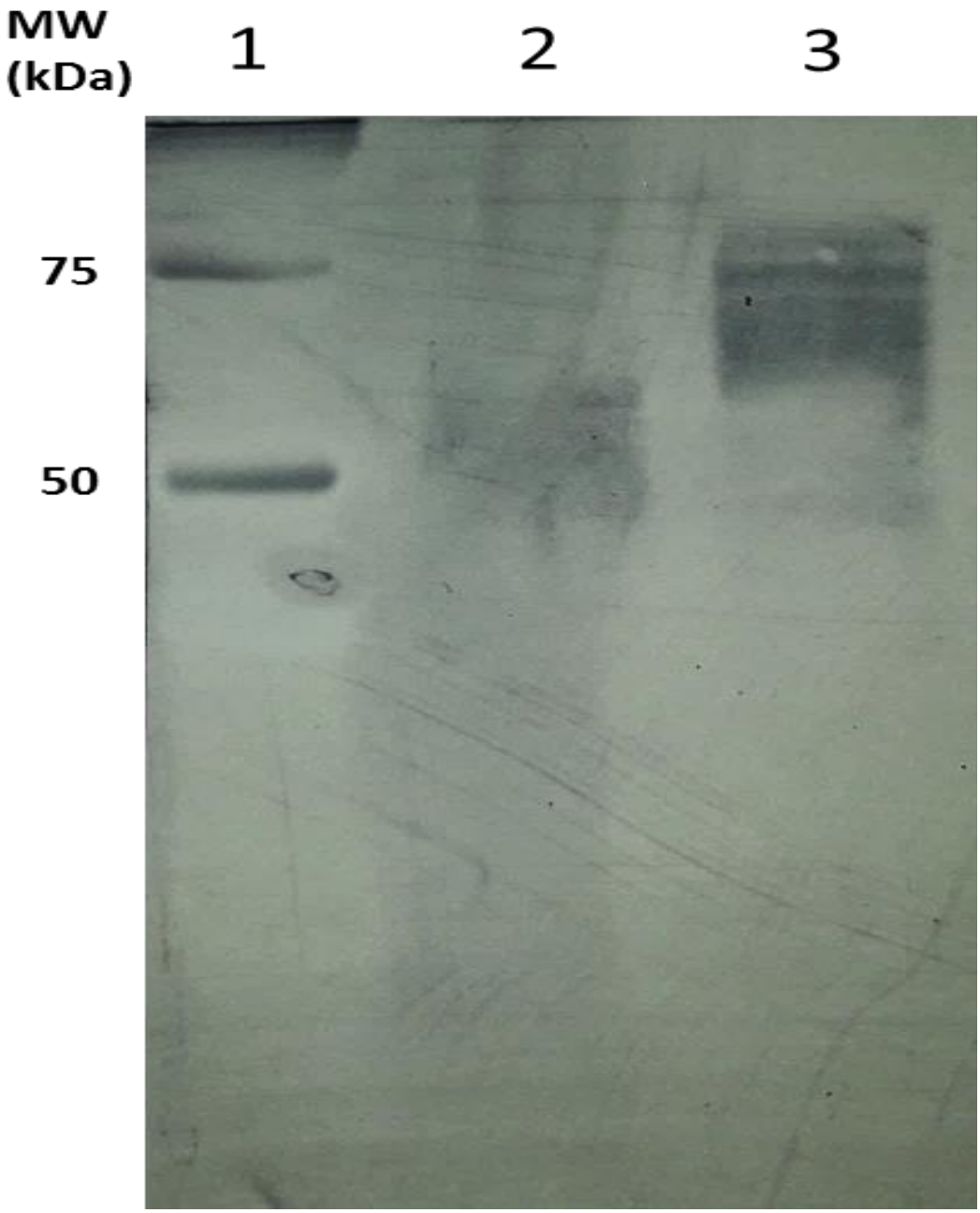

Figure 58: Promastigote stages produce LPG of different molecular weight.

LPG purified from metacyclic and nectomonad stage parasites was run on 12.5% SDS-PAGE gels and transferred onto a PVDF membrane. Blots were incubated with LT6 (1:4, murine antibody specific for Gal-Man-Phosphate repeats found in *Leishmania* glycosylated products). This was followed by alkaline phosphatase conjugated goat anti-mouse antibody. Precipitate deposition on the membrane indicated presence of LPG. 1: Molecular weight standard, 2: Nectomonad LPG, 3: Metacyclic LPG.

3.6.2: Metacyclic LPG has greater CRP binding capacity than nectomonad stage LPG

Previous studies have shown that CRP binds to infective, metacyclic stage LPG of *L donovani*. However, *L.mexicana* binding to CRP had not been investigated to the same extent, although previous studies had indicated that CRP binding to *L.mexicana* promastigotes induces transformation into amastigote-stage parasites (Mbuchi et al., 2006, Bee et al., 2001). As a major acute phase protein that was shown to interact directly with *Leishmania* parasites, it would be reasonable to characterise CRP binding to LPG from different *Leishmania* stages, with relevance to the reported difference in survival against host innate immune mechanisms.

CRP detection ELISA of *L.mexicana* LPG (metacyclic and nectomonad stage) and PCBSA binding to CRP was performed in both orientations (Section 2.15.2). Both ELISA data sets exhibited greater CRP binding detected on metacyclic versus nectomonad stage LPG, indicative of higher CRP binding capacity in the infective stage parasites (Figure 58-59).

Metacyclic and nectomonad LPG was subjected to SDS-PAGE, transferred onto PVDF membranes and probed with CRP (Section 2.15.1). The binding pattern on the membrane indicated that CRP was indeed binding to purified LPG rather than potential contaminants (Figure 60).

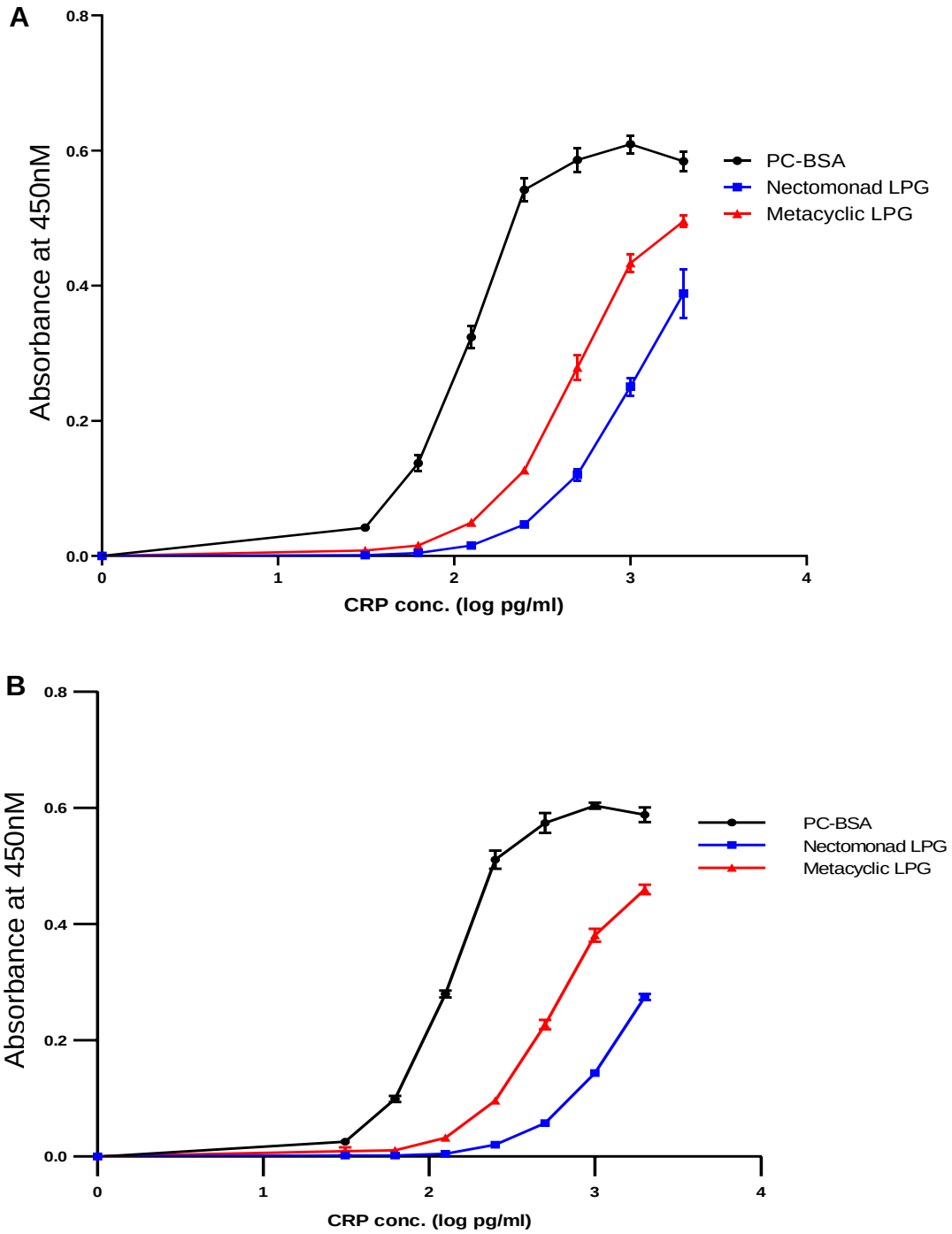

Figure 59: Metacyclic LPG has a higher CRP binding capacity than nectomonad LPG

Dose-response of binding of purified CRP (0-2.0 µg/ml) to immobilised, purified *L.mexicana* LPG from metacyclic and nectomonad promastigote stage parasites (1.0 µg/ml) in the absence (A) and presence (B) of whole serum (1:20). CRP binding was detected using rabbit anti-CRP antibody, HRP-conjugated goat anti rabbit antibody and TMB substrate (OD 450nm). n=4 technical replicates. Error bars represent standard deviation.

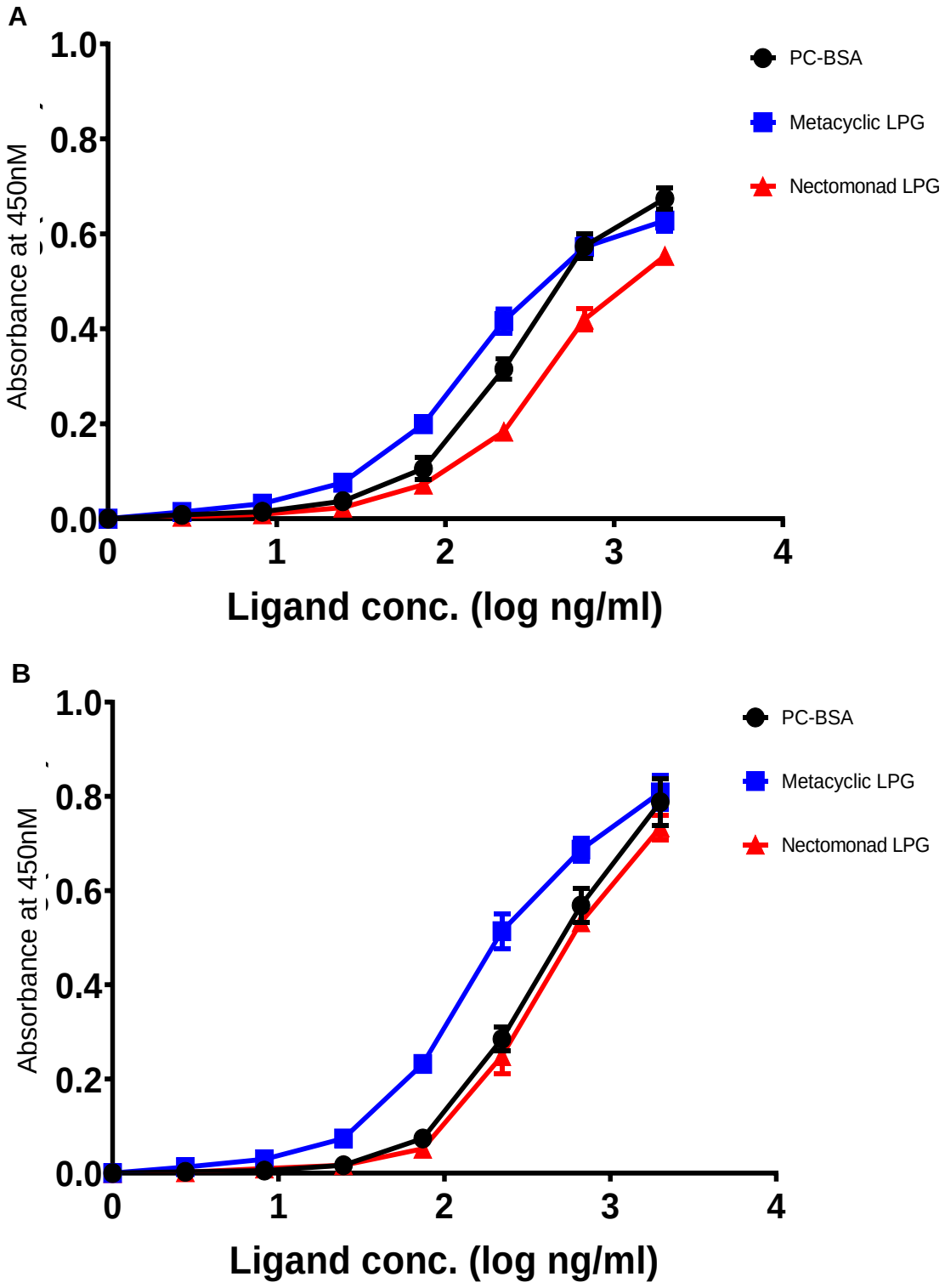

Figure 60: Metacyclic LPG has a higher CRP binding capacity than Nectomonad LPG

Dose-response of binding of CRP-biotin (0-2.0 µg/ml) to immobilised, purified *L.mexicana* LPG from metacyclic and nectomonad promastigote stage parasites (1.0 µg/ml) in the absence (A) and presence (B) of whole serum (1:20). CRP binding was detected suing HRP-conjugated streptavidin and TMB substrate (OD 450nm). n=4 technical replicates. Error bars represent standard deviation.

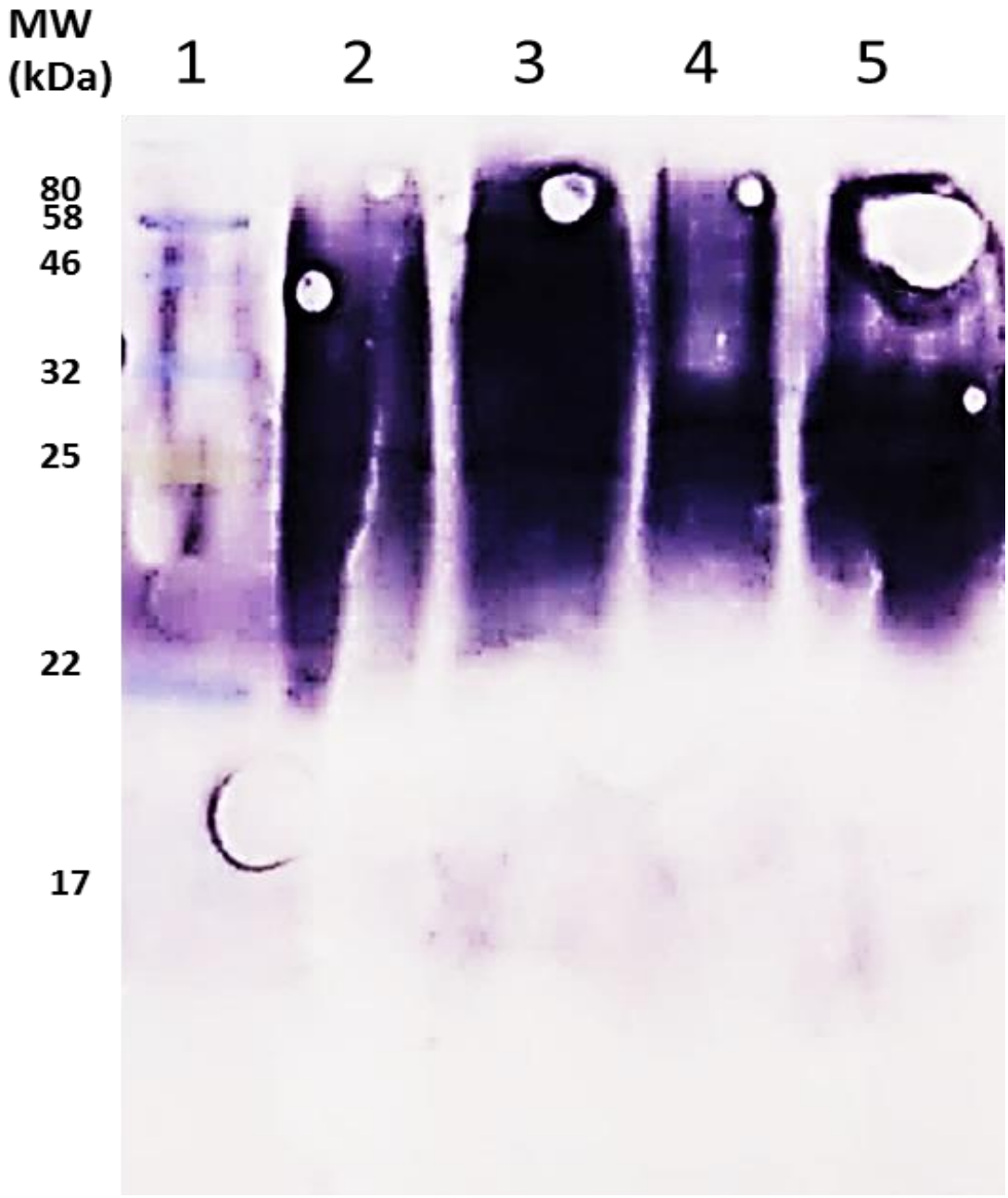

Figure 61: CRP binding to purified *L.mexicana* LPG.

Purified LPG derived from metacyclic and nectomonad-stage parasites was run on 12.5% SDS-PAGE gels and transferred onto a PVDF membrane. Blots were incubated with biotinylated CRP, followed by alkaline phosphatase conjugated streptavidin. Precipitate deposition on the membrane indicates presence of CRP binding.

1: Marker, 2: 7.5 µg Metacyclic LPG, 3: 15 µg Metacyclic LPG, 4: 7.5 µg Nectomonad LPG, 5: 15 µg Nectomonad LPG

3.6.3: CRP binds Metacyclic and Nectomonad stage LPG in a Ca^{2+} dependent manner

CRP had been shown to bind to LPG not via the commonly described PC, but rather to the Gal-Man- PO_4 repeats found in the end of LPG (Culley et al., 1996). As CRP had been shown to be capable of both Ca^{2+} dependent and independent binding mediated via different receptor sites, it was necessary to further characterise CRP binding to LPG, as well as determine if these were consistent between the promastigote stage parasites of different *Leishmania* species.

CRP detection ELISA of immobilised *L.mexicana* nectomonad and metacyclic stage LPG with varying concentrations of CRP, in the presence of either Ca^{2+} and Mg^{2+}, EDTA (Ca^{2+} and Mg^{2+}chelator), or EGTA (Ca^{2+} specific chelator) and Mg^{2+} was performed (Section 2.15.2). While dose-dependent binding of CRP to LPG was observed in the presence of Ca^{2+} and Mg^{2+} for both LPG types, EDTA inhibited LPG-CRP interaction in a non-competitive manner, with complete ablation of binding observed across a range of CRP concentrations. The addback of Mg^{2+} alone did not have any restorative effect on binding, which indicated that CRP-LPG interaction was dependent on Ca^{2+} alone rather than on other divalent cations (Figure 61).

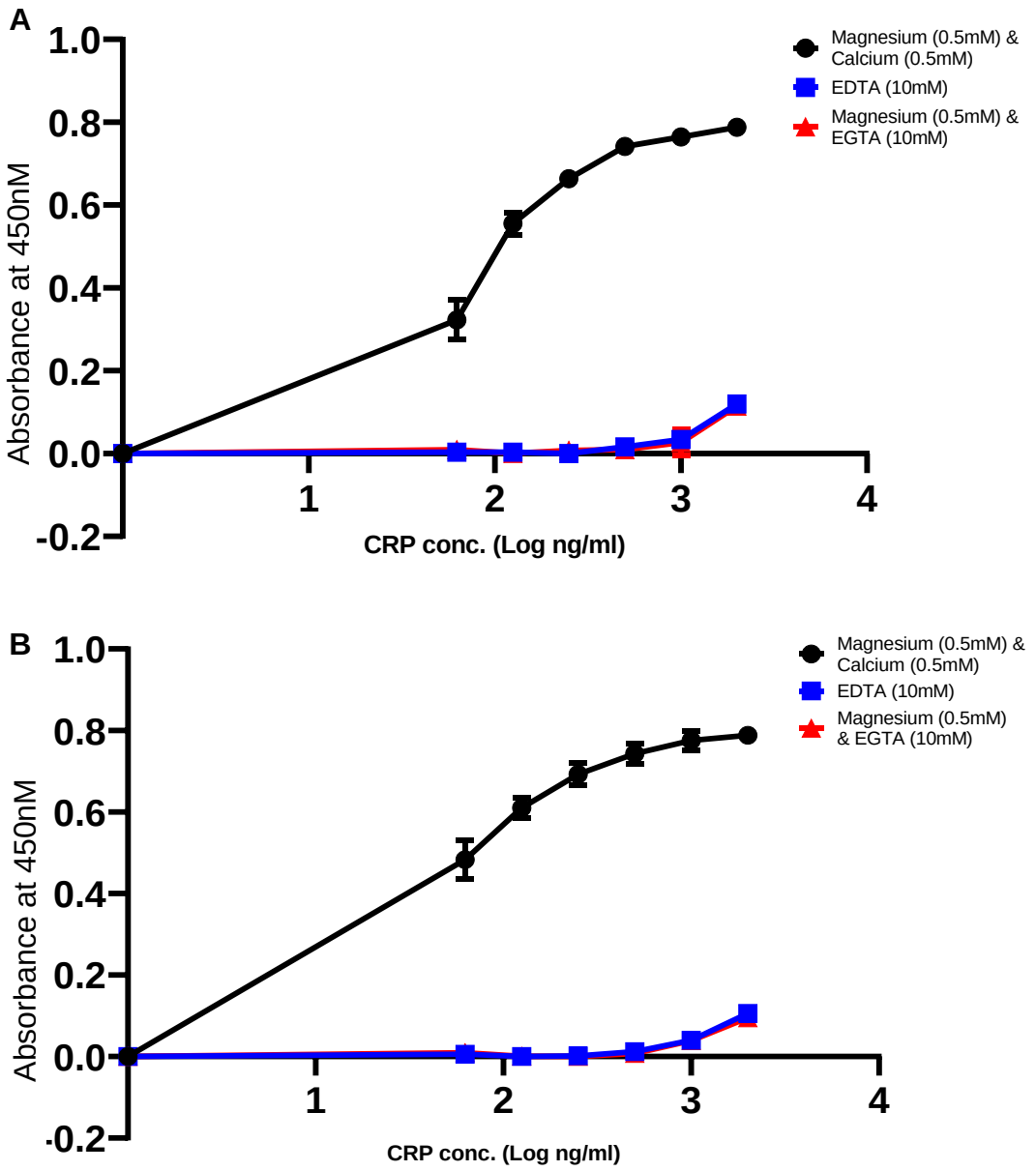

Figure 62: CRP binding to LPG is dependent on calcium and independent of magnesium

Dose-Response of binding of CRP (0-2.0 µg/ml) to immobilised *L.mexicana* wild-type LPG from Metacyclic (A) and Nectomonad (B) stage parasites (1 µg/ml). Binding was observed in the presence of calcium and magnesium (0.5mM), EDTA (10mM), or EGTA (10mM) with Magensium (0.5mM). CRP binding was detected using rabbit anti-CRP antibody (1:1000) and Goat anti-rabbit, HRP conjugated antibody (1:3000). n=4 technical replicates. Error bars represent standard deviation.

3.6.4: CRP binds to LPG via the PC binding site

As previously mentioned, CRP had been shown to bind to LPG to the Gal-Man-PO_4 repeats found in the end of LPG. As a form of confirmation of previous work as well a determination of the comparative availability of said CRP ligand on the different stages of *Leishmania* LPG, a competitive ELISA was performed against the murine antibody LT6, which has been reported to be specific for the Gal-Man- PO_4 moieties common to several *Leishmania* glycosylated products.

A CRP binding ELISA with immobilised *L.mexicana* nectomonad and metacyclic stage LPG with varying concentrations of CRP in the presence of the LT6 antibody previously described (Section 2.15.1). LT6 competitively inhibited CRP binding to both metacyclic and nectomonad LPG, likely through competition for the Gal-Man- PO_4 ligand, which was overcome at higher CRP concentrations. Noticeably, the inhibition was more evident across a range of CRP concentrations in metacyclic LPG. This may be indicative of another CRP ligand present or availability of repeating disaccharide to antibody, either, in nectomonad LPG that may not be bound with high affinity by the LT6 antibody. As LPG side chain substitutions were known to be stage-dependent, it could have been indicative that other glycosylated motifs were present on nectomonad LPG, and that potentially other *Leishmania* glycosylated products may possess CRP binding affinity (Figure 62).

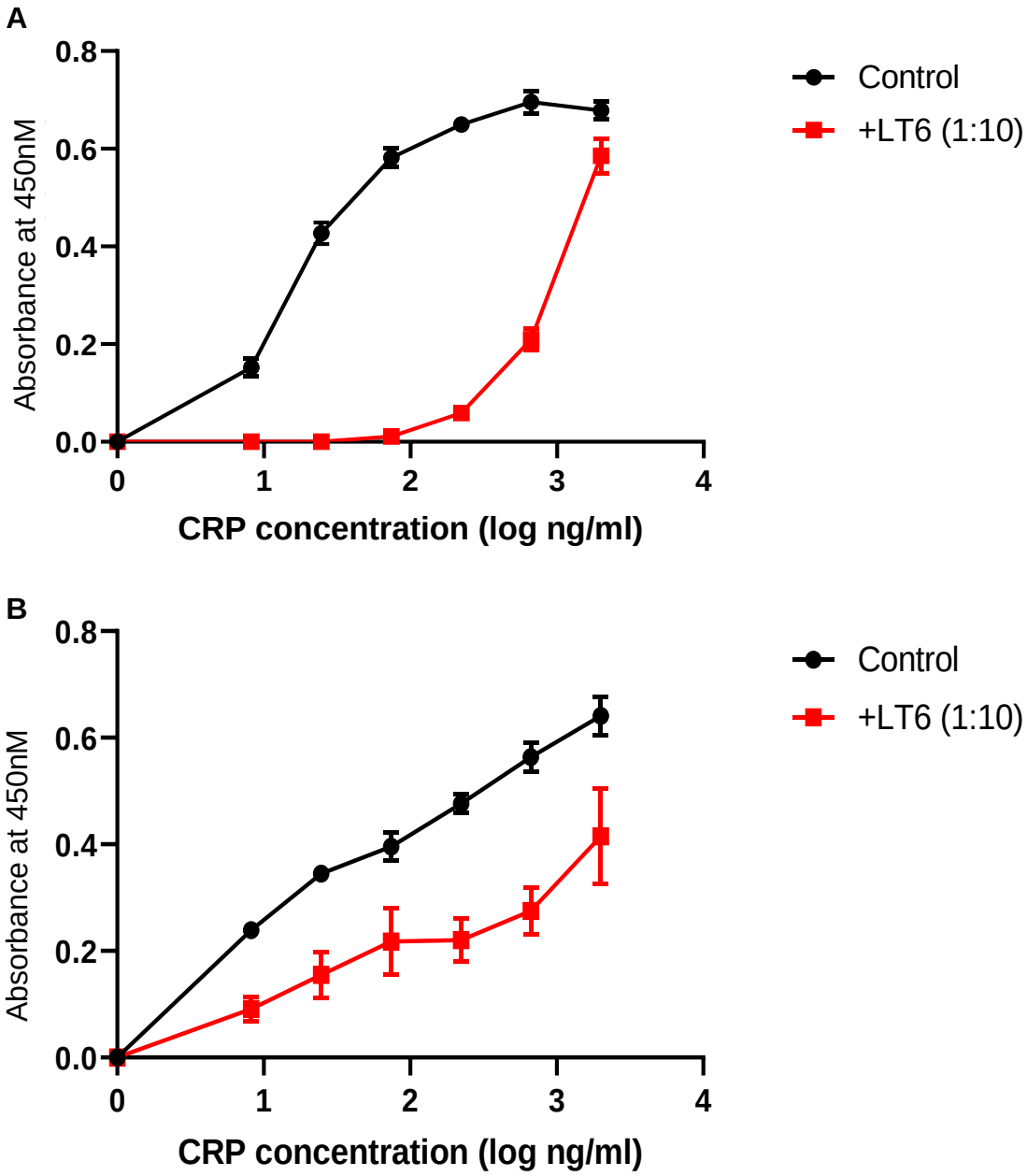

Figure 63: CRP binds to the phosphorylated disaccharide repeats on LPG

Dose-Response of binding of CRP (0-2.0 µg/ml) to immobilised, purified *L.mexicana* LPG from metacyclic (A) and nectomonad (B) promastigote stage parasites (1.0 µg/ml), in the absence and presence of an antibody specific for Gal-Man- PO_4 repeats (LT6). CRP binding was detected using a rabbit anti-CRP antibody, followed by HRP-conjugated goat anti-rabbit antibody. n=3 technical replicates. Error bars represent standard deviation.

3.7: Characterising SAP binding to different stages of LPG expressed by different *Leishmania* promastigote stages

3.7.1: Nectomonad LPG possesses greater SAP binding capacity than metacyclic LPG

SAP, being a widely circulated and highly abundant protein, would likely be present at the site of initial *Leishmania* infection when promastigote stage parasites were injected into the feeding site. In addition, SAP had a number of proposed immune functions. As such, it was of interest to investigate the binding of SAP to LPG, with its possible implications for parasite survival and replication in the early stages of mammalian infection.

An SAP detection ELISA with immobilised *L.mexicana* nectomonad and metacyclic stage LPG or PEC with varying concentrations of SAP-biotin was performed (Section 2.15.2). SAP-biotin was used as attempts to use purified SAP in ELISA resulted in high background, likely due to nonspecific binding of detection antibodies, which was overcome by using a streptavidin-biotin based detection system instead. Approximately 10-fold greater levels of SAP-biotin binding were detected on nectomonad LPG compared to metacyclic LPG across a range of SAP-biotin concentrations, indicating a greater binding capacity in nectomonad LPG (Figure 63).

Metacyclic and nectomonad LPG was subjected to SDS-PAGE, transferred onto PVDF membranes and probed with SAP-biotin (Section 2.15.1). While ligand blotting was a semi-quantitative procedure, the colorimetric intensity for the lanes containing nectomonad LPG was noticeably higher than those containing metacyclic LPG for a given quantity, supporting the previous observation made with the ELISA experiment (Figure 64).

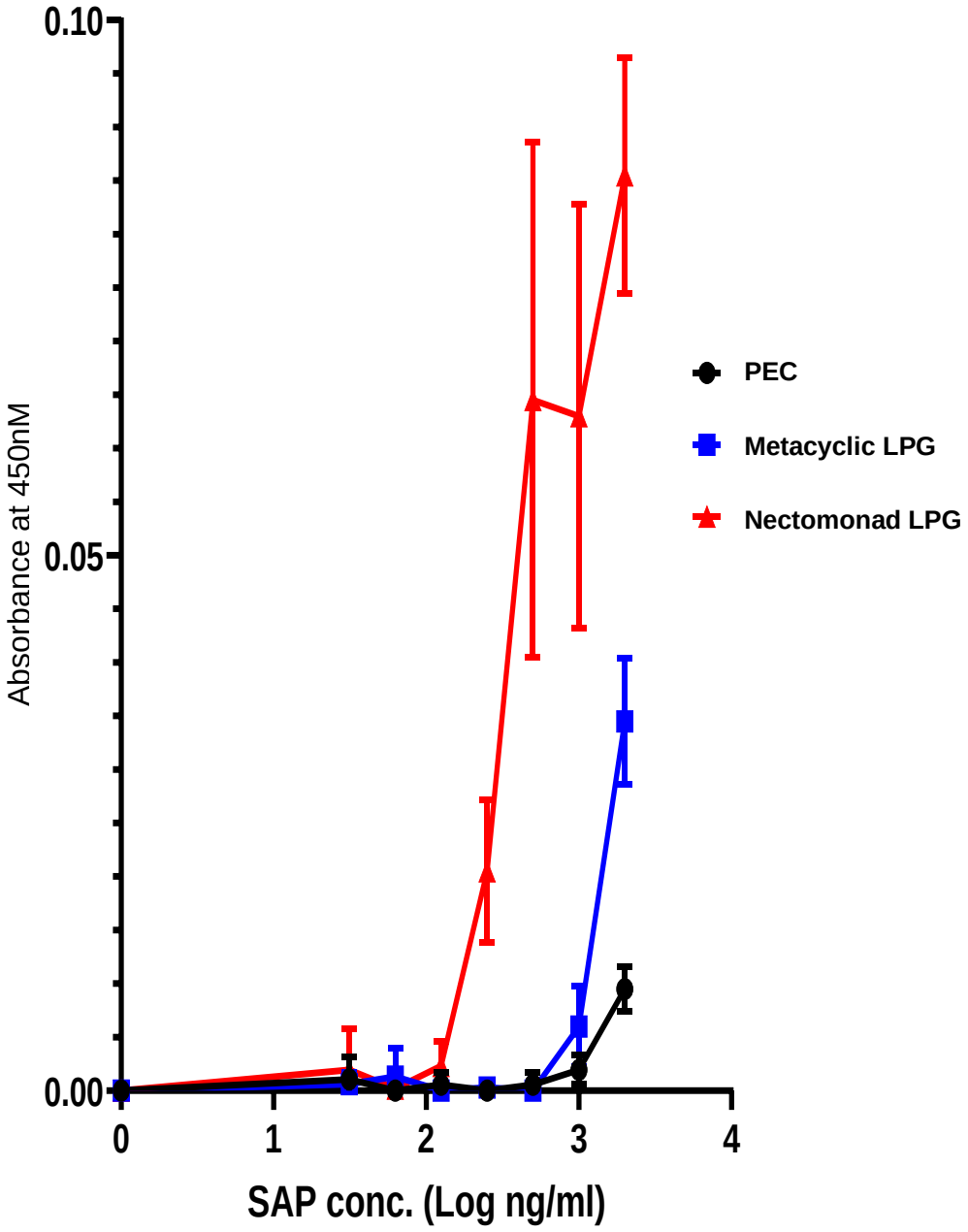

Figure 64: Nectomonad LPG has a higher SAP binding capacity than Metacyclic LPG.

Dose-Response of binding of SAP-biotin (0-2.0 µg/ml) to immobilised, purified *L.mexicana* LPG from metacyclic and nectomonad promastigote stage parasites (1.0 µg/ml), as well as PEC (1:20). SAP-biotin binding was detected using an HRP-conjugated streptavidin. n=4 technical replicates. Error bars represent standard deviation.

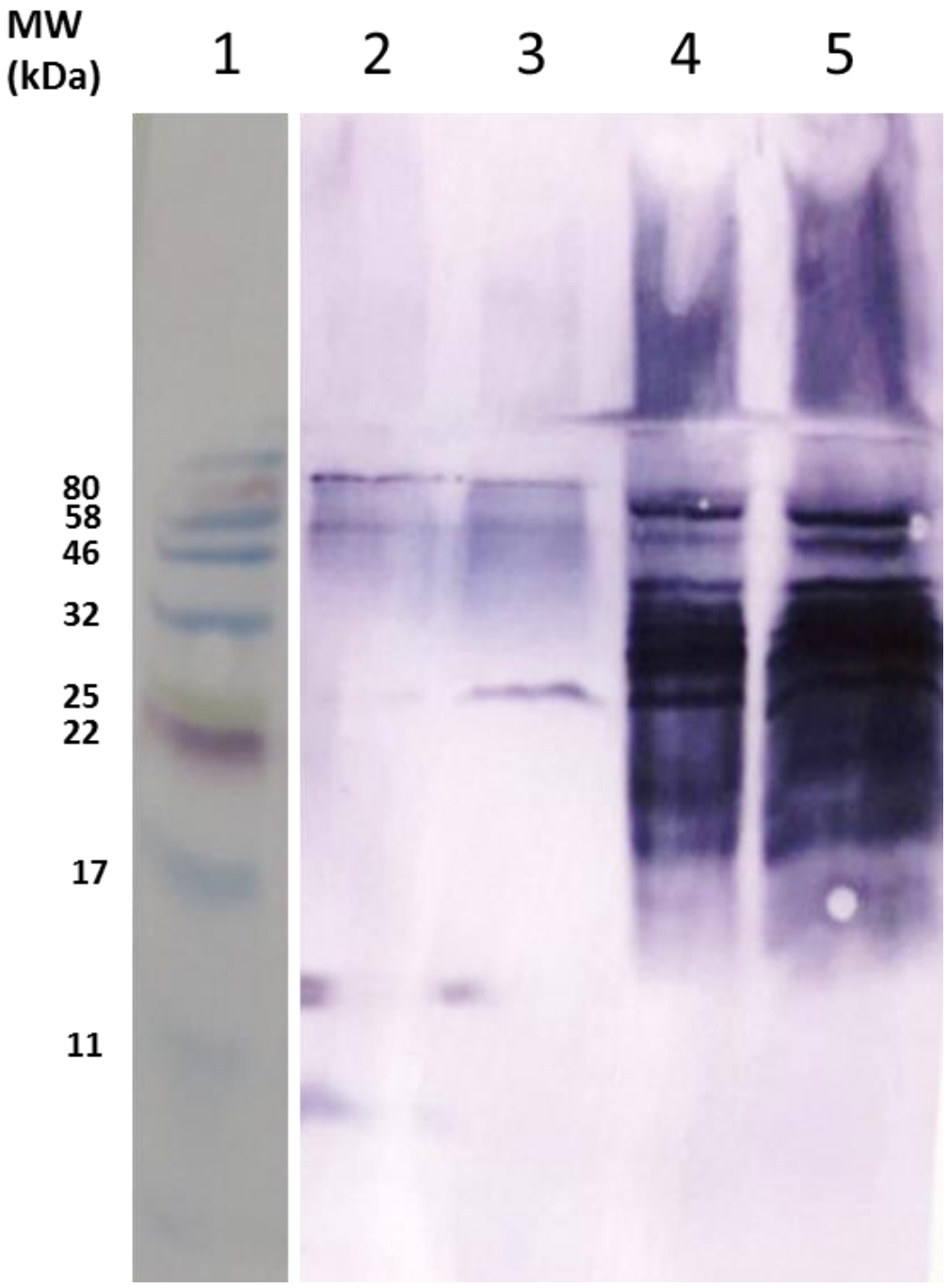

Figure 65: SAP-biotin binding to purified *L.mexicana* LPG.

Purified LPG (Nectomonad and Metacyclic stage parasites) on 12.5% SDS-PAGE gels and transferred onto a PVDF membrane. Blots were incubated with biotinylated SAP, followed by alkaline phosphatase-conjugated streptavidin. Precipitate deposition on the membrane indicates presence of SAP binding. 1: Marker, 2: 7.5 µg metacyclic LPG, 3: 15 µg metacyclic LPG, 4: 7.5 µg nectomonad LPG, 5: 15 µg nectomonad LPG

3.7.2: SAP binds Metacyclic and Nectomonad stage LPG in a Ca^{2+} dependent manner

Similar to CRP, most binding events attributed to SAP has been characterised as Ca^{2+} dependent(Pepys, 2018). As there have been no previous reports on SAP binding to LPG, it was necessary to ascertain if this was consistent SAPs known calcium-dependency.

SAP detection ELISA of immobilised *L.mexicana* nectomonad and metacyclic stage LPG with varying concentrations of SAP, in the presence of either Ca^{2+} and Mg^{2+}, EDTA (Ca^{2+} and Mg^{2+}chelator), or EGTA (Ca^{2+} specific chelator) and Mg^{2+} was performed (Section 2.15.2). Similar to the analogous experiment performed with CRP (Figure 61) dose-dependent binding of SAP-biotin to LPG was observed in the presence of Ca^{2+} and Mg^{2+} for both LPG types. EDTA inhibited LPG-SAP interaction in a non-competitive manner, with complete ablation of binding observed across a range of SAP concentrations. The addback of Mg^{2+} alone did not have any restorative effect on binding, indicating that SAP-LPG interaction was dependent on Ca^{2+} alone rather than on other divalent cations. In this at least, SAP and CRP appeared to have common ground, with binding appearing to be apparently exclusively Ca^{2+} dependent in nature (Figure 65).

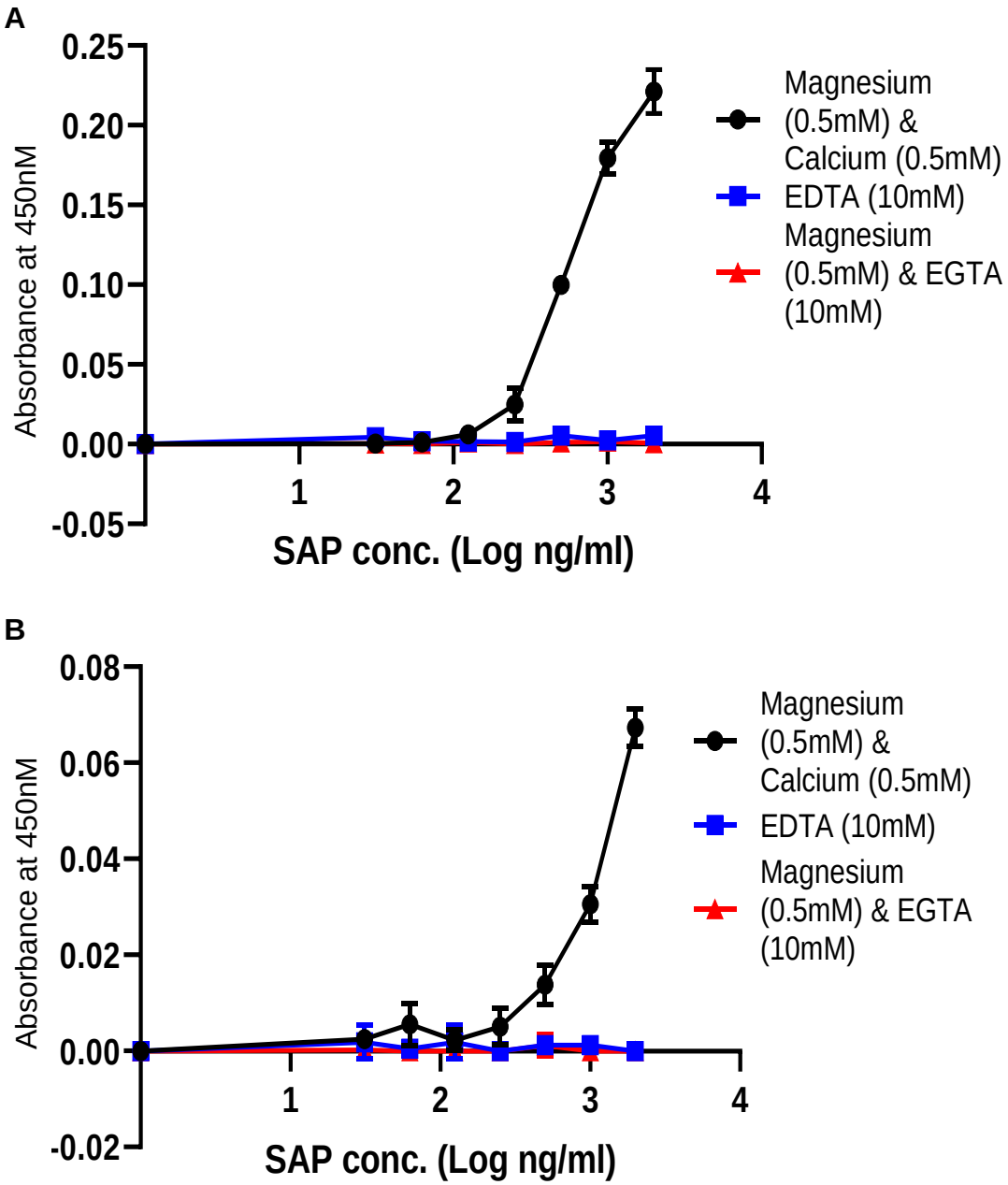

Figure 66: SAP binding to LPG is dependent on Ca^{2+} and independent of Mg^{2+}.

Dose-Response of binding of biotinylated SAP (0-2.0 µg/ml) to immobilised *L.mexicana* wild-type LPG from metacyclic and nectomonad stage parasites (1.0 µg/ml). Binding was observed in the presence of calcium and magnesium (0.5mM), EDTA (10mM), or EGTA (10mM) with Magensium (0.5mM). SAP-biotin binding was detected using HRP-conjugated streptavidin (1:15000). n=4 technical replicates. Error bars represent standard deviation.

3.8: CRP inhibits SAP binding to PSG at high concentrations

Our previous results suggested that CRP and SAP did not bind to the same ligand site on the LPG molecule. Given that SAP was previously reported to be constitutively produced in significant levels and CRP expression can be rapidly upregulated as part of the acute phase response, it was conceivable that both pentraxins were present at the local environment in significant levels in the early stages of *Leishmania* mammalian infection. Understanding the interactions between SAP and CRP was important for a clear understanding of early immune environment regulation and response to pathogenic challenge. In order to further investigate this phenomenon, CRP and SAP binding in the presence varying concentrations of the opposing pentraxin was determined.

CRP binding ELISA with immobilised *L.mexicana* WT LPG (metacyclic or nectomonad), PCBSA and PEC (Section 2.15.2), incubated with a constant concentration of the detected ligand CRP and varying concentrations of the competing ligand SAP, was performed (Figure 66). The opposite assay was also performed, with SAP binding ELISA with immobilised *L.mexicana* LPG (metacyclic or nectomonad), PCBSA and PEC, incubated with a constant concentration of the detected ligand SAP and varying concentrations of the competing ligand CRP (Figure 67). The only inhibition that could be observed occurred in the SAP detection, CRP competition assay (Figure 67), occurring at the equivalent of physiologically achievable levels of CRP (~0.08mg/L and above). This could hav been indicative of steric hinderance or obscuration of the SAP binding site with sufficient levels of CRP binding, or possibly changing the charge profile of the coated surface that ablates SAP binding. However, it should be noted that this occured in the absence of other serum components, and the phenomenon may be an artefact of *in vitro* experimental design limitations.

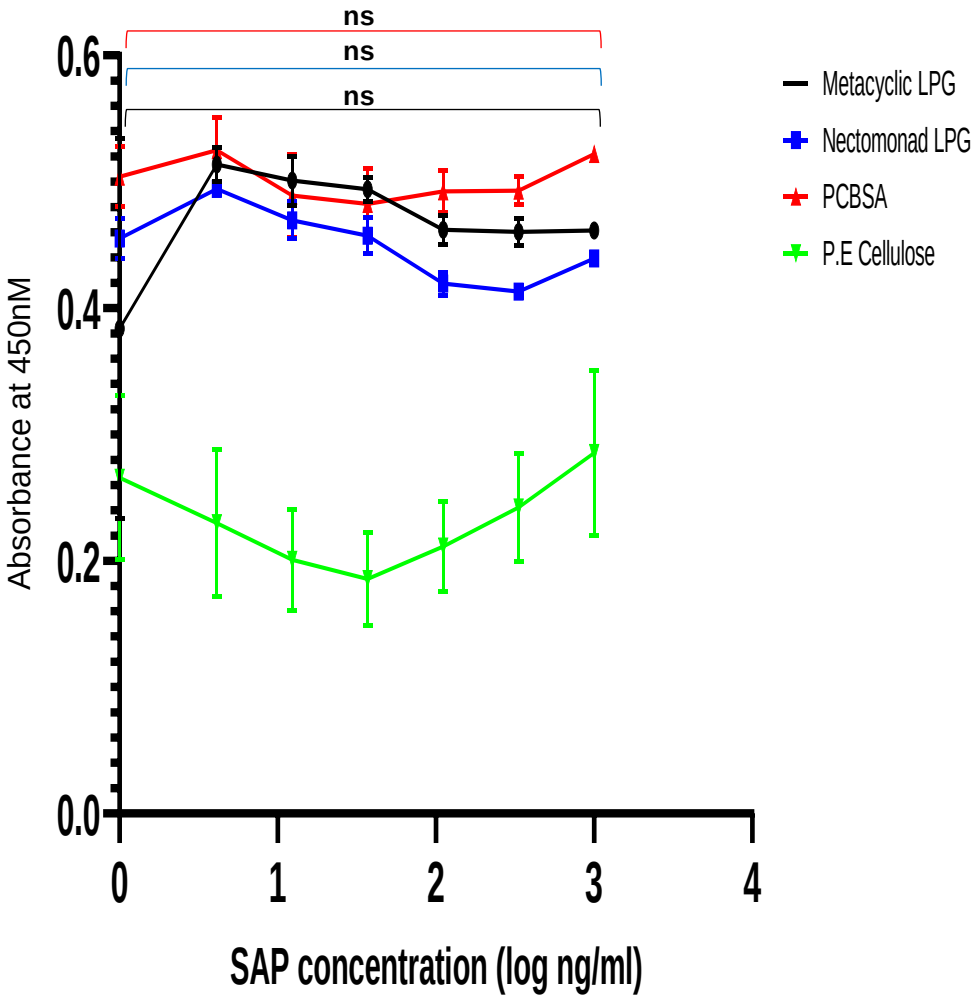

Figure 67: SAP does not inhibit CRP binding to LPG.

Dose-Response of binding of CRP (1.0 µg/ml) to immobilised, purified *L.mexicana* LPG from metacyclic and nectomonad promastigote stage parasites (1.0 µg/ml), in the presence of varying SAP concentrations (20-0 µg/ml). CRP binding was detected using a rabbit anti-CRP antibody, followed by HRP-conjugated goat anti-rabbit antibody. n=3 technical replicates. Error bars represent standard deviation. . *: P ≤ 0.05, **, P ≤ 0.005, ns: Not significant.

Brackets: Black = Metacyclic LPG, blue = nectomonad LPG, red = PCBSA

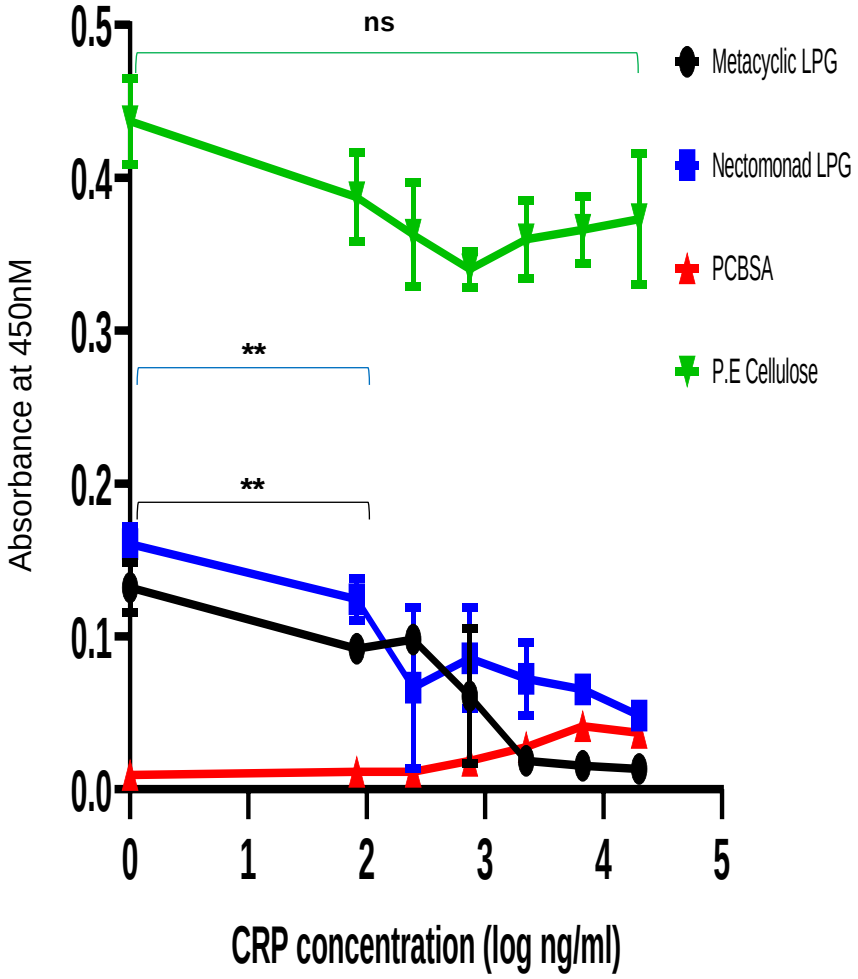

Figure 68: CRP inhibits SAP binding to LPG

Dose-Response of binding of SAP (1.0 µg/ml) to immobilised, purified *L.mexicana* LPG from metacyclic and nectomonad promastigote stage parasites (1.0 µg/ml), in the presence of varying CRP concentrations (0-20 µg/ml). SAP binding was detected using a mouse anti-CRP antibody, followed by HRP-conjugated goat anti-mouse antibody. n=3 technical replicates. Error bars represent standard deviation. *: P ≤ 0.05, **, P ≤ 0.005, ns: Not significant.

Brackets: Black = metacyclic LPG, blue = nectomonad LPG, green = PEC

3.9: Investigation of the ability of LPG to activate the classical complement pathway in complex with different pentraxins

3.9.1: CRP-LPG complex is capable of binding the classical complement pathway initiator molecule C1q

Previous observations with other *Leishmania* products with similar Gal-Man-PO_4 motifs as LPG (i.e. fPPG and ScAP) would suggest that *Leishmania* mainly activates the complement cascade via the classical complement pathway, with significant increases in complement deposition with the addition of CRP (Section 3.3.2). LPG, being a membrane-bound and highly expressed surface marker on *Leishmania* promastigotes, would likely be exposed to CRP and complement factors during early infection in a similar manner to PSG previously discussed. As such, in order to determine if LPG contributes to complement pathway activation, the ability of LPG in complex with CRP to bind to the classical complement pathway initiator molecule C1q was investigated.

CRP detection ELISA of immobilised C1q, incubated with CRP and varying concentrations of PCBSA or *L.mexicana* WT LPG (metacyclic or nectomonad) was performed (Section 2.13.2). The lack of CRP binding in the absence of a corresponding ligand appeared to indicate that CRP alone was incapable of C1q binding, with ligand binding triggering the conformational change in order for it to do so, making the assay an effective measure of CRP-LPG complex binding. Both metacyclic and nectomonad stage LPG exhibit dose-dependent complex binding to C1q, indicating that LPG, like fPPG and ScAP, was capable of initiating classical complement pathway activation. Higher levels of CRP-LPG complex were detected with metacyclic LPG compared to nectomonad LPG at lower ligand concentrations, but this phenomenon appeared to be absent at higher ligand concentrations (approximately 0.2 µg/ml LPG and above). This could have been indicative of inefficient conformational change in CRP in binding to metacyclic LPG moieties compared to nectomonad LPG (Figure 68).

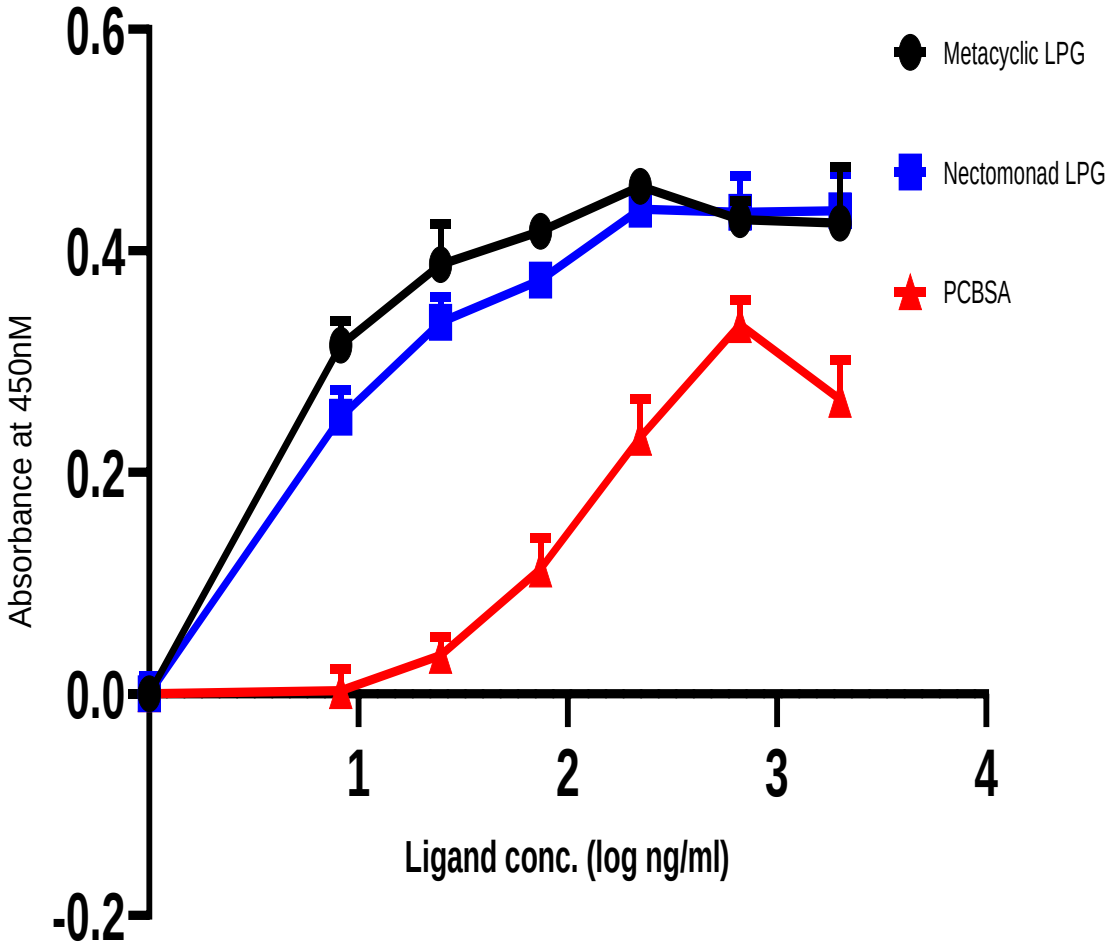

Figure 69: CRP-LPG complexes are capable of binding to the classical complement pathway initiator C1q.

Dose-response of free Metacyclic and Nectomonad LPG (0-2.0 µg/ml) in the presence of CRP (2.0 µg/ml) with immobilised C1q (5.0 µg/ml). CRP-LPG complex binding was detected using a rabbit anti-CRP antibody, followed by HRP-conjugated goat anti-rabbit antibody. n=4 technical replicates. Error bars represent standard deviation.

3.9.2: SAP-LPG complex is unable to activate the classical complement pathway

While literature surrounding the contribution of SAP to innate immune pathogen defence was not as extensive of that related to that of CRP, several studies have suggested that SAP was capable of classical complement activation following ligand binding (de Haas et al., 2000, Yuste et al., 2007). Given the abundance of SAP in circulation and the influence of complement in pathogen elimination and modulation of the local immune environment, the ability of LPG in complex with SAP to bind to C1q was investigated.

SAP detection ELISA of immobilised C1q, incubated with SAP and varying concentrations of PEC or *L.mexicana* WT LPG (metacyclic or nectomonad) was performed (Section 2.13.1). The lack of SAP binding in the absence of a corresponding ligand would indicate that SAP alone was incapable of C1q binding, with ligand binding triggering the conformational change in order for it to do so, making the assay an effective measure of SAP-LPG complex binding. While LPG in complex with the positive control PEC was capable of binding to C1q, neither metacyclic or nectomonad stage LPG exhibited dose-dependent binding to C1q, suggesting that LPG was not capable of initiating classical complement pathway activation. Unlike PEC, the observations indicated that SAP was unable to triggering c1q binding and thereby activate the classical pathway of complement (Figure 69).

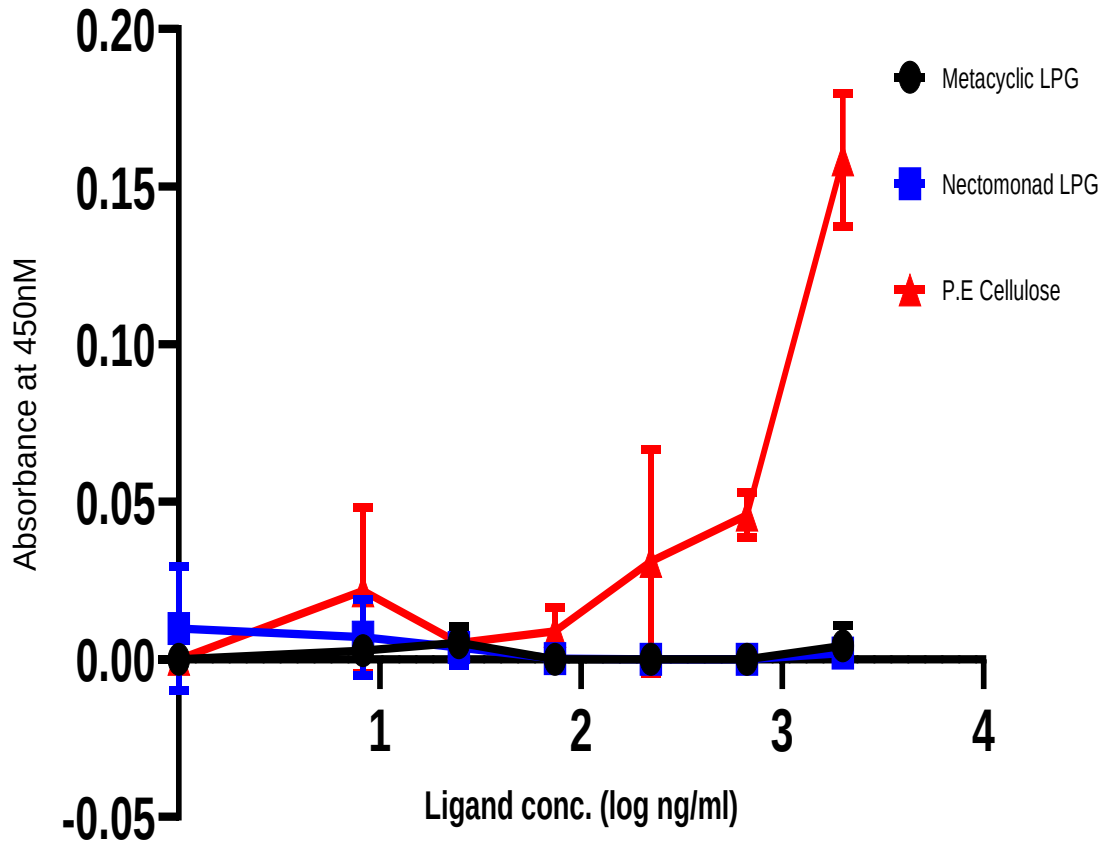

Figure 70: SAP-LPG complexes are not capable of binding to the classical complement pathway initiator C1q.

Dose-response of free Metacyclic and Nectomonad LPG (0-2.0 µg/ml) in the presence of SAP (2.0 µg/ml) with immobilised C1q (5.0 µg/ml). SAP-LPG complex binding was detected using a mouse anti-SAP antibody, followed by HRP-conjugated goat anti-mouse antibody. n=4 technical replicates. Error bars represent standard deviation.

3.10: The influence of CRP in the adherence of different *Leishmania* promastigote stages to PSG

3.10.1: Biotinylated *L.mexicana* WT PSG maintains CRP binding capacity

LPG as part of *Leishmania* parasite glycocalyx and PSG share proximity in the arthropod vector, with PSG forming the blockage from the stomodeal valve to the tegmental midgut within infected sandflies, as well as being co-injected during initial mammalian infection during sandfly feeding attempts, alongside sandfly saliva. The molecular interactions between promastigote LPG and PSG at different stages of development could have multiple potential implications, from affecting the motility of different promastigote stages within the PSG matrix, the probability of expulsion into the feeding site during sandfly regurgitation, and co-uptake during phagocytosis by neutrophils, dendritic cells and macrophages. As infected sandflies have previously been shown to experience mixing of foregut contents and human serum components prior to regurgitation of the mixture into the feeding site by reason of the physical obstruction caused by PSG (Rogers et al., 2002), the ability of CRP to affect the interaction between LPG and PSG was investigated

As *Leishmania* carbohydrate products share many of the same moieties, specific detection of a particular product (e.g. LPG and not fPPG) via the *Leishmania*-specific antibodies we had available (LT6 and LT17: Gal-Man-PO_4 specific) would not have been possible. As such, a biotinylated WT *L.mexicana* PSG was generated which could be detected via biotin-avidin interactions. Carbodiimide linkage of NHS-LC-biotin to amine groups was chosen, as this was predicted to have the least likelihood to alter carbohydrate moieties on PSG that appear to be the exposed ligand binding sites for CRP interaction.

In order to ascertain that biotinylation of PSG did not affect CRP ligand binding capacity and remained an accurate analogue of unmodified PSG, a CRP detection ELISA was performed, with vary concentrations of immobilised

L.mexicana WT PSG, PSG-biotin and PCBSA incubated with CRP (Section 2.12.2). The PSG-biotin exhibited no significant difference in CRP binding capacity in comparison with unmodified PSG across a range of CRP concentrations, indicating that biotinylation did not affect the ligand binding characteristics of *L.mexicana* PSG (Figure 70).

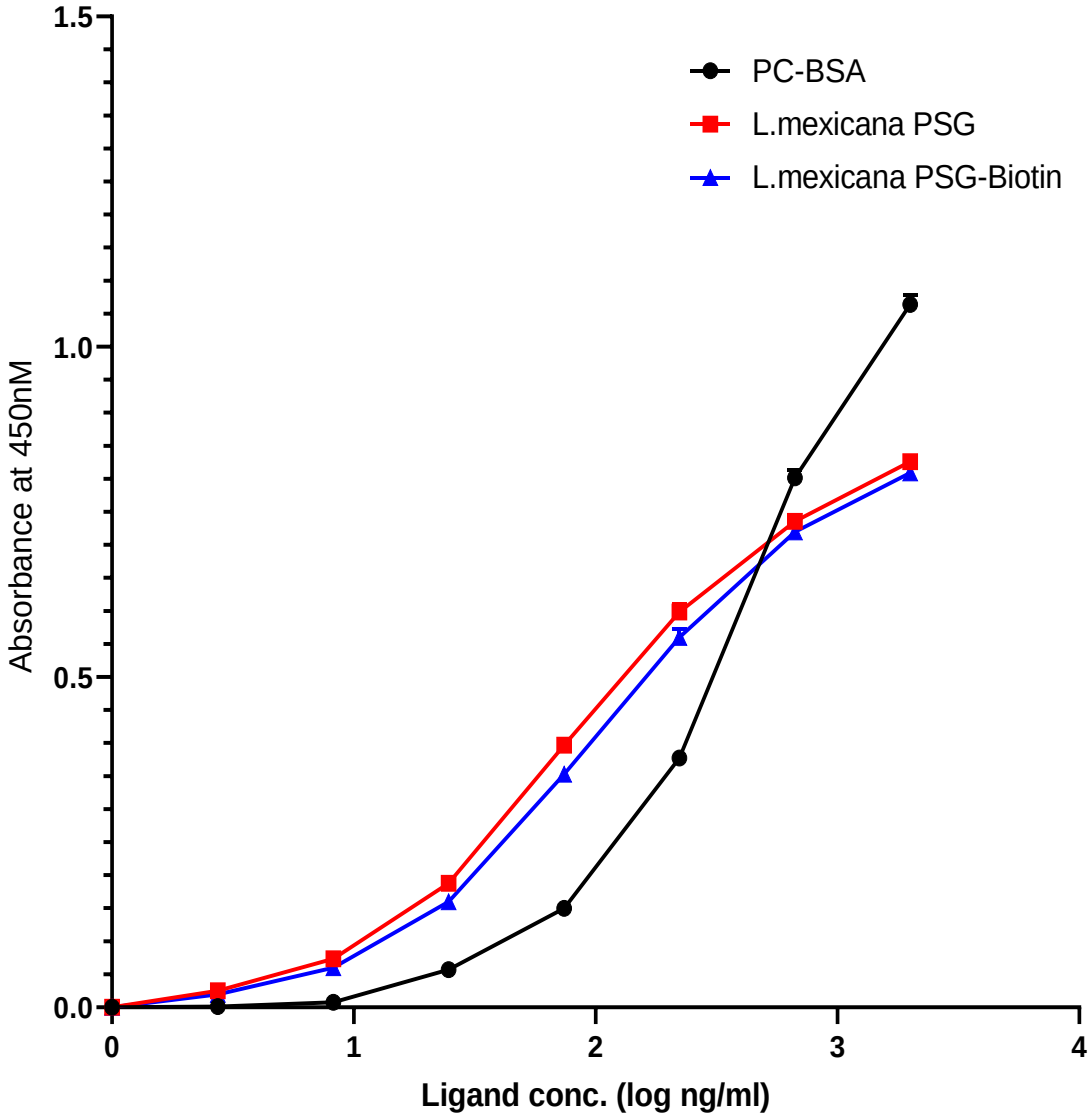

Figure 71: Biotinylation of PSG does not affect CRP binding capacity.

Dose-response purified CRP (1.0 µg/ml) binding to *L.mexicana* PSG or PSG-biotin (0-2.0 µg/ml) coated on an ELISA plate. CRP binding was detected using a rabbit anti-CRP antibody, followed by HRP-conjugated goat anti-rabbit antibody. n=4 technical replicates. Error bars represent standard deviation.

3.10.2: CRP increases LPG-PSG complex formation to a greater extent in metacyclic-stage LPG

Following validation of the biotinylated *L.mexicana* WT PSG product, binding between LPG and PSG was investigated, with particular interest in the influence of CRP and Ca^{2+} on this interaction.

PSG-biotin detection (with streptavidin-HRP) ELISA was performed, with immobilised *L.mexicana* WT metacyclic and nectomonad stage LPG, incubated with *L.mexicana* PSG-biotin with varying concentrations of CRP, in the presence of Ca^{2+} or the cation chelator EDTA (i.e. Ca^{2+} free environment) (Section 2.16).

No LPG-PSG interaction could be detected when CRP concentration was low or absent (≤ 0.04 µg/ml CRP), which indicated a lack of strong direct interaction. Both metacyclic and nectomonad stage LPG exhibited a dose-dependent increase in interaction with PSG with rising CRP concentrations. Metacyclic LPG complex formation with PSG was significantly higher than nectomonad LPG across a range of CRP concentrations (≥ 0.37 µg/ml CRP), LPG-PSG complex formation was completely ablated in the presence of EDTA, suggesting that Ca^{2+} dependent CRP binding to LPG, PSG-biotin, or both, was essential to LPG-PSG complex formation (Figure 71). The orientation of the PC-binding sites on one face of a CRP molecule made cross-linking a less likely scenario than for some other lectins, but binding of repeating disaccharide moieties from PSG and LPG simultaneously by a single CRP molecule was potentially conceivable. Another possibility was that CRP coating of both ligands may overcome the charge-based repulsion between LPG and PSG, allowing the interaction we observed to occur.

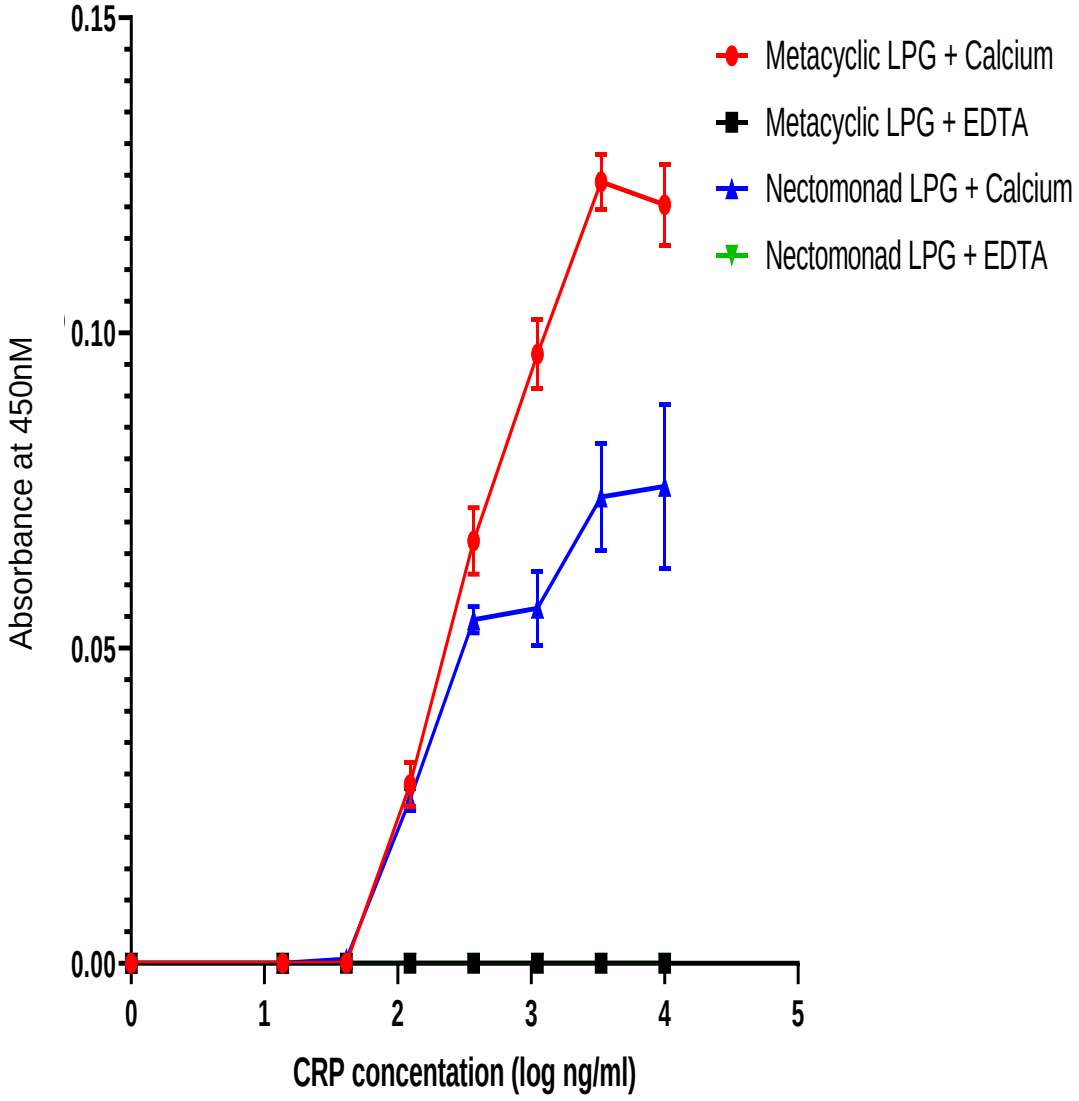

Figure 72: CRP can act as bridge between LPG and PSG

Dose-Response of binding of purified *L.mexicana* PSG-biotin (0.5 µg/ml) to immobilised, purified *L.mexicana* LPG from metacyclic or nectomonad promastigote stage parasites (1.0 µg/ml) in the presence of varying CRP concentrations (0 – 10 µg/ml), and calcium (0.5mM) or EDTA (10mM)-containing HEPES buffer. PSG-biotin binding was detected using HRP-conjugated streptavidin and TMB substrate (OD 450nm). n=4 technical replicates. Error bars represent standard deviation.

3.11: Investigating CRP-PSG binding kinetics using surface plasmon resonance techniques

3.11.1: Initial attempts at immobilisation of PSG ligand

Surface plasmon resonance (SPR) allowed for real-time observation of ligand analyte interaction without the use of labelling molecules. As such, it was chosen as the natural extension of other binding experiments performed previously, such as ELISA and ligand blotting, to further elucidate the biomolecular interactions between the pentraxins (SAP and CRP) and *Leishmania* glycosylated products (LPG, fPPG and ScAP). All SPR experiments were performed on a Biacore 3000 machine, with analytical-grade sensor chips (XanTec and Biacore).

An initial attempt to study CRP and PSG interaction was made by immobilising *L.mexicana* WT PSG (10 µg/ml, pH 4.0, 5mM acetate buffer) on a polycarboxylate surface (dextran-free) with medium charge density (Xantec HC30M) via amine coupling but was unsuccessful (results not shown), with low response unit (RU) change indicating a lack of ligand immobilised on the surface. It was possible that lack of immobilisation was due to charge repulsion between the carboxylate chip surface and the PSG preventing the protein component of PSG from being cross-linked onto the surface. Direct immobilisation of PSG was attempted (Section 2.17) to another carbohydrate-free chip (C1 from Biacore) but association was weak (data not shown) and direct immobilisation of negatively charged carbohydrates to negatively charged biosensor surfaces would likely lead to bias in attachment of heterogeneous PSG.

For both economic and practical purposes, an effort was made to generate a surface wherein biotin-avidin immobilisation of ligand could be performed which could also be stripped completely to allow immobilisation of another cycle of ligand. This work was undertaken by John Raynes (Department of Immune Biology, London School of Hygiene and Tropical Medicine, UK). In principle, desthiobiotin has a strong specific binding to avidin family biotin-binding

proteins, but crucially not so strong that this interaction cannot be dissociated with powerful denaturing agents, such guanidine thiocyanate. Therefore, the desthiobiotin was immobilised covalently, followed by an intermediary avidin layer which can be attached stably, which allows the biotin-labelled ligand of interest (CRP-biotin or PSG-biotin) to be attached stably in turn. The analyte can be flowed over the sensor surface, and in the case of observing CRP-PSG interaction, the analyte can be removed by exposure to EDTA-containing buffer due to the calcium-dependency of the binding. The surface may also be stripped back to the desthiobiotin layer using denaturing agents between different cycles of indirect attachment of various ligands.

A polycarboxylate chip with high charge density (Xantec, C30M) had aminodesthiolbiotin (0.5mM, in sodium maleate buffer, 10mM, pH 6.8) conjugated to the surface of flow cell (FC) 1 and FC2 by amine coupling to the carboxylate (150 RU). Reactive groups on surfaces were blocked with ethanolamine. Neutravidin (10 µg/ml) in calcium-containing HEPES buffer (HBSPC) was then immobilised on the desthiobiotin surface to give a further 150 RU. The ligand, CRP-biotin (10 µg/ml) in HBSPC was immobilized on FC2, with FC1 left blank to serve as a reference surface (Section 2.17.2).

3.11.2: Immobilised CRP binds avidly to *L.mexicana* PSG

To collect kinetic binding data, the analyte (*L.mexicana* PSG: WT, ScAPKO and ScAPAB) in HBSPC was injected over the control flow cell and one loaded with CRP-biotin (150 RU) at varying concentrations (0.16 - 20 µg/ml, 300s association, 300s dissociation) at a temperature of 25°C. Of note, a slow flow rate (5 ul/min) and longer association time was required because of the large size of the PSG and limitations on its association kinetics. The surfaces were regenerated with a 10s injection of EDTA-containing HEPES buffer (HSBPE) (Section 2.17.2.2).

L.mexicana WT PSG was shown to bind with high avidity to CRP, with dissociation rate constant ($k_{d)}$ values calculations by the evaluation software being difficult due to the strength of CRP interaction with PSG having a very slow decrease in RU in the dissociation phase for the given dissociation time period allowed (Figure 72). k_d was a useful measure of the avidity of the interaction, being independent of analyte concentration provided that the mass transport effect was absent, as well as calculable by the SPR analysis software without an estimated molecular weight of the analyte, which has not been accurately determined for PSG. In addition, the suspected heterogenous nature of PSG would make any molecular weight estimation based on one of its individual components dubious at best. A dose response was seen but no saturation, probably because of the limited time of association, suggesting a much greater levels of binding was possible. It was also not possible to generate an on-rate because the due to uncertainty of its molecular weight. When PSG from ScAP mutant PSGs was flowed over the CRP surface (Figure 73), R_{max} (the maximum recorded RU for a given run) values for a given PSG analyte concentration was much higher for ScAPAB (~25 RU) compared to ScAPKO (~10 RU) material for a given CRP analyte concentration (5 µg/ml CRP), with the ScAPAB R_{max} being comparable to that observed for WT *L.mexicana* PSG (Figure 72: ~22 RU), suggesting that ScAP was a major component of CRP binding.

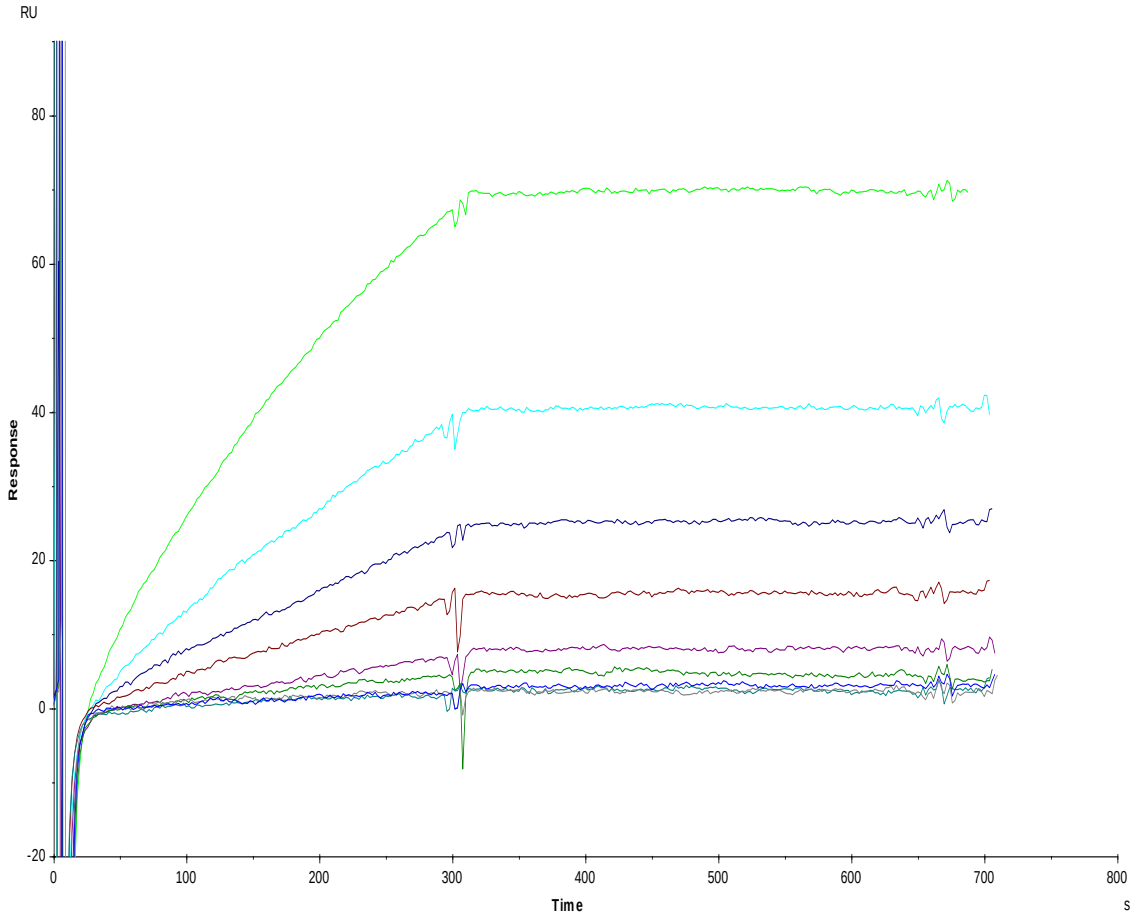

Figure 73: *L.mexicana* WT PSG exhibits strong interaction with CRP.

Surface plasmon resonance of ligand CRP-biotin (150 RU), captured onto neutravidin-desthiobiotin complex captured on XanTec C30M sensor chip, to analyte *L.mexicana* WT PSG at varying analyte concentrations (0.16 - 20 µg/ml, 5 µl/min, 300s association, 300s dissociation) in Ca^{2+} containing HEPES buffer (HBSPC: 10 mM HEPES, 150 mM NaCl, 0.005% P20, 0.5mM $CaCl_2$, pH 7.4). The surfaces were regenerated with a 10s injection of EDTA-containing HEPES buffer (HSBPE: 10 mM HEPES, 150 mM NaCl, 10 mM EDTA, pH 7.4). Data was collected at a rate of 1 Hz. The data was fitted to a simple 1:1 interaction model using the global data analysis option available within BiaEvaluation 3.1 software.

Calculated k_d values:
2.5 ug/ml: 5.41×10^{-5} s^{-1}
1.25 ug/ml: 4.58×10^{-4} s^{-1}
0.63 ug/ml: 2.46×10^{-4} s^{-1}

Average k_d: 4.15×10^{-4} s^{-1}
Standard deviation: 1.2×10^{-4} s^{-1}

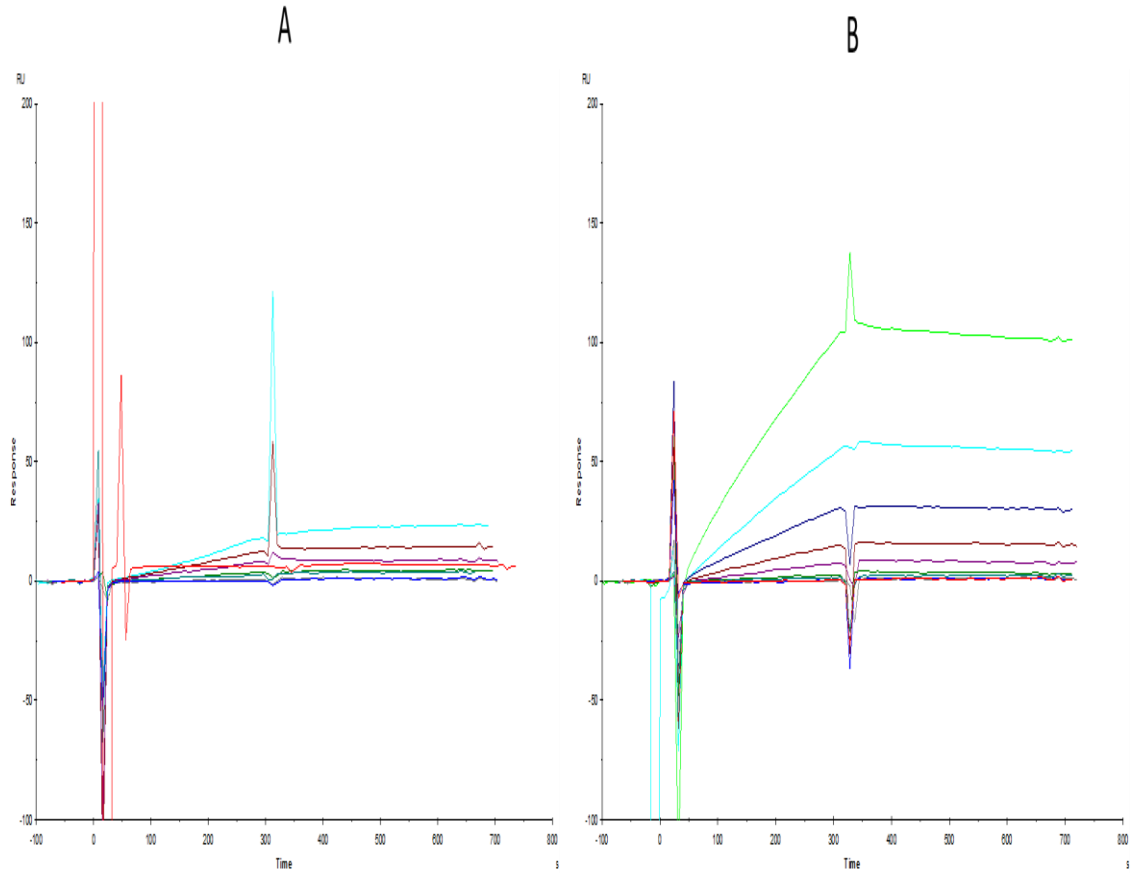

Figure 74: ScAP is a major component of PSG binding to CRP.

Surface plasmon resonance of ligand CRP-biotin (150 RU), immobilised onto neutravidin-desthiobiotin complex captured on XanTec C30M sensor chip, to analyte *L.mexicana* ScAPKO (A) and ScAPAB (B) PSG at varying analyte concentrations (0.16 - 20 µg/ml, 5 µl/min, 300s association, 300s dissociation) in Ca^{2+} containing HEPES buffer (HBSPC: 10 mM HEPES, 150 mM NaCl, 0.005% P20, 0.5mM $CaCl_2$, pH 7.4). The surfaces were regenerated with a 10s injection of EDTA-containing HEPES buffer (HSBPE: 10 mM HEPES, 150 mM NaCl, 10 mM EDTA, pH 7.4). Data was collected at a rate of 1 Hz. The data was fitted to a simple 1:1 interaction model using the global data analysis option available within BiaEvaluation 3.1 software.

3.11.3: PSG-biotin immobilised exhibits high avidity to CRP analyte

In order to overcome the inherent difficulties of having a large molecule analyte in fluid phase, an effort was undertaken to immobilise PSG as the ligand on the chip surface with the aim of flowing CRP analyte over the surface in order to obtain more interpretable binding kinetics data. *L.mexicana* WT PSG was biotinylated and had been validated to retain the CRP binding capacity of unmodified PSG (Figure 72), and as such was chosen as a candidate for capture on the desthiobiotin chip via a neutravidin intermediary.

A polycarboxylate chip with high charge density (Xantec, C30M) covalently modified with aminodesthiolbiotin was loaded with neutravidin as previous. Excess activated surface NHS was deactivated by addition of ethanolamine (Section 2.17.2.1) prior to neutravidin coating. The ligand, *L.mexicana* PSG-biotin (20 µg/ml) in sodium acetate buffer (10mM, pH 5.0) was immobilized on flow cell 2 (340 RU) and flow cell 1 was left blank to serve as a reference surface. To collect kinetic binding data, the analyte (CRP) in HBSPC was injected over the two flow cells at varying concentrations (20 µl/min, 0.16 - 20 µg/ml, 180s association, 300s dissociation) at a temperature of 25°C. The complex was allowed to associate for 300s and dissociate 1200s. The surfaces were regenerated with a 10s injection of EDTA-containing HEPES buffer (Section 2.17.2.3). Residual analysis allowed for determination of the suitability of the kinetic model (Langmuir 1:1 binding) used, with random distribution of data points indicating a good fit. Despite the high amount of available ligand (340 RU) on the chip surface, the amount of analyte CRP bound was low and binding kinetic values were only determined for the higher concentrations (2- 20 µg/ml CRP. It was possible that the lack of binding was due to the binding orientation making CRP binding site unavailable, or that there were few binding sites per PSG molecule. As saturation of binding was approached, stoichiometry, assuming a tentative estimate of a single PSG molecule being approximately 4000 kDa (John Raynes, Department of Immune Biology, London School of Hygiene and Tropical Medicine, UK), would suggest one CRP binding site per PSG molecule (Figure 74).

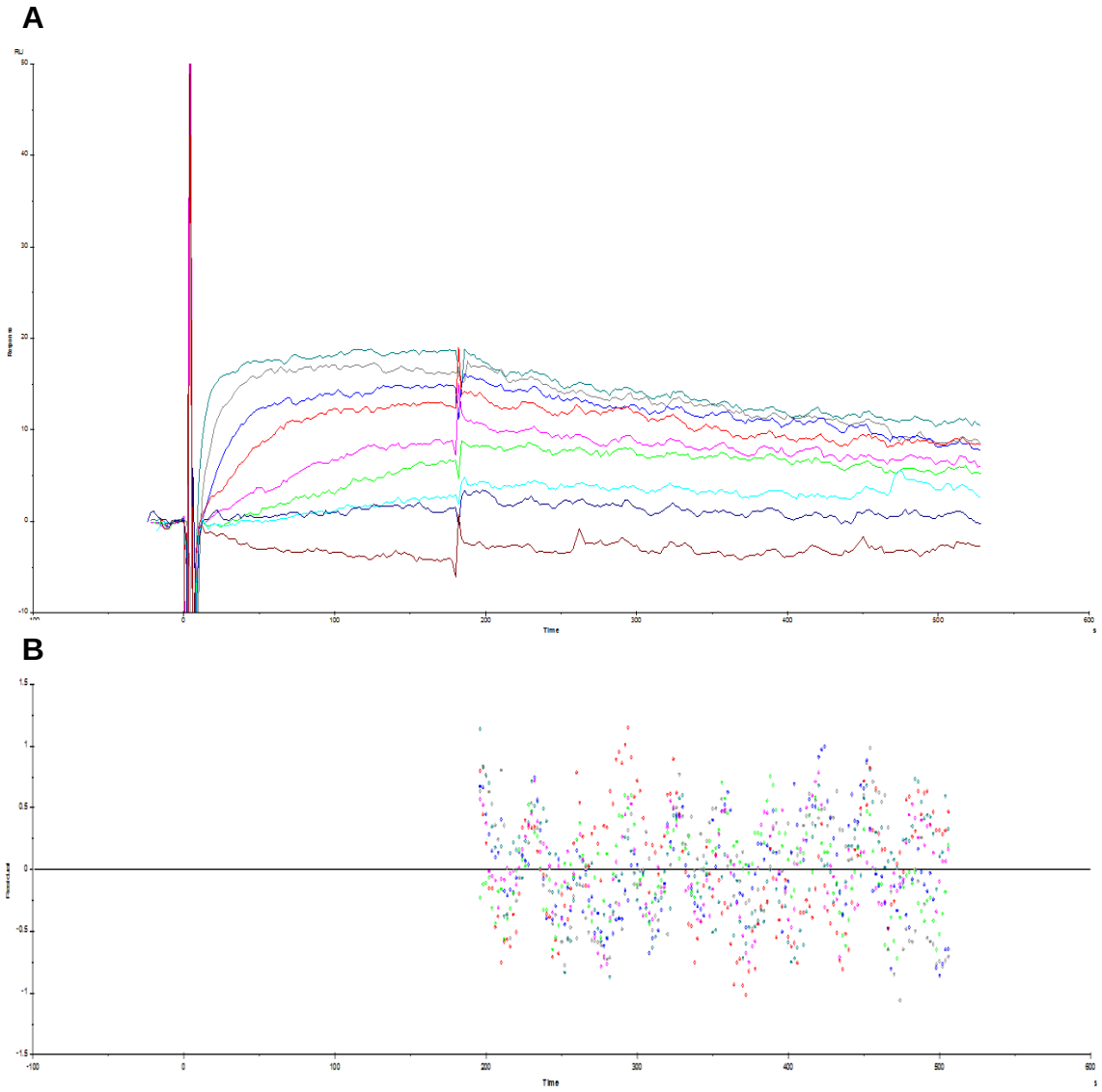

Figure 75: CRP binding to *L.mexicana* PSG biotin immobilised onto neutravidin surface (A) with residual analysis of dissociation (B).

Surface plasmon resonance of WT *L.mexicana* PSG-biotin (340 RU), immobilised onto neutravidin-desthiolbiotin complex captured on XanTec C30M sensor chip, to analyte CRP at varying analyte concentrations (0.16 - 20 µg/ml, 20 µl/min, 180s association, 300s dissociation) in Ca^{2+} containing HEPES buffer (HBSPC: 10 mM HEPES, 150 mM NaCl, 0.005% P20, 0.5mM $CaCl_2$, pH 7.4). The surfaces were regenerated with a 10s injection of EDTA-containing HEPES buffer (HSBPE: 10 mM HEPES, 150 mM NaCl, 10 mM EDTA, pH 7.4). Data was collected at a rate of 1 Hz. The data was fitted to a simple 1:1 interaction model using the global data analysis option available within BiaEvaluation 3.1 software.

Calculated k_d values:
20 ug/ml: 1.40 x 10^{-3} s^{-1}
10 ug/ml: 1.70 x 10^{-3} s^{-1}
5 ug/ml: 1.56 x 10^{-3} s^{-1}
2.5 ug/ml: 1.51 x 10^{-3} s^{-1}

3.11.4: Surface plasmon resonance: Comparison of CRP binding kinetics between different *Leishmania* species

While effort was undertaken to measure binding capacity for PSG among different species previously by ELISA and ligand blotting, we were unable to determine if differences in binding kinetics contributed to the differential binding seen using these experimental models. A series of SPR experiments with CRP-biotin ligand immobilised on a desthiobiotin chip (Section 2.17.2) and varying concentrations of PSG analyte from different *Leishmania* species was performed in order to elucidate this.

As previously CRP-biotin was attached to the neutravidin loaded aminodesthiobiotin C30M chip. To collect kinetic binding data, the analyte (*L.mexicana, L.panamensis, L.donovani, L.aethiopica, L.major, L.tropica* and *L.amazonensis* WT PSG) in HBSPC was injected over the two flow cells at a slow flow rate and at various concentrations (5 µl/min, 6.25-50 µg/ml) at a temperature of 25°C. The complex was allowed to associate for 180s or 300s and dissociate for 600s. The surfaces were regenerated with a 10s injection of EDTA-containing HEPES buffer (HBSPE).

All species where binding could be observed exhibited high binding avidity to CRP, as evidenced by uniformly low dissociation rate constant (k_d) values (Figures 75-78). Difficulties fitting the dissociation curves to the evaluation software was encountered due to the strength of avidity of the binding, meaning that the typical dissociation curve with a drop off in detected RU was not evident, even with the extended dissociation time allowed following experience with similar experiments with immobilised *L.mexicana* WT and mutant PSG (Section 3.11.2). Dissociation rate constant was calculated for all curves except *L.major*, which had binding but widely variable off rates, as well as *L.tropica* and *L.amazonensis*, which demonstrated no discernable binding. The strong avidity would suggest that it was the density of binding sites rather than difference in structure or affinity of CRP ligands on PSG that was the major difference in CRP-PSG driven mechanisms. The data from *Leishmania* PSG

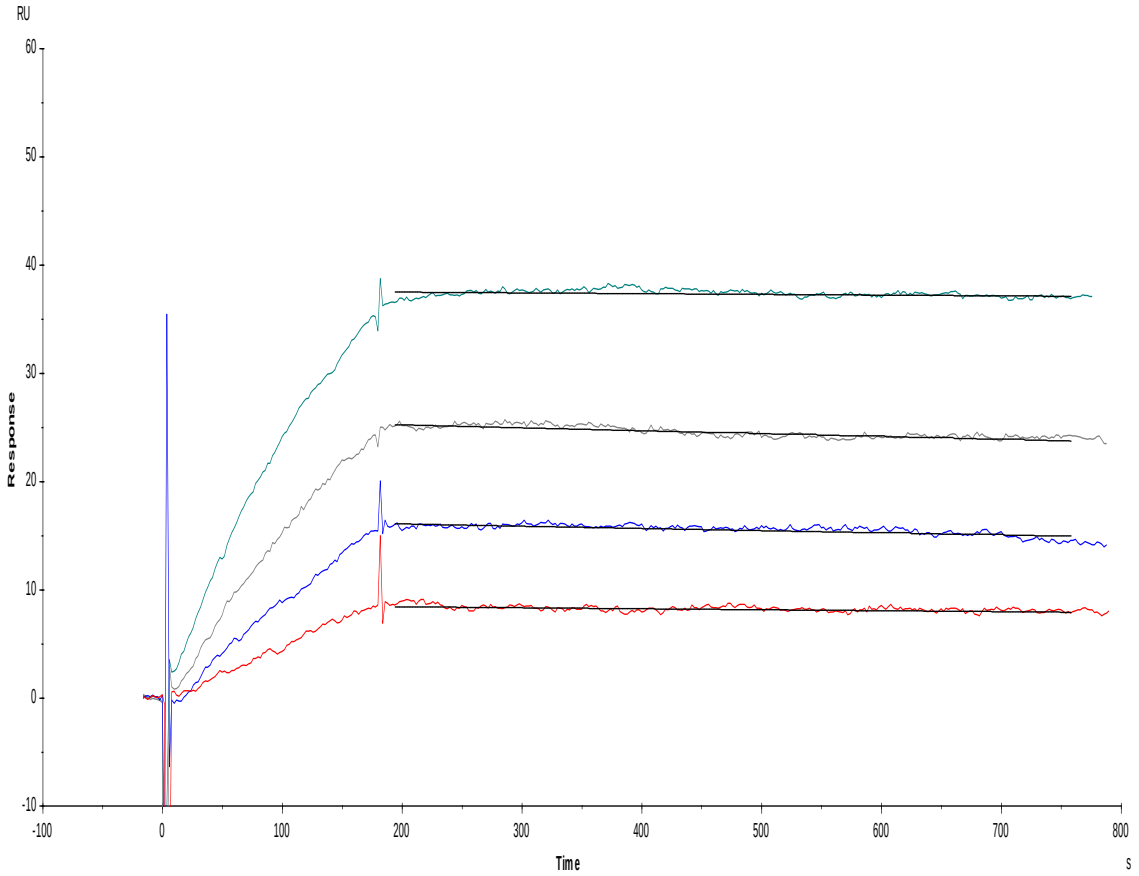

Figure 76: *L.mexicana* WT PSG exhibits binding avidity to immobilised CRP-biotin.

Surface plasmon resonance of ligand CRP-biotin (150 RU), immobilised onto neutravidin-desthiolbiotin complex captured on XanTec C30M sensor chip, to analyte *L.mexicana* WT PSG at varying analyte concentrations (6.25-50 µg/ml, 5 µl/min, 180s association, 600s dissociation) in Ca^{2+} containing HEPES buffer (HBSPC: 10 mM HEPES, 150 mM NaCl, 0.005% P20, 0.5mM $CaCl_2$, pH 7.4). The surfaces were regenerated with a 10s injection of EDTA-containing HEPES buffer (HSBPE: 10 mM HEPES, 150 mM NaCl, 10 mM EDTA, pH 7.4). Data was collected at a rate of 1 Hz. The data was fitted to a simple 1:1 interaction model using the global data analysis option available within BiaEvaluation 3.1 software.

Calculated k_d values:
25 ug/ml: 1.0×10^{-4} s^{-1}
12.5 ug/ml: 1.3×10^{-4} s^{-1}
6.25 ug/ml: 1.03×10^{-4} s^{-1}

Average k_d: 1.11×10^{-4} s^{-1}
Standard deviation: 0.13×10^{-4} s^{-1}

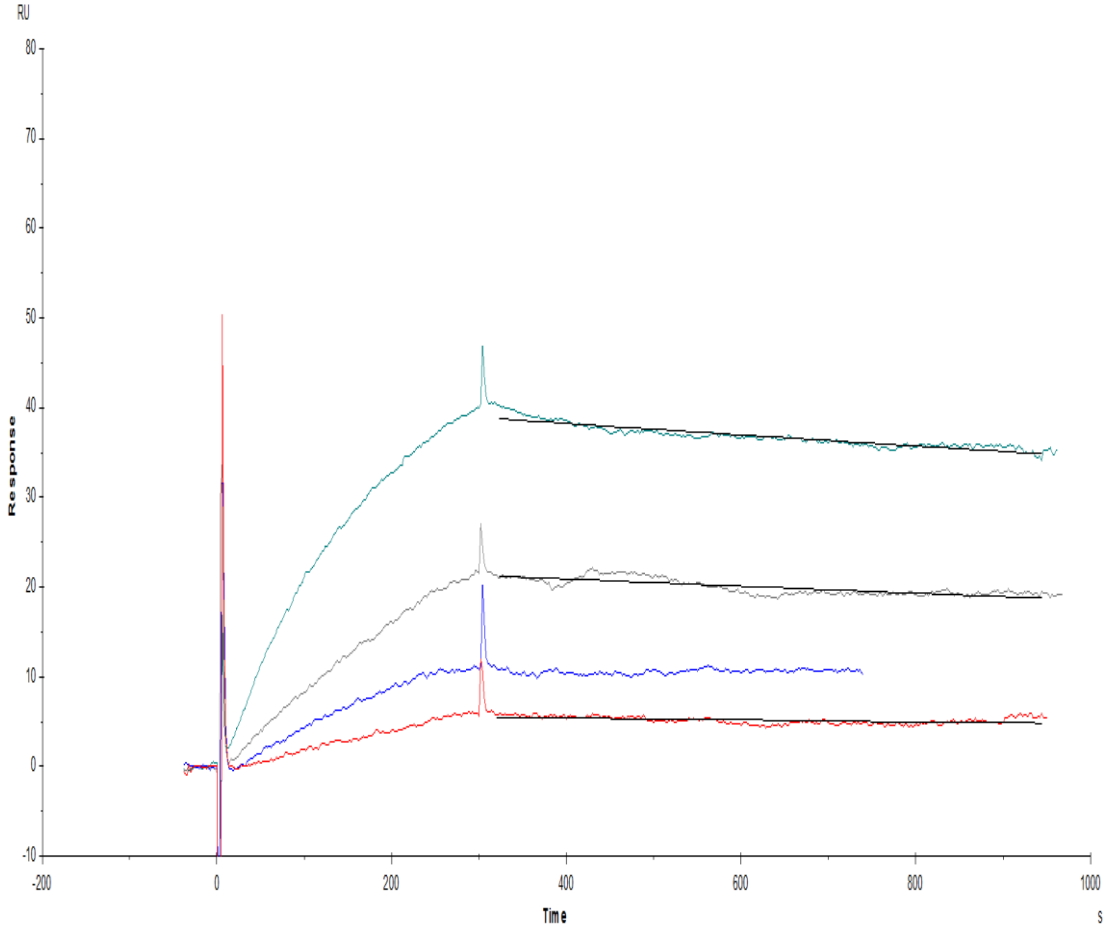

Figure 77: *L.donovani* PSG exhibits binding avidity to immobilised CRP-biotin.

Surface plasmon resonance of ligand CRP-biotin (150 RU), immobilised onto neutravidin-desthiolbiotin complex captured on XanTec C30M sensor chip, to analyte *L.donovani* PSG at varying analyte concentrations (6.25-50 µg/ml, 5 µl/min, 180s association, 600s dissociation) in Ca^{2+} containing HEPES buffer (HBSPC: 10 mM HEPES, 150 mM NaCl, 0.005% P20, 0.5mM $CaCl_2$, pH 7.4). The surfaces were regenerated with a 10s injection of EDTA-containing HEPES buffer (HSBPE: 10 mM HEPES, 150 mM NaCl, 10 mM EDTA, pH 7.4). Data was collected at a rate of 1 Hz. The data was fitted to a simple 1:1 interaction model using the global data analysis option available within BiaEvaluation 3.1 software.

Calculated k_d values:
50 ug/ml: 1.63×10^{-4} s^{-1}
25 ug/ml: 1.89×10^{-4} s^{-1}
6.25 ug/ml: 1.88×10^{-4} s^{-1}

Average k_d: 1.8×10^{-4} s^{-1}
Standard deviation: 0.12×10^{-4} s^{-1}

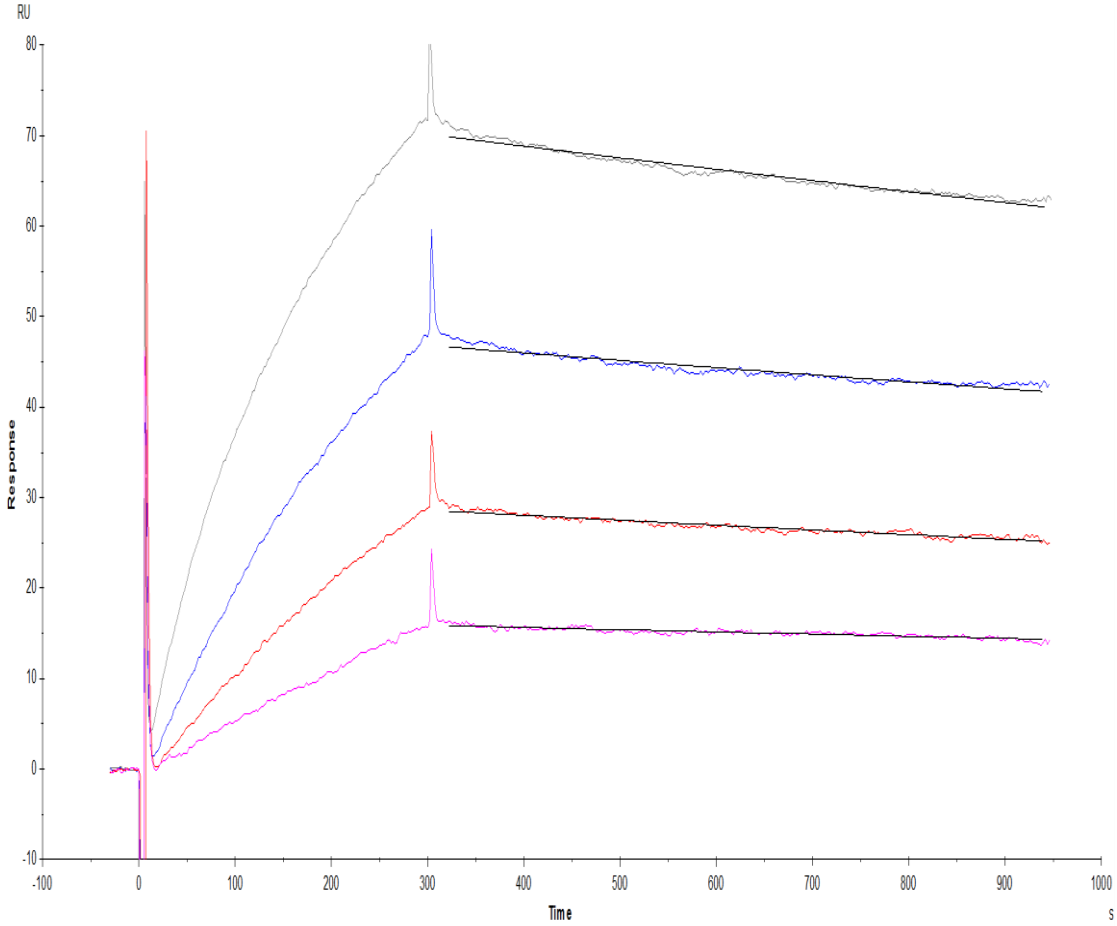

Figure 78: *L.panamensis* PSG exhibits binding avidity to immobilised CRP-biotin.

Surface plasmon resonance of ligand CRP-biotin (150 RU), immobilised onto neutravidin-desthiolbiotin complex captured on XanTec C30M sensor chip, to analyte *L.panamensis* PSG at varying analyte concentrations (6.25-50 µg/ml, 5 µl/min, 300s association, 600s dissociation) in Ca^{2+} containing HEPES buffer (HBSPC: 10 mM HEPES, 150 mM NaCl, 0.005% P20, 0.5mM $CaCl_2$, pH 7.4). The surfaces were regenerated with a 10s injection of EDTA-containing HEPES buffer (HSBPE: 10 mM HEPES, 150 mM NaCl, 10 mM EDTA, pH 7.4). Data was collected at a rate of 1 Hz. The data was fitted to a simple 1:1 interaction model using the global data analysis option available within BiaEvaluation 3.1 software.

Calculated k_d values:
50 ug/ml: 1.85×10^{-4} s^{-1}
25 ug/ml: 1.75×10^{-4} s^{-1}
12.5 ug/ml: 1.93×10^{-4} s^{-1}
6.25 ug/ml: 1.57×10^{-4} s^{-1}

Average k_d: 1.775×10^{-4} s^{-1}
Standard deviation: 0.13×10^{-4} s^{-1}

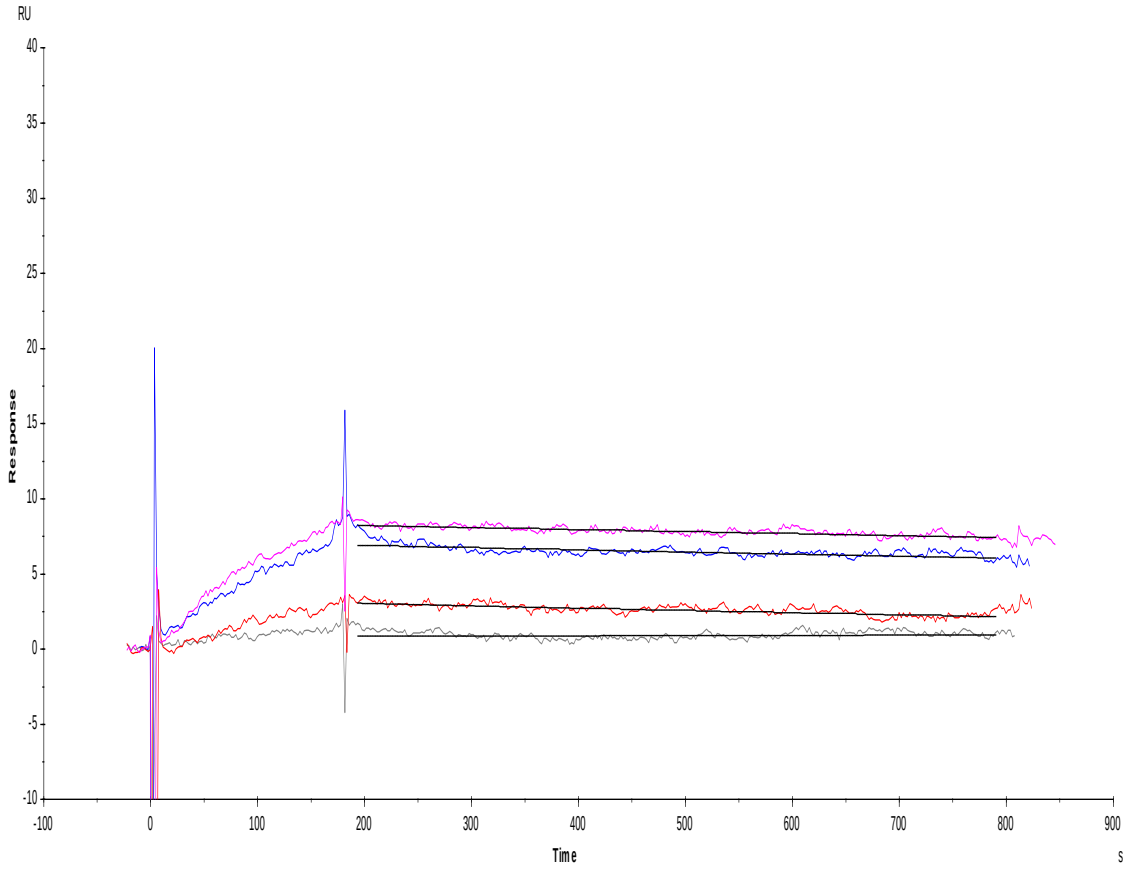

Figure 79: *L.aethiopica* PSG exhibits binding avidity to immobilised CRP-biotin.

Surface plasmon resonance of ligand CRP-biotin (150 RU), immobilised onto neutravidin-desthiolbiotin complex captured on XanTec C30M sensor chip, to analyte *L.aethiopica* PSG at varying analyte concentrations (6.25-50 µg/ml, 5 µl/min, 180s association, 600s dissociation) in Ca^{2+} containing HEPES buffer (HBSPC: 10 mM HEPES, 150 mM NaCl, 0.005% P20, 0.5mM $CaCl_2$, pH 7.4). The surfaces were regenerated with a 10s injection of EDTA-containing HEPES buffer (HSBPE: 10 mM HEPES, 150 mM NaCl, 10 mM EDTA, pH 7.4). Data was collected at a rate of 1 Hz. The data was fitted to a simple 1:1 interaction model using the global data analysis option available within BiaEvaluation 3.1 software.

Calculated k_d values:
25 ug/ml: 1.80 $x10^{-4}$ s^{-1}
12.5 ug/ml: 5.04 $x10^{-4}$ s^{-1}
6.25 ug/ml: 1.64 $x10^{-4}$ s^{-1}

Average k_d: 2.82 x 10^{-4} s^{-1}
Standard deviation: 1.56 x 10^{-4} s^{-1}

from species (*L.major, L.tropica* and *L.amazonensis*) which were previously shown to have low CRP binding capacity (Section 3.2.3), directly corresponded with low RU during SPR (Figures 79-80).

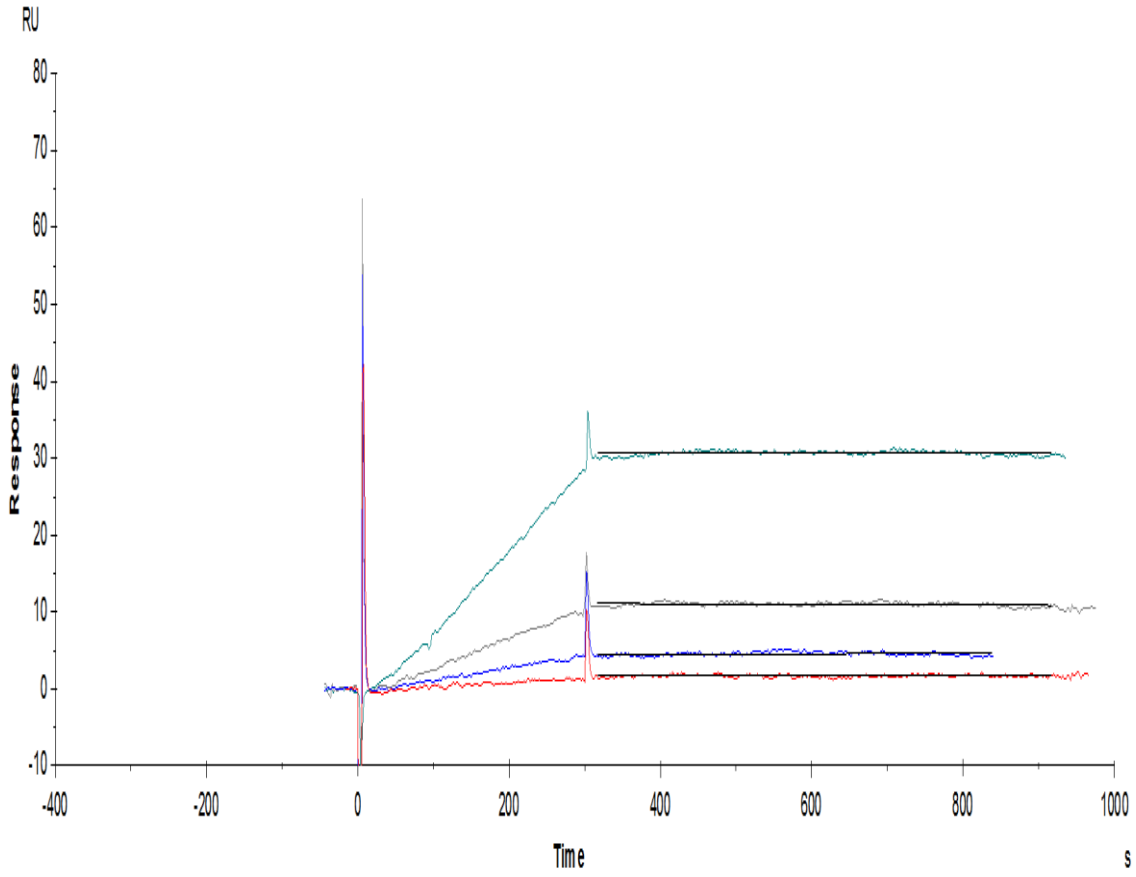

Figure 80: *L.major* PSG binding to CRP-biotin insufficient to calculate binding kinetics.

Surface plasmon resonance of ligand CRP-biotin (150 RU), immobilised onto neutravidin-desthiolbiotin complex captured on XanTec C30M sensor chip, to analyte *L.major* PSG at varying analyte concentrations (6.25-50 µg/ml, 5 µl/min, 180s association, 600s dissociation) in Ca^{2+} containing HEPES buffer (HBSPC: 10 mM HEPES, 150 mM NaCl, 0.005% P20, 0.5mM $CaCl_2$, pH 7.4). The surfaces were regenerated with a 10s injection of EDTA-containing HEPES buffer (HSBPE: 10 mM HEPES, 150 mM NaCl, 10 mM EDTA, pH 7.4). Data was collected at a rate of 1 Hz. The data was fitted to a simple 1:1 interaction model using the global data analysis option available within BiaEvaluation 3.1 software.

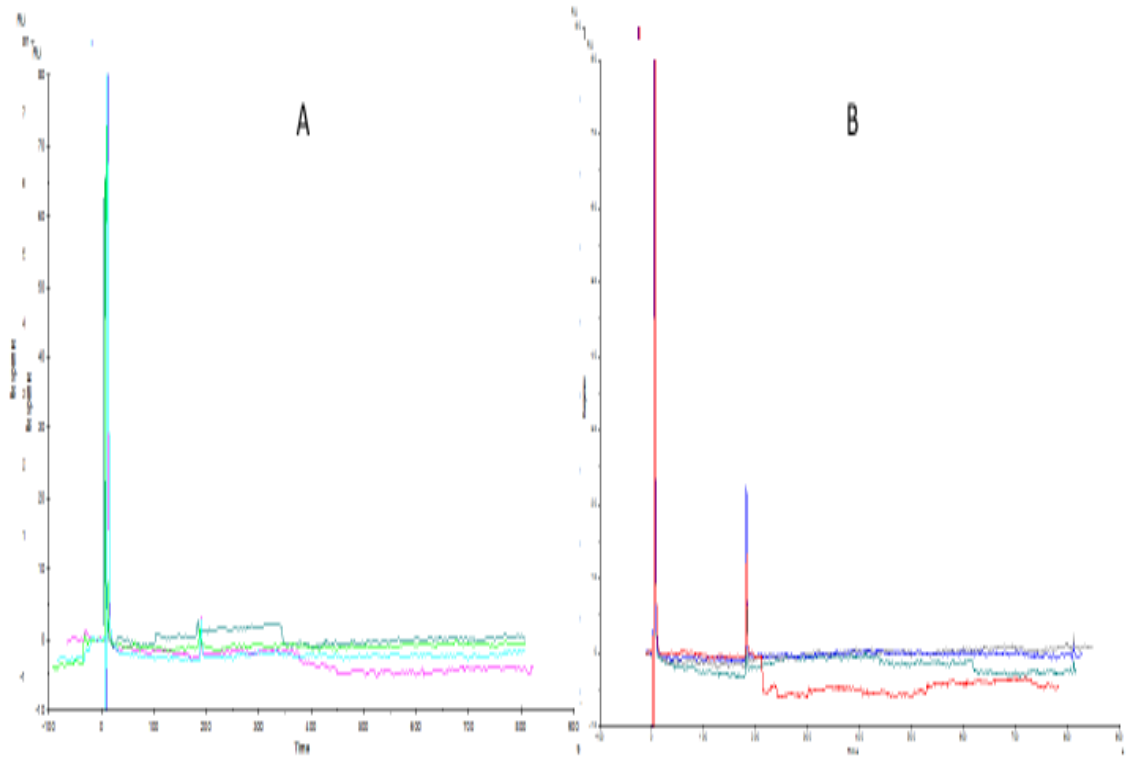

Figure 81: *L.tropica* and *L.amazonensis* PSG exhibit poor CRP binding avidity

Surface plasmon resonance of ligand CRP-biotin (150 RU), immobilised onto neutravidin-desthiolbiotin complex captured on XanTec C30M sensor chip, to analyte *L. tropica* (A) and *L.amazonensis* (B) PSG at varying analyte concentrations (6.25-50 µg/ml, 5 µl/min, 180s association, 600s dissociation) in Ca^{2+} containing HEPES buffer (HBSPC: 10 mM HEPES, 150 mM NaCl, 0.005% P20, 0.5mM $CaCl_2$, pH 7.4). The surfaces were regenerated with a 10s injection of EDTA-containing HEPES buffer (HSBPE: 10 mM HEPES, 150 mM NaCl, 10 mM EDTA, pH 7.4). Data was collected at a rate of 1 Hz. The data was fitted to a simple 1:1 interaction model using the global data analysis option available within BiaEvaluation 3.1 software.

3.11.5: PSG binding to CRP is based on multiple low-affinity binding events

In order to determine the optimal flow rate to observe the binding of an analyte as large as PSG to the immobilised CRP ligand, binding was observed at varying flow rates.

CRP was immobilised to the chip surface as previously (Section 2.17.2.2). WT *L.mexicana* PSG (20 ug/ml) appears to bind to surface with greater avidity when flow rate was reduced (5, 10 and 20 µl/min). This suggests that PSG binding to CRP may be due to multiple binding events, with the reduction in flow rate allowing the multiple interactions between the large PSG analyte and the CRP ligand surface required for the binding event to occur and be detected. This was perhaps unsurprising, considering the multimeric nature of CRP as well as the abundance of the repeating phosphorylated disaccharide on some *Leishmania* glycosylated products (Figure 81). In addition, CRP has been observed to have low binding affinity to single phosphorylated saccharides(Culley et al., 2000).

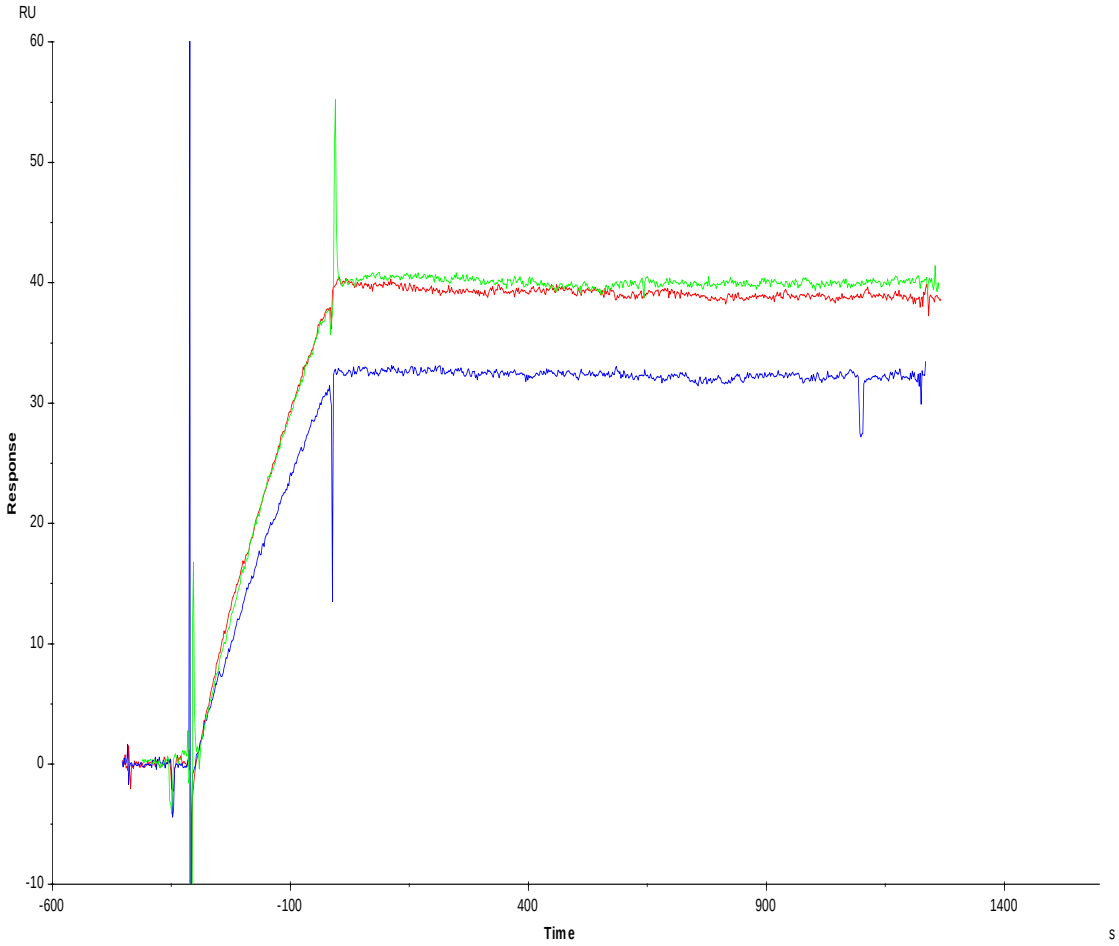

Figure 82: ***L****.mexicana* WT PSG association rate to CRP-biotin is reduced at high flow rates

Surface plasmon resonance of CRP-biotin ligand (150 RU) immobilised onto neutravidin-desthiolbiotin complex captured on XanTec C30M sensor chip. To collect kinetic binding data, the analyte (*L.mexicana* WT PSG) in HBSPC was injected over the two flow cells (20 µg/ml) at various flow rates(5, 10 and 20 µl/min) at a temperature of 25°C. The complex was allowed to associate for 300s and dissociate 1200s. The surfaces were regenerated with a 10s injection of EDTA-containing HEPES buffer (HSBPE: 10 mM HEPES, 150 mM NaCl, 0.005% P20, 0.5mM EDTA pH 7.4). Data was collected at a rate of 1 Hz. The data was fitted to a simple 1:1 interaction model using the global data analysis option available within BiaEvaluation 3.1 software.

Flow rate**:** Blue: 20 µl/min, Red: 10 µl/min, Green: 5 µl/min

Calculated k_d values:
5 µl/min: 1.97 x10^{-5} s^{-1}
10 µl/min: 1.97 x10^{-5} s^{-1}
20 µl/min: 2.42 x10^{-5} s^{-1}

Average k_d:2.12 x10^{-5} s^{-1}
Standard deviation: 0.21 x10^{-5} s^{-1}

3.11.6: CRP binding to immobilised PSG is affected by ligand capture method and heterogenous composition

PSG had been reported to be a very large molecule, with the phosphorylated disaccharide present on multiple surfaces, and as such the method of capture should affect only a small proportion of the available surface. Therefore, CRP was added back to see if it would bind to PSG previously captured by CRP-biotin. Although this analysis required reassociation of PSG each time after EDTA elution, this was determined to be reproducible (Section 2.17.2.4). A relatively small amount of PSG (8-15 RU) was bound to the CRP-biotin surface given the amount of available ligand on the surface. However, a subsequent injection of CRP (20 µg/ml, 5 µl/min, 300s association, 600s dissociation) over the now immobilised PSG resulted in far higher levels of analyte CRP bound (Figure 82: 106 RU) in comparison to prior experiments with more direct immobilisation strategies for PSG ligand on the surface (Figures 72, 74 and 75). This allowed better kinetic data and was performed with PSG from multiple *Leishmania* species immobilised on the surface, with CRP as the free-flowing analyte.

The ligand (*L.mexicana* PSG*:* 15 RU*, L.panamensis* PSG*:* 8 RU and *L.donovani* PSG: 8 RU) was immobilised on FC2, with FC1 left blank (i.e. no PSG loaded) to serve as a reference surface. To collect kinetic binding data, the analyte CRP in HBSPC was injected over the two flow cells at varying concentrations (0.1-6.4 µg/ml) at 20 µl/min at a temperature of 25°C. The complex was allowed to associate for 180s and dissociate for 600s. The surfaces were regenerated with a 10s injection of EDTA-containing HEPES buffer (HSBPE: 10 mM HEPES, 150 mM NaCl, 0.005% P20, 0.5mM EDTA pH 7.4) and reloaded with the appropriate PSG (Figure 83-85; Table 3).

In all instances, CRP binding stoichiometry to PSG appears to increase substantially, despite the much lower RU of available ligand immobilised on the surface. This result indicated that PSG binding to CRP may be subject to the orientation or change of conformation of the PSG molecules captured, or perhaps more likely that the CRP-biotin capture selects for one of the forms which has high CRP binding in a heterogeneous population of PSG molecules.

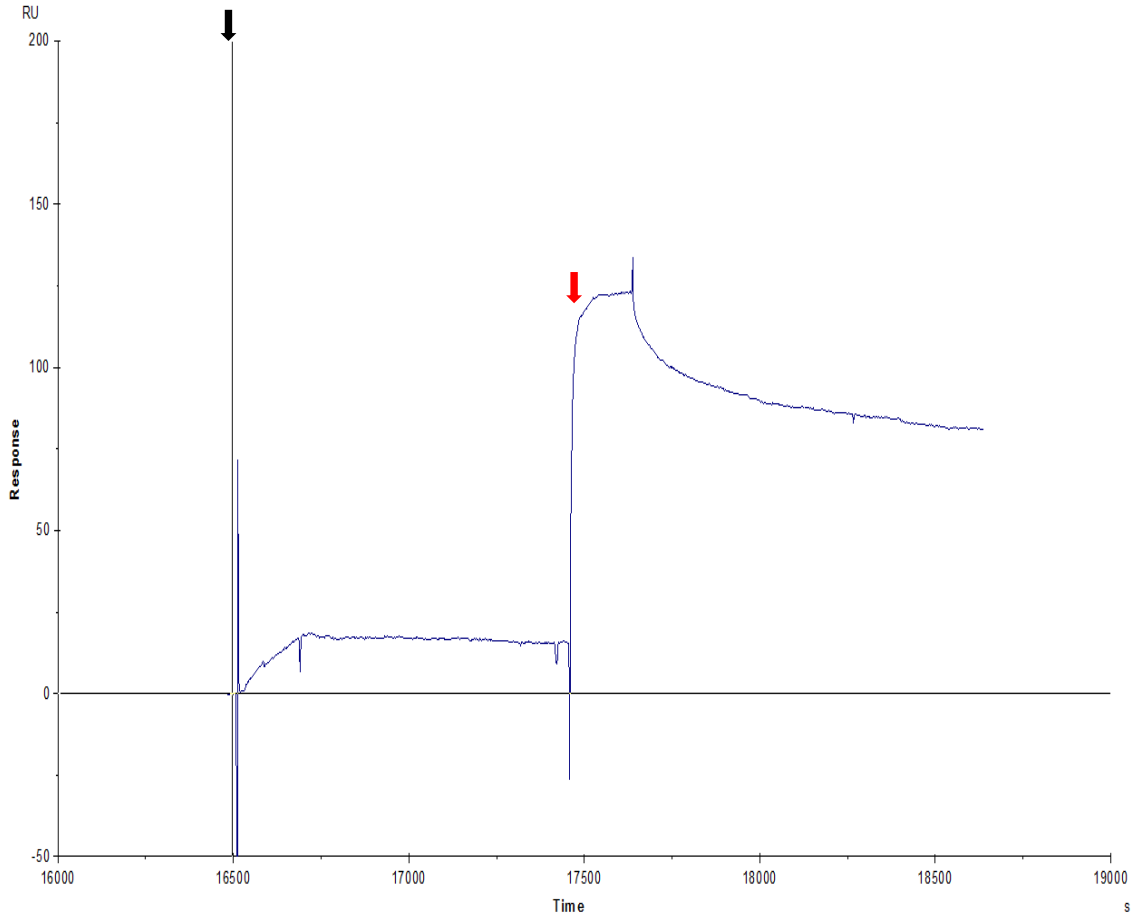

Figure 83: *L.mexicana* WT PSG captured on CRP-biotin exhibits greater CRP binding capacity compared to directly immobilised PSG (Figures 74, 76 and 77).

Initially, *L.mexicana* WT PSG (16 RU) was immobilised onto CRP-biotin (150 RU) bound to neutravidin-desthiolbiotin complex captured on XanTec C30M sensor chip, by a single injection (50 µg/ml, 5 µl/min) in HBSPC at a temperature of 25°C. The complex was allowed to associate for 300s and dissociate 600s. Time of injection was indicated by the black arrow (→). Analyte CRP in HBSPC (20 µg/ml, 5 µl/min) was then injected at a temperature of 25°C. The complex was allowed to associate for 300s and dissociate 600s. Time of injection was indicated by the red arrow (→).

Data was collected at a rate of 1 Hz. The data were fit to a simple 1:1 interaction model using the global data analysis option available within BiaEvaluation 3.1 software.

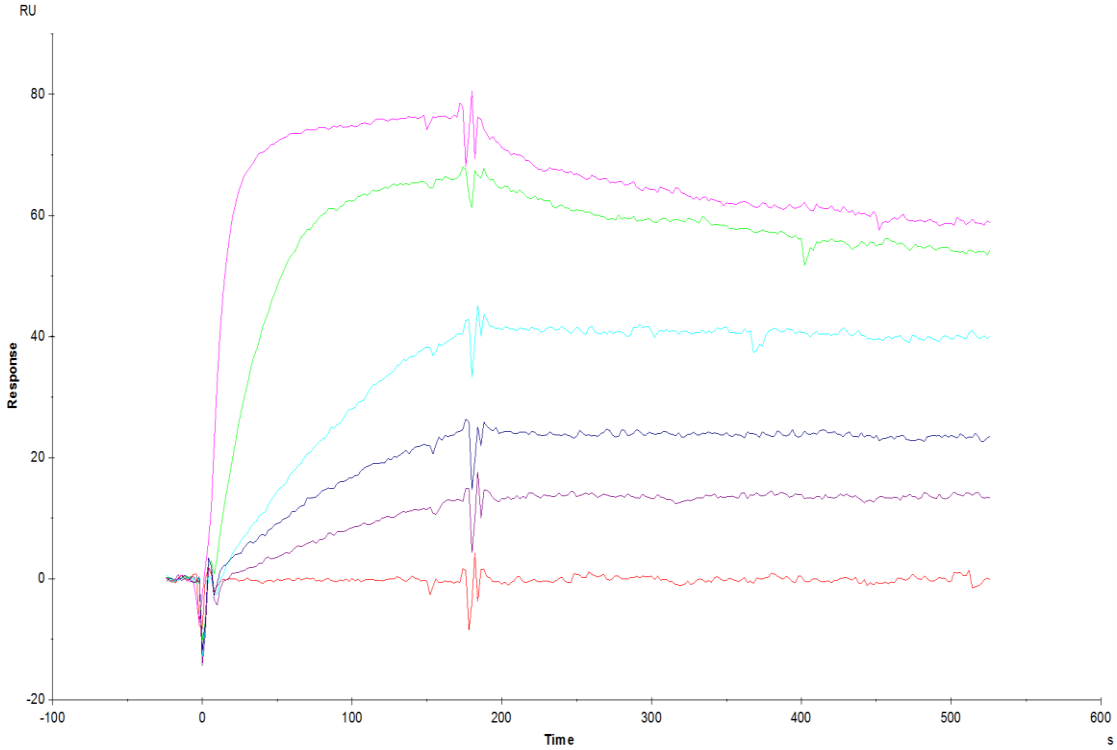

Figure 84: CRP-biotin captured *L.mexicana* PSG exhibits increased binding sites for CRP.

Surface plasmon resonance of the ligand *L.mexicana* PSG (15 RU) in was immobilised on CRP-biotin/neutravidin/desthiolbiotin complex on the XanTec C30M sensor chip. To collect kinetic binding data, the analyte (CRP) in HBSPC was injected over the two flow cells at various concentrations (6.4, 1.6, 0.8, 0.4, 0.1 µg/ml) at 20 µl/min at a temperature of 25°C. The complex was allowed to associate for 180s and dissociate for 300s. The surfaces were regenerated with a 10s injection of 10 mM EDTA buffer.

Data was collected at a rate of 1 Hz. The data was fitted to a simple 1:1 interaction model using the global data analysis option available within BiaEvaluation 3.1 software.

k_a (1/Ms)	k_d (1/s)	R_{max} (RU)	RI (RU)	Analyte conc. (M)	K_A (1/M)	K_D (M)	R_{eq} (RU)	k_{obs} (1/s)
$1.88e^{6}$	$5e^{-4}$	71.4	2.77	$5e^{-8}$	$3.77e^{9}$	$2.65e^{-10}$	71	0.0947
$2.21e^{6}$	$5e^{-4}$	70.6	0.119	$1.25e^{-8}$	$4.42e^{9}$	$2.26e^{-10}$	69.3	0.0281
$2.12e^{6}$	$2e^{-4}$	63.5	1.39	$3e^{-9}$	$1.06e^{10}$	$9.44e^{-11}$	61.6	$6.56e^{-3}$
$1.94e^{6}$	$2e^{-4}$	67.1	1.68	$1.6e^{-9}$	$9.72e^{9}$	$1.03e^{-10}$	63.1	$3.31e^{-3}$
$4.77e^{5}$	$2e^{-4}$	30.5	0.671	$8e^{-9}$	$2.38e^{9}$	$4.2e^{-10}$	28.9	$4.01e^{-3}$

Table 3: Table of kinetic values for SPR of CRP analyte binding to ligand WT *L.mexicana* PSG captured on CRP-biotin (Figure 83).

k_a: Association Rate Constant (i.e. Rate of complex formation)
k_d: Dissociation Rate Constant (i.e. Fraction of complex decay)
R_{max}: Maximum observed Response Units
RI: RU detected at beginning of analysis
Analyte conc.: Concentration of injected analyte
K_A: Association Constant
K_D: Dissociation Constant
R_{eq}: Response Units at equilibrium
R_{obs}: Observed rate constant ($k_aC + k_d$)

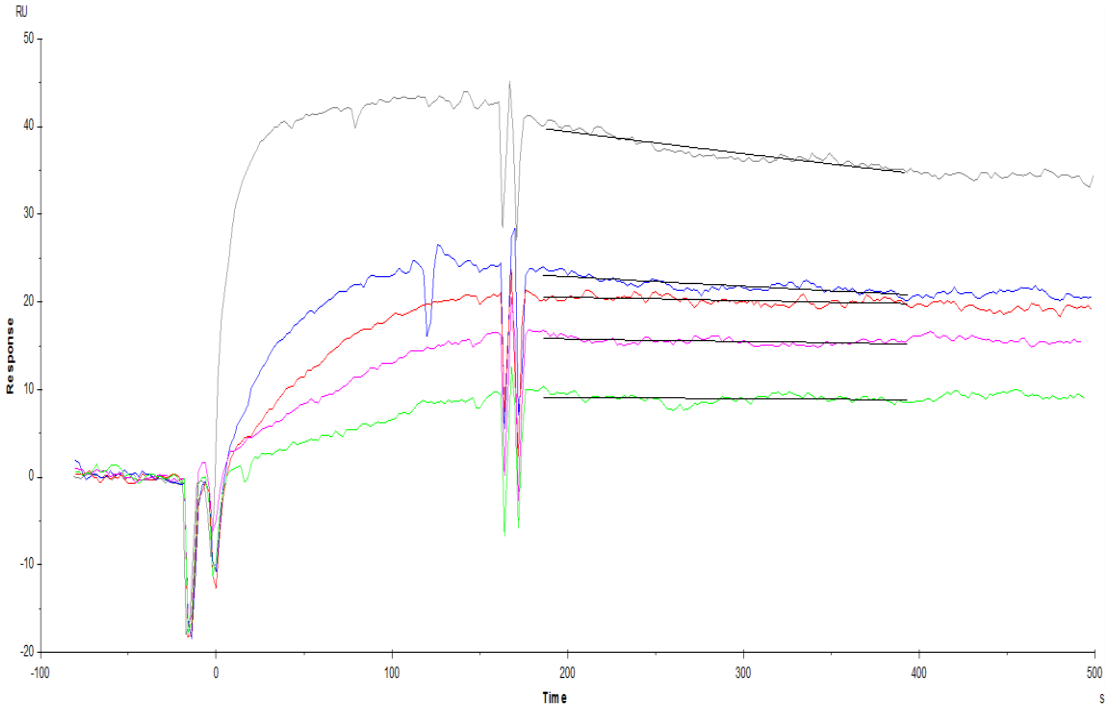

Figure 85: CRP-biotin captured *L.panamensis* PSG exhibits increased binding sites for CRP.

Surface plasmon resonance of the ligand *L.panamensis* PSG (8 RU) in was immobilised on CRP-biotin/neutravidin/desthiolbiotin complex on the XanTec C30M sensor chip. To collect kinetic binding data, the analyte (CRP) in HBSPC was injected over the two flow cells at various concentrations (6.4, 1.6, 0.8, 0.4, 0.1 µg/ml) at 20 µl/min at a temperature of 25°C. The complex was allowed to associate for 180s and dissociate for 300s. The surfaces were regenerated with a 10s injection of 10 mM EDTA buffer. Data was collected at a rate of 1 Hz. The data was fitted to a simple 1:1 interaction model using the global data analysis option available within BiaEvaluation 3.1 software.

Calculated k_d values:
6.4 ug/ml: 6.35 x 10^{-4} s^{-1}
1.6 ug/ml: 4.62 x 10^{-4} s^{-1}
0.8 ug/ml: 1.78 x 10^{-4} s^{-1}
0.4 ug/ml: 1.77 x 10^{-4} s^{-1}
0.1 ug/ml: 1.56 x 10^{-4} s^{-1}

For analyte CRP concentration 1.6-6.4 ug/ml:
Average k_d: 5.485 x10^{-4} s^{-1}
Standard deviation: 0.865 x 10^{-4} s^{-1}
For analyte CRP concentration 0.1-0.8 ug/ml:
Average k_d: 1.7 x10^{-4} s^{-1}
Standard deviation: 0.10 x10^{-4} s^{-1}

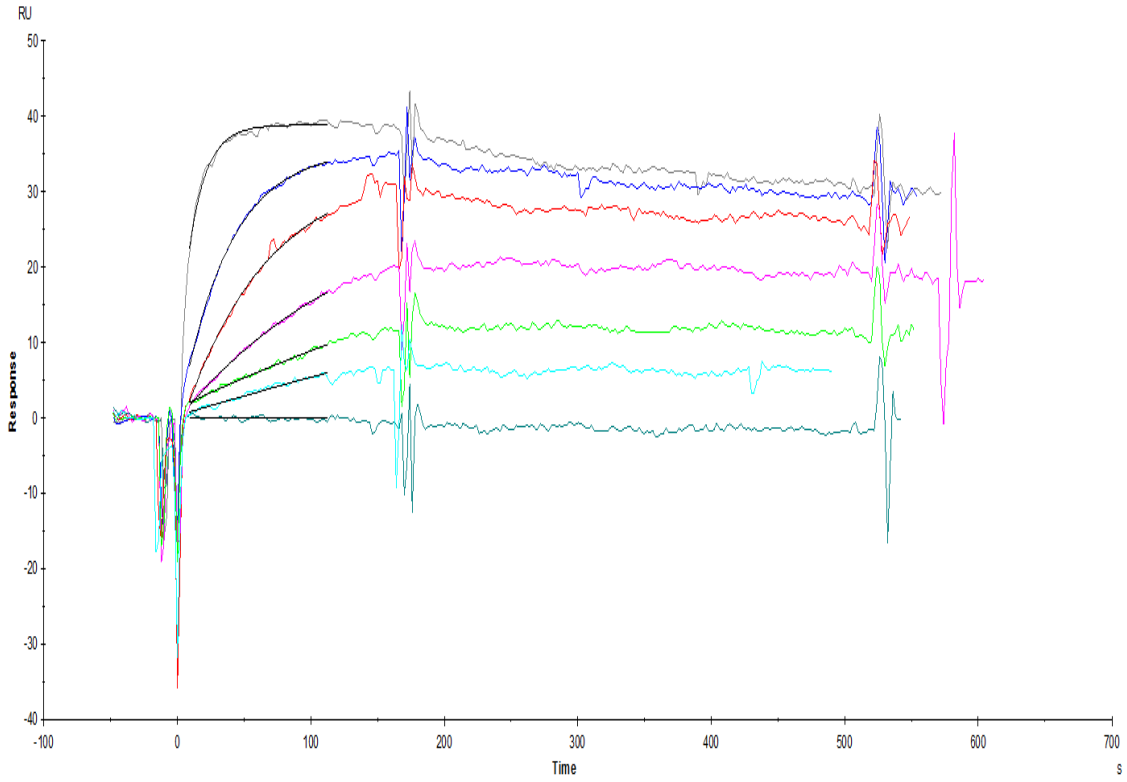

Figure 86: CRP-biotin captured *L.donovani* PSG exhibits increased binding sites for CRP

Surface plasmon resonance of the ligand *L.donovani PSG* (8 RU) in was immobilised on CRP-biotin/neutravidin/desthiolbiotin complex on the XanTec C30M sensor chip. To collect kinetic binding data, the analyte (CRP) in HBSPC was injected over the two flow cells at various concentrations (6.4, 1.6, 0.8, 0.4, 0.1 µg/ml) at 20 µl/min at a temperature of 25°C. The complex was allowed to associate for 180s and dissociate for 300s. The surfaces were regenerated with a 10s injection of 10 mM EDTA buffer. Data was collected at a rate of 1 Hz. The data was fitted to a simple 1:1 interaction model using the global data analysis option available within BiaEvaluation 3.1 software.

Calculated k_d values:
6.4 ug/ml: 5.12 x 10^{-4} s^{-1}
1.6 ug/ml: 4.5 x 10^{-4} s^{-1}
0.8 ug/ml: 3.3 x 10^{-4} s^{-1}
0.4 ug/ml: 2.3 x 10^{-4} s^{-1}
0.2 ug/ml: 1.53 x 10^{-4} s^{-1}
0.1 ug/ml: 1.47 x 10^{-4} s^{-1}

For analyte CRP concentration 1.6-6.4 ug/ml:
Average k_d: 4.81 x10^{-4} s^{-1}
Standard deviation: 0.31 x 10^{-4} s^{-1}
For analyte CRP concentration 0.1-0.8 ug/ml:
Average k_d: 2.15 x10^{-4} s^{-1}
Standard deviation: 0.740236449 x10^{-4} s^{-1}

We also observed that binding affinity appears to change with different concentrations of CRP analyte, with the k_d value decreasing with an increasing concentration of CRP analyte flowed over the PSG ligand surface. This would appear to indicate a lower affinity binding event present only at high analyte concentrations (~20 ug/ml CRP), significant binding to which only appears to occur once the higher affinity sites were occupied. Nevertheless, it was possible to calculate a dissociation constant for binding of CRP to the PSG (~1 $x10^{-10}$ M). Of note, the on-rate was also faster at higher concentrations, which was unexpected as this was rare in binding interactions. This phenomenon will be re-visited in LPG-CRP SPR experiments (Section 3.12.2).

3.12: Investigating pentraxin binding to LPG using Surface plasmon resonance techniques

3.12.1: Early LPG ligand Immobilisation strategies

Previous attempts to study LPG-CRP interactions were made by John Raynes (Department of Infection Biology, London School of Hygiene and Tropical Medicine, UK) and Jan-Hendrik Schroeder (Department of Inflammation Biology, King's College London, UK), where LPG was immobilised onto C1 surface using aldehyde-hydrazine based coupling, following surface activation with EDC/NHS (Section 2.18.1). CRP analyte was performed on metacyclic and nectomonad stage *L.mexicana* LPG (approx. 205 RU), where the early observation was made that CRP bound with greater avidity to the former compared to the latter (R_{max} for 40 µg/ml CRP analyte: Metacyclic LPG 380 RU, nectomonad LPG 58 RU). Binding was also characterised for infective stage (i.e. metacyclic) stage parasites for other various *Leishmania* species, including *L.donovani* (Not shown).

In its native state, LPG was reported to be anchored by the insertion of the lysoalkyl phosphinositol portion of the molecule into the cell membrane, presumably leaving the glycosylated regions exposed (section 1.5.1). As such, there was a concern that the immobilisation strategy used could have resulted in an orientation that did not accurately reflect LPG in *vivo,* due to the possibility of attachment to the chip surface via the aforementioned glycosylated regions. In addition, the oxidation process required for carbodiimide coupling could have fundamentally altered the chemical structure of LPG, leading to anomalous binding characteristics.

3.12.2: Metacyclic-stage LPG exhibits higher CRP binding avidity than nectomonad LPG at higher ligand densities

In order to more accurately represent the orientation of LPG as it would be on the *Leishmania* cell surface, a new method of LPG attachment to the chip surface was developed, aiming to immobilise the ligand via hydrophobic interaction to the glycoinositol lipid anchor, leaving the glycosylated region exposed and in its native state. This new attachment strategy would also be able to be stripped completely with detergent, and can thus be reused, making it more cost efficient (Section 2.18.2).

A hydrophobic planar alkyl surface (XanTec HPP) was first washed with Octyl β-glucoside (40mM, 10 µl/min, 600s) in order to remove any residual contaminants. *L.mexicana* LPG (50 µg/ml, 2 µl/min metacyclic or nectomonad LPG) in HBSC (10 mM HEPES, 150 mM NaCl, 0.5mM $CaCl_2$ pH 7.4) was then immobilised on the surface a lower (Figure 86-87, Both 25 RU) or higher (Figure Figure 88 & Table 4: Metacyclic LPG 290 RU, Figure 89 & Table 5: Nectomonad LPG 270 RU). CRP (30 µl/min, 0.02 – 40 µg/ml, 180s association, 300s dissociation) analyte was then flowed over the surface. Surface was regenerated with EDTA containing buffer (10 mM HEPES, 150 mM NaCl, 0.5mM EDTA pH 7.4). Care was taken to ensure no detergent was present in any samples or buffers, due to the potential for disruption of the hydrophobic binding mechanism.

At low ligand density, there does not appear to be any discernible difference in CRP avidity between metacyclic and nectomonad LPG, with similar levels of CRP binding R_{max} detected for a given analyte concentration. There was however a higher avidity of CRP when the LPG was at higher density as seen for the dissociation constant (Low density: ~$5.0x10^{-10}$ M, high density: ~$1.0 x10^{-10}$ M). Of note, the k_d values appear to be analyte concentration dependent, with the k_d values observed in both LPG types being approximate twofold higher at higher CRP concentrations (1.25-10 ug/ml) compared to values obtained at lower CRP concentrations (0.08-0.63 ug/ml). This could be indicative of the presence of

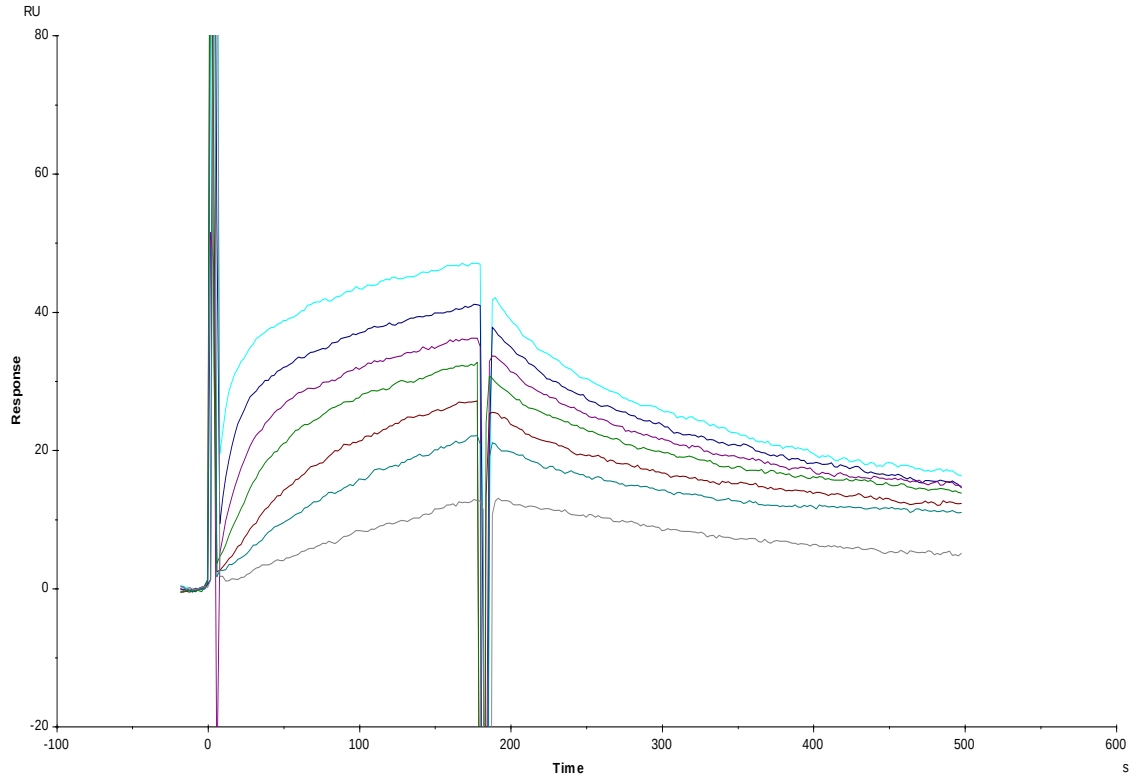

Figure 87: CRP exhibits similar binding avidity to metacyclic LPG at low ligand densities.

Surface plasmon resonance of ligand metacyclic LPG (25 RU) immobilised by hydrophobic attachment to a Xantec HPP alkyl chip, to analyte CRP (0.16 – 10 µg/ml, 30 µl/min, 180s association, 300s dissociation) in HBSC (10 mM HEPES, 150 mM NaCl, 0.5mM $CaCl_2$, pH 7.4). The surfaces were regenerated with a 10s injection of EDTA-containing HEPES buffer (HSBPE: 10 mM HEPES, 150 mM NaCl, 10 mM EDTA, pH 7.4). Data was collected at a rate of 1 Hz. The data was fitted to a simple 1:1 interaction model using the global data analysis option available within BiaEvaluation 3.1 software.

Calculated k_d values:
10 ug/ml: 2.65 x 10^{-3} s^{-1}
5 ug/ml: 2.61 x 10^{-3} s^{-1}
2.5 ug/ml: 2.06 x 10^{-3} s^{-1}
1.25 ug/ml: 2.38 x 10^{-3} s^{-1}
0.63 ug/ml: 2.17 x 10^{-3} s^{-1}
0.31 ug/ml: 1.89 x 10^{-4} s^{-1}
0.16 ug/ml: 3.34 x 10^{-4} s^{-1}

Average k_d: 1.80175 x 10^{-3} s^{-1}
Standard deviation: 0.38 x 10^{-3} s^{-1}

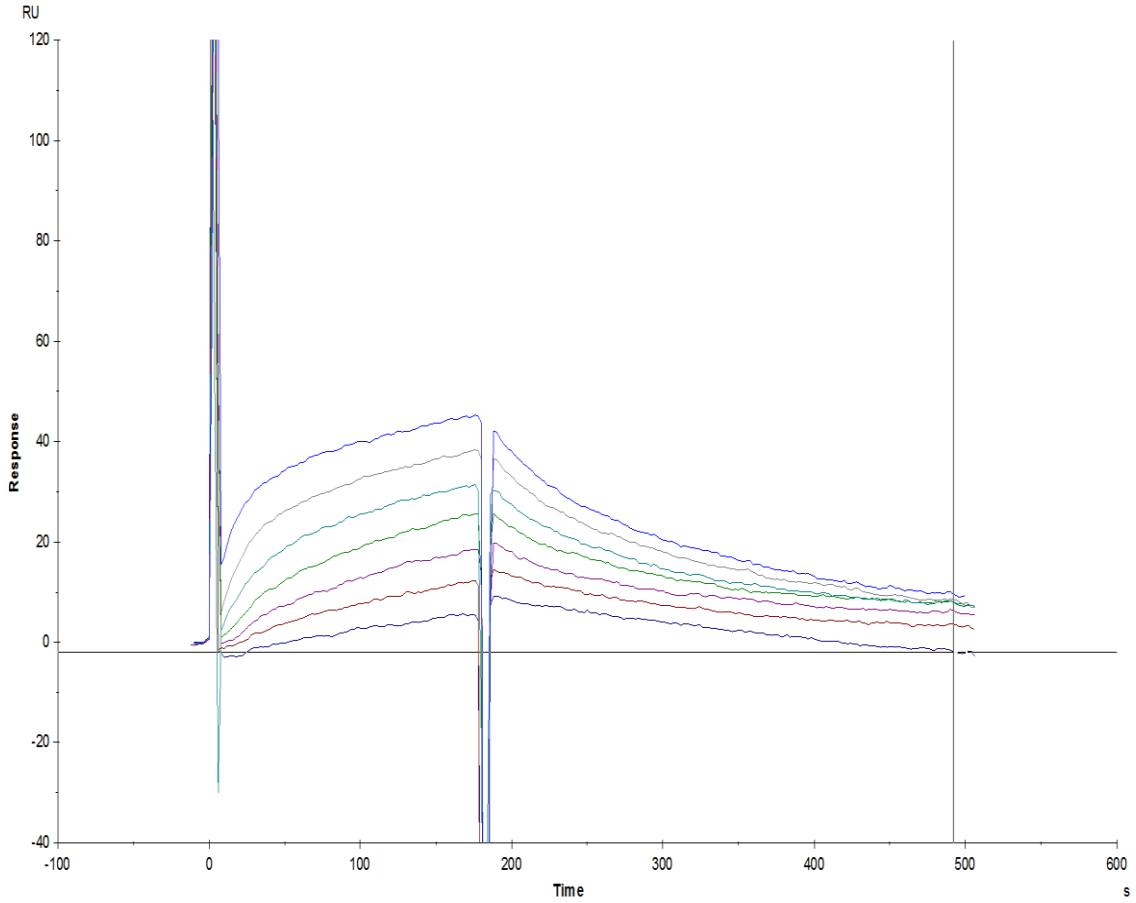

Figure 88: CRP exhibits similar binding avidity to nectomonad LPG at low ligand densities.

Surface plasmon resonance of ligand nectomonad LPG (25 RU), immobilised by hydrophobic attachment to a XanTec HPP alkyl chip, to analyte CRP (0.16 – 10 µg/ml, 30 µl/min, 180s association, 300s dissociation) in HBSC (10 mM HEPES, 150 mM NaCl, 0.5mM $CaCl_2$, pH 7.4). The surfaces were regenerated with a 10s injection of EDTA-containing HEPES buffer (HSBPE: 10 mM HEPES, 150 mM NaCl, 10 mM EDTA, pH 7.4). Data was collected at a rate of 1 Hz. The data was fitted to a simple 1:1 interaction model using the global data analysis option available within BiaEvaluation 3.1 software.

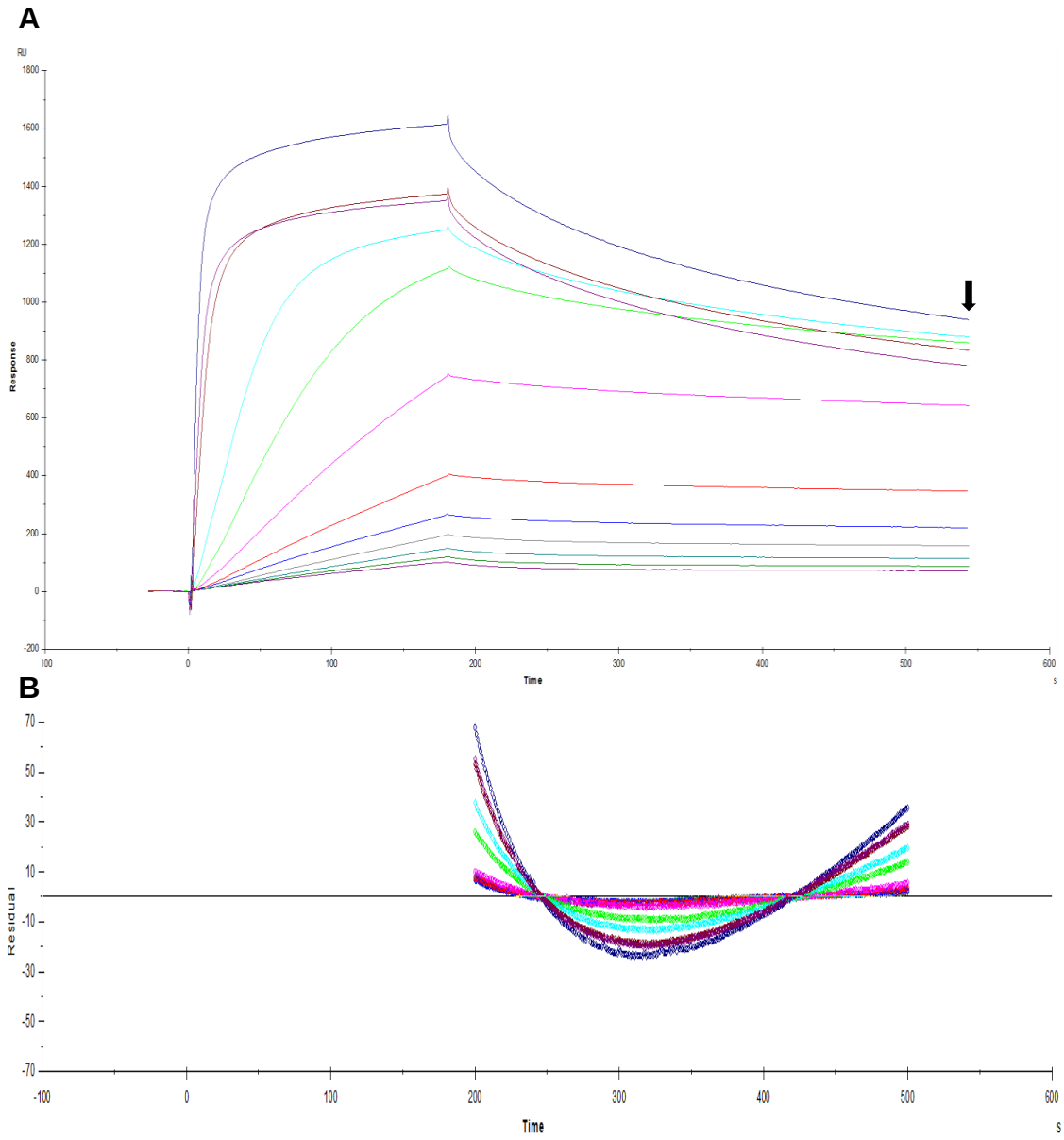

Figure 89: CRP binding to *L.mexicana* metacyclic LPG immobilised at high density exhibits changes in kinetics at higher CRP concentrations (A), with residual analysis of dissociation (B).

SPR of ligand metacyclic LPG (290 RU), immobilised by hydrophobic attachment to a Xantec HPP alkyl chip, to analyte CRP (0.02 – 40 µg/ml, 30 µl/min, 180s association, 300s dissociation) in HBSC (10 mM HEPES, 150 mM NaCl, 0.5mM $CaCl_2$, pH 7.4). The surfaces were regenerated with a 10s injection of EDTA-containing HEPES buffer (HSBPE: 10 mM HEPES, 150 mM NaCl, 10 mM EDTA, pH 7.4). Data was collected at a rate of 1 Hz. The data was fitted to a simple 1:1 interaction model using the global data analysis option available within BiaEvaluation 3.1 software.

CRP analyte concentrations per run, from highest to lowest RU recorded at timepoint indicated by the black arrow (→): 10, 5, 2.5, 20, 40, 1.25, 0.63, 0.31, 0.16, 0.08, 0.04 and 0.02 µg/ml.

Analyte conc. (µg/ml)	k_a (1/Ms)	k_d (1/s)	R_{max} (RU)	RI (RU)	Analyte conc. (M)	K_A (1/M)	K_D (M)	R_{eq} (RU)	k_{obs} (1/s)
1.25	$3.85e^4$	$4e^{-4}$	$1.25e^4$	-6.02	$1e^{-8}$	$9.63e^7$	$1.04e^{-8}$	$6.12e^3$	$7.85e^{-4}$
2.5	$2.34e^5$	$6.5e^{-4}$	$2.43e^3$	-27.5	$2e^{-8}$	$3.6e^8$	$2.77e^{-9}$	$2.14e^3$	$5.34e^{-3}$
5	$4.92e^5$	$8.6e^{-4}$	$1.47e^3$	-46.3	$4e^{-8}$	$5.72e^8$	$1.75e^{-9}$	$1.41e^3$	0.0205
10	$2.13e^6$	$1.3e^{-3}$	$1.07e^3$	448	$8e^{-8}$	$1.64e^9$	$6.09e^{-10}$	$1.06e^3$	0.172
20	$5.56e^5$	$1.2e^{-3}$	$1.19e^3$	114	$1.6e^{-7}$	$4.63e^8$	$2.16e^{-9}$	$1.18e^3$	0.0901
40	$3.69e^5$	$1.3e^{-3}$	$1.03e^3$	259	$3.2e^{-7}$	$2.84e^8$	$3.52e^{-9}$	$1.01e^3$	0.119

Table 4: Table of kinetic values for SPR of CRP analyte binding to ligand *L.mexicana* metacyclic LPG immobilised by hydrophobic attachment (Figure 88).

k_a: Association rate constant (i.e. Rate of complex formation)
k_d: Dissociation rate constant (i.e. Fraction of complex decay)
R_{max}: Maximum observed response units
RI: RU detected at beginning of analysis
Analyte conc.: Concentration of injected analyte
K_A: Association constant
K_D: Dissociation constant
R_{eq}: Response Units at equilibrium
R_{obs}: Observed rate constant ($k_aC + k_d$)

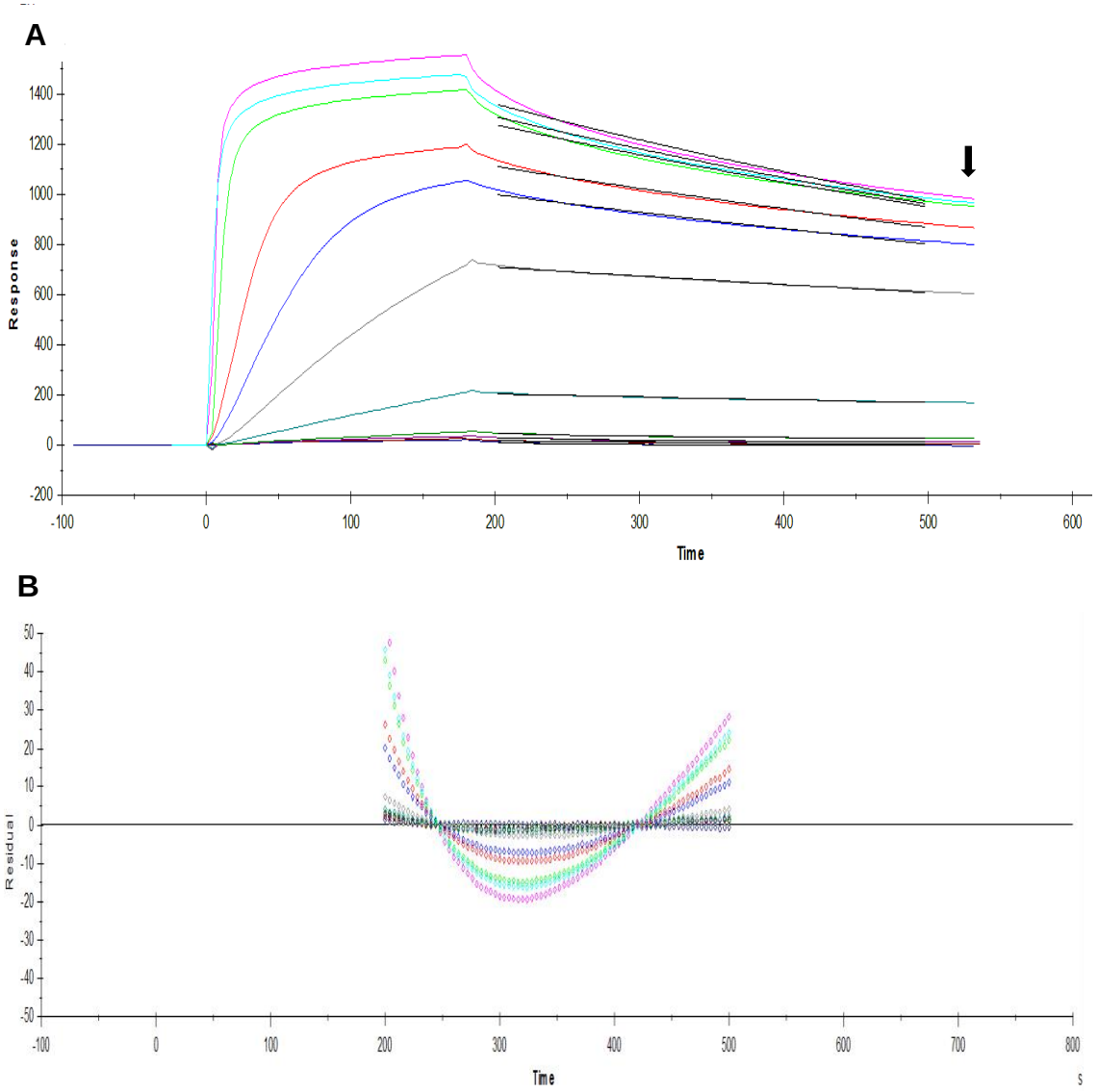

Figure 90: CRP at higher concentrations shows changes in kinetics of binding to nectomonad LPG from *L.mexicana* immobilised at high ligand density (A), with residual analysis of association (B).

Surface plasmon resonance of ligand nectomonad LPG (270 RU), immobilised by hydrophobic attachment to a Xantec HPP alkyl chip, to analyte CRP (0.02 – 40 µg/ml, 30 µl/min, 180s association, 300s dissociation) in HBSC (10 mM HEPES, 150 mM NaCl, 0.5mM $CaCl_2$, pH 7.4). The surfaces were regenerated with a 10s injection of EDTA-containing HEPES buffer (HSBPE: 10 mM HEPES, 150 mM NaCl, 10 mM EDTA, pH 7.4). Data was collected at a rate of 1 Hz. The data was fitted to a simple 1:1 interaction model using the global data analysis option available within BiaEvaluation 3.1 software.

CRP analyte concentrations per run, from highest to lowest RU recorded at timepoint indicated by the black arrow (→): 10, 40, 20, 5, 2.5, 1.25, 0.63, 0.31, 0.16, 0.08, 0.04 and 0.02 µg/ml.

Analyte conc. (µg/ml)	k_a (1/Ms)	k_d (1/s)	R_{max} (RU)	RI (RU)	Analyte conc. (M)	K_A (1/M)	K_D (M)	R_{eq} (RU)	k_{obs} (1/s)
1.25	$5.43e^4$	$5e^{-4}$	$9.02e^3$	-3.96	$1e^{-8}$	$1.09e^8$	$9.2e^{-9}$	$4.7e^3$	$1.04e^{-3}$
2.5	$5.68e^5$	$7e^{-4}$	$1.4e^3$	4.71	$2e^{-8}$	$8.11e^8$	$1.23e^{-9}$	$1.32e^3$	0.0121
5	$8.37e^5$	$8e^{-4}$	$1.16e^3$	53.5	$4e^{-8}$	$1.05e^9$	$9.55e^{-10}$	$1.13e^3$	0.0343
10	$2.02e^6$	$1e^{-3}$	$1.05e^3$	426	$8e^{-8}$	$2.02e^9$	$4.95e^{-10}$	$1.04e^3$	0.163
20	$6.97e^5$	$1e^{-3}$	$1.31e^3$	39.7	$1.6e^{-7}$	$6.97e^8$	$1.43e^{-9}$	$1.3e^3$	0.113
40	$5.07e^5$	$1e^{-3}$	725	662	$3.2e^{-7}$	$5.07e^8$	$1.97e^{-9}$	721	0.163

Table 5: Table of kinetic values for SPR of CRP analyte binding to ligand *L.mexicana* Nectomonad LPG immobilised by hydrophobic attachment (Figure 89).

k_a: Association rate constant (i.e. Rate of complex formation)
k_d: Dissociation rate constant (i.e. Fraction of complex decay)
R_{max}: Maximum observed response units
RI: RU detected at beginning of analysis
Analyte conc.: Concentration of injected analyte
K_A: Association constant
K_D: Dissociation constant
R_{eq}: Response Units at equilibrium
R_{obs}: Observed rate constant ($k_aC + k_d$)

multiple CRP binding sites on CRP with different binding affinities with an increase in percentage of CRP binding through fewer of the 5 subunits. CRP binding capacity increases with the density of the LPG ligand coupled to the surface for both promastigote stages, with increased R_{max} values observed for any given CRP analyte concentration flowed across the surface, with data comparison between runs being broadly compatible when flow rates and association/dissociation periods were constant.

Interestingly, at high ligand densities, the R_{max} and R_{eq} achieved in each run was not entirely analyte concentration-dependent, peaking at 5 µg/ml CRP for metacyclic and nectomonad LPG, with the subsequent run at 10 µg/ml CRP achieving corresponding lower values. There appears to be critical point of CRP binding on the LPG surface that appears to change the binding properties at the surface with regard to CRP binding capacity, possibly by structural disruption of the immobilised LPG.

The strongest evidence for this comes from the analysis of the k_a which increases noticeably at CRP analyte above 1.25 ug/ml, particularly for high density nectomonad LPG (Figure 90 & Table 6). Although association of CRP was proportional to concentration, the k_a between two given components should be constant if the two interacting partners remain unchanged. This was likely a reversible phenomenon as removal of CRP does not seem to affect the subsequent association run. As such, the increase in k_a suggested an alteration of LPG structure, associated with faster binding of CRP to the LPG surface. Metacyclic LPG appears to undergo a similar change at lower CRP analyte concentrations (above 0.16 µg/ml), although a repeat of this experiment suggests a similar threshold level to that observed for nectomonad LPG. The same phenomena were seen previously for CRP binding to *L.mexicana* PSG (Section 3.11.6).

Of note, this phenomenon was not observed in non-*Leishmania* CRP ligands. The k_a for CRP binding to PCBSA, amine coupled in a similar manner to PSG (Section 2.17.1.1) was fairly consistent (~1-2 $x10^6$ $M^{-1}s^{-1}$), independent of CRP analyte concentration between 0.16-20 ug/ml (Figure 91 & Table 6). In addition, previous work performed by the Raynes group (Ahmed et al., 2016) revealed a

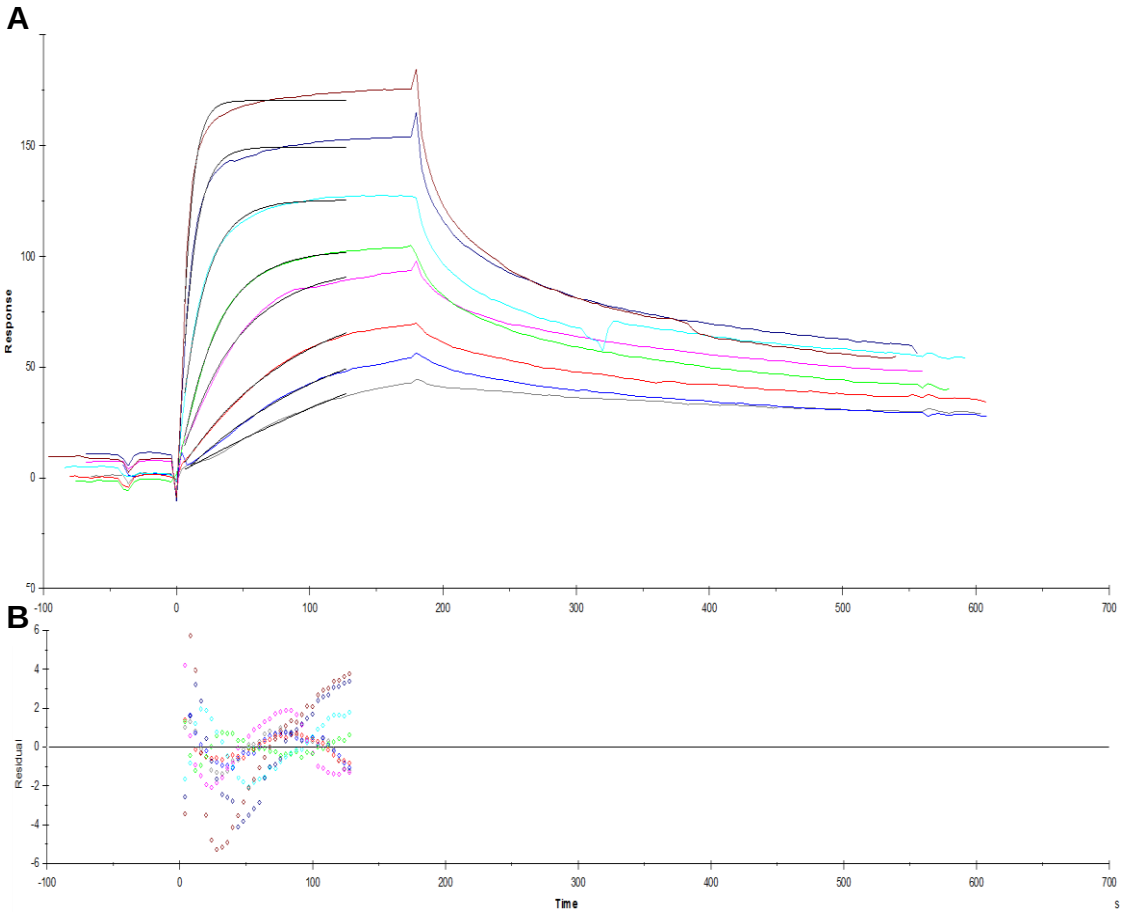

Figure 91: CRP exhibits no change in kinetics of binding to PCBSA (A), with residual analysis of association (B).

Surface plasmon resonance of ligand PCBSA (420 RU), immobilised by amine coupling (Section 2.17.1.1.) to a Biacore C1 chip, to CRP at varying analyte concentrations (0.16 - 20 µg/ml, 20 µl/min, 180s association, 420s dissociation) in Ca^{2+} containing HEPES buffer (HBSPC: 10 mM HEPES, 150 mM NaCl, 0.005% P20, 0.5mM $CaCl_2$, pH 7.4). The surfaces were regenerated with a 10s injection of EDTA-containing HEPES buffer (HSBPE: 10 mM HEPES, 150 mM NaCl, 10 mM EDTA, pH 7.4). Data was collected at a rate of 1 Hz. The data was fitted to a simple 1:1 interaction model using the global data analysis option available within BiaEvaluation 3.1 software.

Analyte conc. (µg/ml)	k_a (1/Ms)	k_d (1/s)	R_{max} (RU)	RI (RU)	Analyte conc. (M)	K_A (1/M)	K_D (M)	R_{eq} (RU)	k_{obs} (1/s)
0.16	$1.53e^5$	$2e^{-3}$	$1.72e^3$	3.14	1.25e-9	7.65e7	1.31e-8	150	2.19e-3
0.3	$1.65e^6$	$2e^{-3}$	132	4.51	$2.5e^{-9}$	$8.24e^8$	$1.21e^{-9}$	89.2	6.12e-3
0.6	$1.62e^6$	$2e^{-3}$	108	5.34	$5e^{-9}$	$8.09e^8$	$1.24e^{-9}$	86.5	0.0101
1.25	$1.65e^6$	$2e^{-3}$	105	12	$1e^{-8}$	$8.25e^8$	$1.21e^{-9}$	93.7	0.0185
2.5	$1.72e^6$	$2e^{-3}$	96.4	11.4	$2e^{-8}$	$8.58e^8$	$1.17e^{-9}$	91.1	0.0363
5	$1.46e^6$	$2e^{-3}$	101	25.2	$4e^{-8}$	$7.28e^8$	1.37e-9	97.8	0.0602
10	$1.35e^6$	$2e^{-3}$	111	36.6	$8e^{-8}$	$6.75e^8$	$1.48e^{-9}$	109	0.11
20	$1.02e^6$	$2e^{-3}$	125	41.9	$1.6e^{-7}$	$5.11e^8$	$1.96e^{-9}$	124	0.166

Table 6: Table of kinetic values for SPR of CRP analyte binding to ligand PCBSA immobilised by amine coupling (Figure 90).

k_a: Association rate constant (i.e. Rate of complex formation)
k_d: Dissociation rate constant (i.e. Fraction of complex decay)
R_{max}: Maximum observed response units
RI: RU detected at beginning of analysis
Analyte conc.: Concentration of injected analyte
K_A: Association constant
K_D: Dissociation constant
R_{eq}: Response Units at equilibrium
R_{obs}: Observed rate constant ($k_aC + k_d$)

similarly consistent, albeit slightly higher k_a (~2-4 x 10^6 $M^{-1}s^{-1}$) during SPR analysis of ES-62, another PC-containing ligand (Figure 91 and Table 7).

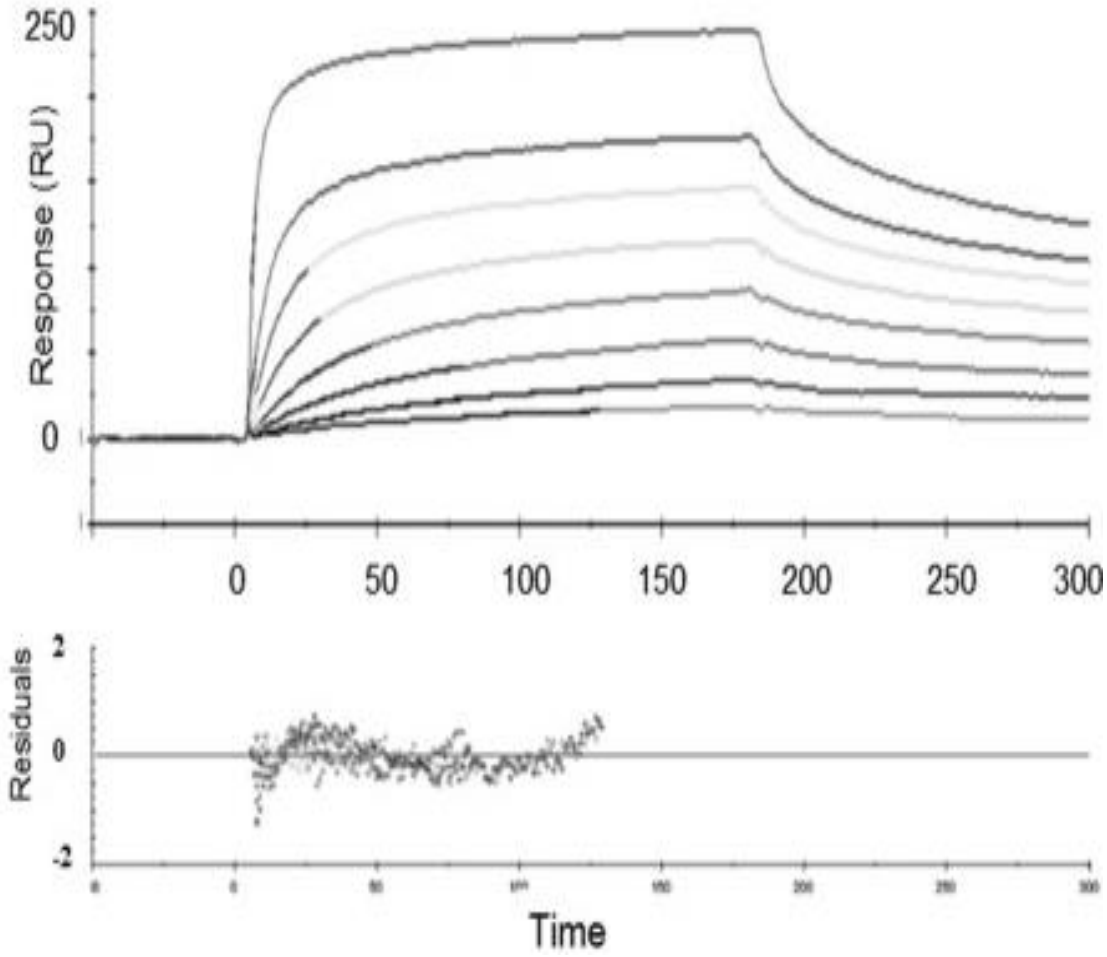

Figure 92: CRP exhibits no change in kinetics of binding to ES-62 (A), with residual analysis of association (B) (Ahmed et al., 2016).

Surface plasmon resonance of ligand ES-62 (300 RU), immobilised by amine coupling (Section 2.17.1.1.) to a Biacore CM5 chip, to CRP at varying analyte concentrations (0.02 - 10 µg/ml, 10 µl/min, 180s association, 300s dissociation) in Ca^{2+} containing HEPES buffer (HBSPC: 10 mM HEPES, 150 mM NaCl, 0.005% P20, 0.5mM $CaCl_2$, pH 7.4). The surfaces were regenerated with a 10s injection of EDTA-containing HEPES buffer (HSBPE: 10 mM HEPES, 150 mM NaCl, 10 mM EDTA, pH 7.4). Data was collected at a rate of 1 Hz. The data was fitted to a simple 1:1 interaction model using the global data analysis option available within BiaEvaluation 3.1 software.

k_a (1/Ms)	k_d (1/s)	R_{max} (RU)	RI (RU)	Analyte conc. (M)	K_A (1/M)	K_D (M)	R_{eq} (RU)	k_{obs} (1/s)
$6.29e^{6}$	$5.5e^{-4}$	19.7	2.99	$2.5e^{-9}$	$1.14e^{10}$	$8.74e^{-11}$	19	0.0163
$4.07e^{6}$	$6e^{-4}$	26.2	5.26	$5e^{-9}$	$6.79e^{9}$	$1.47e^{-10}$	25.4	0.021
$6.22e^{6}$	$8.6e^{-4}$	35.8	12.2	$1e^{-8}$	$7.23e^{9}$	$1.38e^{-10}$	35.3	0.063
$4.89e^{6}$	$1e^{-3}$	49.8	9.15	$2e^{-8}$	$4.89e^{9}$	$2.05e^{-10}$	49.3	0.0988
$2.5e^{6}$	$1.1e^{-3}$	53.4	15.4	$4e^{-8}$	$2.28e^{9}$	$4.39e^{-10}$	52.8	0.101
$2.96e^{6}$	$1.3e^{-3}$	61.4	24.7	$8e^{-8}$	$2.28e^{9}$	$4.39e^{-10}$	61.1	0.238
$2.21e^{6}$	$1.4e^{-3}$	86.9	11.2	$1.6e^{-7}$	$1.58e^{9}$	$6.34e^{-10}$	86.5	0.355
$1.56e^{6}$	$1.5e^{-3}$	112	8.23	$3e^{-7}$	$1.04e^{9}$	$9.63e^{-10}$	111	0.469
$8.72e^{5}$	$1.5e^{-3}$	108	30.5	$6e^{-7}$	$5.81e^{8}$	$1.72e^{-9}$	108	0.525

Table 7: Table of kinetic values for SPR of CRP analyte binding to ligand ES-62 (Ahmed et al., 2016).

k_a: Association rate constant (i.e. Rate of complex formation)
k_d: Dissociation rate constant (i.e. Fraction of complex decay)
R_{max}: Maximum observed response units
RI: RU detected at beginning of analysis
Analyte conc.: Concentration of injected analyte
K_A: Association constant
K_D: Dissociation constant
R_{eq}: Response Units at equilibrium
R_{obs}: Observed rate constant ($k_aC + k_d$)

3.12.3: CRP analyte association with *L.mexicana* metacyclic LPG ligand is not influenced by mass transport effect

Anomalous binding kinetic data could be derived if the rate of delivery of the analyte out of the bulk flow to the surface by convection and diffusion (i.e. mass transfer) was slower than the rate of analyte-ligand binding, due to the limitation of analyte availability to the surface influencing the probability of association and subsequent dissociation events occurring.

In order to ascertain if mass transport effect was present, *L.mexicana* LPG ligand from metacyclic stage parasites was immobilised to a Xantec HPP chip at high ligand density as previously described (section 3.12.2). CRP analyte (1µg/ml, 180s association, 300s dissociation) was then flowed over the surface at various rates (15, 30 and 60 µl/min) (Figure 92).

The relative constancy of the rate of association (k_a) would suggest that mass transfer effect was not a significant factor at the flow rate (30ul/min) used in prior LPG-CRP experiments, suggesting that previously obtained data accurately reflected the binding kinetics of the interaction. Similar data was obtained for nectomonad LPG (Figure 93).

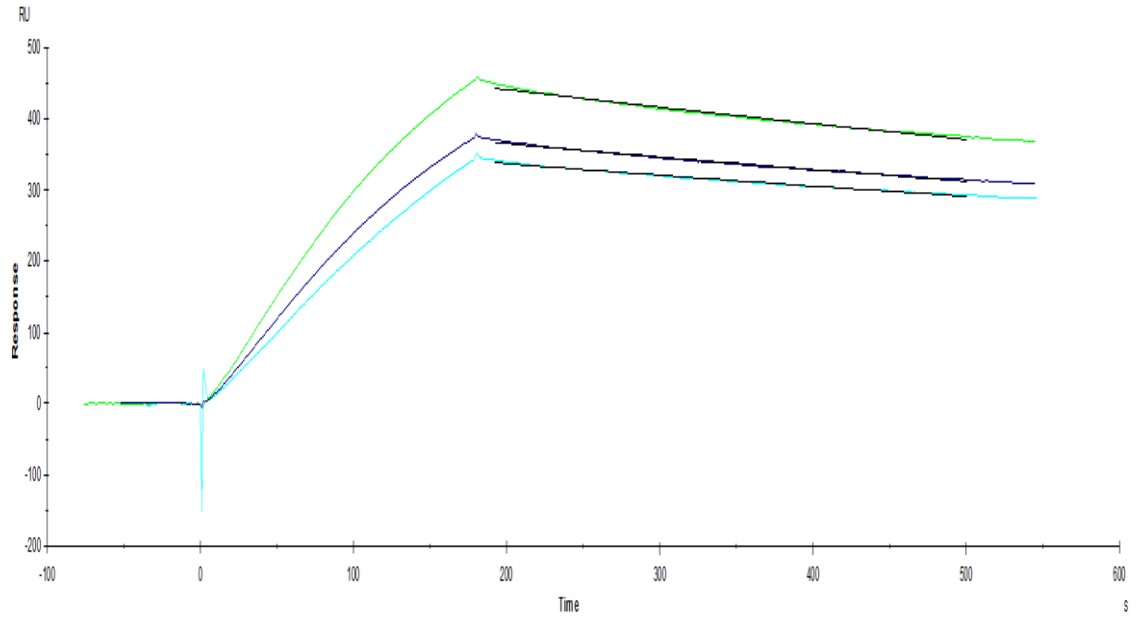

Figure 93: CRP analyte association rate to *L.mexicana* metacyclic LPG ligand was not mass transfer dependent.

Surface plasmon resonance of ligand metacyclic LPG (290 RU), immobilised by hydrophobic attachment to a Xantec HPP alkyl chip. To collect kinetic binding data, the analyte CRP in HBSC was injected over the two flow cells (1 µg/ml) at various flow rates (15, 30 and 60 µl/min) at a temperature of 25°C. The complex was allowed to associate for 180s and dissociate 300s. The surfaces were regenerated with a 10s injection of EDTA-containing HEPES buffer (HSBPE: 10 mM HEPES, 150 mM NaCl, 0.005% P20, 0.5mM EDTA pH 7.4). Data was collected at a rate of 1 Hz. The data was fitted to a simple 1:1 interaction model using the global data analysis option available within BiaEvaluation 3.1 software.

Flow rate**:** Dark blue: 60 µl/min, Green: 30 µl/min, Light blue: 15 µl/min

Calculated k_d values:
15 µl/min: 5.14 x10^{-4} s^{-1}
30 µl/min: 4.83 x10^{-4} s^{-1}
60 µl/min: 5.65 x10^{-4} s^{-1}

Average k_d: 5.21 x10^{-4} s^{-1} 0.33 x10^{-4} s^{-1}

Calculated k_a values:
15 µl/min: 3.58 x10^{-5} s^{-1}
30 µl/min: 6.74 x10^{-5} s^{-1}
60 µl/min: 5.63 x10^{-5} s^{-1}

Average k_a: 5.32 x10^{-5} s^{-1}
Standard deviation: 1.30x10^{-5} s^{-1}

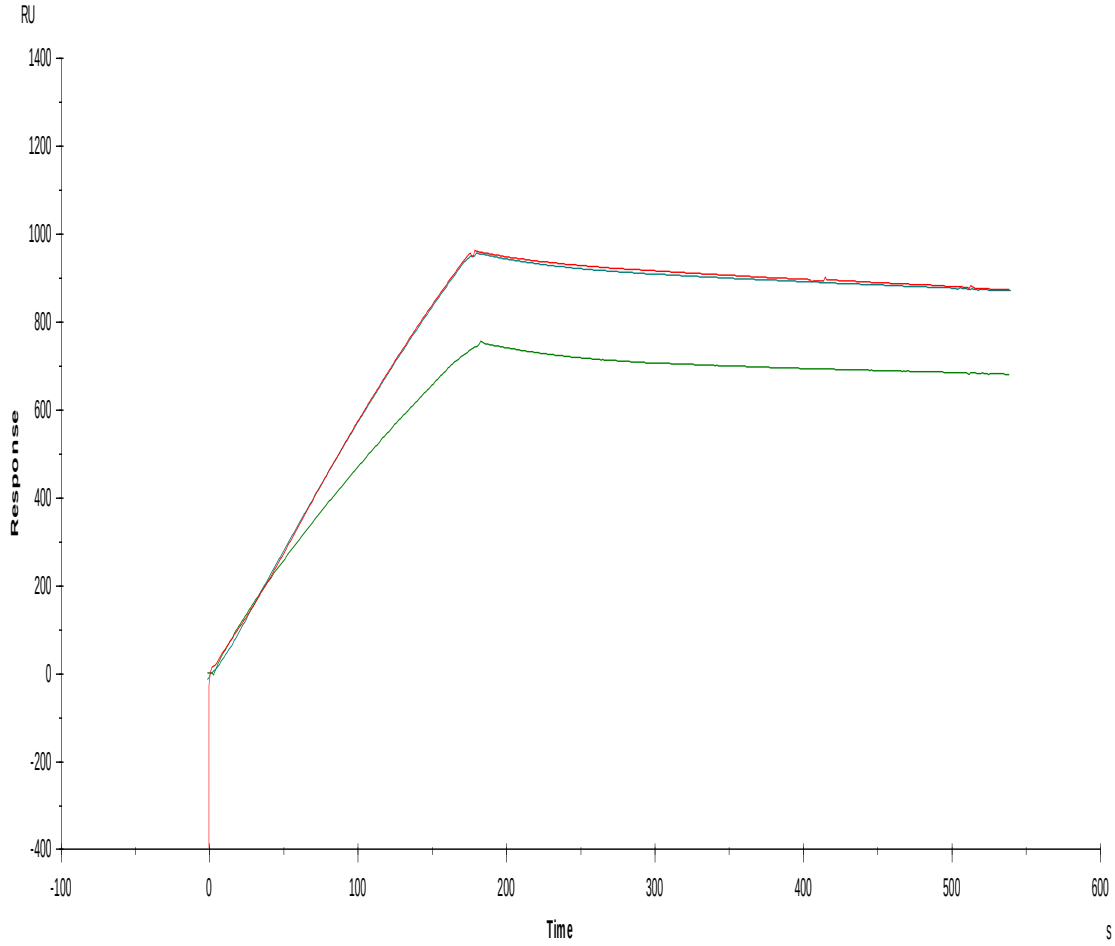

Figure 94: CRP analyte association rate to *L.mexicana* nectomonad LPG ligand is not mass transfer dependent.

Surface plasmon resonance of ligand nectomonad LPG (290 RU), immobilised by hydrophobic attachment to a Xantec HPP alkyl chip. To collect kinetic binding data, the analyte CRP in HBSC was injected over the two flow cells (1 µg/ml) at various flow rates (15, 30 and 60 µl/min) at a temperature of 25°C. The complex was allowed to associate for 180s and dissociate 300s. The surfaces were regenerated with a 10s injection of EDTA-containing HEPES buffer (HSBPE: 10 mM HEPES, 150 mM NaCl, 0.005% P20, 0.5mM EDTA pH 7.4). Data was collected at a rate of 1 Hz. The data was fitted to a simple 1:1 interaction model using the global data analysis option available within BiaEvaluation 3.1 software.

Flow rate**:** Red: 60 µl/min, Blue: 30 µl/min, Green: 15 µl/min

Chapter 4
Discussion

4.1: Preface

This project aimed to investigate the ability of *Leishmania*-derived glycosylated products ability to modulate the local innate immune environment in order to encourage infection of mammalian host. It was postulated that these potential virulence factors could interact with the classical pentraxins and/or other innate immune factors, triggering associated downstream effects, such as opsonisation, stimulation of host immune cell recruitment and manipulation of the complement pathway. We believed that our findings could contribute to the optimisation of vaccines and therapeutics against leishmaniasis, in addition to being potentially relevant to the discovery of novel immunomodulator candidates for treatment of assorted autoimmune conditions.

4.2: Pentraxin purification and modification

4.2.1: Pentraxin purification

Pentraxins were purified from acute-phase human plasma through calcium-dependent affinity chromatography, as described in existing protocols (Volanakis, 2001). Material was then validated with western blot and Coomassie protein gel staining following each purification, with most pentraxin purification attempts producing a pure product, as indicated by a single band of the appropriate molecular weight. However, an isolated CRP purification attempt noted two distinct bands following SDS-PAGE and Coomassie Blue gel staining,

This phenomenon could also be indicative of *in vivo* modifications of CRP, which has been reported under certain conditions. Given that CRP was purified was human plasma obtained from individuals with inflammatory conditions due

to the dramatic upregulation of CRP in the acute phase, it was plausible that the generation of a glycosylated isoform of CRP may have occurred during synthesis in hepatocytes (Das et al., 2003), although it should be noted that such occurrences were uncommon.

Following this, commercially available CRP was used for all experiments. This was done for practical purposes, being of reasonable cost, high purity and circumventing the need for patient ethical approval for plasma that would otherwise be disposed of as clinical waste.

In order to confirm the data of binding studies was not due to denaturation or contamination from the purification process many of the experiments were also repeated with a recombinant CRP generated in *Pichia pestis*, which was not contaminated with SAP or other proteins. However, it should be noted that rCRP potentially contaminated with yeast derived contaminants, although this was unlikely to affect the binding character of CRP, as determined in multiple instances where native and recombinant CRP display similar binding characteristics in the course of this study.

4.2.2: Biotinylation of SAP

The methodology for labelling of SAP (Section 2.8.2.2) with biotin was developed by John Raynes (Department of Infection Biology, Faculty of Infectious and Tropical Diseases, London School of Hygiene and Tropical Medicine, UK), in order to observe SAP binding without the use of antibodies, reducing the probability of nonspecific interactions during the detection steps, which had been an ongoing issue with early ELISA and ligand blot experiments using unlabelled SAP.

The first attempt at biotinylation of SAP at low pH (sodium acetate buffer, 0.1M, pH 5.5) with the aim to generate reactive aldehyde groups by oxidising the glycosylated domains of SAP with sodium-meta-periodate (20mM) for later addition of an NHS-ester activated biotinylation reagent conjugated to a long chain spacer (EZ-Link™ NHS-LC-Biotin, Thermo Fisher Scientific) was unsuccessful. This was likely due to the denaturation of the protein under acidic

conditions, with loss of PE ligand binding capacity evident from the lack of SAP captured during affinity chromatography on PE-conjugated Sepharose.

Taking the acid-labile nature of SAP into consideration, a second attempt at biotinylation at near-neutral pH was performed in a similar manner to that used successfully for CRP (Section 2.8.2.1) in Tris-buffered Saline (10mM Tris-HCl, 0.15M NaCl, pH 8.0), due to previous observations in the Raynes Group of SAP being prone to aggregation in other buffer types. This too did not produce observable SAP-biotin, again evidenced by the lack of capture by the PE affinity chromatography column described previously. This was likely due to the excessive labelling of biotin moieties on the PE ligand binding site, leading to a loss of function in the biotinylated SAP molecule. Of note, the SAP ligand binding site contains a lysine residue (K79) that was not present in CRP (Mikolajek et al., 2011), which may be targeted by the succinimide based amine coupling method thereby preventing labelled SAP binding to PE (Figure 94). CRP on the other hand retained binding activity using this method.

The eventual method used to successfully generate biotinylated SAP used aldehyde coupling of the biotin-spacer conjugate following oxidation of the carbohydrate region of SAP with sodium metaperiodate, similar to the first attempt, but at near-neutral pH (7.6), which allowed for biotinylation of glycosylated regions independent of the binding site, and without SAP denaturation associated with acidic conditions. It was interesting to note however that even this method only generated a low recovery (results not shown) following affinity chromatography repurification of the labelled material, suggesting that even with the additional consideration of biotinylation sites, a significant amount of SAP-biotin appears to lose its binding specificity during the labelling process.

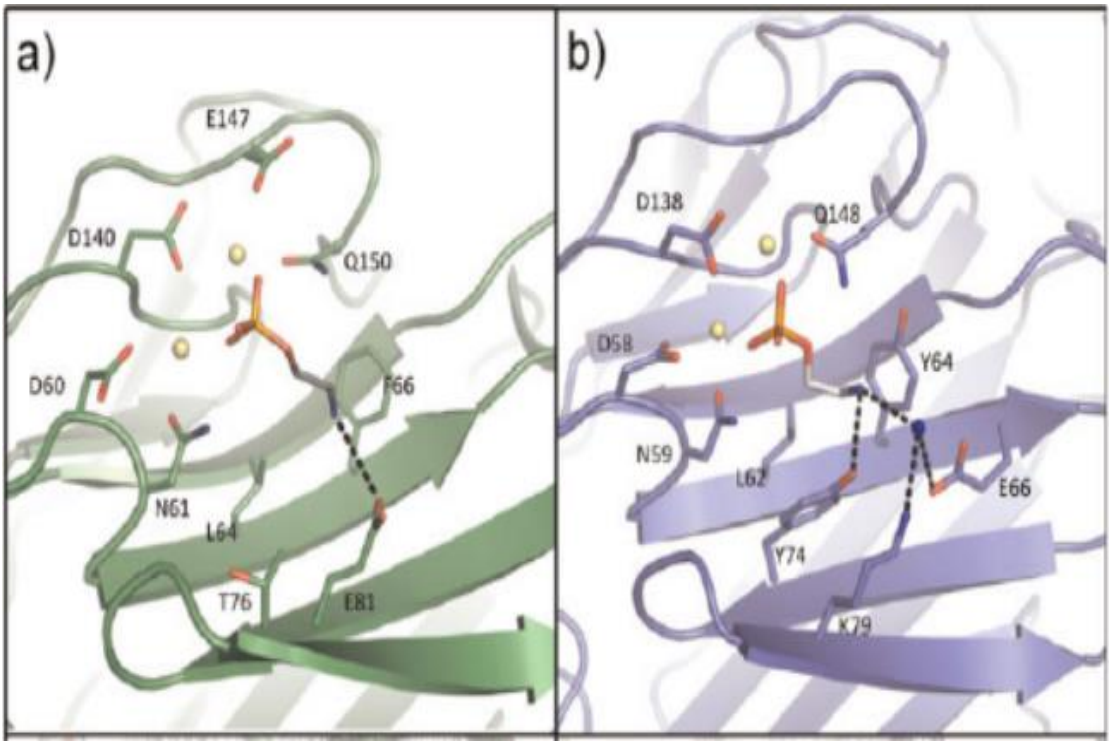

Figure 95: Ligand binding site structure for CRP (A) and SAP (B) (Mikolajek et al., 2011)

Protein structure visualisation was generated with pyMOL software (DeLano Scientific LLC). Ca^{2+} binding required for ligand binding were represented by yellow spheres, while H_2O was represented by blue spheres.

4.2.3: Conclusions

Protocols for the purification of the classical pentraxins CRP and SAP from human plasma or serum using affinity chromatography on solid-phase PC or PE-conjugated columns were well established. However, determination of the potential contaminant by Coomassie Blue protein gel staining and Western blotting techniques following SDS-PAGE of product for estimation of molecular weight should still be performed per purification batch, due to the potential for *in vivo* modifications of CRP, such as glycosylation, which has been reported in certain inflammatory conditions.

The successful biotinylation of CRP and SAP, while retaining their native binding characteristics, is of value to the study of these innate immune proteins. In addition, our attempts at biotinylation of the pentraxins highlighted the importance in the consideration of the protein in question prior to choosing a labelling strategy. The chemical modification of moieties involved in ligand binding may lead to loss of function, while denaturation of the protein, such as might occur with exposure to acidic conditions, might lead to the loss of the 3D structures required for complex interaction and ligation.

4.3: Composition of PSG

4.3.1: PSG derived from promastigote culture supernatant

PSG *in vivo* forms a 3-dimensional gel matrix within the infected sandfly digestive tract, extending from the tegmental midgut to the stomodeal valve. PSG has been suggested to have a number of functions that encourage *Leishmania* transmission, including being key to the 'blocked fly' hypothesis, as well as being a virulence factor which was previously demonstrated to promote mammalian infection, being transmitted alongside metacyclic promastigotes and sandfly saliva into the feeding site. However, the interactions of PSG with the innate immune system, particularly its acellular components, was not well understood, a clearer understanding of which could have implications in the development of vaccines and therapeutics against leishmaniasis.

The use of PSG derived from parasites grown in culture supernatant as an alternative to extraction from infected sandflies has been well-established in previous studies. This was in large part a response to a practical issue, with the extraction of *in vivo* generated, native PSG being a laborious process. In addition, material extracted from the sandfly gut would likely contain sandfly-derived contaminants, with removal via purification processes, such as the ones described in this study, being impractical due to the typically small volumes of PSG that were capable of being extracted via dissection of infected sandflies.

4.3.2: Corroboration of PSG purified in-house with previous work

Early reports of *L.mexicana* PSG purification exhibited material trapped in an extended stacking gel layer (approximately 20mm, 4%) when subjected to discontinuous SDS-PAGE. In these studies, ligand blots were performed, with a gradient resolving gel (7.5%-20%), compared with the resolving gel layer of constant concentration (6%) used for our study. However, estimation of molecular weight as indicated by molecular weight markers appears broadly

consistent with previous reports of PSG purification (>100 kDa) (Ilg et al., 1996). Previous SDS-PAGE and ligand blot experiments on *L.donovani* culture supernatant (Culley et al., 1996), which would predominantly contain PSG components, reveals a similar smear pattern to that which we observed with purified PSG for both LT6 and CRP probing for *L donovani* and *L.mexicana*.

The decision to use an alternative polyacrylamide gel format was undertaken early on in the study. Reproducibility of gradient gels by hand-casting methods was difficult to achieve, with variability in polyacrylamide density in the resolving layer between different gels making comparison of subsequent Coomassie gel staining and ligand blotting untenable. In addition, commercially available precast gradient gels do not feature a stacking gel layer, making them unsuitable from the discontinuous SDS-PAGE model required for fPPG visualisation. We determined that a discontinuous SDS-PAGE system with a low percentage resolving polyacrylamide gel layer would allow for optimal visualisation of PSG components, allowing sufficient travel of the larger products for molecular weight estimation, while allowing for comparison between ligand blots due to the consistency of the gel composition.

Previous studies have indicated that PSG was composed primarily of fPPG, although ScAP was also part of the secretory products of promastigote stage parasites and may be present. The broad smear patterns in the lower molecular weight stacking gel layer observed in LT6 ligand blotting of *L.mexicana* WT PSG indicates that PSG in multiple species was a composite and heterogeneous in nature, possibly suggesting that ScAP, or perhaps other as yet defined phosphoglycans, were present in PSG at more significant levels than previous literature would suggest (T Ilg, 1991). It should be noted that ligand blot detection was semi-quantitative, and further investigation would be required to determine the relative level of expression of the disparate PSG components in promastigote culture supernatant and *in vivo*.

4.3.3: Individual characterisation of PSG components

Previous studies have described the partial purification of ScAP by isolation of fractions that display acid phosphatase activity following anion exchange chromatography of *Leishmania* culture supernatant (Ilg et al., 1991b). The

similarity in chemical and ligand composition, as well as the unusually large size of both molecules, has made further separation of fPPG and ScAP difficult, both in terms of purification of individual PSG components (e.g. affinity chromatography) and visualisation following separation under dissociating conditions (e.g. SDS-PAGE).

4.3.4: Conclusions

While it had been previously reported PSG was primarily composed of fPPG, the *Leishmania* secretory glycome is complex and diverse, with ScAP being expressed by all *Leishmania* promastigotes with the notable exception of *L.major*. Positive identification of individual PSG components by molecular weight estimation was hampered by its highly glycosylated nature causing the generation of a smear pattern during SDS-PAGE. In addition, the similar moieties present in ScAP and fPPG makes antibody-based affinity techniques difficult for identification and purification of the individual PSG components. The generation of monoclonal antibodies specific to the protein components of ScAP and/or fPPG would greatly aid future research, but would require the significant investment in time and funds. In addition, the carbohydrate moieties in PSG and ScAP may sterically hinder antibody binding to the obscured amino acid chains.

Despite the limitations of methodology above *L.mexicana* mutants partially or completely deficient in ScAP production allowed characterisation of the importance of ScAP to binding data or PSG, bypassing the need to separate the compositionally similar *Leishmania* PPGs (Ilg, 2000b). In addition, material purified from culture supernatants of *L.mexicana* mutants deficient in LPG ($LPG1^{-/-}$) or entirely deficient in PG synthesis ($LPG2^{-/-}$) showed that interaction observed isn't an artefact of LPG contamination and was dependent on the presence of PGs present, respectively.

4.4: PSG Binding to pentraxins

4.4.1: Binding affinity and capacity of PSG to pentraxins

Using an ELISA format, we determined that PSG from different *Leishmania* species have varying capacity for CRP and SAP binding, with the lack of correspondence between the CRP and SAP data suggesting that the two pentraxins were specific for different epitopes on PSG components or associated molecules. The methods used to purify were non-dissociating, and as such it was possible that other components may be part of the high molecular complex. This was further indicated by SAP and CRP binding to components of different molecular weight on Western blot NIR images. Using ligand blotting techniques and ELISA format PSG-CRP inhibition assays, we demonstrated that the CRP-PSG binding was a calcium-dependent interaction that involves the same binding site as it does for PC. Using ligand blotting techniques, we determined that PSG from different species have varying compositions of phosphoglycans, and was not solely fPPG, which was identifiable by its higher molecular weight trapping it in the stacking gel layer (Ilg et al., 1996). This was expected from the proposed structure of fPPG, being an extremely large molecule, preventing travel of the molecule into the higher percentage resolving gel layer with its reduced pore size.

Binding of CRP to the phosphoglycans in PSG were analysed by SPR in a number of orientations. All these orientations show similarly slow dissociation rates for PSG binding to CRP and a strong binding with dissociation constants of approximately 1 $x10^{-10}$ Ms^{-1}. Interestingly, SPR experiments appear to show a higher rate of PSG analyte association with reduction of flow rate, suggesting that fluid-phase PSG binding to the solid-phase CRP-biotin and subsequent detection was dependent on multiple CRP-PSG interactions.

The generation of a similar series of mutants for other *Leishmania* species would allow experiments to determine whether any observations made are species-specific.

4.4.2: LPG was not a major CRP binding component in PSG

While a membrane-associated product, LPG has been observed to be shed into surrounding environment in *L.donovani* (Kaneshiro and Wyder, 1993). In addition, previous studies have shown CRP binding to *L.mexicana* LPG. Positive identification of possible LPG contaminants by sequential SDS-PAGE and ligand blotting are complicated by the similarity in phosphorylated carbohydrate moieties shared between *Leishmania* glycosylated products. While monoclonal antibodies specific to the disparate glycan structures in *Leishmania* PG products have been described in previous studies, these were not available. In addition, LPG experiences aberrant mobility during SDS-PAGE, due to being entirely bereft of amino acid residues and having potential for hydrophobic association with other molecules, and when pure generating a smear pattern that makes molecular weight estimation subjective. In order to ascertain that any binding events were not an artefact of LPG contamination, PSG purified from *L.mexicana* mutant deficient in LPG expression ($LPG1^{-/-}$) was subjected to ELISA-format pentraxin binding assays alongside PSG derived from WT and entirely PG-deficient ($LPG2^{-/-}$) *L.mexicana*, which indicated no significant difference in CRP binding capacity between $LPG1^{-/-}$ PSG, and a complete ablation of binding observed in $LPG2^{-/-}$ PSG, suggesting that the purified WT PSG contains at best negligible levels of LPG contamination, and that the PPGs, fPPG and ScAP, are responsible for CRP binding (Figure 38). Ligand blots of WT and $LPG1^{-/-}$ PSG with CRP, however, seem to indicate a loss of low molecular weight components capable of binding CRP with $LPG1^{-/-}$ PSG (Figure 39).

4.4.3: Individual pentraxin binding characteristics of the PSG components fPPG and ScAP

Investigation of pentraxin binding to PSG derived from WT, ScAPKO and ScAPAB *L.mexicana* parasite cultures suggests that ScAP accounts for the majority of CRP-binding capacity in PSG, reflected in both ELISA (Figure 41) and SPR (Figure 73) experimental methods. CRP binding capacity appears to

be higher in ScAPKO and ScAPAB PSG compared to WT, positively correlating with the proportion of fPPG present. Ligand blots of CRP binding to PSG from multiple *leishmania* species seems to indicate that in addition to fPPG, which previous literature would suggest remains trapped in the stacking layer (Ilg et al., 1996), CRP also binds to ScAP, other undefined PPGs present in the *Leishmania* promastigote secretome, or denaturation products of fPPG (Figure 35-36).

ELISA experiments appeared to suggest that SAP capacity in ScAPKO and ScAPAB PSG appears to be higher than that of WT (ScAPKO > ScAPAB> WT) in *L.mexicana* strains (Figure 56). Given the higher proportion of fPPG in the PSG of mutants partially or completely deficient in ScAP expression, this would seemingly suggest that fPPG possessed greater SAP binding capacity per weight relative to ScAP. However, ligand blots of PSG from multiple *Leishmania* species demonstrates that binding of SAP was to lower molecular weight components found in PSG rather that fPPG, which would likely be trapped in stacking gel layer. The amount of SAP binding observed was very low as indicated by the requirement for very sensitive fluorescent detection and lack of observed binding in some other binding methodologies, and as such further investigation would be required to determine the veracity of this observation. Unfortunately, due to time constraints and the prioritisation of other lines of inquiry, *L.panamensis* and *L.aethiopica* PSG, which in plate assays appear to show saturable binding of SAP even at low SAP concentrations (Figure 53), was not subjected to SDS-PAGE. These two particular *Leishmania* species appear to express an abundance of a ligand that was not seen in the other *Leishmania* species. Further work on identification of the SAP-binding ligand might focus on these parasites. While the most likely SAP ligand candidate present in PSG was PE, which has been found expressed in other parasitic products, SAP binding has also been reported with various phosphorylated and sulphated carbohydrate ligands. (Loveless et al., 1992)

Adding to the difficulty of positive identification of individual PSG components, the relatively low protein content of the *Leishmania* PPGs generates the diffuse band pattern we observed following ligand blots of material subjected to SDS-PAGE, rather than tight bands typical to proteins processed in a similar manner for molecular weight indication.

4.5: PSG-driven complement activation

4.5.1: Classical Pathway activation by CRP-PSG complex

An ELISA of C1q capture, in which the ability of a ligand added in solution to form a complex with CRP that was capable of binding to purified C1q immobilised to the plate surface, was performed in order to ascertain the ability of the ligand to fulfil the prerequisite of CRP-driven CP activation after binding in the 'recognition' face. The recognition face binding induces conformational change in CRP 'effector' face that allows C1q binding and activation.

Results indicate that CRP in complex with PSG ligand from multiple *Leishmania* species was capable of binding C1q (Figure 43-44). This was inhibited by the presence of the PC chloride-calcium salt, suggesting that secondary structures in PC ligands may play a role in the efficiency of induction of the conformational change in the CRP 'effector' face required for C1q binding (Figure 45). Of note, there was a lack of correlation between the ranking order of CRP binding capacity observed between different *Leishmania* species (Figure 34) and the level of C1q binding observed (Figure 43), possibly due to differences in the size of PSG from different species, as well as the innate heterogeneity of PSG itself.

Comparisons of ligand blots probing with either CRP or LT6 (antibody specific for *Leishmania* carbohydrate repeats) WT and LPG1$^-$ *L.mexicana* PSG confirms that the above interactions are not dependent on the presence of LPG, supporting current reports that LPG was not a component of PSG(Rogers et al., 2004). ELISA testing indicates that PSG activates the classical complement pathway with minor alternative pathway activation, as evidenced by the generation of the C3 convertase product C3b.

4.5.2: Lectin pathway activation via MBL-binding

PSG, similar to other *Leishmania* glycosylated products, was a carbohydrate-rich molecule, and as such may be subject to binding by lectins. LPG, which

has similar carbohydrate moieties to PSG, has been reported to have affinity to lectins expressed within the sandfly gut (Soares et al., 2002), mediating parasite attachment to the digestive tract wall and promoting parasite survival by preventing excretion with the bloodmeal.

Using ELISA analysis, we determined that PSG from different *Leishmania* species have varying binding capacities for the lectin MBL (Figure 51). Further investigation seemed to indicate an element of calcium-independent binding to *L.aethiopica* PSG that was not observed in the positive control ligand, mannan, which experienced complete ablation of binding with the same level of EDTA introduced (Figure 52). Of note, MBL binding to amyloid-β in a manner inhibitable by negatively charged polysaccharides, but not entirely inhibitable by EDTA, had been observed, suggesting binding via MBL's calcium-dependent carbohydrate recognition domain (CRD) as well as the cysteine-rich domain in a calcium-independent manner (Larvie et al., 2012). It was possible that a similar interaction occurs between MBL and PSG.

As MBL is an initiator molecule for LP activation, we attempted to determine the extent to which the LP contributes to PSG-mediated complement activation by selective inhibition using sodium polyanethole sulphonate (SPS) in a manner indicated by a previous study (Palarasah et al., 2011). In short, SPS was a polyanionic compound that was reported to inhibit the AP and CP while leaving the LP intact, following preincubation of serum with 0.5 mg/ml SPS during ELISA experiments measuring the generation of complement components. However, our own attempts at this was unsuccessful, as determined by the failure of SPS inhibition by mannan-driven complement activation (results not shown). It should be noted that SPS was a polymer compound that was subject to batch variability, and as such the reported inhibitory concentration may also be variable.

4.5.3: *Leishmania* survival and complement

In a previous study, ES-62 bound C1q, but failed to generate C3 convertase(Ahmed et al., 2016). Previous data suggests that this due to the flexible attachment of the PC substitution to a flexible N-glycan chain. The lack of spatial rigidity likely leads to inefficient C4b and C2b deposition on ES-62,

with reduced proximity of the C3 convertase components leading to reduced formation and inactivation of the classical complement pathway. Given that filarial nematodes are extracellular in the mammalian host and are constantly exposed to innate immune mediators, the depletion of complement pathway mediators would likely promote survival.

We demonstrated that promastigote secretory products, unlike ES-62, activated the classical complement pathway thereby refuting our original hypothesis. However, given that promastigotes are a transitionary stage for the parasite in the mammalian host(Bates, 2007, Gupta et al., 2013, Ilg, 2000a), in direct opposition to the persistent nature of filarial nematodes, there are other ways in which this could be beneficial to *Leishmania* infection.

When evaluating the respective merits of parasite ligands in modulating the innate immune environment, it is worth considering the survival strategy employed by the parasite responsible for its production.

Complement pathway activation broadly leads to three consequences: The generation of anaphylatoxins C3a, C4a and C5a; opsonisation by C3b; and direct lysis by membrane attack complex (MAC) formation with C5b, C6, C7, C8, C9. Other studies have observed, however, that activation of the CP by CRP was inefficient in the generation of MAC, an antimicrobial action which could be deleterious to the parasite. Anaphylatoxin release, on the other hand, could be beneficial to early stages of mammalian infection by signalling the migration of immune cells to the sandfly feeding site, with opsonisation by C3b enhancing uptake of promastigotes by macrophages, either directly or via intermediary apoptotic neutrophils. A key determinant to the outcome of promastigotes within the phagosome compartment would be the activation state of the macrophage in question, with some studies indicating that PSG may promote intracellular *Leishmania* survival by selective promotion (Figure 95).

Data from our study suggests that PSG was heterogenous in nature, indicated by binding of innate immune mediators (i.e. CRP and SAP) to material of various molecular weights in ligand blot experiments, rather than any single purified component, such as fPPG, as evidenced by the presence of CRP and SAP binding to components of molecular weight too low to be attributable to

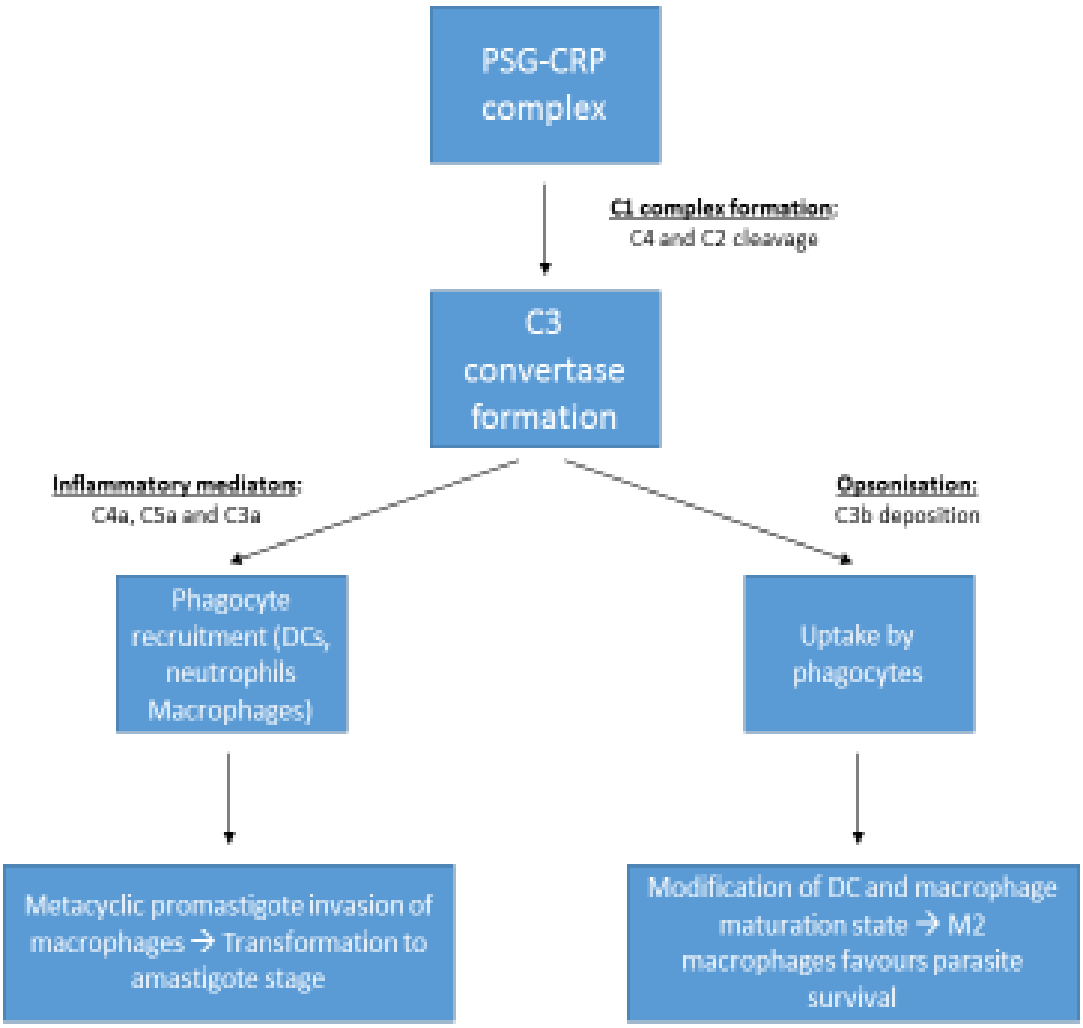

Figure 96: Model of proposed PSG innate immune manipulation and how it may promote *Leishmania* survival and persistence

As PSG was a secreted molecule with no associated membrane, the generation of Membrane complex seems unlikely to be relevant to PSG action on the classical complement pathway

fPPG alone. Other *Leishmania* promastigote secretory products, including ScAP, share a similar PG structure to LPG and fPPG, as evidenced by the cross reactivity of antibodies specific to the abundant carbohydrate moieties. ScAP has been shown to be present in the vector midgut and foregut, suggesting expression by promastigote stage parasites, with high concentrations of ScAP being detected in the flagellar pocket of late stage promastigotes(Ilg et al., 1996, Stierhof et al., 1999).

Given the structural glycosylation similarities between ScAP and fPPG, as well as their co-concurrence in promastigote secretory gel, it was possible that they perform a similar function with respect to innate immune manipulation. Further study will be required to clarify the role of ScAP in immune modulation. Given the low protein content of promastigote PPGs it seems unlikely that the protein backbone of either ScAP or fPPG have a major immunological role, aside from mediating presentation of the glycosylated moieties. In addition, given the carbohydrate repeating chains obscuring them it seems unlikely that any interactions can occur in any reasonable conceived scenario between the protein backbone and innate immune molecules. However, deglycosylation of PPG using the mild acid hydrolysis method described in previous studies may provide a useful alternative to molecular weight markers on Western blots for the differentiation of fPPG from ScAP (Rogers et al., 2004, Rogers et al., 2009).

4.5.4: ScAP and intracellular nutrition

Other intracellular pathogens, such as *Plasmodium falciparum* (Muller et al., 2010) and *Mycobacterium tuberculosis* (Saleh and Belisle, 2000), secrete ScAP within the macrophage in order to obtain nutrients from the host cell, promoting their own survival and persistence. *M.tuberculosis* and *P.falciparum* ScAP appears to have similar functionality to *Leishmania* ScAP, with a broad substrate specificity and activity at acidic conditions, but notably does not share the highly glycosylated composition that *Leishmania* ScAP. However, structural differences would be secondary in determining similarities in function in comparison to evidence of ScAP within the intracellular environment, either by phagocytosis or intracellular expression, as well as intracellular enzymatic activity.

4.5.5: Conclusions

Complement is a key aspect of the early innate immune response, and must be taken into consideration when assessing the survival mechanisms and strategies of any pathogen. We have demonstrated that PSG has the ability to activate the CP when bound with CRP as determined by the generation of C3 convertase products, with a minor contribution made by the AP. The involvement of CRP at the relatively low concentration used for *in vitro* experiments was significant, as it demonstrates that the effect was present at normal, physiological concentrations, and would not be reliant on upregulation by inflammation. In addition, CRP is an innate immune protein and therefore its expressionis independent to potential previous exposure to *Leishmania* antigens, making the scenario conceivable in both naïve and previously infected individuals.

Being a highly glycosylated product, LP-driven complement activation by PSG cannot be ruled out, and indeed we demonstrated binding capacity for PSG to one of one of the LP's' initiator molecules, MBL. Our attempts to selectively inhibit the LP during complement activation experiments were unfortunately unsuccessful. Further investigation would have to be made to determine what role the LP plays in early PSG-driven complement activation.

4.6: Characterisation of pentraxin binding to *L.mexicana* LPG

4.6.1: CRP binding to LPG

The first report of binding to a *Leishmania* factor was by Emanuela Handman, who demonstrated parasite release of a secretory factor that interacted with macrophages. (Handman et al., 1987). subsequently CRP binding to *Leishmania* parasites was observed in multiple *Leishmania* species (Raynes et al., 1994). Further investigation by the Raynes Group determined that CRP bound to LPG, which forms a glycocalyx surrounding the parasite. Stage specificity of CRP binding to LPG was demonstrated in *L. donovani.* CRP binding also appeared to be species specific, with CRP binding with greater avidity *to L.donovani* compared to *L.major* (Culley et al., 1996). It was proposed that the interaction in *L.major* was inhibited by the extensive side chain substitution.

Using ELISA, we determined that stage specific variations in LPG were also present in *L.mexicana*. with LPG derived from infective, metacyclic stage promastigotes possessing a higher binding capacity for CRP in comparison to LPG derived from non-infective, nectomonad stage promastigotes. Using an inhibition ELISA model, we determined that CRP binding to LPG was mediated via the PC-binding site, being competitively inhibited by the presence of PC chloride-calcium salt. Similar to the findings in previous with *L.donovani*, CRP binding to *L.mexicana* LPG was calcium dependent, being non-competitively inhibited by the divalent cation chelator EDTA. Inhibition assays with the Gal-Man-PO_4 specific antibody LT6 appears to indicate that CRP binding to *L.mexicana* LPG was via the phosphorylated disaccharide moieties present. Further confirmation of this was observed in a separate study, where inhibition assays of CRP binding to *L.donovani* LPG with a series of unsubstituted or modified monosaccharides, demonstrated competitive inhibition only with phosphorylated monosaccharides(Culley et al., 2000).

Using ligand blotting, we determined *that L.mexicana* metacyclic-stage parasite produce a larger variant of LPG than nectomonad stage promastigotes, with the

binding pattern roughly corresponding between a probe with CRP and LT6 (Gal-Man-PO_4 specific) on LPG transferred onto PVDF membranes following SDS-PAGE. This would corroborate with previous studies indicating stage-dependent differences in LPG of other *Leishmania* species correlating to an increased number of phosphorylated disaccharide repeats present following metacyclogenesis (McConville et al., 1992), although differences in side chain substitution type between metacyclic and nectomonad LPG may also affect the CRP binding capacity of LPG.

Metacyclic and nectomonad *L.mexicana* promastigote LPG appeared to demonstrate similar levels of binding avidity to CRP analyte when subjected to SPR analysis with lower levels of immobilised LPG ligand on the hydrophobic alkyl chip surface (approximately 25 RU). However, similar runs with higher densities of immobilised LPG (approximately 290 RU) appeared to indicate that metacyclic LPG has higher binding avidity to CRP compared to nectomonad LPG. In addition, both metacyclic and nectomonad LPG at high ligand densities appeared to suggest biphasic binding to the CRP analyte, with binding occurring at higher concentrations (≥1.25 μg/ml) seeming to indicate lower binding avidity events compared to those at lower concentrations, indicating the presence of separate CRP ligands present on LPG. It was also possible that this was representative of homotropic allosteric interaction between CRP and LPG, where CRP binding to the phosphorylated disaccharide moieties regulated the availability of the ligand for subsequent binding between the same two partners (Monod et al., 1965). In this particular scenario, CRP appears to increase the number of subsequent available ligand binding sites, making CRP was a positive allosteric regulator.

4.6.2: LPG binding to SAP

ELISA experiments appeared to indicate that nectomonad LPG has higher binding capacity for SAP in comparison to metacyclic LPG. This was supported by ligand blotting with semi-quantitative ligand blotting of LPG following SDS-PAGE, which shows a markedly more chromogenic deposition on lanes containing nectomonad LPG material. Inhibition assays with EDTA and EGTA indicate that this was a calcium-dependent event, while the lack of inhibition in

the presence of LT6 indicates that SAP does not bind to the phosphorylated disaccharide moieties on LPG.

Of note, we observed that the SAP-LPG complex was incapable of binding to C1q in ELISA format experiments, in contrast to complexes formed with the positive control ligand, PEC. While he matter of SAP's role in complement activation itself is a contentious issue, our observations suggest that SAP activation of the CP independent of anti-SAP IgG/IgM may be dependent on a conformational change elicited in the pentraxins' structure triggered by ligand binding which LPG does not achieve. Given the relative concentration of SAP and CRP in circulation, this may have implications for previously reported effects of CRP binding to the parasite surface via LPG, especially if they experience competition for binding. Our own attempts at exploring the possibility of SAP-CRP cross inhibition binding suggest that CRP may inhibit SAP binding at higher concentrations, whereas we did not observe competition vice versa. One potential explanation might be that CRP binding results in steric exclusion of the SAP from its corresponding ligand rather than direct competition. However, the experimental had several limitations, including the incubation of a relatively low concentration of SAP (1.0 µg/ml) in the ELISA compared to that observed under physiological conditions (20-60 µg/ml) due to concerns regarding SAP aggregation at high concentrations in the presence of calcium.

4.6.3: CRP and SAP binding sites on LPG

Given the concurrence of CRP and SAP in normal human serum, it was conceivable that the parasite membrane and associated LPG was exposed to both pentraxins in the initial stages of infection. While SAP was a constitutively expressed protein, CRP concentrations vary greatly with the inflammatory state of the individual, although a previous study estimate that the normal serum concentration of CRP in areas with endemic VL at 3.95±1.9µg/ml (Wasunna et al., 1995). Given the varied innate immune functions ascribed to CRP and SAP, any competition in binding to LPG on the parasite surface would likely influence the survival and persistence of *Leishmania* in the mammalian host.

Our own experiments, in line with previous studies, demonstrate that CRP binds to LPG via the phosphorylated disaccharide repeat in a calcium-dependent

manner, as evidenced by competition inhibition by the Gal-Man-PO_4 specific antibody LT6 and non-competitive inhibition by both the divalent cation chelator EDTA and the calcium-specific chelator EGTA.

The lack of LT6 inhibition for SAP binding to LPG would suggest that they do not share binding sites, as well as the relative lack of cross-inhibition between CRP and SAP within physiological serum concentrations of either pentraxin. This would also corroborate with the lack of increase in SAP binding capacity, unlike CRP, following the transformation from nectomonad to metacyclic stage promastigotes, wherein a stage-specific change in LPG expression observed in other species, such as *L.major* (McConville and Ferguson, 1993), sees an elongation of the molecule correlating to an increase in the number of Gal-Man-PO_4 repeats present per molecule.

4.6.4: Conclusions

Metacyclic LPG contains greater binding capacity and avidity to CRP compared to nectomonad LPG in *L.mexicana*, with inhibition assays suggesting that binding was dependent Ca^{2+} and to Gal-Man-PO_4 present on LPG, in a similar manner to the observations made for *L.donovani* by previous studies. The difference in binding avidity was only apparent at higher densities of immobilised LPG when subjected to SPR experiments. Another phenomenon that was only observed at high ligand LPG densities was that LPG ligand from both promastigote stages appeared to experience biphasic binding when subjected to SPR experiments, with markedly higher avidity binding observed below approximately 1.25 µg/ml CRP analyte compared to a gradually decreasing avidity above it. This was likely to be related to saturation of higher avidity sites first. While drawing an equivalence in LPG density on a chip surface compared to that on a promastigote cell surface was difficult, previous data would indicate that LPG forms a thick glycocalyx surrounding the parasite, suggesting that LPG was both highly available and expressed on the surface, and that therefore the observations at high ligand densities are likely to be more meaningful.

Nectomonad LPG contains greater binding capacity for SAP compared to metacyclic LPG in *L.mexicana*. Inhibition assays suggest that this interaction

was Ca^{2+} dependent and does not occur to Gal-Man-PO_4. Determination of differences in binding avidity between the two stages of LPG to SAP could be performed with SPR experimentation, in a similar to that done for CRP binding to LPG, although caution should be taken with fluid-phase SAP analyte, given its propensity to aggregate in the presence of Ca^{2+} and the absence of albumin, which could compromise both the chip surface and potentially the microfluidics of the SPR machine. But initial studies demonstrated no interaction of SAP for LPG immobilised on hydrophobic chips or when LPG was immobilised by aldehyde hydrazide coupling. This may be due to unavailability of the site particularly in flow conditions. Previous attempts at removal of aggregated SAP on a PSG-immobilised chip (results not shown) showed that chip surface aggregation was resistant to multiple methods on surface regeneration, including EDTA, NaOH and glycine. Experiments testing SAP binding to whole promastigotes, such as confocal microscopy following immunofluorescent probing, as well as surfaces better representing LPG as it would on the cell membrane, could determine that SAP binding to LPG was not an artefact of the experimental methods used. In addition, deglycosylation of LPG using established methods such as mild acid hydrolysis used for PSG, as well as inhibition assays with antibodies specific to other moieties common to Leishmania ligands such as L7.25, which was specific for the mannose end-cap of LPG, could help further characterisation of SAP-LPG binding.

Investigation into SAP and CRP cross inhibition appears to indicate some inhibition of SAP binding to LPG, with increasing concentrations of competing CRP (Figure 67), but not vice versa (Figure 66). It should be noted that the SAP concentration used in the ELISA was relatively low compared to that found in serum from healthy individuals (~20-60 µg/ml) (Pilling and Gomer, 2018), due to concerns regarding aggregation at higher concentrations. Further investigation would be required to determine if these observations are accurate.

4.7: Surface Binding Resonance

4.7.1: Binding kinetics

All calculations of binding kinetics for interactions between *Leishmania* glycosylated products and CRP/SAP was performed on BioEvaluation software (GE Healthcare), using a Langmuir model, which assumes a 1:1 interaction between the ligand and analyte molecules (Oshannessy et al., 1993). Given that pentraxins are by their very nature multivalent proteins, which each subunit containing ligand binding capacity, and that *Leishmania* glycosylated products contain multiple, exposed repeats of the hypothesised CRP ligand in the form of phosphorylated disaccharides, it seems unlikely that this would be the case, either *in vivo* or *in vitro*. However, given the complexity of the predicted binding mechanics between pentraxin and *Leishmania* products, and the given kinetic models available in the software, the Langmuir model provides the most appropriate representation. Attempts to generate more complex models that might provide more accurate data were resisted as these are therefore more likely to generate erroneous accuracy or unsubstantiated models of interaction.

The Langmuir model has been shown to be reasonably accurate with immobilised LPG ligand and CRP analyte until higher concentration of analyte was introduced, likely due to the increased variability of numbers of repeating disaccharide bound by a CRP pentamer and an increase in percentage with a single repeating disaccharide and a fast off rate.

4.7.2: PSG orientation and ligand availability

PSG captured by CRP immobilised of the chip surface demonstrated a far greater relative CRP binding capacity than PSG ligand coupled to the surface in a more direct fashion, with the phenomenon being demonstrated in PSG derived from several species (*L.mexicana, L.panamensis* and *L.donovani*). In addition, *L.mexicana* PSG-biotin immobilised to the surface exhibits similar low CRP binding capacity when compared to its unmodified counterpart. Given that the immobilisation strategy used in the latter direct method which involved avidin capture of biotinylated amino acid moieties in PSG, it seems unlikely that

chemical modification of the proposed CRP ligands, the phosphorylated carbohydrate groups, was responsible for the relative lack of binding observed. Rather it was perhaps likely that all PSG does not have equal amounts of the CRP ligand of repeating disaccharide and that the direct coupling leads to more of the form with a lower ligand component which may be preferentially biotinylated and the captured form preferentially has more ligand for further CRP binding.

The use of CRP-biotin to look at the binding of the PSG was interesting in that the flow rate showed greater binding at a lower flow rate. This was consistent with a large extended molecule with relatively few binding sites and an on-rate that was restricted by the access of the ligand to the CRP on the surface. However, the data in terms of the relative binding of different parasites and binding parameters were consistent with the data in the reverse orientation. Again, these interactions showed the same features of calcium-dependency and were similar for recombinant and purified CRP.

It was possible that prior attempts at PSG ligand immobilisation to the surface caused denaturation due to the exposure of the PSG to low pH buffer (sodium acetate, pH 5.0). PSG has been shown to be susceptible chemical modification in acidic conditions, as seen in other studies demonstrating PSG deglycosylation following a mild acid hydrolysis process (Ilg et al., 1996). Given that this would directly impact on the availability of the proposed CRP ligand, this could potentially explain the relative lack of CRP binding seen.

It seems likely that the orientation of PSG captured to the surface would influence the CRP binding capacity observed as well, with CRP-biotin captured PSG possibly exposing more of the phosphorylated carbohydrate moieties than the previously discussed methods. Consideration should also be taken to determine that the ligand coupled to the chip surface was not denatured by the procedure, such as might occur by exposure to low pH, or that any labelling process, such as biotinylation, does not affect any relevant binding functionality that would otherwise be present in the unmodified molecule. The binding orientation of the ligand should also be done in a manner to closely represent that which would occur in its native state.

4.8: LPG-PSG interaction

4.8.1: LPG and PSG in the arthropod digestive tract

Previous studies have shown that LPG was a stage-specific molecule, with LPG size, directly correlating to the number of disaccharide repeats expressed, and side-chain substitutions varying between promastigote stages. This has been demonstrated to affect binding of the parasite to the midgut, an essential mechanism to establishing infection in the sandfly vector by preventing excretion of the parasite as part of the normal digestive process. LPG side chain substitutions have also been shown to influence the species of arthropod vector for a given *Leishmania* species, with side chain substitutions facilitating attachment of the parasites via lectin expressed on the surface of the sandfly gut (Soares et al., 2002).

Of interest, the PSG matrix has been reported to be predominantly embedded with infectious, metacyclic stage promastigotes. This would suggest some form of selective mechanism which facilitates the localisation of the infectious stage parasites in the region most likely to be introduced to the feeding site during the infected sandfly regurgitation event, as well as co-transmission of said parasites with a virulence factor that promotes *Leishmania* infection in the mammalian host in the form of PSG. As previous studies have demonstrated that LPG was the predominant surface marker of *Leishmania* promastigotes, forming a thick glycocalyx that likely obscures other surface molecules, we investigated if the stage-specific nature of LPG in promastigotes extended to parasite motility in the PSG matrix.

CRP facilitates LPG-PSG interaction in a calcium-dependent manner. In addition to being dose-dependent with regard to CRP, it also appears to be a stage-specific phenomenon, with metacyclic-stage LPG exhibiting far greater adhesion to PSG compared to nectomonad-stage LPG. This could have implications in the *in vivo* migration patterns of the *Leishmania* parasite in the sandfly gut, as well as potentially facilitating co-transmission of the infective stage metacyclic *Leishmania* promastigotes with PSG during infected sandfly feeding. To further investigate this interaction, it would be possible to develop

SPR experimental models, which would have the added advantage of being able to use unlabelled molecules. ELISA experiments that would allow rapid analysis of multiple different media conditions of calcium and CRP concentrations and pH will require at least one component to have a defined label and or detection antibody which poses problems because of the similarity in ligands observed between the various *Leishmania* glycosylated products.

4.8.2: LPG and PSG in the mammalian host

As noted in previous studies, PSG components and LPG share similar moieties in regard to their glycosylated domains. While it was unknown if PSG experience stage and species-specific side-chain substitutions and levels of expression in the same manner that LPG has been observed to, the two molecules are at the very least similar in their ability to bind to CRP and subsequently activate the CP through the above-mentioned Gal-Man-PO_4 domains. With regard to modulation of the innate immune environment by via the complement system and independent CRP action, it was conceivable that fPPG and ScAP act to exaggerate the effects on innate immunity previously attributed to LPG that might not be otherwise achieved with the relatively lower levels of the salient CRP ligand that can be found expressed on the parasite LPG glycocalyx alone.

A key determining factor in testing this hypothesis would be further elucidation of the PSG side-chain structures, as well as an estimation of the level of PSG that was introduced to the feeding site relative to the number of parasites and sandfly saliva. Given the evidence that PSG was a virulence factor of *leishmania* mammalian infection, it may be advisable that future *in vivo* and *in vitro* experiments take it into account with regard to infection models, in order to better represent the innate immune environment as it would be during early, natural infection.

4.9: Role of Serum Amyloid P (SAP) in innate immunity

Despite its relative abundance in circulation, relatively little was known about the role of SAP in immunity compared to CRP. The lack of naturally occurring SAP deficient mutants would suggest that SAP has an essential role in maintaining organism viability. There was evidence that SAP has a role in opsonisation and complement activation following binding of *Streptococcus pneumoniae* in animal models(Yuste et al., 2007), as well as inhibition of dermal wound healing in mice(Naik-Mathuria et al., 2008), suggesting that SAP has an innate immune role.

The ability of SAP to activate complement was also subject to debate, with some evidence that SAP-bound bacteria prevents activation of the classical complement pathway by preventing the deposition of C1q on the bacterial cell surface lipopolysaccharide(de Haas et al., 2000). This was in direct contradiction of other reports, which suggest that SAP was capable of aiding complement-mediated immunity (Yuste et al., 2007).

We observed no binding of the LPG-SAP complex to C1q. This was in contrast to binding to the SAP positive control ligand, PEC, which appears to be able to form a complex with SAP that binds to C1q, although the exact nature of the binding event was unknown. Indeed, there was no reports of SAP undergoing a conformational change following calcium-dependent binding at the time of this writing.

Further investigation using similar experimental models of complement deposition ELISA (Section 2.13.3-4) could be performed to further elucidate the role of SAP in complement.

4.10: The lectin pathway in *Leishmania*-mediated complement activation

As highly glycosylated products, it was plausible that LPG and PSG interact with and activate the LP, due to its initiator signalling molecules having specificity to carbohydrate moieties present on various pathogenic products. Indeed, LP pathway activation has been observed with *L.mexicana* amastigote-stage secreted proteophosphoglycan, which contains chemically similar structures to the *Leishmania* products investigated in this study (Peters et al., 1997).

We investigated the ability of MBL, an LP initiator molecule, to bind to PSG, revealing widely varying MBL binding capacity between different species (Figure 53). In *L.aethiopica* at least, the interaction appears to be largely independent of the presence of calcium. This was in contrast to the MBL positive control ligand, mannan (Figure 54). In the future, it would be of interest to investigate this interaction further, such as with SPR techniques, as well as to expand the scope to the other LP initiator molecules, such as ficolin-class lectins.

Further investigation into potential LP activation by PSG was hindered by the inability to selectively inhibit was using SPS in a similar manner reported in a separate study (Palarasah et al., 2011). It may be possible to optimise the existing protocol, as it was noted that SPS was subject to batch variability, which may account for the lack of inhibition experienced. Selective depletion of serum of the various LP initiator molecules using antibody-based affinity chromatography techniques may be possible, but would have to account for the wide variety of LP initiator molecules, including MBL, M-ficolin, L-ficolin, H-ficolin and Collectin-11. Other candidates for depletion may include the MASP proteins, downstream activation of which drives LP activation (Section 1.3.4).

4.11: Phosphorylcholine containing molecules: The search for an immunomodulatory small molecule derivative

Other parasites have been observed to express phosphorylated ligands containing specificity towards pentraxins, either in the form of PC or PE towards CRP and SAP respectively. In addition, we have demonstrated that *Leishmania* PGs, such as LPG and PSG, bind to CRP via the repeating phosphorylated disaccharide structure.

ES-62 has been the subject of previous related studies, with a range of potentially therapeutic effects including dendritic cell modulation and IL-17 inhibition. Previous studies have also demonstrated classical complement pathway inhibition linked to a lack of C3 convertase formation. In addition, ES-62 has been shown to improve the condition of experimental models of asthma and rheumatoid arthritis.

The role of PC in the immunomodulatory effects of ES-62 was supported by the use of other PC containing molecules, such as, *Ascaris suum* derived glycosphingolipids (GSL), PCBSA conjugates and PC alone, which have been shown to have similar immunomodulatory effects in experimental models. On the other hand, GL2, a synthetic glycosphingolipid with similar structures to *Ascaris suum*-GSLs but with a ceramide substitution for PC, exhibits no immunomodulatory effects. Two other PC containing synthetic GSL, GL1 and GL3, exhibit widely varying regulatory effects. While PC has been shown to be an immunomodulatory component, the importance of attached structural features are evident.

One aspect of ES-62's immunomodulatory effects was its reported ability to inhibit complement activation by forming a complex with CRP without subsequent activation of the CP, causing a net reduction in inflammatory effects and antipathogenic mechanisms (Figure 96). Our observations of PSG and LPG components would suggest that these Leishmania PG products do not share this quality, our investigations have highlighted the importance of the

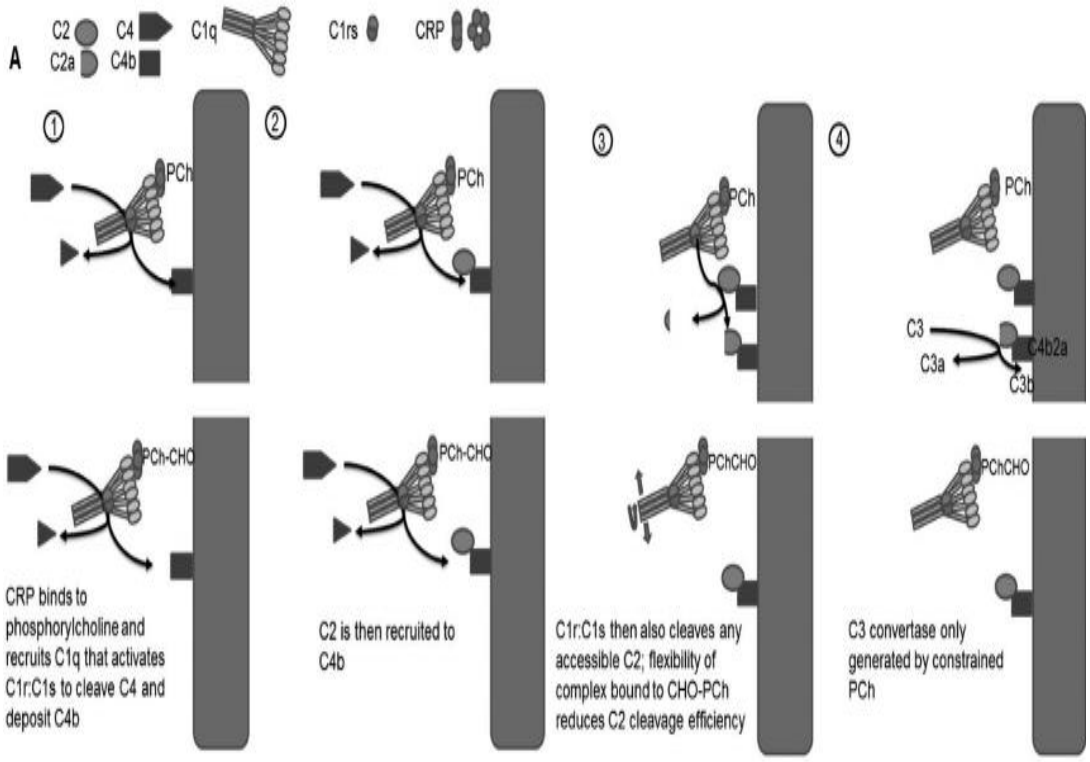

Figure 97: Proposed mechanism of CP inactivation by the *Acanthocheilonema viteae* CRP ligand ES-62 (below), compared to complement activation by conventional CRP ligands (above) (Ahmed et al., 2016).

secondary, non-binding site structures of CRP-ligands in determining the activation of the CP. ES-62's unique function has been hypothesised to be due to the placement of its PC-binding head to 30 Angstrom-long, flexible glycan linkage, reducing the efficiency of the rate of cleavage of surface-deposited C2C4b by bound C1q due to its mobility and ability to shift from a position proximal to the surface. This was in direct contrast to the rigidly-bound PC ligands found on *S.pneumoniae* and likely for the dense ligand presentation of LPG on the parasite cell membrane and PSG.

4.12: Summary

The main focus of our study and this thesis has been the interaction of *Leishmania* PG products with the pentraxins CRP and SAP (Table 8). This was done in order determine their role in the establishment of early infection in the mammalian host, as well as the pentraxins' effects on *Leishmania* within the context of the infected sandfly when introduced into the digestive tract as part of the bloodmeal.

We have demonstrated that CRP binds with avidity to various *Leishmania* ligands, with the strength of the binding interaction correlating with the presence of the phosphorylated disaccharide repeats common to many of its' glycosylated products. We observed calcium-dependent CRP binding to PSG components with subsequent complement activation capacity, being driven mainly via the CP with a minor AP contribution, although we were unable to ascertain the role of the LP within the observed complement activation. In the context of PSG, we have determined that ScAP, rather than fPPG, was the major CRP binding component. CRP in complex with PSG has been demonstrated to be an efficient activator of complement mainly via the CP, a mechanism that may be beneficial in establishing early infection, especially since PSG was not membrane-associated, allowing complement activation to occur at the proverbial 'safe distance'. One feature revealed by SPR was that a large component of the high avidity was driven by the very slow off-rate which might be expected for CRP binding to a large molecule like PSG with multiple chains that can contain repeating disaccharide ligand.

We established that *L.mexicana* LPG exhibits stage-specific variations to its structure, which in turn affects the CRP binding capacity and affinity. Further investigation using SPR analysis, which notably allowed for a more accurate representation of LPG as it would appear in its native state as part of the cell membrane in terms of orientation, revealed that this was a high avidity interaction, as evidenced by the calculated low dissociation constant values, with metacyclic-stage LPG displaying markedly stronger binding in comparison to nectomonad-stage LPG. In addition, SPR analysis allowed estimation of binding stoichiometry between CRP and LPG. While there was variance

Species	ELISA	Ligand blot	SPR: Carbodiimide-linked PSG ligand, CRP analyte	SPR: PSG-biotin ligand, CRP analyte	SPR: CRP-captured PSG ligand, CRP analyte	SPR: CRP-biotin ligand, PSG analyte
L.donovani	+++++	+	NA	NA	+++	++++
L.panamensis	+++++	+++	NA	NA	++++	++++
L.aethiopica	+++++	NA	NA	NA	+	NA
L.infantum	+++	+++++	NA	NA	NA	NA
L.major	++	NA	NA	NA	+	NA
L.tropica	-	-	NA	NA	-	NA
L.amazonensis	-	NA	NA	NA	-	NA
L.mexicana WT	++++	++	+	+	+++	+++
***L.mexicana* LPG1$^{-/-}$**	++++	++	NA	NA	NA	NA
***L.mexicana* LPG2$^{-/-}$**	-	-	NA	NA	NA	NA
***L.mexicana* ScAPKO**	+	NA	NA	NA	+	NA
***L.mexicana* ScAPAB**	++	NA	NA	NA	+++	NA

Table 8: Table of CRP binding interaction to PSG in different *Leishmania* species observed with various experimental techniques in the course of this study.

+++++: Very high avidity/capacity
++++: High avidity/capacity
+++: Moderate avidity/capacity
++: Weak avidity/capacity
+: Very weak avidity/capacity
-: Negligible or no detectable avidity/capacity
NA: Non-applicable i.e. not tested for a given technique

dependent on the amount of LPG loaded coupled to the chip, results obtained from sensor surfaces coupled with high LPG ligand densities suggests approximately 5 CRP subunits binding per LPG molecule, which would indicate LPG molecules binding to multiple CRP pentamers in a 'bridging' action. This was perhaps unsurprising with the multiple ligand binding sites present on CRP, the highly available repeating disaccharide ligand present per molecule and the close proximity of the LPG molecules on the surface. Change of association constant values as CRP analyte concentrations reached a threshold point (approximately 2.5 µg/ml) appears to indicate that CRP binding to LPG caused a conformational change on the chip surface, allowing for further ligand binding. While such allosteric modifications of ligands have been noted in proteins, equivalent observations in carbohydrate products have rarely been made. The corresponding increase in dissociation rate at these high CRP concentrations suggests that the newly available CRP binding sites are of lower avidity in comparison to those available at lower CRP concentrations. Interestingly, the observed R_{max} was reduced at the highest CRP analyte concentrations tested, suggesting a disruption of the LPG-coupled chip surface present after removal of bound CRP with EDTA buffer. Of note, the CRP threshold associated with these phenomenon was similar to that which was previously reported to elicit transformation from metacyclic promastigote to amastigote stage parasites in *L.donovani* and *L.mexicana* (Mbuchi et al., 2006), although further investigation would be required to elucidate potential links between the two phenomenon.

CRP binding to LPG was likely influenced by a number of structural characteristics of the molecule, and should be thought about in the context *in vivo*, which suggests LPG forming a highly expressed, dense glycocalyx structure on the promastigote surface. Prior investigation into the 3-dimensional structure of LPG using *L.donovani* as a model suggest that the phosphorylated disaccharide repeat region of LPG forms a helical structure with approximately 6 repeats per turn, capable of expansion and contraction from 90-160 angstroms for an LPG molecule of 16 repeats (Homans et al., 1992). The level of spacing between the turns in the helical structure would likely influence the availability of the CRP binding sites. While *L.donovani* was a group I LPG molecule with entirely unsubstituted phosphorylated disaccharide repeats, *L.mexicana* was a group II LPG molecule, with branching modifications from the

C3 position of the galactose residue (McConville et al., 1995). A separate study into suggests that approximately 20% of the phosphorylated disaccharide repeats found in LPG derived from late logarithmic phase/early stationary phase *L.mexicana* promastigotes are modified with glucose (Ilg et al., 1992). The elongation of LPG in metacyclogenesis has also been associated with the proposed 'hairpin' turn in *L.donovani* LPG, associated with the obscuration on the mannose end-cap structure, which may also serve to increase presentation of the CRP-binding phosphorylated disaccharide repeats (Sacks et al., 1995), in addition to increasing the net amount of CRP ligand sites available due to the increase in the number of repeats expressed per LPG molecule. While this was not thought to occur with occur in *L.major*, likely due to its highly branched structure preventing folding while densely packed, *L.mexicana* LPG was observed to have a relatively low level of side-chain modification in comparison.

CRP has been noted to bind in high densities to the target pathogen surface, likely due to its' affinity for repeating ligands on the surface, such as CWPS on *S.pneumoniae*. Given the levels of expression of the phosphorylated disaccharide indicated by structural analysis of secreted PSG, as well as LPG as expressed on the promastigote membrane, it was conceivable that this relevant to these *Leishmania* ligands as well. A potential effect of CRP binding, particularly at high levels, would be the alteration of the surface charge profile. Such an effect could have multiple implications, including alterations of the surface architecture, which has been observed in mucins, which bear a similar composition to PSG. SPR experiments have noted a reduction in the association constant when high CRP analyte concentrations were flowed over surface-coupled LPG, indicative of modifications of the surface.

Further studies have been undertaken in collaboration with Alaa Riziek (Department of Infection Biology, Infectious and Tropical Diseases, London School of Hygiene and Tropical Medicine, UK) in order to investigate the effect of CRP binding on the charge profile of *Leishmania* parasites and or PSG ligands. This was achieved using electrophoretic light scattering (ELS) techniques with a Zetasizer (Malvern Panalytical), which measures the movement of the molecule of interest in response to a charge field. Early results with *L.mexicana* metacyclic and nectomonad stage parasites indicate that in the absence of CRP, with or without calcium, the parasite surface bears a highly

negative charge, likely due to the presence of phosphate groups present as part of the phosphorylated disaccharide moieties in LPG. CRP (3 µg/ml) in the presence of calcium (2mM) eliminates the surface charge of *L.mexicana* promastigotes. A similar effect was seen with *L.mexicana* PSG, with calcium-dependent binding reducing the net negative charge. Further investigation with a wider range of CRP and calcium concentrations, as well as SAP, would be of interest.

The mechanism of PSG gelation was not completely understood, but analysis of human intestinal mucin assembly, which was structurally and compositionally similar, indicate a complex interplay of factors, including hydrogen bonding and calcium-mediated linkages (Meldrum et al., 2018). As such, CRP binding and change in surface charge profile could conceivably disrupt the assembly of the gel matrix and affect its viscosity. This may have implications in promastigote motility within the gel matrix present in the sandfly gut, as well as the introduction of PSG into the feeding site, and would be of interest for future investigation.

Future work could be undertaken to estimate the time-course of CRP binding to *L.mexicana* LPG, which could be performed in a similar manner previously used on *L.donovani* promastigotes (Culley et al., 1996). While pentraxin binding data between cultures of metacyclic promastigote LPG are reasonably reproducible, we have observed some variation between nectomonad LPG cultures, which could illustrate the need for better definitions for the various intermediary promastigote stages. The use of immunofluorescence probing of CRP/SAP whole promastigotes, coupled with confocal microscopy analysis, was currently being investigated to determine the distribution of ligand on the parasite surface.

Our attempts at characterisation of SAP binding to *Leishmania* ligands were arguably less successful than that for CRP. While SAP binding was demonstrated in both ELISA and ligand blot experiments, early observations (Eve Doran, Department of Infection Biology, Infectious and Tropical Diseases, London School of Hygiene and Tropical Medicine, UK) using SPR techniques with LPG coupled to the hydrophobic HPP chip and fluid-phase SAP analyte have yielded no binding. This could be indicative of an SAP ligand, such as PE,

which was obscured in LPG's native orientation. It should be noted, however, that SAP was prone to aggregation in the presence of calcium and the absence of calcium, affecting its binding characteristics. Determination of the presence of PE in LPG achieved using mass spectrometry techniques, with consideration being taken so as to prevent removal of possible PE structures during material preparation (Paschinger and Wilson, 2016).

PEC, which was generated by gram-negative bacteria *Escherichia coli* as part of its biofilm, was observed to contain SAP binding affinity, and as such was used as a positive control ligand. PEC in complex with SAP was shown to be able to bind to C1q, although subsequent ability to generate complement through this interaction was not demonstrated. LPG, on the other hand, was unable to generate a C1q binding complex with SAP. However, this in itself could represent a difference in the two organisms' survival strategies in the mammalian host, as SAP has been reported to have complement-independent immune effects. Of note, it has been observed that SAP-deficient mice are less susceptible to *E.coli* infection than their WT counterparts, with SAP binding reducing bacterial opsonisation (Noursadeghi et al., 2000). Our own observations indicate that SAP does not independently activate complement through LPG binding, introducing another potential element of innate immune modulation by SAP-binding pathogens. It would be of interest to see if this phenomenon was dependent on C1q.

It was currently unclear as to why nectomonad-stage LPG has a greater SAP binding capacity compared to metacyclic LPG, although inhibition assays with antibodies specific to the other glycan structures present on LPG that have been described in previous studies may help elucidate the target ligand. Currently, studies are ongoing into the significance of differential SAP binding to LPG and hence the *Leishmania* promastigote surface, within the context of the mammalian and arthropod hosts.

A summary of the key findings of this project and their potential, wider implications had been provided (Figure 97).

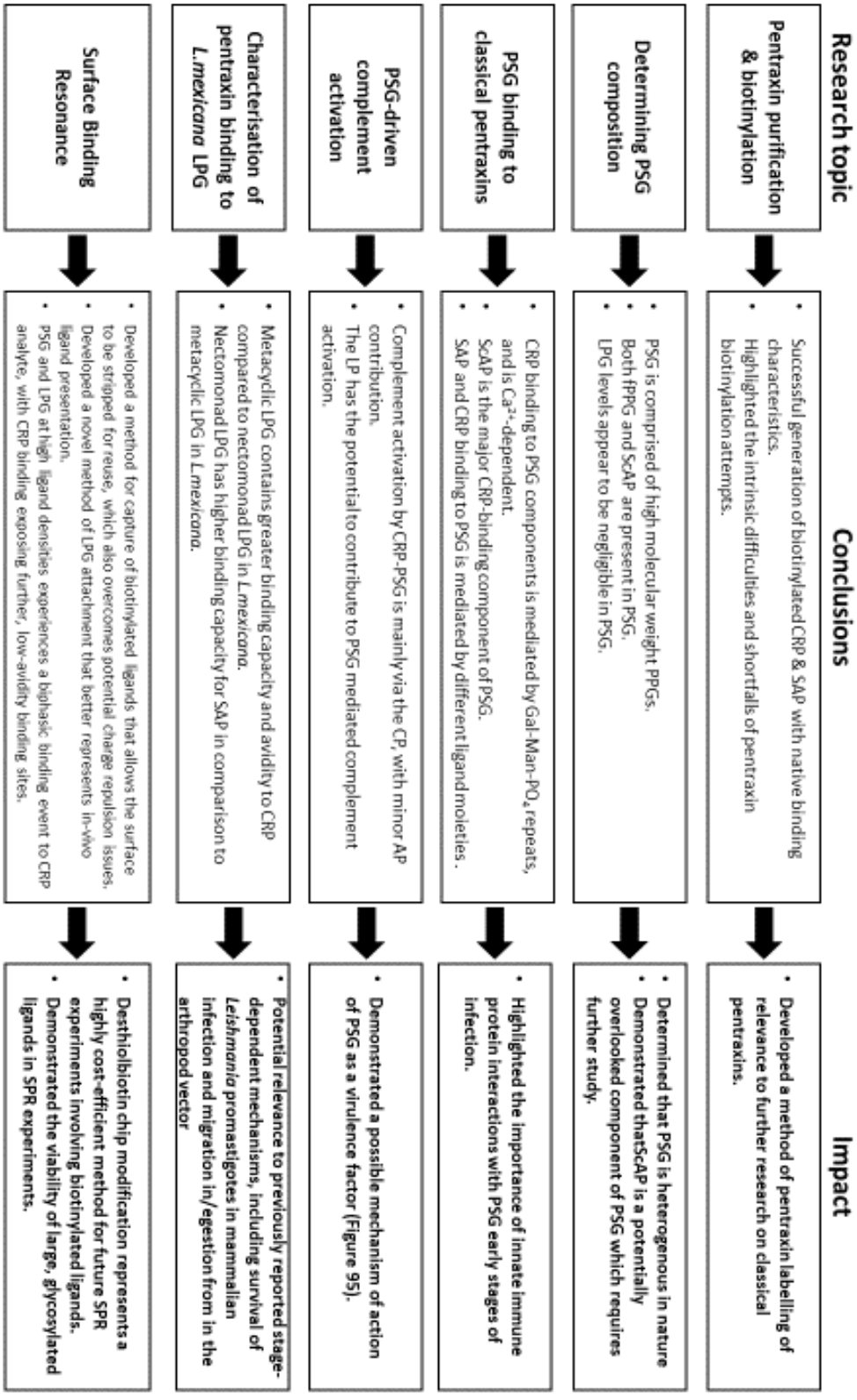

Figure 98: Summary of the initial research topics, the conclusions drawn and their potential, wider impact/relevance to the field.

References

AFONSO, L., BORGES, V. M., CRUZ, H., RIBEIRO-GOMES, F. L., DOSREIS, G. A., DUTRA, A. N., CLARENCIO, J., DE OLIVEIRA, C. I., BARRAL, A., BARRAL-NETTO, M. & BRODSKYN, C. I. 2008. Interactions with apoptotic but not with necrotic neutrophils increase parasite burden in human macrophages infected with Leishmania amazonensis. *J Leukoc Biol,* 84**,** 389-96.

AGA, E., KATSCHINSKI, D. M., VAN ZANDBERGEN, G., LAUFS, H., HANSEN, B., MULLER, K., SOLBACH, W. & LASKAY, T. 2002. Inhibition of the spontaneous apoptosis of neutrophil granulocytes by the intracellular parasite Leishmania major. *J Immunol,* 169**,** 898-905.

AGRAWAL, A. 2005. CRP after 2004. *Mol Immunol,* 42**,** 927-30.

AHMED, U. K., MALLER, N. C., IQBAL, A. J., AL-RIYAMI, L., HARNETT, W. & RAYNES, J. G. 2016. The Carbohydrate-linked Phosphorylcholine of the Parasitic Nematode Product ES-62 Modulates Complement Activation. *J Biol Chem,* 291**,** 11939-53.

AL-SHAWI, R., TENNENT, G. A., MILLAR, D. J. & AL., E. 2016. Pharmacological Removal of Serum Amyloid P Component From Intracerebral Plaques and Cerebrovascular Aβ Amyloid Deposits in Vivo. *Open Biology,* 6.

ALBALASMEH, A. A., BERHE, A. A. & GHEZZEHEI, T. A. 2013. A new method for rapid determination of carbohydrate and total carbon concentrations using UV spectrophotometry. *Carbohydr Polym,* 97**,** 253-61.

ALBERTI, S., MARQUES, G., CAMPRUBI, S., MERINO, S., TOMAS, J. M., VIVANCO, F. & BENEDI, V. J. 1993. C1q binding and activation of the complement classical pathway by Klebsiella pneumoniae outer membrane proteins. *Infect Immun,* 61**,** 852-60.

ALI, Y. M., LYNCH, N. J., HALEEM, K. S., FUJITA, T., ENDO, Y., HANSEN, S., HOLMSKOV, U., TAKAHASHI, K., STAHL, G. L., DUDLER, T., GIRIJA, U. V., WALLIS, R., KADIOGLU, A., STOVER, C. M., ANDREW, P. W. & SCHWAEBLE, W. J. 2012. The lectin pathway of complement activation is a

critical component of the innate immune response to pneumococcal infection. *PLoS Pathog,* 8**,** e1002793.

AMBRUS, G., GAL, P., KOJIMA, M., SZILAGYI, K., BALCZER, J., ANTAL, J., GRAF, L., LAICH, A., MOFFATT, B. E., SCHWAEBLE, W., SIM, R. B. & ZAVODSZKY, P. 2003. Natural substrates and inhibitors of mannan-binding lectin-associated serine protease-1 and -2: a study on recombinant catalytic fragments. *J Immunol,* 170**,** 1374-82.

ANDERSEN, O., VILSGAARD RAVN, K., JUUL SORENSEN, I., JONSON, G., HOLM NIELSEN, E. & SVEHAG, S. E. 1997. Serum amyloid P component binds to influenza A virus haemagglutinin and inhibits the virus infection in vitro. *Scand J Immunol,* 46**,** 331-7.

ANTONELLI, L. R., DUTRA, W. O., ALMEIDA, R. P., BACELLAR, O. & GOLLOB, K. J. 2004. Antigen specific correlations of cellular immune responses in human leishmaniasis suggests mechanisms for immunoregulation. *Clin Exp Immunol,* 136**,** 341-8.

ARBORE, G., WEST, E. E., SPOLSKI, R., ROBERTSON, A. A. B., KLOS, A., RHEINHEIMER, C., DUTOW, P., WOODRUFF, T. M., YU, Z. X., O'NEILL, L. A., COLL, R. C., SHER, A., LEONARD, W. J., KOHL, J., MONK, P., COOPER, M. A., ARNO, M., AFZALI, B., LACHMANN, H. J., COPE, A. P., MAYER-BARBER, K. D. & KEMPER, C. 2016. T helper 1 immunity requires complement-driven NLRP3 inflammasome activity in CD4(+) T cells. *Science,* 352**,** aad1210.

ASHFORD, R. W. E. A. 2020. Report of a meeting of the WHO Expert Committee on the Control of Leishmaniases, Geneva, 22–26 March 2010. WHO Library: World Health Organisation.

ASHOK, D., SCHUSTER, S., RONET, C., ROSA, M., MACK, V., LAVANCHY, C., MARRACO, S. F., FASEL, N., MURPHY, K. M., TACCHINI-COTTIER, F. & ACHA-ORBEA, H. 2014. Cross-presenting dendritic cells are required for control of Leishmania major infection. *Eur J Immunol,* 44**,** 1422-32.

ASHWELL, G. & HARFORD, J. 1982. Carbohydrate-specific receptors of the liver. *Annu Rev Biochem,* 51**,** 531-554.

AURITI, C., PRENCIPE, G., MORIONDO, M., BERSANI, I., BERTAINA, C., MONDI, V. & INGLESE, R. 2017. Mannose-Binding Lectin: Biologic Characteristics and Role in the Susceptibility to Infections and Ischemia-Reperfusion Related Injury in Critically Ill Neonates. *J Immunol Res,* 2017**,** 7045630.

BANG, R., MARNELL, L., MOLD, C., STEIN, M. P., CLOS, K. T., CHIVINGTON-BUCK, C. & CLOS, T. W. 2005. Analysis of binding sites in human C-reactive protein for Fc{gamma}RI, Fc{gamma}RIIA, and C1q by site-directed mutagenesis. *J Biol Chem,* 280**,** 25095-102.

BANKS, R. E., FORBES, M. A., STORR, M., HIGGINSON, J., THOMPSON, D., RAYNES, J., ILLINGWORTH, J. M., PERREN, T. J., SELBY, P. J. & WHICHER, J. T. 1995. The acute phase protein response in patients receiving subcutaneous IL-6. *Clin Exp Immunol,* 102**,** 217-23.

BANSIL, R. & TURNER, B. S. 2006. Mucin structure, aggregation, physiological functions and biomedical applications. *Current Opinion in Colloid & Interface Science,* 11**,** 164-170.

BARTEL, Y., BAUER, B. & STEINLE, A. 2013. Modulation of NK cell function by genetically coupled C-type lectin-like receptor/ligand pairs encoded in the human natural killer gene complex. *Front Immunol,* 4**,** 362.

BATES, P. A. 2007. Transmission of Leishmania metacyclic promastigotes by phlebotomine sand flies. *Int J Parasitol,* 37**,** 1097-106.

BATES, P. A., HERMES, I. & DWYER, D. M. 1989. Leishmania donovani: immunochemical localization and secretory mechanism of soluble acid phosphatase. *Exp Parasitol,* 68**,** 335-46.

BATES, P. A., HERMES, I. & DWYER, D. M. 1990. Golgi-mediated post-translational processing of secretory acid phosphatase by Leishmania donovani promastigotes. *Mol Biochem Parasitol,* 39**,** 247-55.

BEE, A., CULLEY, F. J., ALKHALIFE, I. S., BODMAN-SMITH, K. B., RAYNES, J. G. & BATES, P. A. 2001. Transformation of Leishmania mexicana metacyclic promastigotes to amastigote-like forms mediated by binding of human C-reactive protein. *Parasitology,* 122**,** 521-9.

BENOIT, M. E., CLARKE, E. V., MORGADO, P., FRASER, D. A. & TENNER, A. J. 2012. Complement protein C1q directs macrophage polarization and limits inflammasome activity during the uptake of apoptotic cells. *J Immunol,* 188**,** 5682-93.

BIDULA, S., SEXTON, D. W. & SCHELENZ, S. 2019. Ficolins and the Recognition of Pathogenic Microorganisms: An Overview of the Innate Immune Response and Contribution of Single Nucleotide Polymorphisms. *J Immunol Res,* 2019**,** 3205072.

BIRO, A., ROVO, Z., PAPP, D., CERVENAK, L., VARGA, L., FUST, G., THIELENS, N. M., ARLAUD, G. J. & PROHASZKA, Z. 2007. Studies on the interactions between C-reactive protein and complement proteins. *Immunology,* 121**,** 40-50.

BLACK, S., KUSHNER, I. & SAMOLS, D. 2004. C-reactive Protein. *J Biol Chem,* 279**,** 48487-90.

BODIN, K., ELLMERICH, S., KAHAN, M. C., TENNENT, G. A., LOESCH, A., GILBERTSON, J. A., HUTCHINSON, W. L., MANGIONE, P. P., GALLIMORE, J. R., MILLAR, D. J., MINOGUE, S., DHILLON, A. P., TAYLOR, G. W., BRADWELL, A. R., PETRIE, A., GILLMORE, J. D., BELLOTTI, V., BOTTO, M., HAWKINS, P. N. & PEPYS, M. B. 2010. Antibodies to human serum amyloid P component eliminate visceral amyloid deposits. *Nature,* 468**,** 93-7.

BODMAN-SMITH, K. B., GREGORY, R. E., HARRISON, P. T. & RAYNES, J. G. 2004. FcgammaRIIa expression with FcgammaRI results in C-reactive protein- and IgG-mediated phagocytosis. *J Leukoc Biol,* 75**,** 1029-35.

BODMAN-SMITH, K. B., MBUCHI, M., CULLEY, F. J., BATES, P. A. & RAYNES, J. G. 2002a. C-reactive protein-mediated phagocytosis of Leishmania donovani promastigotes does not alter parasite survival or macrophage responses. *Parasite Immunol,* 24**,** 447-54.

BODMAN-SMITH, K. B., MELENDEZ, A. J., CAMPBELL, I., HARRISON, P. T., ALLEN, J. M. & RAYNES, J. G. 2002b. C-reactive protein-mediated phagocytosis and phospholipase D signalling through the high-affinity receptor for immunoglobulin G (FcgammaRI). *Immunology,* 107**,** 252-260.

BONGRAZIO, M., PRIES, A. R. & ZAKRZEWICZ, A. 2003. The endothelium as physiological source of properdin: role of wall shear stress. *Molecular Immunology,* 39**,** 669-675.

BOTTO, M., HAWKINS, P. N., BICKERSTAFF, M. C. & AL., E. 1997. Amyloid Deposition Is Delayed in Mice With Targeted Deletion of the Serum Amyloid P Component Gene. *Nat Med,* 3**,** 855-859.

BRAIG, D., NERO, T. L., KOCH, H. G., KAISER, B., WANG, X., THIELE, J. R., MORTON, C. J., ZELLER, J., KIEFER, J., POTEMPA, L. A., MELLETT, N. A., MILES, L. A., DU, X. J., MEIKLE, P. J., HUBER-LANG, M., STARK, G. B., PARKER, M. W., PETER, K. & EISENHARDT, S. U. 2017. Transitional changes in the CRP structure lead to the exposure of proinflammatory binding sites. *Nat Commun,* 8**,** 14188.

BRETON, M., TREMBLAY, M. J., OUELLETTE, M. & PAPADOPOULOU, B. 2005. Live nonpathogenic parasitic vector as a candidate vaccine against visceral leishmaniasis. *Infection and Immunity,* 73**,** 6372-6382.

BROOIMANS, R. A., HIEMSTRA, P. S., VAN DER ARK, A. A., SIM, R. B., VAN ES, L. A. & DAHA, M. R. 1989. Biosynthesis of complement factor H by human umbilical vein endothelial cells. Regulation by T cell growth factor and IFN-gamma. *J Immunol,* 142**,** 2024-30.

BROOKS, G. C., BLAHA, M. J. & BLUMENTHAL, R. S. 2010. Relation of C-reactive protein to abdominal adiposity. *Am J Cardiol,* 106**,** 56-61.

BRUHN, K. W., BIRNBAUM, R., HASKELL, J., VANCHINATHAN, V., GREGER, S., NARAYAN, R., CHANG, P. L., TRAN, T. A., HICKERSON, S. M., BEVERLEY, S. M., WILSON, M. E. & CRAFT, N. 2012. Killed but Metabolically Active Leishmania infantum as a Novel Whole-Cell Vaccine for Visceral Leishmaniasis. *Clinical and Vaccine Immunology,* 19**,** 490-498.

CAMOUS, L., ROUMENINA, L., BIGOT, S., BRACHEMI, S., FREMEAUX-BACCHI, V., LESAVRE, P. & HALBWACHS-MECARELLI, L. 2011. Complement alternative pathway acts as a positive feedback amplification of neutrophil activation. *Blood,* 117**,** 1340-1349.

CASTELLANO, G., WOLTMAN, A. M., SCHLAGWEIN, N., XU, W., SCHENA, F. P., DAHA, M. R. & VAN KOOTEN, C. 2007. Immune modulation of human dendritic cells by complement. *Eur J Immunol,* 37**,** 2803-11.

CECILIO, P., PEREZ-CABEZAS, B., SANTAREM, N., MACIEL, J., RODRIGUES, V. & CORDEIRO DA SILVA, A. 2014. Deception and manipulation: the arms of leishmania, a successful parasite. *Front Immunol,* 5**,** 480.

CHEN, C. B. & WALLIS, R. 2001. Stoichiometry of complexes between mannose-binding protein and its associated serine proteases - Defining functional units for complement activation. *Journal of Biological Chemistry,* 276**,** 25894-25902.

CHEN, C. B. & WALLIS, R. 2004. Two mechanisms for mannose-binding protein modulation of the activity of its associated serine proteases. *J Biol Chem,* 279**,** 26058-65.

CHUNG, H. L., FENG, L. C. & FENG, S. L. 1950. Observations concerning the successful transmission of kala-azar in North China by the bites of naturally infected Phlebotomus chinensis. *Peking Natural History Bulletin* 19**,** 302-26.

CLABORN, D. M. 2010. The biology and control of leishmaniasis vectors. *J Glob Infect Dis,* 2**,** 127-34.

CLARKE, E. V., WEIST, B. M., WALSH, C. M. & TENNER, A. J. 2015. Complement protein C1q bound to apoptotic cells suppresses human macrophage and dendritic cell-mediated Th17 and Th1 T cell subset proliferation. *J Leukoc Biol,* 97**,** 147-60.

COBB, B. A. & KASPER, D. L. 2005. Coming of age: carbohydrates and immunity. *Eur J Immunol,* 35**,** 352-6.

COLER, R. N., SKEIKY, Y. A. W., BERNARDS, K., GREESON, K., CARTER, D., CORNELLISON, C. D., MODABBER, F., CAMPOS-NETO, A. & REED, S. G. 2002. Immunization with a polyprotein vaccine consisting of the T-cell antigens thiol-specific antioxidant, Leishmania major stress-inducible protein 1, and Leishmania elongation initiation factor protects against leishmaniasis. *Infection and Immunity,* 70**,** 4215-4225.

CONVIT, J., CASTELLANOS, P. L., RONDON, A., PINARDI, M. E., ULRICH, M., CASTES, M., BLOOM, B. & GARCIA, L. 1987. Immunotherapy versus chemotherapy in localised cutaneous leishmaniasis. *Lancet,* 1**,** 401-5.

COULTHARD, L. G. & WOODRUFF, T. M. 2015. Is the complement activation product C3a a proinflammatory molecule? Re-evaluating the evidence and the myth. *J Immunol,* 194**,** 3542-8.

COX, N., PILLING, D. & GOMER, R. H. 2015. DC-SIGN activation mediates the differential effects of SAP and CRP on the innate immune system and inhibits fibrosis in mice. *Proc Natl Acad Sci U S A,* 112**,** 8385-90.

CRAY, C., ZAIAS, J. & ALTMAN, N. H. 2009. Acute Phase Response in Animals: A Review. *Comparative Msedicine,* 59**,** 517–526.

CULLEY, F. J., BODMAN-SMITH, K. B., FERGUSON, M. A., NIKOLAEV, A. V., SHANTILAL, N. & RAYNES, J. G. 2000. C-reactive protein binds to phosphorylated carbohydrates. *Glycobiology,* 10**,** 59-65.

CULLEY, F. J., HARRIS, R. A., KAYE, P. M., MCADAM, K. P. W. J. & RAYNES, J. G. 1996. C-reactive protein binds to a novel ligand on Leishmania donovani and increases uptake into human macrophages. *Journal of Immunology,* 156**,** 4691-4696.

DAHL, M. R., THIEL, S., MATSUSHITA, M., FUJITA, T., WILLIS, A. C., CHRISTENSEN, T., VORUP-JENSEN, T. & JENSENIUS, J. C. 2001. MASP-3 and its association with distinct complexes of the mannan-binding lectin complement activation pathway. *Immunity,* 15**,** 127-35.

DAS, T., SEN, A. K., KEMPF, T., PRAMANIK, S. R., MANDAL, C. & MANDAL, C. 2003. Induction of glycosylation in human C-reactive protein under different pathological conditions. *Biochem J,* 373**,** 345-55.

DAVIS, B. S., CHANG, G. J. J., CROPP, B., ROEHRIG, J. T., MARTIN, D. A., MITCHELL, C. J., BOWEN, R. & BUNNING, M. L. 2001. West Nile virus recombinant DNA vaccine protects mouse and horse from virus challenge and expresses in vitro a noninfectious recombinant antigen that can be used in enzyme-linked immunosorbent assays. *Journal of Virology,* 75**,** 4040-4047.

DE BEER, F. C., BALTZ, M. L., HOLFORD, S., FEINSTEIN, A. & PEPYS, M. B. 1981. Fibronectin and C4-binding protein are selectively bound by aggregated amyloid P component. *J Exp Med,* 154**,** 1134-9.

DE BEER, F. C., BALTZ, M. L., MUNN, E. A., FEINSTEIN, A., TAYLOR, J., BRUTON, C., CLAMP, J. R. & PEPYS, M. B. 1982. Isolation and characterization of C-reactive protein and serum amyloid P component in the rat. *Immunology,* 45**,** 55-70.

DE HAAS, C. J., VAN LEEUWEN, E. M., VAN BOMMEL, T., VERHOEF, J., VAN KESSEL, K. P. & VAN STRIJP, J. A. 2000. Serum amyloid P component bound to gram-negative bacteria prevents lipopolysaccharide-mediated classical pathway complement activation. *Infect Immun,* 68**,** 1753-9.

DE HAAS, C. J. C. 1999. New insights into the role of serum amyloid P component, a novel lipopolysaccharide-binding protein. *Fems Immunology and Medical Microbiology,* 26**,** 197-202.

DEBEER, F. C. & PEPYS, M. B. 1982. Isolation of Human C-Reactive Protein and Serum Amyloid P Component. *Journal of Immunological Methods,* 50**,** 17-31.

DHALIWAL, J. S. & LIEW, F. Y. 1987. Induction of delayed-type hypersensitivity to Leishmania major and the concomitant acceleration of disease development in progressive murine cutaneous leishmaniasis. *Infect Immun,* 55**,** 645-51.

DI NAPOLI, M., SLEVIN, M., POPA-WAGNER, A., SINGH, P., LATTANZI, S. & DIVANI, A. A. 2018. Monomeric C-Reactive Protein and Cerebral Hemorrhage: From Bench to Bedside. *Front Immunol,* 9**,** 1921.

DOBO, J., SZAKACS, D., OROSZLAN, G., KORTVELY, E., KISS, B., BOROS, E., SZASZ, R., ZAVODSZKY, P., GAL, P. & PAL, G. 2016. MASP-3 is the exclusive pro-factor D activator in resting blood: the lectin and the alternative complement pathways are fundamentally linked. *Scientific Reports,* 6.

DOSTALOVA, A., VOTYPKA, J., FAVREAU, A. J., BARBIAN, K. D., VOLF, P., VALENZUELA, J. G. & JOCHIM, R. C. 2011. The midgut transcriptome of Phlebotomus (Larroussius) perniciosus, a vector of Leishmania infantum: comparison of sugar fed and blood fed sand flies. *BMC Genomics,* 12**,** 223.

DU CLOS, T. W. 2013. Pentraxins: structure, function, and role in inflammation. *ISRN Inflamm,* 2013**,** 379040.

DUNKELBERGER, J. R. & SONG, W. C. 2010. Complement and its role in innate and adaptive immune responses. *Cell Res,* 20**,** 34-50.

EASON, R. J., BELL, K. S., MARSHALL, F. A., RODGERS, D. T., PINEDA, M. A., STEIGER, C. N., AL-RIYAMI, L., HARNETT, W. & HARNETT, M. M. 2016. The helminth product, ES-62 modulates dendritic cell responses by inducing the selective autophagolysosomal degradation of TLR-transducers, as exemplified by PKCdelta. *Sci Rep,* 6**,** 37276.

EHRENGRUBER, M. U., GEISER, T. & DERANLEAU, D. A. 1994. Activation of human neutrophils by C3a and C5A Comparison of the effects on shape changes, chemotaxis, secretion, and respiratory burst. *FEBS Letters,* 346**,** 181-184.

EHRNTHALLER, C., IGNATIUS, A., GEBHARD, F. & HUBER-LANG, M. 2011. New insights of an old defense system: structure, function, and clinical relevance of the complement system. *Mol Med,* 17**,** 317-29.

EILAM, Y., EL-ON, J. & SPIRA, D. T. 1985. Leishmania major: excreted factor, calcium ions, and the survival of amastigotes. *Exp Parasitol,* 59**,** 161-8.

EMSLEY, J., WHITE, H. E., O'HARA, B. P., OLIVA, G., SRINIVASAN, N., TICKLE, I. J., BLUNDELL, T. L., PEPYS, M. B. & WOOD, S. P. 1994. Structure of pentameric human serum amyloid P component. *Nature,* 367**,** 338-45.

ENDOA, Y., MATSUSHITA, M. & FUJITA, T. 2011. The role of ficolins in the lectin pathway of innate immunity. *The International Journal of Biochemistry & Cell Biology,* 43**,** 705–712.

FEIJO, D., TIBURCIO, R., AMPUERO, M., BRODSKYN, C. & TAVARES, N. 2016. Dendritic Cells and Leishmania Infection: Adding Layers of Complexity to a Complex Disease. *J Immunol Res,* 2016**,** 3967436.

FILARDY, A. A., PIRES, D. R., NUNES, M. P., TAKIYA, C. M., FREIRE-DE-LIMA, C. G., RIBEIRO-GOMES, F. L. & DOSREIS, G. A. 2010. Proinflammatory clearance of apoptotic neutrophils induces an IL-12(low)IL-10(high) regulatory phenotype in macrophages. *J Immunol,* 185**,** 2044-50.

FRANKE, E. D., MCGREEVY, P. B., KATZ, S. P. & SACKS, D. L. 1985. Growth cycle-dependent generation of complement-resistant Leishmania promastigotes. *J Immunol,* 134**,** 2713-8.

FRASCH, C. E. & CONCEPCION, N. F. 2000. Specificity of human antibodies reactive with pneumococcal C polysaccharide. *Infect Immun,* 68**,** 2333-7.

FUJITA, T. 2002. Evolution of the lectin–complement pathway and its role in innate immunity. *Nat Rev Immunol,* 2**,** 346–353.

GABORIAUD, C., JUANHUIX, J., GRUEZ, A., LACROIX, M., DARNAULT, C., PIGNOL, D., VERGER, D., FONTECILLA-CAMPS, J. C. & ARLAUD, G. J. 2003. The crystal structure of the globular head of complement protein C1q provides a basis for its versatile recognition properties. *J Biol Chem,* 278**,** 46974-82.

GARRED, P., LARSEN, F., SEYFARTH, J., FUJITA, R. & MADSEN, H. O. 2006. Mannose-binding lectin and its genetic variants. *Genes and Immunity,* 7**,** 85–94.

GETTNER, H. R. R. S. S. S. 1969. Leishmania tropica, L. donovani and L. enriettii: Immune rabbit serum inhibitory in vitro. *Experimental Parasitology,* 26**,** 257-263.

GIDWANI, K., PICADO, A., RIJAL, S., SINGH, S. P., ROY, L., VOLFOVA, V., ANDERSEN, E. W., URANW, S., OSTYN, B., SUDARSHAN, M., CHAKRAVARTY, J., VOLF, P., SUNDAR, S., BOELAERT, M. & ROGERS, M. E. 2011. Serological markers of sand fly exposure to evaluate insecticidal nets against visceral leishmaniasis in India and Nepal: a cluster-randomized trial. *PLoS Negl Trop Dis,* 5**,** e1296.

GOLLOB, K. J., ANTONELLI, L. R. V. & DUTRA, W. O. 2005. Insights into CD4(+) memory T cells following Leishmania infection. *Trends in Parasitology,* 21**,** 347-350.

GOMER, R. H., PILLING, D., KAUVAR, L. M., ELLSWORTH, S., RONKAINEN, S. D., ROIFE, D. & DAVIS, S. C. 2009. A serum amyloid P-binding hydrogel speeds healing of partial thickness wounds in pigs. *Wound Repair Regen,* 17**,** 397-404.

GOODMAN, A. R., CARDOZO, T., ABAGYAN, R., ALTMEYER, A., WISNIEWSKI, H. G. & VILCEK, J. 1996. Long pentraxins: an emerging group of proteins with diverse functions. *Cytokine Growth Factor Rev,* 7**,** 191-202.

GOSSAGE, S. M., ROGERS, M. E. & BATES, P. A. 2003. Two separate growth phases during the development of Leishmania in sand flies: implications for understanding the life cycle. *Int J Parasitol.,* 33**,** 1027–1034.

GRIMALDI, G., JR., TEVA, A., DOS-SANTOS, C. B., SANTOS, F. N., PINTO, I. D., FUX, B., LEITE, G. R. & FALQUETO, A. 2017. Field trial of efficacy of the Leish-tec(R) vaccine against canine leishmaniasis caused by Leishmania infantum in an endemic area with high transmission rates. *PLoS One,* 12**,** e0185438.

GUIMARAES, A. C., NOGUEIRA, P. M., SILVA, S. O., SADLOVA, J., PRUZINOVA, K., HLAVACOVA, J., MELO, M. N. & SOARES, R. P. 2018. Lower galactosylation levels of the Lipophosphoglycan from Leishmania (Leishmania) major-like strains affect interaction with Phlebotomus papatasi and Lutzomyia longipalpis. *Mem Inst Oswaldo Cruz,* 113**,** e170333.

GUPTA, G., OGHUMU, S. & SATOSKAR, A. R. 2013. Mechanisms of immune evasion in leishmaniasis. *Adv Appl Microbiol,* 82**,** 155-84.

HAJISHENGALLIS, G. & RUSSELL, M. W. 2015. Innate Humoral Defense Factors. *Mucosal Immunology***,** 251–70.

HANDMAN, E., MCCONVILLE, M. J. & GODING, J. W. 1987. Carbohydrate Antigens as Possible Parasite Vaccines - a Case for the Leishmania Glycolipid. *Immunology Today,* 8**,** 181-185.

HARNETT, W. & HARNETT, M. M. 2006. Filarial nematode secreted product ES-62 is an anti-inflammatory agent: therapeutic potential of small molecule derivatives and ES-62 peptide mimetics. *Clin Exp Pharmacol Physiol,* 33**,** 511-8.

HARNETT†, W. H. A. M. M. 2006. FILARIAL NEMATODE SECRETED PRODUCT ES-62 IS AN ANTIINFLAMMATORY AGENT: THERAPEUTIC POTENTIAL OF SMALL MOLECULE DERIVATIVES AND ES-62 PEPTIDE

MIMETICS. *Clinical and Experimental Pharmacology and Physiology,* 33**,** 511-518.

HASSANI, K., SHIO, M. T., MARTEL, C., FAUBERT, D. & OLIVIER, M. 2014. Absence of metalloprotease GP63 alters the protein content of Leishmania exosomes. *PLoS One,* 9**,** e95007.

HEINZEL, F. P., SADICK, M. D., HOLADAY, B. J., COFFMAN, R. L. & LOCKSLEY, R. M. 1989. Reciprocal expression of interferon gamma or interleukin 4 during the resolution or progression of murine leishmaniasis. Evidence for expansion of distinct helper T cell subsets. *J Exp Med,* 169**,** 59-72.

HEJA, D., KOCSIS, A., DOBO, J., SZILAGYI, K., SZASZ, R., ZAVODSZKY, P., PAL, G. & GAL, P. 2012. Revised mechanism of complement lectin-pathway activation revealing the role of serine protease MASP-1 as the exclusive activator of MASP-2. *Proceedings of the National Academy of Sciences of the United States of America,* 109**,** 10498-10503.

HEWITSON, J. P., GRAINGER, J. R. & MAIZELS, R. M. 2009. Helminth immunoregulation: the role of parasite secreted proteins in modulating host immunity. *Mol Biochem Parasitol,* 167**,** 1-11.

HOFFMAN, W., LAKKIS, F. G. & CHALASANI, G. 2016. B Cells, Antibodies, and More. *Clinical journal of the American Society of Nephrology* 11**,** 137-154.

HOMANS, S. W., MEHLERT, A. & TURCO, S. J. 1992. Solution structure of the lipophosphoglycan of Leishmania donovani. *Biochemistry,* 31**,** 654-61.

HUTCHINSON, W. L., HOHENESTER, E. & PEPYS, M. B. 2000. Human serum amyloid P component is a single uncomplexed pentamer in whole serum. *Molecular Medicine,* 6**,** 482-493.

ILG, T. 2000a. Lipophosphoglycan is not required for infection of macrophages or mice by *Leishmania mexicana*. *EMBO J,* 19**,** 1953-62.

ILG, T. 2000b. Proteophosphoglycans of Leishmania. *Parasitol Today,* 16**,** 489-97.

ILG, T., DEMAR, M. & HARBECKE, D. 2001. Phosphoglycan repeat-deficient Leishmania mexicana parasites remain infectious to macrophages and mice. *J Biol Chem,* 276**,** 4988-97.

ILG, T., ETGES, R., OVERATH, P., MCCONVILLE, M. J., THOMAS-OATES, J., THOMAS, J., HOMANS, S. W. & FERGUSON, M. A. 1992. Structure of Leishmania mexicana lipophosphoglycan. *J Biol Chem,* 267**,** 6834-40.

ILG, T., HANDMAN, E., NG, K., STIERHOF, Y. D. & BACIC, A. 1999. Mucin-like proteophosphoglycans from the protozoan parasite Leishmania. *Trends in Glycoscience and Glycotechnology,* 11**,** 53-71.

ILG, T., MENZ, B., WINTER, G., RUSSELL, D. G., ETGES, R., SCHELL, D. & OVERATH, P. 1991a. Monoclonal antibodies to Leishmania mexicana promastigote antigens. I. Secreted acid phosphatase and other proteins share epitopes with lipophosphoglycan. *J Cell Sci,* 99**,** 175-80.

ILG, T., OVERATH, P., FERGUSON, M. A., RUTHERFORD, T., CAMPBELL, D. G. & MCCONVILLE, M. J. 1994. O- and N-glycosylation of the Leishmania mexicana-secreted acid phosphatase. Characterization of a new class of phosphoserine-linked glycans. *J Biol Chem,* 269**,** 24073-81.

ILG, T., STIERHOF, Y. D., CRAIK, D., SIMPSON, R., HANDMAN, E. & BACIC, A. 1996. Purification and structural characterization of a filamentous, mucin-like proteophosphoglycan secreted by Leishmania parasites. *J Biol Chem,* 271**,** 21583-96.

ILG, T., STIERHOF, Y. D., ETGES, R., ADRIAN, M., HARBECKE, D. & OVERATH, P. 1991b. Secreted acid phosphatase of Leishmania mexicana: A filamentous phosphoglycoprotein polymer. *Proceedings of the National Academy of Sciences,* 88.

ILG, T., STIERHOF, Y. D., MCCONVILLE, M. J. & OVERATH, P. 1995. Purification, partial characterization and immunolocalization of a proteophosphoglycan secreted by Leishmania mexicana amastigotes. *Eur J Cell Biol,* 66**,** 205-15.

ITABE, H., MORI, M., FUJIMOTO, Y., HIGASHI, Y. & TAKANO, T. 2003. Minimally modified LDL is an oxidized LDL enriched with oxidized phosphatidylcholines. *J Biochem,* 134**,** 459-65.

JI, S. R., WU, Y., ZHU, L., POTEMPA, L. A., SHENG, F. L., LU, W. & ZHAO, J. 2007. Cell membranes and liposomes dissociate C-reactive protein (CRP) to

form a new, biologically active structural intermediate: mCRPm. *FASEB J,* 21**,** 284-294.

JI, Z., KE, Z. J. & GENG, J. G. 2012. SAP suppresses the development of experimental autoimmune encephalomyelitis in C57BL/6 mice. *Immunol Cell Biol,* 90**,** 388-95.

JIANG, H. X., SIEGEL, J. N. & GEWURZ, H. 1991. Binding and Complement Activation by C-Reactive Protein Via the Collagen-Like Region of C1q and Inhibition of These Reactions by Monoclonal-Antibodies to C-Reactive Protein and C1q. *Journal of Immunology,* 146**,** 2324-2330.

JOSHI, M. B., MALLINSON, D. J. & DWYER, D. M. 2004. The human pathogen Leishmania donovani secretes a histidine acid phosphatase activity that is resistant to proteolytic degradation. *Journal of Eukaryotic Microbiology,* 51**,** 108-112.

JOSHI, P. B., SACKS, D. L., MODI, G. & MCMASTER, W. R. 1998. Targeted gene deletion of Leishmania major genes encoding developmental stage-specific leishmanolysin (GP63). *Mol Microbiol,* 27**,** 519-30.

KANESHIRO, E. S. & WYDER, M. A. 1993. Lipophosphoglycan antigen shedding by Leishmania donovani. *J Eukaryot Microbiol,* 40**,** 336-40.

KILLICK-KENDRICK, R. 1990. The life-cycle of Leishmania in the sandfly with special reference to the form infective to the vertebrate host. *Ann Parasitol Hum Comp,* 65 Suppl 1**,** 37-42.

KILLICK-KENDRICK, R., LEANEY, A. J., READY, P. D. & MOLYNEUX, D. H. 1977. Leishmania in phlebotomid sandflies. IV. The transmission of Leishmania mexicana amazonensis to hamsters by the bite of experimentally infected Lutzomyia longipalpis. *Proc R Soc Lond B Biol Sci,* 196**,** 105-15.

KIM, S. H., JIA, W., PARREIRA, V. R., BISHOP, R. E. & GYLES, C. L. 2006. Phosphoethanolamine substitution in the lipid A of Escherichia coli O157 : H7 and its association with PmrC. *Microbiology,* 152**,** 657-666.

KIMA, P. E. & SOONG, L. 2013. Interferon gamma in leishmaniasis. *Front Immunol,* 4**,** 156.

KOTTGEN, E., HELL, B., KAGE, A. & TAUBER, R. 1992. Lectin specificity and binding characteristics of human C-reactive protein. *J Immunol,* 149**,** 445-53.

KOUSER, L., ABDUL-AZIZ, M., NAYAK, A., STOVER, C. M., SIM, R. B. & KISHORE, U. 2013. Properdin and factor h: opposing players on the alternative complement pathway "see-saw". *Front Immunol,* 4**,** 93.

KOUSER, L., MADHUKARAN, S. P., SHASTRI, A., SARAON, A., FERLUGA, J., AL-MOZAINI, M. & KISHORE, U. 2015. Emerging and Novel Functions of Complement Protein C1q. *Front Immunol,* 6**,** 317.

KRISHNAN, L., GUILBERT, L. J., RUSSELL, A. S., WEGMANN, T. G., MOSMANN, T. R. & BELOSEVIC, M. 2020. Pregnancy impairs resistance of C57BL/6 mice to Leishmania major infection and causes decreased antigen-specific IFN-gamma response and increased production of T helper 2 cytokines. *The Journal of Immunology,* 156**,** 644-652.

LAEMMLI, U. K. 1970. Cleavage of structural proteins during the assembly of the head of bacteriophage T4. *Nature,* 227**,** 680-5.

LARVIE, M., SHOUP, T., CHANG, W.-C., CHIGWESHE, L., HARTSHORN, K., WHITE, M. R., STAHL, G. L., ELMALEH, D. R. & TAKAHASHI, K. 2012. Mannose-Binding Lectin Binds to Amyloid Protein and Modulates Inflammation. *Journal of Biomedicine and Biotechnology,* 2012**,** 1-12.

LASKAY, T., VAN ZANDBERGEN, G. & SOLBACH, W. 2003. Neutrophil granulocytes--Trojan horses for Leishmania major and other intracellular microbes? *Trends Microbiol,* 11**,** 210-4.

LAUFS, H., MULLER, K., FLEISCHER, J., REILING, N., JAHNKE, N., JENSENIUS, J. C., SOLBACH, W. & LASKAY, T. 2002. Intracellular survival of Leishmania major in neutrophil granulocytes after uptake in the absence of heat-labile serum factors. *Infect Immun,* 70**,** 826-35.

LAURENTI, M. D., ORN, A., SINHORINI, I. L. & CORBETT, C. E. P. 2004. The role of complement in the early phase of Leishmania (Leishmania) amazonensis infection in BALB/c mice. *Brazilian Journal of Medical and Biological Research,* 37**,** 427-434.

LIPPERT, D. N., DWYER, D. W., LI, F. & OLAFSON, R. W. 1999. Phosphoglycosylation of a secreted acid phosphatase from Leishmania donovani. *Glycobiology,* 9**,** 627-36.

LOVELACE, J. K. & GOTTLIEB, M. 1986. Comparison of Extracellular Acid-Phosphatases from Various Isolates of Leishmania. *American Journal of Tropical Medicine and Hygiene,* 35**,** 1121-1128.

LOVELESS, R. W., FLOYD-O'SULLIVAN, G., RAYNES, J. G., C.T., Y. & FEIZI, T. 1992. Human Serum Amyloid P Is a Multispecific Adhesive Protein Whose Ligands Include 6-phosphorylated Mannose and the 3-sulphated Saccharides Galactose, N-acetylgalactosamine and Glucuronic Acid. *EMBO J. ,* 11**,** 813-819.

LUMB, F. E., DOONAN, J., BELL, K. S., PINEDA, M. A., CORBET, M., SUCKLING, C. J., HARNETT, M. M. & HARNETT, W. 2017. Dendritic cells provide a therapeutic target for synthetic small molecule analogues of the parasitic worm product, ES-62. *Sci Rep,* 7**,** 1704.

MA, Y. J., SKJOEDT, M. O. & GARRED, P. 2013. Collectin-11/MASP complex formation triggers activation of the lectin complement pathway--the fifth lectin pathway initiation complex. *J Innate Immun,* 5**,** 242-50.

MAEKAWA, Y., HIMENO, K., ISHIKAWA, H., HISAEDA, H., SAKAI, T., DAINICHI, T., ASAO, T., GOOD, R. A. & KATUNUMA, N. 1998. Switch of CD4(+) T cell differentiation from Th2 to Th1 by treatment with cathepsin B inhibitor in experimental Leishmaniasis. *Journal of Immunology,* 161**,** 2120-2127.

MAHONEY, A. B., SACKS, D. L., SARAIVA, E., MODI, G. & TURCO, S. J. 1999. Intra-species and stage-specific polymorphisms in lipophosphoglycan structure control Leishmania donovani-sand fly interactions. *Biochemistry,* 38**,** 9813-23.

MASUKO, T., MINAMI, A., IWASAKI, N., MAJIMA, T., NISHIMURA, S. & LEE, Y. C. 2005. Carbohydrate analysis by a phenol-sulfuric acid method in microplate format. *Anal Biochem,* 339**,** 69-72.

MATSUSHITA, M. 2013. Ficolins in complement activation. *Mol Immunol,* 55**,** 22-6.

MATTE, C. & OLIVIER, M. 2002. Leishmania-induced cellular recruitment during the early inflammatory response: modulation of proinflammatory mediators. *J Infect Dis,* 185**,** 673-81.

MAYRINK, W., DA COSTA, C. A., MAGALHAES, P. A., MELO, M. N., DIAS, M., LIMA, A. O., MICHALICK, M. S. & WILLIAMS, P. 1979. A field trial of a vaccine against American dermal leishmaniasis. *Trans R Soc Trop Med Hyg,* 73**,** 385-7.

MBUCHI, M., BATES, P. A., ILG, T., COE, J. E. & RAYNES, J. G. 2006. C-reactive protein initiates transformation of Leishmania donovani and L-mexicana through binding to lipophosphoglycan. *Molecular and Biochemical Parasitology,* 146**,** 259-264.

MCCONVILLE, M. J., BACIC, A., MITCHELL, G. F. & HANDMAN, E. 1987. Lipophosphoglycan of Leishmania-Major That Vaccinates against Cutaneous Leishmaniasis Contains an Alkylglycerophosphoinositol Lipid Anchor. *Proceedings of the National Academy of Sciences of the United States of America,* 84**,** 8941-8945.

MCCONVILLE, M. J. & FERGUSON, M. A. 1993. The structure, biosynthesis and function of glycosylated phosphatidylinositols in the parasitic protozoa and higher eukaryotes. *Biochem J,* 294 (Pt 2)**,** 305-24.

MCCONVILLE, M. J., SCHNUR, L. F., JAFFE, C. & SCHNEIDER, P. 1995. Structure of Leishmania lipophosphoglycan: inter- and intra-specific polymorphism in Old World species. *Biochem J,* 310 (Pt 3)**,** 807-18.

MCCONVILLE, M. J., TURCO, S. J., FERGUSON, M. A. & SACKS, D. L. 1992. Developmental modification of lipophosphoglycan during the differentiation of Leishmania major promastigotes to an infectious stage. *EMBO J,* 11**,** 3593-600.

MCMAHON-PRATT , D. & ALEXANDER, J. 2004. Does the Leishmania major paradigm of pathogenesis and protection hold for New World cutaneous leishmaniasis or the visceral disease? *Immunol. Rev. ,* 201**,** 206–224.

MCSORLEY, H. J. & MAIZELS, R. M. 2012. Helminth infections and host immune regulation. *Clin Microbiol Rev,* 25**,** 585-608.

MELDRUM, O. W., YAKUBOV, G. E., BONILLA, M. R., DESHMUKH, O., MCGUCKIN, M. A. & GIDLEY, M. J. 2018. Mucin gel assembly is controlled by a collective action of non-mucin proteins, disulfide bridges, Ca(2+)-mediated links, and hydrogen bonding. *Sci Rep,* 8**,** 5802.

MEYER-FERNANDES, M. A. V.-S. A. J. R. July 1995. Leishmanial PKC modulate host cell infection via secreted acid phosphatase. *European Journal of Cell Biology*.

MIKOLAJEK, H., KOLSTOE, S. E., PYE, V. E., MANGIONE, P., PEPYS, M. B. & WOOD, S. P. 2011. Structural basis of ligand specificity in the human pentraxins, C-reactive protein and serum amyloid P component. *J Mol Recognit,* 24**,** 371-7.

MODABBER, F. 1995. Vaccines against leishmaniasis. *Ann Trop Med Parasitol,* 89 Suppl 1**,** 83-8.

MOLD, C., GEWURZ, H. & DU CLOS, T. W. 1999. Regulation of complement activation by C-reactive protein. *Immunopharmacology,* 42**,** 23-30.

MOLENAAR, E. T., VOSKUYL, A. E., FAMILIAN, A., VAN MIERLO, G. J., DIJKMANS, B. A. & HACK, C. E. 2001. Complement activation in patients with rheumatoid arthritis mediated in part by C-reactive protein. *Arthritis Rheum,* 44**,** 997-1002.

MOLINS, B., FUENTES-PRIOR, P., ADAN, A., ANTON, R., AROSTEGUI, J. I., YAGUE, J. & DICK, A. D. 2016. Complement factor H binding of monomeric C-reactive protein downregulates proinflammatory activity and is impaired with at risk polymorphic CFH variants. *Scientific Reports,* 6.

MOLLER-KRISTENSEN, M., THIEL, S., SJOHOLM, A., MATSUSHITA, M. & JENSENIUS, J. C. 2007. Cooperation between MASP-1 and MASP-2 in the generation of C3 convertase through the MBL pathway. *Int Immunol,* 19**,** 141-9.

MOLLINEDO, F., JANSSEN, H., DE LA IGLESIA-VICENTE, J., VILLA-PULGARIN, J. A. & CALAFAT, J. 2010. Selective fusion of azurophilic granules with Leishmania-containing phagosomes in human neutrophils. *J Biol Chem,* 285**,** 34528-36.

MONOD, J., WYMAN, J. & CHANGEUX, J. P. 1965. On the Nature of Allosteric Transitions: A Plausible Model. *J Mol Biol,* 12**,** 88-118.

MOSSER, D. M., BURKE, S. K., COUTAVAS, E. E., WEDGWOOD, J. F. & EDELSON, P. J. 1986. Leishmania species: mechanisms of complement activation by five strains of promastigotes. *Exp Parasitol,* 62**,** 394-404.

MUKBEL, R. M. 2005. Leishmania amazonensis and macrophage interactions: immune factors necessary to kill the parasite. *Iowa State University: Retrospective Theses and Dissertations,* 1841.

MUKHOPADHYAY, S. & MANDAL, C. 2006. Glycobiology of Leishmania donovani. *Indian J Med Res,* 123**,** 203-20.

MULLER, I. B., KNOCKEL, J., ESCHBACH, M. L., BERGMANN, B., WALTER, R. D. & WRENGER, C. 2010. Secretion of an acid phosphatase provides a possible mechanism to acquire host nutrients by Plasmodium falciparum. *Cell Microbiol,* 12**,** 677-91.

MULLER, K., VAN ZANDBERGEN, G., HANSEN, B., LAUFS, H., JAHNKE, N., SOLBACH, W. & LASKAY, T. 2001. Chemokines, natural killer cells and granulocytes in the early course of Leishmania major infection in mice. *Med Microbiol Immunol,* 190**,** 73-6.

MURRAY, L. A., KRAMER, M. S., HESSON, D. P., WATKINS, B. A., FEY, E. G., ARGENTIERI, R. L., SHAHEEN, F., KNIGHT, D. A. & SONIS, S. T. 2010. Serum amyloid P ameliorates radiation-induced oral mucositis and fibrosis. *Fibrogenesis Tissue Repair,* 3**,** 11.

NAIK-MATHURIA, B., PILLING, D., CRAWFORD, J. R., GAY, A. N., SMITH, C. W., GOMER, R. H. & OLUTOYE, O. O. 2008. Serum amyloid P inhibits dermal wound healing. *Wound Repair Regen,* 16**,** 266-73.

NAUSER, C. L., HOWARD, M. C., FANELLI, G., FARRAR, C. A. & SACKS, S. 2018. Collectin-11 (CL-11) Is a Major Sentinel at Epithelial Surfaces and Key Pattern Recognition Molecule in Complement-Mediated Ischaemic Injury. *Frontiers in Immunology,* 9.

NOURSADEGHI, M., BICKERSTAFF, M. C., GALLIMORE, J. R., HERBERT, J., COHEN, J. & PEPYS, M. B. 2000. Role of serum amyloid P component in

bacterial infection: protection of the host or protection of the pathogen. *Proc Natl Acad Sci U S A,* 97**,** 14584-9.

OKADA, H., KUHN, C., FEILLET, H. & BACH, J. F. 2010. The 'hygiene hypothesis' for autoimmune and allergic diseases: an update. *Clin Exp Immunol,* 160**,** 1-9.

OLIVEIRA, F., JOCHIM, R. C., VALENZUELA, J. G. & KAMHAWI, S. 2009. Sand flies, Leishmania, and transcriptome-borne solutions. *Parasitol Int,* 58**,** 1-5.

OSHANNESSY, D. J., BRIGHAMBURKE, M., SONESON, K. K., HENSLEY, P. & BROOKS, I. 1993. Determination of Rate and Equilibrium Binding Constants for Macromolecular Interactions Using Surface-Plasmon Resonance - Use of Nonlinear Least-Squares Analysis-Methods. *Analytical Biochemistry,* 212**,** 457-468.

PALARASAH, Y., NIELSEN, C., SPROGOE, U., CHRISTENSEN, M. L., LILLEVANG, S., MADSEN, H. O., BYGUM, A., KOCH, C., SKJODT, K. & SKJOEDT, M. O. 2011. Novel assays to assess the functional capacity of the classical, the alternative and the lectin pathways of the complement system. *Clin Exp Immunol,* 164**,** 388-95.

PARRA, L. E., BORJA-CABRERA, G. P., SANTOS, F. N., SOUZA, L. O. P., PALATNIK-DE-SOUSA, C. B. & MENZ, I. 2007. Safety trial using the Leishmune (R) vaccine against canine visceral leishmaniasis in Brazil. *Vaccine,* 25**,** 2180-2186.

PASCHINGER, K. & WILSON, I. B. H. 2016. Analysis of zwitterionic and anionic N-linked glycans from invertebrates and protists by mass spectrometry. *Glycoconjugate Journal,* 33**,** 273-283.

PEPYS, M. B. 2018. The Pentraxins 1975–2018: Serendipity, Diagnostics and Drugs. *Frontiers in Immunology,* 9.

PEPYS, M. B., DASH, A. C. & ASHLEY, M. J. 1977. Isolation of C-reactive protein by affinity chromatography. *Clinical and experimental immunology,* 30**,** 32-37.

PEPYS, M. B., HERBERT, J., HUTCHINSON, W. L., TENNENT, G. A., LACHMANN, H. J., GALLIMORE, J. R., LOVAT, L. B., BARTFAI, T., ALANINE, A., HERTEL, C., HOFFMANN, T., JAKOB-ROETNE, R., NORCROSS, R. D., KEMP, J. A., YAMAMURA, K., SUZUKI, M., TAYLOR, G. W., MURRAY, S., THOMPSON, D., PURVIS, A., KOLSTOE, S., WOOD, S. P. & HAWKINS, P. N. 2002. Targeted pharmacological depletion of serum amyloid P component for treatment of human amyloidosis. *Nature,* 417**,** 254-9.

PEPYS, M. B., HIRSCHFIELD, G. M., TENNENT, G. A., GALLIMORE, J. R., KAHAN, M. C., BELLOTTI, V., HAWKINS, P. N., MYERS, R. M., SMITH, M. D., POLARA, A., COBB, A. J., LEY, S. V., AQUILINA, J. A., ROBINSON, C. V., SHARIF, I., GRAY, G. A., SABIN, C. A., JENVEY, M. C., KOLSTOE, S. E., THOMPSON, D. & WOOD, S. P. 2006. Targeting C-reactive protein for the treatment of cardiovascular disease. *Nature,* 440**,** 1217-21.

PEPYS, M. B., RADEMACHER, T. W., AMATAYAKUL-CHANTLER, S., WILLIAMS, P., NOBLE, G. E., HUTCHINSON, W. L., HAWKINS, P. N., NELSON, S. R., GALLIMORE, J. R., HERBERT, J. & ET AL. 1994. Human serum amyloid P component is an invariant constituent of amyloid deposits and has a uniquely homogeneous glycostructure. *Proc Natl Acad Sci U S A,* 91**,** 5602-6.

PETERS, C., KAWAKAMI, M., KAUL, M., ILG, T., OVERATH, P. & AEBISCHER, T. 1997. Secreted proteophosphoglycan of Leishmania mexicana amastigotes activates complement by triggering the mannan binding lectin pathway. *Eur J Immunol,* 27**,** 2666-72.

PETERS, N. C., EGEN, J. G., SECUNDINO, N., DEBRABANT, A., KIMBLIN, N., KAMHAWI, S., LAWYER, P., FAY, M. P., GERMAIN, R. N. & SACKS, D. 2008. In vivo imaging reveals an essential role for neutrophils in leishmaniasis transmitted by sand flies. *Science,* 321**,** 970-4.

PILLING, D. & GOMER, R. H. 2018. The Development of Serum Amyloid P as a Possible Therapeutic. *Front Immunol,* 9**,** 2328.

PILLING, D., ROIFE, D., WANG, M., RONKAINEN, S. D., CRAWFORD, J. R., TRAVIS, E. L. & GOMER, R. H. 2007. Reduction of bleomycin-induced pulmonary fibrosis by serum amyloid P. *J Immunol,* 179**,** 4035-44.

PINEDA, M. A., AL-RIYAMI, L., HARNETT, W. & HARNETT, M. M. 2014. Lessons from helminth infections: ES-62 highlights new interventional approaches in rheumatoid arthritis. *Clin Exp Immunol,* 177**,** 13-23.

POMPEU, M. L., FREITAS, L. A., SANTOS, M. L. V., KHOURI, M. & BARRAL-NETTO, M. 1991. Granulocytes in the inflammatory process of BALB/c mice infected by Leishmania amazonensis. A quantitative approach. *Acta Tropica,* 48**,** 185-193.

POSTIGO, J. A. R. 2020. *Clinical Forms of the Leishmaniases* [Online]. https://www.who.int/leishmaniasis/disease/clinical_forms_leishmaniases/en/: World Health Organisation. [Accessed 15.2.20 2020].

POTEMPA, L. A., SIEGEL, J. N., FIEDEL, B. A., POTEMPA, R. T. & GEWURZ, H. 1987. Expression, detection and assay of a neoantigen (Neo-CRP) associated with a free, human C-reactive protein subunit. *Mol Immunol,* 24**,** 531-41.

POTEMPA, L. A., SIEGEL, J. N. & GEWURZ, H. 1981. Binding reactivity of C-reactive protein for polycations. II. Modulatory effects of calcium and phosphocholine. *J Immunol,* 127**,** 1509-14.

POULSEN, E. T., PEDERSEN, K. W., MARZEDA, A. M. & ENGHILD, J. J. 2017. Serum Amyloid P Component (SAP) Interactome in Human Plasma Containing Physiological Calcium Levels. *Biochemistry,* 56**,** 896-902.

PRATES, D. B., ARAUJO-SANTOS, T., LUZ, N. F., ANDRADE, B. B., FRANCA-COSTA, J., AFONSO, L., CLARENCIO, J., MIRANDA, J. C., BOZZA, P. T., DOSREIS, G. A., BRODSKYN, C., BARRAL-NETTO, M., BORGES, V. M. & BARRAL, A. 2011. Lutzomyia longipalpis saliva drives apoptosis and enhances parasite burden in neutrophils. *J Leukoc Biol,* 90**,** 575-82.

PUENTES, S. M., SACKS, D. L., DA SILVA, R. P. & JOINER, K. A. 1988. Complement binding by two developmental stages of Leishmania major promastigotes varying in expression of a surface lipophosphoglycan. *J Exp Med,* 167**,** 887-902.

PUGLISI, M. J. & FERNANDEZ, M. L. 2008. Modulation of C-reactive protein, tumor necrosis factor-alpha, and adiponectin by diet, exercise, and weight loss. *J Nutr,* 138**,** 2293-6.

RAMALHO-ORTIGAO, M., JOCHIM, R. C., ANDERSON, J. M., LAWYER, P. G., PHAM, V. M., KAMHAWI, S. & VALENZUELA, J. G. 2007. Exploring the midgut transcriptome of Phlebotomus papatasi: comparative analysis of expression profiles of sugar-fed, blood-fed and Leishmania-major-infected sandflies. *BMC Genomics,* 8**,** 300.

RAYNES, J. G. 1994. The acute phase response. *Biochem Soc Trans,* 22**,** 69-74.

RAYNES, J. G., CURRY, A. & HARRIS, R. A. 1994. Binding of C-reactive protein to Leishmania. *Biochem Soc Trans,* 22**,** 3S.

REITHINGER, R., DUJARDIN, J. C., LOUZIR, H., PIRMEZ, C., ALEXANDER, B. & BROOKER, S. 2007. Cutaneous leishmaniasis. *Lancet Infect Dis,* 7**,** 581-596.

REN, Y., DING, Q. & ZHANG, X. 2014. Ficolins and infectious diseases. *Virol Sin,* 29**,** 25-32.

RHEA N. COLER, Y. G., LISA BOGATZKI, VANITHA RAMAN, AND STEVEN G. REED 2007. Leish-111f, a Recombinant Polyprotein Vaccine That Protects againstVisceral Leishmaniasis by Elicitation of CD4 T Cells. *INFECTION AND IMMUNITY,* 75**,** 4648–4654.

RIBEIRO-GOMES, F. L., PETERS, N. C., DEBRABANT, A. & SACKS, D. L. 2012. Efficient capture of infected neutrophils by dendritic cells in the skin inhibits the early anti-leishmania response. *PLoS Pathog,* 8**,** e1002536.

RIBEIRO-GOMES, F. L., ROMANO, A., LEE, S., ROFFE, E., PETERS, N. C., DEBRABANT, A. & SACKS, D. 2015. Apoptotic cell clearance of Leishmania major-infected neutrophils by dendritic cells inhibits CD8(+) T-cell priming in vitro by Mer tyrosine kinase-dependent signaling. *Cell Death Dis,* 6**,** e2018.

RICHARDS, D. B., COOKSON, L. M., BERGES, A. C., BARTON, S. V., LANE, T., RITTER, J. M., FONTANA, M., MOON, J. C., PINZANI, M., GILLMORE, J.

D., HAWKINS, P. N. & PEPYS, M. B. 2015. Therapeutic Clearance of Amyloid by Antibodies to Serum Amyloid P Component. *N Engl J Med,* 373**,** 1106-14.

RIDKER, P. M. 2003. Clinical application of C-reactive protein for cardiovascular disease detection and prevention. *Circulation,* 107**,** 363-9.

RITTER, U., FRISCHKNECHT, F. & VAN ZANDBERGEN, G. 2009. Are neutrophils important host cells for Leishmania parasites? *Trends Parasitol,* 25**,** 505-10.

ROGERS, M., KROPF, P., CHOI, B. S., DILLON, R., PODINOVSKAIA, M., BATES, P. & MULLER, I. 2009. Proteophosophoglycans regurgitated by Leishmania-infected sand flies target the L-arginine metabolism of host macrophages to promote parasite survival. *PLoS Pathog,* 5**,** e1000555.

ROGERS, M. E. 2012. The role of leishmania proteophosphoglycans in sand fly transmission and infection of the Mammalian host. *Front Microbiol,* 3**,** 223.

ROGERS, M. E., CHANCE, M. L. & BATES, P. A. 2002. The role of promastigote secretory gel in the origin and transmission of the infective stage of Leishmania mexicana by the sandfly Lutzomyia longipalpis. *Parasitology,* 124**,** 495-507.

ROGERS, M. E., CORWARE, K., MULLER, I. & BATES, P. A. 2010. Leishmania infantum proteophosphoglycans regurgitated by the bite of its natural sand fly vector, Lutzomyia longipalpis, promote parasite establishment in mouse skin and skin-distant tissues. *Microbes Infect,* 12**,** 875-9.

ROGERS, M. E., ILG, T., NIKOLAEV, A. V., FERGUSON, M. A. J. & BATES, P. A. 2004. Transmission of cutaneous leishmaniasis by sand flies is enhanced by regurgitation of fPPG. *Nature,* 430**,** 463-467.

ROOS, A., BOUWMAN, L. H., MUNOZ, J., ZUIVERLOON, T., FABER-KROL, M. C., FALLAUX-VAN DEN HOUTEN, F. C., KLAR-MOHAMAD, N., HACK, C. E., TILANUS, M. G. & DAHA, M. R. 2003. Functional characterization of the lectin pathway of complement in human serum. *Mol Immunol,* 39**,** 655-68.

ROUMENINA, L. T., RUSEVA, M. M., ZLATAROVA, A., GHAI, R., KOLEV, M., OLOVA, N., GADJEVA, M., AGRAWAL, A., BOTTAZZI, B., MANTOVANI, A., REID, K. B. M., KISHORE, U. & KOJOUHAROVA, M. S. 2006. Interaction of

C1q with IgG1, C-reactive protein and pentraxin 3: Mutational studies using recombinant globular head modules of human C1q A, B, and C chains. *Biochemistry,* 45**,** 4093-4104.

ROY, N., OHTANI, K., HIDAKA, Y., AMANO, Y., MATSUDA, Y., MORI, K., HWANG, I., INOUE, N. & WAKAMIYA, N. 2017. Three pentraxins C-reactive protein, serum amyloid p component and pentraxin 3 mediate complement activation using Collectin CL-P1. *Biochimica Et Biophysica Acta-General Subjects,* 1861**,** 1-14.

RUB, A., DEY, R., JADHAV, M., KAMAT, R., CHAKKARAMAKKIL, S., MAJUMDAR, S., MUKHOPADHYAYA, R. & SAHA, B. 2009. Cholesterol depletion associated with Leishmania major infection alters macrophage CD40 signalosome composition and effector function. *Nat Immunol,* 10**,** 273-80.

SACKS, D. L., MODI, G., ROWTON, E., SPATH, G., EPSTEIN, L., TURCO, S. J. & BEVERLEY, S. M. 2000. The role of phosphoglycans in Leishmania-sand fly interactions. *Proc Natl Acad Sci U S A,* 97**,** 406-11.

SACKS, D. L., PIMENTA, P. F. P., MCCONVILLE, M. J., SCHNEIDER, P. & TURCO, S. J. 1995. Stage-Specific Binding of Leishmania-Donovani to the Sand Fly Vector Midgut Is Regulated by Conformational-Changes in the Abundant Surface Lipophosphoglycan. *Journal of Experimental Medicine,* 181**,** 685-697.

SALAZAR, J., MARTINEZ, M. S., CHAVEZ-CASTILLO, M., NUNEZ, V., ANEZ, R., TORRES, Y., TOLEDO, A., CHACIN, M., SILVA, C., PACHECO, E., ROJAS, J. & BERMUDEZ, V. 2014. C-Reactive Protein: An In-Depth Look into Structure, Function, and Regulation. *Int Sch Res Notices,* 2014**,** 653045.

SALEH, M. T. & BELISLE, J. T. 2000. Secretion of an acid phosphatase (SapM) by Mycobacterium tuberculosis that is similar to eukaryotic acid phosphatases. *J Bacteriol,* 182**,** 6850-3.

SALEHI-SANGANI, G., MOHEBALI, M., JAJARMI, V., KHAMESIPOUR, A., BANDEHPOUR, M., MAHMOUDI, M. & ZAHEDI-ZAVARAM, H. 2019. Immunization against Leishmania major infection in BALB/c mice using a subunit-based DNA vaccine derived from TSA, LmSTI1, KMP11, and LACK predominant antigens. *Iran J Basic Med Sci,* 22**,** 1493-1501.

SANDRI, T. L., ANDRADE, F. A., LIDANI, K. C. F., EINIG, E., BOLDT, A. B. W., MORDMULLER, B., ESEN, M. & MESSIAS-REASON, I. J. 2019. Human collectin-11 (COLEC11) and its synergic genetic interaction with MASP2 are associated with the pathophysiology of Chagas Disease. *PLoS Negl Trop Dis,* 13**,** e0007324.

SANTER, D. M., WIEDEMAN, A. E., TEAL, T. H., GHOSH, P. & ELKON, K. B. 2012. Plasmacytoid dendritic cells and C1q differentially regulate inflammatory gene induction by lupus immune complexes. *J Immunol,* 188**,** 902-15.

SANTOS, I. K., COSTA, C. H., KRIEGER, H., FEITOSA, M. F., ZURAKOWSKI, D., FARDIN, B., GOMES, R. B., WEINER, D. L., HARN, D. A., EZEKOWITZ, R. A. & EPSTEIN, J. E. 2001. Mannan-binding lectin enhances susceptibility to visceral leishmaniasis. *Infect Immun,* 69**,** 5212-5.

SCAPINI, P., LAPINET-VERA, J. A., GASPERINI, S., CALZETTI, F., BAZZONI, F. & CASSATELLA, M. A. 2000. The neutrophil as a cellular source of chemokines. *Immunological Reviews,* 177**,** 195-203.

SCHLEIN, Y., JACOBSON, R. L. & MESSER, G. 1992. Leishmania infections damage the feeding mechanism of the sandfly vector and implement parasite transmission by bite. *Proc Natl Acad Sci U S A,* 89**,** 9944-8.

SCHULTE, W., BERNHAGEN, J. & BUCALA, R. 2013. Cytokines in sepsis: potent immunoregulators and potential therapeutic targets--an updated view. *Mediators Inflamm,* 2013**,** 165974.

SCHWAEBLE, W. J., LYNCH, N. J., CLARK, J. E., MARBER, M., SAMANI, N. J., ALI, Y. M., DUDLER, T., PARENT, B., LHOTTA, K., WALLIS, R., FARRAR, C. A., SACKS, S., LEE, H., ZHANG, M., IWAKI, D., TAKAHASHI, M., FUJITA, T., TEDFORD, C. E. & STOVER, C. M. 2011. Targeting of mannan-binding lectin-associated serine protease-2 confers protection from myocardial and gastrointestinal ischemia/reperfusion injury. *Proc Natl Acad Sci U S A,* 108**,** 7523-8.

SCOTECE, M., CONDE, J., GOMEZ, R., LOPEZ, V., PINO, J., GONZALEZ, A., LAGO, F., GOMEZ-REINO, J. J. & GUALILLO, O. 2012. Role of adipokines in atherosclerosis: interferences with cardiovascular complications in rheumatic diseases. *Mediators Inflamm,* 2012**,** 125458.

SHIH, H. H., ZHANG, S. W., CAO, W., HAHN, A., WANG, J., PAULSEN, J. E. & HARNISH, D. C. 2009. CRP is a novel ligand for the oxidized LDL receptor LOX-1. *American Journal of Physiology-Heart and Circulatory Physiology,* 296**,** H1643-H1650.

SIEGEL, J., OSMAND, A. P., WILSON, M. F. & GEWURZ, H. 1975. Interactions of C-reactive protein with the complement system. II. C-reactive protein-mediated consumption of complement by poly-L-lysine polymers and other polycations. *J Exp Med,* 142**,** 709-21.

SIMONS, J. P., LOEFFLER, J. M., AL-SHAWI, R., ELLMERICH, S., HUTCHINSON, W. L., TENNENT, G. A., PETRIE, A., RAYNES, J. G., DE SOUZA, J. B., LAWRENCE, R. A., READ, K. D. & PEPYS, M. B. 2014. C-reactive protein is essential for innate resistance to pneumococcal infection. *Immunology,* 142**,** 414-420.

SINGH, P., HOFFMANN, M., WOLK, R., SHAMSUZZAMAN, A. S. & SOMERS, V. K. 2007. Leptin induces C-reactive protein expression in vascular endothelial cells. *Arterioscler Thromb Vasc Biol,* 27**,** e302-7.

SJOBERG, A. P., TROUW, L. A. & BLOM, A. M. 2009. Complement activation and inhibition: a delicate balance. *Trends Immunol,* 30**,** 83-90.

SJOBERG, A. P., TROUW, L. A., MCGRATH, F. D., HACK, C. E. & BLOM, A. M. 2006. Regulation of complement activation by C-reactive protein: targeting of the inhibitory activity of C4b-binding protein. *J Immunol,* 176**,** 7612-20.

SOARES, R. P., MACEDO, M. E., ROPERT, C., GONTIJO, N. F., ALMEIDA, I. C., GAZZINELLI, R. T., PIMENTA, P. F. & TURCO, S. J. 2002. Leishmania chagasi: lipophosphoglycan characterization and binding to the midgut of the sand fly vector Lutzomyia longipalpis. *Mol Biochem Parasitol,* 121**,** 213-24.

SONA, M., SANTIAGO-SCHWARZA, F., AL-ABEDC, Y. & DIAMOND, B. 2012. C1q limits dendritic cell differentiation and activation by engaging LAIR-1. *PNAS,* 109**,** E3160–E3167.

SORENSEN, I. J., ANDERSEN, O., NIELSEN, E. H. & SVEHAG, S. E. 1995. Native Human Serum Amyloid P-Component Is a Single Pentamer. *Scandinavian Journal of Immunology,* 41**,** 263-267.

SORENSEN, I. J., NIELSEN, E. H., ANDERSEN, O., DANIELSEN, B. & SVEHAG, S. E. 1996. Binding of complement proteins C1q and C4bp to serum amyloid P component (SAP) in solid contra liquid phase. *Scand J Immunol,* 44**,** 401-7.

SRIVASTAVA, N., SUDAN, R. & SAHA, B. 2011. CD40-modulated dual-specificity phosphatases MAPK phosphatase (MKP)-1 and MKP-3 reciprocally regulate Leishmania major infection. *J Immunol,* 186**,** 5863-72.

STIERHOF, Y. D., BATES, P. A., JACOBSON, R. L., ROGERS, M. E., SCHLEIN, Y., HANDMAN, E. & ILG, T. 1999. Filamentous proteophosphoglycan secreted by Leishmania promastigotes forms gel-like three-dimensional networks that obstruct the digestive tract of infected sandfly vectors. *European Journal of Cell Biology,* 78**,** 675-689.

STIERHOF, Y. D., ILG, T., RUSSELL, D. G., HOHENBERG, H. & OVERATH, P. 1994. Characterization of polymer release from the flagellar pocket of Leishmania mexicana promastigotes. *J Cell Biol,* 125**,** 321-31.

SUNDAR, S. & SINGH, B. 2014. Identifying vaccine targets for anti-leishmanial vaccine development. *Expert Review of Vaccines,* 13**,** 489-505.

SVÁROVSKÁ, A., ANT, T. H., SEBLOVÁ, V., JECNÁ, L., BEVERLEY, S. M. & VOLF, P. 2010. Leishmania major glycosylation mutants require phosphoglycans (lpg2-) but not lipophosphoglycan (lpg1-) for survival in permissive sand fly vectors. *PLoS Negl Trop Dis,* 4**,** e580.

T ILG, Y. D. S., R ETGES, M ADRIAN, D HARBECKE, AND P OVERATH 1991. Secreted acid phosphatase of Leishmania mexicana: A filamentous phosphoglycoprotein polymer. *PNAS,* 88**,** 8774-8778.

TAKAHASHI, H., CARLSON, R. W., MUSZYNSKI, A., CHOUDHURY, B., KIM, K. S., STEPHENS, D. S. & WATANABE, H. 2008a. Modification of lipooligosaccharide with phosphoethanolamine by LptA in Neisseria meningitidis enhances meningococcal adhesion to human endothelial and epithelial cells. *Infect Immun,* 76**,** 5777-89.

TAKAHASHI, M., IWAKI, D., KANNO, K., ISHIDA, Y., XIONG, J., MATSUSHITA, M., ENDO, Y., MIURA, S., ISHII, N., SUGAMURA, K. & FUJITA,

T. 2008b. Mannose-binding lectin (MBL)-associated serine protease (MASP)-1 contributes to activation of the lectin complement pathway. *J Immunol,* 180**,** 6132-8.

TELLERIA, E. L., DE ARAUJO, A. P. O., SECUNDINO, N. F., D'AVILA-LEVY, C. M. & TRAUB-CSEKO, Y. M. 2010. Trypsin-Like Serine Proteases in Lutzomyia longipalpis - Expression, Activity and Possible Modulation by Leishmania infantum chagasi. *Plos One,* 5.

TENNENT, G. A., BUTLER, P. J., HUTTON, T., WOOLFITT, A. R., HARVEY, D. J., RADEMACHER, T. W. & PEPYS, M. B. 1993. Molecular characterization of Limulus polyphemus C-reactive protein. I. Subunit composition. *Eur J Biochem,* 214**,** 91-7.

TENNENT, G. A., LOVAT, L. B. & PEPYS, M. B. 1995. Serum amyloid P component prevents proteolysis of the amyloid fibrils of Alzheimer disease and systemic amyloidosis. *Proc Natl Acad Sci U S A,* 92**,** 4299-303.

THANEI, S. & TRENDELENBURG, M. 2017. Anti-C1q autoantibodies from patients with systemic lupus erythematosus induce C1q production by macrophages. *J Leukoc Biol,* 101**,** 481-491.

THIAKAKI, M., KOLLI, B., CHANG, K. P. & SOTERIADOU, K. 2006. Down-regulation of gp63 level in Leishmania amazonensis promastigotes reduces their infectivity in BALB/c mice. *Microbes and Infection,* 8**,** 1455-1463.

THOMPSON, D., PEPYS, M. B. & WOOD, S. P. 1999. The physiological structure of human C-reactive protein and its complex with phosphocholine. *Structure,* 7**,** 169-77.

THONGSOMBOON, W., SERRA, D. O., POSSLING, A., HADJINEOPHYTOU, C., HENGGE, R. & CEGELSKI, L. 2018. Phosphoethanolamine cellulose: A naturally produced chemically modified cellulose. *Science,* 359**,** 334-338.

THURMAN, J. M. & HOLERS, V. M. 2006. The central role of the alternative complement pathway in human disease. *J Immunol,* 176**,** 1305-10.

TIMAR, K. K., PASCH, M. C., VAN DEN BOSCH, N. H. A., JARVA, H., JUNNIKKALA, S., MERI, S., BOS, J. D. & ASGHAR, S. S. 2006. Human

keratinocytes produce the complement inhibitor factor H: Synthesis is regulated by interferon-gamma. *Molecular Immunology,* 43**,** 317-325.

TROUW, L. A., PICKERING, M. C. & BLOM, A. M. 2017. The complement system as a potential therapeutic target in rheumatic disease. *Nature Reviews Rheumatology,* 13.

TSUJIMOTO M, I. K., NOJIMA S. 1983. Purification and characterisation of human C-reactive Protein. *J Biochem.,* 94**,** 1367-1373.

UDAY KISHORE A, K. B. M. R. B. 2000. C1q: structure, function, and receptors. *UImmunpharmacology,* 49.

UENO, N. & WILSON, M. E. 2012. Receptor-mediated phagocytosis of Leishmania: implications for intracellular survival. *Trends Parasitol,* 28**,** 335-44.

VAN ASBECK, E. C., HOEPELMAN, A. I., SCHARRINGA, J., HERPERS, B. L. & VERHOEF, J. 2008. Mannose binding lectin plays a crucial role in innate immunity against yeast by enhanced complement activation and enhanced uptake of polymorphonuclear cells. *BMC Microbiol,* 8**,** 229.

VAN DER AUWERA, G. & DUJARDIN, J. C. 2015. Species typing in dermal leishmaniasis. *Clin Microbiol Rev,* 28**,** 265-94.

VAN ZANDBERGEN, G., BOLLINGER, A., WENZEL, A., KAMHAWI, S., VOLL, R., KLINGER, M., MULLER, A., HOLSCHER, C., HERRMANN, M., SACKS, D., SOLBACH, W. & LASKAY, T. 2006. Leishmania disease development depends on the presence of apoptotic promastigotes in the virulent inoculum. *Proc Natl Acad Sci U S A,* 103**,** 13837-42.

VAN ZANDBERGEN, G., KLINGER, M., MUELLER, A., DANNENBERG, S., GEBERT, A., SOLBACH, W. & LASKAY, T. 2004. Cutting edge: Neutrophil granulocyte serves as a vector for Leishmania entry into macrophages. *Journal of Immunology,* 173**,** 6521-6525.

VOLANAKIS, J. E. 2001. Human C-reactive protein: expression, structure, and function. *Mol Immunol,* 38**,** 189-97.

VORUP-JENSEN, T., PETERSEN, S. V., HANSEN, A. G., POULSEN, K., SCHWAEBLE, W., SIM, R. B., REID, K. B., DAVIS, S. J., THIEL, S. & JENSENIUS, J. C. 2000. Distinct pathways of mannan-binding lectin (MBL)-

and C1-complex autoactivation revealed by reconstitution of MBL with recombinant MBL-associated serine protease-2. *J Immunol,* 165**,** 2093-100.

WANDERLEY, J. L., PINTO DA SILVA, L. H., DEOLINDO, P., SOONG, L., BORGES, V. M., PRATES, D. B., DE SOUZA, A. P., BARRAL, A., BALANCO, J. M., DO NASCIMENTO, M. T., SARAIVA, E. M. & BARCINSKI, M. A. 2009. Cooperation between apoptotic and viable metacyclics enhances the pathogenesis of Leishmaniasis. *PLoS One,* 4**,** e5733.

WANDERLEY, J. L. M., THORPE, P. E., BARCINSKI, M. A. & SOONG, L. 2013. Phosphatidylserine exposure on the surface of Leishmania amazonensis amastigotes modulates in vivo infection and dendritic cell function. *Parasite Immunol,* 35**,** 109-119.

WANG, Y., GUO, Y., WANG, X., HUANG, J., SHANG, J. & SUN, S. 2012. Serum amyloid P component facilitates DNA clearance and inhibits plasmid transfection: implications for human DNA vaccine. *Gene Therapy,* 19**,** 70–77

WANG, Y., SMITH, W., HAO, D., HE, B. & KONG, L. 2019. M1 and M2 macrophage polarization and potentially therapeutic naturally occurring compounds. *Int Immunopharmacol,* 70**,** 459-466.

WASUNNA, K. M., RAYNES, J. G., WERE, J. B., MUIGAI, R., SHERWOOD, J., GACHIHI, G., CARPENTER, L. & MCADAM, K. P. 1995. Acute phase protein concentrations predict parasite clearance rate during therapy for visceral leishmaniasis. *Trans R Soc Trop Med Hyg,* 89**,** 678-81.

WEINGARTNER, A., KEMMER, G., MULLER, F. D., ZAMPIERI, R. A., GONZAGA DOS SANTOS, M., SCHILLER, J. & POMORSKI, T. G. 2012. Leishmania promastigotes lack phosphatidylserine but bind annexin V upon permeabilization or miltefosine treatment. *PLoS One,* 7**,** e42070.

WIESE, M. 1998. A mitogen-activated protein (MAP) kinase homologue of Leishmania mexicana is essential for parasite survival in the infected host. *EMBO J,* 17**,** 2619-28.

WIESE, M., ILG, T., LOTTSPEICH, F. & OVERATH, P. 1995. Ser/Thr-rich repetitive motifs as targets for phosphoglycan modifications in Leishmania mexicana secreted acid phosphatase. *EMBO Journal,* 14**,** 1067-74.

WILSON, M. E., INNES, D. J., DE Q. SOUSA, A. & PEARSON, R. D. 1987. Early Histopathology of Experimental Infection with Leishmania donovani in Hamsters. *The Journal of Parasitology,* 73.

WILSON, M. E. & PEARSON, R. D. 1988. Roles of CR3 and mannose receptors in the attachment and ingestion of Leishmania donovani by human mononuclear phagocytes. *Infect Immun,* 56**,** 363-9.

WRIGHT, S. D. & SILVERSTEIN, S. C. 1983. Receptors for C3b and C3bi promote phagocytosis but not the release of toxic oxygen from human phagocytes. *The Journal of experimental medicine,* 158**,** 2016-2023.

XU, Y., MA, M., IPPOLITO, G. C., SCHROEDER, H. W., JR., CARROLL, M. C. & VOLANAKIS, J. E. 2001. Complement activation in factor D-deficient mice. *Proc Natl Acad Sci U S A,* 98**,** 14577-82.

YUSTE, J., BOTTO, M., BOTTOMS, S. E. & BROWN, J. S. 2007. Serum amyloid P aids complement-mediated immunity to Streptococcus pneumoniae. *PLoS Pathog,* 3**,** 1208-19.

ZIJLSTRA, E. E. 2016. The immunology of post-kala-azar dermal leishmaniasis (PKDL). *Parasit Vectors,* 9**,** 464.